

THE ROLE OF INHIBITORY TRANSMISSION IN BIRDSONG AUDITORY  
PROCESSING

By  
Raphael Pinaud

A DISSERTATION

Presented to the Department of Neuroscience  
and the Oregon Health and Science University

School of Medicine

in partial fulfillment of  
the requirements for the degree of

Doctor of Philosophy

August 2005

School of Medicine  
Oregon Health and Science University

---

CERTIFICATE OF APPROVAL

---


This is to certify that the Ph.D. dissertation of


**Raphael Pinaud**


has been approved

  
Mentor/Advisor - Dr. Claudio V. Mello

  
Member / Dr. Curtis Bell (Chair)

  
Member – Dr. Matthew Frerking

  
Member – Dr. Jane MacPherson

  
Member – Dr. Henrique von Gersdorff

## TABLE OF CONTENTS

ANATOMICAL ABBREVIATIONS .....	vii
ACKNOWLEDGMENTS .....	viii
ABSTRACT.....	xii
DEDICATION.....	xvii
CHAPTER 1 - INTRODUCTION.....	1
Song Learning.....	3
The Song Control System.....	5
Song Learning and Maintenance Requires Auditory Feedback: A Brief Look at the Ascending Auditory System in Songbirds.....	7
The Immediate Early Gene zenk.....	10
Activity-Dependent zenk Expression Reveals Functional Properties of the Songbird Auditory Telencephalon.....	12
GABA and Inhibition in Birdsong Auditory Processing .....	15
GABA Neurotransmission .....	17
GABAergic Receptors .....	18
Sources of GABAergic Input.....	20
Roles of GABAergic Transmission in Sensory Processing.....	22
a) GABA Regulation of RFs in the Somatosensory Cortex .....	22
b) GABA Regulation of RFs in the Visual Cortex .....	23
c) GABA Regulation of RFs in the Auditory Cortex .....	26
GABAergic Transmission and Auditory Processing in the Zebra Finch: Thesis Goals .....	27

CHAPTER 2 - GABA IMMUNOREACTIVITY IN AUDITORY AND SONG CONTROL BRAIN AREAS OF ZEBRA FINCHES .....	47
INTRODUCTION .....	48
MATERIAL AND METHODS .....	52
RESULTS .....	57
DISCUSSION .....	96
CHAPTER 3 - GABAERGIC NEURONS PARTICIPATE IN THE BRAIN'S RESPONSE TO BIRDSONG AUDITORY STIMULATION.....	108
INTRODUCTION .....	109
MATERIAL AND METHODS .....	113
RESULTS .....	122
DISCUSSION .....	142
CHAPTER 4 - A NOVEL MECHANISM FOR AUDITORY PROCESSING DYNAMICS INVOLVING DISINHIBITION IN THE SONGBIRD ANALOGUE OF THE AUDITORY CORTEX.....	152
INTRODUCTION .....	153
MATERIAL AND METHODS .....	156
RESULTS .....	160
DISCUSSION .....	186
CHAPTER 5 - CALBINDIN-POSITIVE NEURONS REVEAL A SEXUAL DIMORPHISM WITHIN THE SONGBIRD ANALOGUE OF THE MAMMALIAN AUDITORY CORTEX.....	192
INTRODUCTION .....	193



MATERIAL AND METHODS.....	197
RESULTS .....	205
DISCUSSION .....	225
CHAPTER 6 - SUMMARY AND CONCLUSIONS.....	233
Summary of Key Contributions .....	234
An Operational Model for NCM.....	237
a) Active GABAergic Synapses at Rest Suppress Excitatory Network .....	238
b) A Double Inhibitory Circuit .....	239
c) Disinhibition During Sensory Processing.....	240
d) Physical Requirements of the Double Inhibitory Model.....	241
NCM and the Mammalian Primary Auditory Cortex: Analogous Structures?.....	242
a) General Anatomical Organization .....	242
b) Organization of the GABAergic Network.....	243
c) Roles for GABAergic Transmission During Sensory Processing .....	244
d) Mechanisms Underlying Frequency Discrimination.....	245
e) Biophysical Properties of Auditory Neurons.....	246
Is NCM a Single Brain Region? .....	247
Orexin Regulation by Song and Its Role in Auditory Processing in NCM.....	249
Final Comments .....	255
APPENDIX I - PRELIMINARY EVIDENCE FOR THE NEUROCHEMICAL IDENTITY OF PROJECTION NEURONS IN THE SONGBIRD FIELD L AND NCM .....	265

APPENDIX II - FURTHER ANALYSIS ON THE EFFECTS OF BICUCULLINE ON FREQUENCY TUNING CURVES IN THE NCM OF AWAKE-RESTRAINED ZEBRA FINCHES.....	270
REFERENCES .....	277

## ANATOMICAL ABBREVIATIONS

A – arcopallium  
AFP – anterior forebrain pathway  
area X – area X of the striatum  
Cb – cerebellum  
CLM – caudolateral mesopallium  
CMM – caudomedial mesopallium  
DLM - medial nucleus of dorsolateral thalamus  
DM - dorsal medial nucleus of the midbrain  
FLM – medial longitudinal fasciculus  
GP – globus pallidus  
H – hyperpallium  
Hp – hippocampus  
HVC – nucleus HVC (a letter-based name)  
IC – inferior colliculus  
ICo - intercollicular nucleus  
IV – fourth ventricle  
L1, L2a, L3 – field L subdivisions  
LaM – lamina mesopallialis  
LMAN – medial subdivision of the magnocellular nucleus of the anterior nidopallium  
M – mesopallium  
MLd – dorsal part of the lateral mesencephalic nucleus  
MGN – medial geniculate nucleus  
N – nidopallium  
NA – nucleus angularis  
NCM – caudomedial nidopallium  
Nif – nucleus interfascialis of the nidopallium  
NL – nucleus laminaris  
NM – nucleus magnocellularis  
Ov – nucleus ovoidalis of the thalamus  
P – pons  
PFP – posterior forebrain pathway  
RA – robust nucleus of the arcopallium  
sh – nidopallial shelf region adjacent to HVC  
SON – superior olivary nucleus  
St – striatum  
CSt – caudal striatum  
TeO – optic tectum  
Th – thalamus  
tOM – occipitomesencephalic tract  
V- ventricle  
VeL – lateral vestibular nucleus  
VII n. – nucleus of the seventh cranial (facial) nerve

## ACKNOWLEDGMENTS

First and foremost I would like to thank my supervisor Claudio Mello for the opportunity to conduct my doctoral work under his direction. Claudio has played a major role in my scientific formation, beginning with his influence during my undergraduate work in Brazil and as an intern at Rockefeller University. I would also like to thank Claudio for imprinting on me the heaviest scientific stringency and for his meticulous guidance throughout the development of this work.

Jane MacPherson has seen and lived most of the ups and downs of this thesis work along with me. Always with sound advice, tireless guidance and words of wisdom, Jane played a critical role in my development as a young scientist. Apart from our work relation, Jane became part of our family; she became my half-Portlander, half-Canadian second mother. I will certainly miss our meetings, dinners, breakfasts and laughter when I move onto the next step of my career, but am confident that our friendship will remain strong.

David Vicario for allowing me the opportunity to conduct research under his direction at Rutgers University. During my stay at David's laboratory I had the opportunity to accomplish a life-long dream: to record electrophysiological responses from awake animals. The sights and sounds of real-time neural activity provided me with one of the most memorable experiences of my entire neuro-scientific path, for which I will always be grateful.

Tom Terleph, a post-doctoral fellow in David Vicario's lab at Rutgers, conducted the extracellular recordings with me, side-by-side, and therefore was a critical participant of this thesis. During my training in David's lab I lived in the Terleph household for a number of weeks where I was spoiled with home-made high quality beer and treated as a member of the family. Tom and Kristi became very close friends and were dragged to Brazil last year for a quick tropical vacation!

I am deeply indebted to Henrique von Gersdorff. In my first year, as a requirement for the graduate program, I had to rotate through three labs; one of my choices was Henrique's lab. From my first day at OHSU, I made it clear to all my rotation supervisors that I had made my decision as to what lab I had chosen to conduct my graduate work. Henrique gracefully accepted me as a rotation student in his lab despite knowing of my decision. His generosity extended beyond this point! Henrique allowed me to use equipment in his lab to conduct the first patch-clamp recordings in NCM during my rotation; part of the data collected during this training period are included in this thesis.

During my first year as a graduate student, Ricardo Leão, then a post-doctoral fellow in the von Gersdorff lab at the Vollum Institute, and I developed a slice preparation and conduct the first patch-clamp recordings in the songbird NCM! Since then Ricardo has become a great friend and has continued to explore the biophysical mysteries of NCM, since his return to Brazil, in his own laboratory.

I would especially like to thank the members of my thesis committee: Curtis Bell, Jane MacPherson, Henrique von Gersdorff and Claudio Mello for their guidance, support and enthusiasm. I also thank them for their collective intellectual stringency which contributed significantly to my scientific blooming.

Jin Kwon Jeong has provided incredible technical support for the Mello laboratory throughout most of my graduate work. Jin contributed to the early stages of my graduate training, particularly during my first year at OHSU, when graduate students are typically swamped with coursework. His very pleasant personality contributed to a nice environment in the Mello laboratory and was certainly missed after his return to South Korea. Aesoon Bensen passed through our lab for a relatively short period of time; this time, however, was sufficient enough for her to provide excellent technical help, especially with routine laboratory tasks, allowing me to focus on other critical methodologies employed in my thesis.

Matthew Frerking has played a major advisory role in my transition from graduate school to the post-doctoral level. Matt always made time in his busy schedule to provide me with critical and thorough advice, feedback and information about my next scientific move. His guidance allowed me to make a very informed decision on my next move and has made this otherwise stressful transition period significantly smoother.

Antonio Fortes, my great "Land of 10,000 Lakes" friend, for unmatched remote support, advice and friendship. In addition to being a true friend, Antonio became my official Matlab and Adobe Illustrator live guide, Federal tax consultant and Forum of European Neuroscience and Society for Neuroscience roommate. Antonio's professional photographic skills were certainly Godsend when he came for his only visit during my life in Portland...and arrived the day my son Daniel was born, allowing me to have full documentation of the day my life changed, for better.

I am indebted also to Rich Simerly, for constantly refreshing my memory on the complexity and beauty of the mammalian neuroanatomy. I also thank Rich for plenty of great advice through the ups and downs of my graduate work and for careful and insightful feedback on the calbindin findings discussed in this thesis.

Jane Rosato has provided incredible support throughout my years here at OHSU. Her unconditional and timely help made my life as a graduate student much less complicated and significantly more efficient. Likewise, Gary Rowell has always provided immediate help through my administrative and bureaucratic struggles.

Paul Cordo has assembled and directs a group of incredibly talented scientists in the Neurological Sciences Institute. This environment allowed me the opportunity of valuable scientific exchanges that certainly contributed to my formation as a young scientist. In addition, Paul has trusted my credentials as a professional volunteer in several of his microneurographic inquiries.

Francesca Fleming, our library guru, provided critical help during my adventures in the primary (often ancient) literature that could not be found online.

Many people contributed to sharpening my thinking in neurobiological questions. I would like to especially thank Jennifer Alden, Ana Karla Jansen de Amorim, Lutgarde Arckens, Curtis Bell, Johan Bolhuis, Heather Cameron, Bill Currie, Peter De Weerd, Mike Dragunow, Antonio Fortes, Tim Gentner, Rainer Goebel, Cheryl Harding, Erich Jarvis, Leszek Kaczmarek, Alfredo Kirkwood, Chris Kushmerick, Peter Larsson, Ricardo Leão, Jane MacPherson, Edwin McCleskey, Rob Malenka, Claudio Mello, Charles Meshul, Kathy Nordeen, Ernie Nordeen, David Perkel, Jennifer Petersen, Jacob Raber, Pat Roberts, Roberto Santiago, Kazue Semba, Rich Simerly, Bob Stackman, Tom Terleph, Shelly Tillman, Liisa Tremere, Sriharsha Vemana, Paulo Vianney, David Vicario, Henrique von Gersdorff, John Welsh, John Williams, Sean Wolfson and Bill Woodward.

I thank all members of the Mello lab for interesting discussions.

I also thank teachers and mentors that contributed to all stages of my intellectual formation.

To all the animals used in this thesis, my most sincere gratitude.

My in-laws Arnold and Marcella Tremere provided incredible help and support throughout these years. The home-made “Raphael’s cookies” were often times the key to successful scientific experimentation and progress. Evelyn and Sean Studer have always been supportive and encouraging throughout the course of my graduate work. In addition, Ev and Sean superbly hosted me in Calgary numerous times during the endless visa renewals. Special thanks also go to Sean who took me to the Calgary Saddledome to watch my beloved Calgary Flames, on front row seats (really nose on the glass)!

I thank my cousins Krika, Robertão, Naldo and Dani for their friendship and support.

I owe a great debt to my Great-Aunt Eunice for her constant care and attention. For keeping me linked to the Brazilian culture and news. Eunice has kept her tradition of sending me great Brazilian magazines and postcards every other week, religiously. Te amo Tetê e obrigado por toda sua atenção, apoio e amor.

Vó Vilma e Vô Nêu, for making my life a priority over their own! My grandparents came to Portland a number of times during my graduate work to help with non-thesis related issues thereby freeing my time to focus on my experiments and career. I thank you both from the bottom of my heart for all your love and support. Vó e Vô, eu amo vocês demais e agradeço do fundo do meu coração todos seus esforços e sacrifícios durante toda minha vida e, principalmente, nestes últimos anos em que estive aqui.

I offer my efforts in this thesis and thank my father Luiz Fernando, my mother Sandra and my brother Rodolpho for their love and support, and for encouraging my personal and professional development despite the strain of us being far apart. This thesis is our victory! Vocês são minha vida.

I thank Liisa Tremere, my wife, my friend, my lover, my confidant, my editor, my collaborator, my teacher, my shoulder, my coach, my idol, my fan, my mentor, my heart, my energy and my soul, for giving me strength (always giving me strength; always) for your unconditional love and support and for showing me the path to complete this convoluted and often arduous journey. I also would like to especially thank you for being a fantastic mother to our son.

Finally I thank you, Daniel, my son, my life. For your smiles, for your hugs and for understanding why daddy sometimes could not spend more time playing with you and holding you. For gracefully understanding why sometimes I was too tired to stay with you until you slept. I thank you for giving my life and this effort a purpose.

## ABSTRACT

The telencephalic caudo-medial nidopallium (NCM) participates in auditory processing of vocalizations in songbirds. Knowledge on the anatomical and functional organization of NCM is still in its infancy. Given that GABA is one of the most prevalent neurotransmitter systems in the vertebrate brain and plays critical roles in sensory processing, the present work addresses the anatomo-functional organization of the GABAergic system in the songbird brain, with a specific focus in auditory areas. We have investigated this system in three sets of studies.

First we used GABA immunocytochemistry to reveal GABAergic cells and processes in zebra finch brain, and emphasized auditory areas and song control nuclei. We found that several nuclei of the ascending auditory pathway showed a moderate to high density of GABAergic neurons including the cochlear nuclei, nucleus laminaris, superior olivary nucleus, mesencephalic nucleus lateralis pars dorsalis, and nucleus ovoidalis. Telencephalic auditory areas, including field L subfields L1, L2a and L3, caudomedial nidopallium (NCM) and mesopallium (CMM), contained GABAergic cells at particularly high densities, approximately 50% of neuronal cells. This high prevalence of GABAergic neurons in auditory areas suggested a major role for inhibition in network dynamics, and a possible GABAergic influence on auditory response properties of NCM neurons. Considerable GABA labeling was also seen in the shelf area of caudodorsal nidopallium, and the cup area in the arcopallium, as well area X, the lateral magnocellular nucleus of the anterior nidopallium, the robust nucleus of the arcopallium and nidopallial nucleus HVC. GABAergic cells were typically small, most likely local inhibitory interneurons,



although large GABA-positive cells that were sparsely distributed were also identified. GABA-positive neurites and puncta were identified in most nuclei of the ascending auditory pathway and in song control nuclei. These anatomical data are in accordance with a prominent role of GABAergic mechanisms in regulating the neural circuits involved in song perceptual processing, motor production, and vocal learning in songbirds.

Second, we cloned a zebra finch homologue of the gene encoding the 65 kD isoform of glutamic-acid decarboxylase (GAD-65), a specific GABAergic marker, and conducted an expression analysis by in-situ hybridization to identify and to map the brain distribution of GABAergic cells. The results using this methodology confirmed the previous results that auditory telencephalic areas Field L2, NCM and CMM contain a high number of GABAergic cells. Next, using double fluorescence in-situ hybridization and double-immunocytochemical labeling, we demonstrated that large numbers of GABAergic cells in NCM and CMM show inducible expression of the transcription regulator *zenk* in response to song auditory stimulation and are thus, song-responsive. Next, whole-cell patch clamp recordings from NCM neurons in a slice preparation were used to explore the relative contributions of inhibitory and excitatory inputs to spontaneous activity. Application of bicuculline methiodide (BMI), a competitive antagonist for GABA-A receptors, abolished inhibitory post-synaptic currents (IPSCs) and spontaneous IPSCs, a phenomenon that was accompanied by dramatic increases in activity. These findings suggested that tonic inhibition via GABA-A transmission plays a significant role in modulating excitability of NCM neurons.

Third, multi-electrode extracellular recordings were combined with local injections of BMI in the NCM of awake, restrained adult zebra finches during song playback to study the role of inhibition in the patterning of auditory responses. Simultaneous recordings were made from multiple NCM sites bilaterally, both before and after pressure injection of BMI into the right hemisphere at a dose just below threshold for local seizure-like activity. Before injection, song stimuli elicited responses in both hemispheres consisting of phasic bursts to most syllables and sustained firing between syllables that continued after the end of the stimulus. After BMI application, the right hemisphere showed changes in firing pattern: 1) the phasic responses increased dramatically, especially to the first song syllable, and 2) the sustained firing between syllables was largely abolished; however, the overall response magnitude was not changed. BMI application did not affect frequency tuning of NCM units but appeared to decrease significantly the fidelity of information coding. These findings suggested that GABA-A transmission contributes not only to excitability but also to the temporal dynamics of auditory responses in NCM.

In an attempt to further characterize the neurochemical identity of GABAergic neurons in NCM, immunocytochemistry was conducted to identify calbindin-positive neurons. Our results provided evidence for a sexual dimorphism in the population of calbindin-positive neurons in NCM. We showed that cells immunolabeled for calbindin are primarily localized to caudal NCM and are almost twice as numerous in males as in females. This dimorphism was neither a reflection of higher neuronal cell density nor higher number of GABAergic neurons in this area. Calbindin-positive neurons did not exhibit song-induced *zenk* expression and their numbers were not

regulated by auditory experience in males or females. Caudal NCM also expressed high levels of the estrogen-generating enzyme aromatase and could represent a site of estrogen production. Thus, NCM contains neurochemically-defined subdomains, with possible distinct functional properties, and a sexually dimorphic neuronal population. These observations suggest that auditory processing of birdsong may differ across genders, and that local sex steroids may play a role in the processing of auditory information.

“I am of the opinion that the brain exercises  
the greatest power in the man”

- Hippocrates

## DEDICATION

This thesis is dedicated  
to my father Luiz Fernando  
and my mother Sandra,  
for believing...  
...and for their unconditional love and unlimited support.

## **CHAPTER 1**

### **INTRODUCTION**

One of the great challenges in the field of sensory physiology is how the brain encodes environmental information. A great deal of effort has been placed at trying to understand the neural substrates and mechanisms that underlie the representation of external information in the vertebrate brain. A key player in this process appears to be the main inhibitory neurotransmitter in the vertebrate central nervous system (CNS), the gamma-aminobutyric acid (GABA). In the present thesis I have investigated the general organization and function of GABAergic system in the zebra finch auditory telencephalon, with a particular focus in the caudomedial nidopallium (NCM), using a combination of molecular, cellular and electrophysiological approaches.

In the following paragraphs it is my hope to provide the reader with background that is relevant to put in perspective the rationale of the experiments conducted herein, as well as critical research findings that facilitate the interpretation and discussion of the data collected in this thesis. First I will present a brief overview of the relevance of songbirds as an experimental model for vocal learning and auditory processing. Next I will present a summary of how activity-dependent tools, especially the expression of the immediate early gene *zenk*, have helped songbird neurobiological quests aimed at understanding the functional organization of NCM. Finally I will discuss critical properties of the GABAergic system, with a particular focus on data obtained by other research groups in mammalian models, where most scientific inquiries directed at the GABAergic circuit have been studied. I will close this introductory chapter by stating this thesis' goals and its general organizational structure.

## **Song Learning**

The genesis of contemporary birdsong neurobiology, especially the study of vocal learning behavior, begun in the 1950's with the earliest descriptions of formal experimentation conducted by William Thorpe, from Cambridge University. These early studies demonstrated that acoustic isolation of juvenile chaffinches from same-species (conspecific) male vocalizations led to anomalous song development (Thorpe, 1958). Interestingly, playback of pre-recorded adult chaffinch songs to the young isolates rescued their normal song development (Thorpe, 1958). In addition to highlighting the importance of suitable tutor song for normal birdsong development, these early experiments also confirmed that song learning occurred within a "critical period" that preceded sexual maturity. Hence, early experiments provided the first evidence that young songbirds learn the structure of their own vocalizations from adult conspecifics and must do so before exiting a critical period of their development. This original finding differs from evidence subsequently collected in other songbirds, such as canaries, whose song continues to be modified throughout life, usually on a seasonal basis (for reviews see Doupe, 1993; Mooney, 1999; Brainard and Doupe, 2000; Mello et al., 2004; Nordeen and Nordeen, 2004). As the field of songbird neurobiology evolved over the years it was agreed that species such as chaffinches, that learn a single song that is maintained throughout the animal's life, would be referred to as "age-limited learners", while species such as the canary, who modify their vocalizations on a seasonal basis, would be referred to as "open-ended learners". Following Thorpe's pioneering efforts on how age-limited song learners require both tutor songs and a critical period in order to engage in song learning



behaviors, songbirds have been extensively and successfully used as a model for vocal learning. Vocal learning is defined as the ability to learn vocalizations through imitation, as opposed to intuition, using auditory information.

For my own work in this field I have used zebra finches (*Taeniopygia guttata*), another age-limited learner, whose vocal learning also occurs only during a critical period early in life. This songbird is the most extensively studied species in the songbird neurobiology field, perhaps because its songs are relatively simple and highly structured. In addition, this songbird species tends to breed well in captivity.

In zebra finches, the period in which song learning behavior occurs lasts for approximately 90 days. This behavior has been conveniently divided into three stages that exhibit some degree of overlap (Fig. 1A). During the (1)*sensory phase*, which in zebra finches begins approximately 2 to 3 weeks post-hatching, young animals are exposed to direct vocalizations of their tutors, often their fathers. Zebra finches, like chaffinches, require these initial exposures to tutor song in order to generate memories of that song used as a template in the subsequent construction of their own song.

The second stage of song learning behavior is referred to as the (2) *sensorimotor phase*. Early in this second stage, juvenile birds start to spontaneously vocalize. Initially their songs are highly unstructured in both syntax and phonology. It is thought that during this phase, developing animals use auditory feedback to tune their own outputs; juvenile birds appear to compare their own vocalizations with traces of the tutor's song that had been memorized during the sensory phase. As the sensorimotor phase progresses, young birds' vocalizations notably improve in

structure and, by the end of this phase, are significantly less variable, more structured and with most elements clearly incorporated from the tutor's song. In zebra finches, the sensorimotor phase begins around the first month of age, and extends approximately to three months post-hatch. Once a firm pattern of song repetition has been achieved, vocalizations will not change throughout the life of the zebra finch at which point it is said to be crystallized. During the (3) *crystallization phase* the song becomes highly stereotyped, that is, basically invariant across renditions. It has been proposed, therefore, that crystallization constitutes the final phase of the vocal learning behavior.

### **The Song Control System**

Fernando Nottebohm, in the mid-1970's, shed considerable light upon the neural circuitry that enables vocal learning in songbirds. It became clear that vocal learning behavior is under the tight control of a set of interconnected telencephalic nuclei commonly referred to as the *song control nuclei*, or the *song control system* (Fig.1B). The presence of telencephalic song control nuclei is directly related to the ability to learn and sing songs, but not to vocalize.

In most songbird species, especially in temperate regions, only males sing. This behavioral distinction is associated with the presence of song control nuclei only in males, but not females. In females, the song system is highly atrophied, if existent, providing one of the earliest and clearest examples of brain sexual dimorphism in vertebrates (Nottebohm and Arnold, 1976, 1979). Interestingly, treatment of female birds with male sex hormones in some species triggers the development of song

control nuclei as well as the ability to sing (Nottebohm and Arnold, 1976; Nottebohm, 1980; Schlinger, 1997).

The song control system is divided into two main pathways: 1) the posterior forebrain pathway (PFP), which is reportedly involved in vocal production and 2) the anterior forebrain pathway (AFP) which plays a role in sensory learning (reviewed in Zeigler and Marler, 2004). The PFP encompasses descending projections from the telencephalic nucleus HVC to the robust nucleus of the arcopallium (RA), and from there to the tracheosyringeal section of the hypoglossal nucleus, where motoneurons finally innervate muscles of the syrinx, the vocal organ in songbirds (Nottebohm et al., 1982; Wild, 2004). In experiments where stations of the PFP were lesioned, animals were rendered incompetent to vocalize, presumably because these circuits are part of a descending pre-motor pathway (Nottebohm et al., 1976) (Fig. 1B).

The AFP is originated from projections of HVC onto area X of the striatum (Nottebohm et al., 1976; Bottjer et al., 1989). Cells in area X project to the dorsal mediolateral nucleus of the thalamus (DLM) and these area X recipient cells, in turn, project to the telencephalic lateral magnocellular nucleus (LMAN) (Bottjer et al., 1989). LMAN neurons target two brain nuclei. One set of cells projects to area X, forming an anatomical arrangement that has been proposed by some to form a closed loop dedicated to processing information related to song learning (Vates and Nottebohm, 1995; reviewed in Zeigler and Marler, 2004). The second target region of LMAN neurons is the nucleus RA, which is part of the descending pre-motor output of the PFP (Bottjer et al., 1989; reviewed in Nordeen and Nordeen, 1997; Zeigler and Marler, 2004) (Fig. 1B). Lesions targeting the AFP in juvenile birds impair song

acquisition and/or development as animals cannot improve their vocalizations towards the normal stereotypical adult songs during the critical period, and end-up crystallizing those aberrantly. Conversely, lesions in the AFP of adult birds, that were allowed to develop and crystallize normal songs, fail to generate any measurable impairment in song production or maintenance (Bottjer et al., 1984; Sohrabji et al., 1990; Scharff and Nottebohm, 1991; Nordeen and Nordeen, 1993).

### **Song Learning and Maintenance Requires Auditory Feedback: A Brief Look at the Ascending Auditory System in Songbirds**

It has been shown that intact hearing is critical for the normal development of vocal learning behavior. For example, birds raised in acoustic isolation or deafened at a young age fail to develop normal song structure (Konishi, 1965b; reviewed in Nordeen and Nordeen, 1997; Zeigler and Marler, 2004). Normal auditory experience continues to be required throughout life for the maintenance of the adult state, crystallized song in zebra finches. Experiments in animals that underwent cochlear lesions or experienced computer-guided auditory feedback interference provided clear evidence that the structure of the adult song degrades after extended periods of time when auditory feedback mechanisms that are used to validate song structure become compromised (Nordeen and Nordeen, 1992; Woolley and Rubel, 1997; Leonardo and Konishi, 1999). Given that normal auditory processing is required for both vocal learning and the maintenance of adult songs, it is understandable that a great deal of effort has been directed at characterizing the anatomo-functional organization of auditory processing stations in the songbird brain.

The basic anatomical organization of the songbird ascending auditory system appears to be highly conserved when compared to other avian species and other vertebrates (Vates et al., 1996; Mello et al., 1998; Reiner et al., 2004). The avian auditory pathway consists of brainstem and thalamic stations that process and transmit auditory information to the auditory telencephalon (Fig. 2A). Briefly, auditory information reaches the CNS through the auditory branch of the 8<sup>th</sup> cranial nerve (vestibulo-cochlear nerve). Auditory input reaches the cochlear nuclei (nuclei magnocellularis [NM] and angularis [NA]). Cell bodies in the NM project bilaterally to nucleus laminaris (NL), whereas those in the NA send bilateral ascending projections to the superior olivary nucleus (SON) and the dorsal lateral mesencephalic nucleus (MLd). MLd has been postulated to be the avian homologue of the mammalian inferior colliculus (Conlee and Parks, 1986) (Fig. 2A). NL projections also target the SON and MLd. The main source of SON projections consists of descending GABAergic projections directed at the cochlear nuclei and NL (Lachica et al., 1994). The output of MLd targets the thalamic nucleus ovoidalis (Ov), which is the anatomical, and possibly functional, equivalent of the mammalian medial geniculate nucleus, in avian species (Fig. 2B). Ov axons target the auditory telencephalon. A fraction of the sub-telencephalic projections detailed above have not been characterized in songbirds, especially in stations that precede MLd, but have been extensively studied in non-oscine species such as the barn-owl, pigeons and chicks (Karten, 1967, 1968; Parks and Rubel, 1975; Rubel and Parks, 1975; Parks and Rubel, 1978; Brauth et al., 1987; Takahashi and Konishi, 1988; Lachica et al., 1994;

Levin et al., 1997). The physiological roles of regions in the ascending auditory pathway are discussed in Chapter 2.

The caudomedial aspect of the auditory telencephalon has a prominent lobe that contains the thalamo-recipient zone field L, as well as the principal field L targets, the NCM and the caudomedial and caudolateral mesopallium (CMM and CLM, respectively) (Vates et al., 1996) (Fig. 2B). Even though the precise role of each individual nucleus in this pathway in sensory processing has not yet been clearly defined, it has been proposed that each area contributes uniquely to song auditory processing and perception (for reviews see Gentner, 2004; Mello et al., 2004). In addition, a few areas in this auditory lobe have been proposed to participate in processes of song memorization required for vocal learning (for review see Mello et al., 2004). These interpretations are based on a series of electrophysiological and gene expression studies that were conducted in a number of songbird species.

It has been shown that field L of zebra finches and starlings exhibit song- and pure-tone evoked auditory responses (Muller and Leppelsack, 1985; Gehr et al., 1999) and are organized in a tonotopic fashion for several songbird species (Muller and Leppelsack, 1985; Capsius and Leppelsack, 1999; Gehr et al., 1999). Field L is divided into three subfields (field L1, L2 and L3; field L2 being further subdivided into field L2a and L2b based on anatomical criteria). Field L2, which is the major target of auditory thalamo-telencephalic projections, exhibits auditory responses that are less selective for complex auditory stimuli than its target regions including NCM and field L1 and L3, suggesting that field L2 is hierarchically located at a lower position as compared to its targets (Muller and Leppelsack, 1985; Sen et al., 2001).

NCM, which is the primary area of interest of this thesis, also displays robust song- and tone-evoked responses (Chew et al., 1995; Chew et al., 1996).

Electrophysiological responses recorded at this level, however, revealed that NCM exhibits a significantly higher degree of response selectivity, as compared to lower regions such as field L. For example, Chew and colleagues have reported that NCM units preferentially respond to conspecific songs, rather than other-species (heterospecific) ones, white noise or pure-tones (Chew et al., 1995; Chew et al., 1996).

A great deal of information regarding the anatomical and functional organization of NCM has also been obtained with gene expression studies. On the forefront of these gene expression studies is the activity-dependent gene *zenk*, which appears to be sensitive to neuronal depolarization and, therefore, has been used as a mapping tool for neuronal activation in songbird neurobiological studies. In the following paragraphs I will detail aspects of *zenk* structure and function. Subsequently, I will discuss key experiments where *zenk* expression enhanced our knowledge of the anatomy and physiology of the songbird brain, with a focus in the auditory area NCM.

### **The Immediate Early Gene *zenk***

The immediate early gene (IEG) *zenk* (also known as NGFI-A, *egr-1*, *krox-24* and *zif268*) encodes a transcriptional regulator that belongs to the zinc-finger class. Finger-like protuberances in its structure are stabilized by ionic zinc and interact with

a specific DNA motif found in the promoter of a wide variety of genes expressed within the nervous system, thereby potentially regulating their expression.

*zenk* is an activity-regulated gene (Murphy et al., 1991; Worley et al., 1991; Herdegen and Leah, 1998; Knapska and Kaczmarek, 2004). Furthermore, its expression depends on the activation of the N-methyl-D-aspartate (NMDA) receptors (Cole et al., 1989; Wisden et al., 1990), which have been involved in various aspects of synaptic reinforcement and facilitation in a number of experimental systems (reviewed in Cotman et al., 1988; Daw et al., 1993; Hollmann and Heinemann, 1994). Expression of *zenk* appears to be coupled to the activation of the ERK/mitogen-activated protein kinase (MAP) kinase pathway, as well as other kinase cascades such as the protein kinase A (PKA) and calcium/calmodulin kinase II pathways, and putatively coordinates the expression of other genes that possess the *zenk* binding domain in their promoters or enhancer regions (Herdegen and Leah, 1998; Dziema et al., 2003; Pinaud, 2005) (Fig. 3).

Significant attention has been paid to *zenk* over the years; this heightened scientific interest has coincided in part, with the elucidation of the identity of many genes regulated by this transcription factor. Some of these putative *zenk* target genes have been implicated in normal neuronal and synaptic functioning, as well as plasticity. It has, for example, been demonstrated that the ZENK protein is involved in the transcriptional regulation of synapsin I and synapsin II genes, as well as the gene that encodes for synaptobrevin II (Thiel et al., 1994; Petersohn et al., 1995; Petersohn and Thiel, 1996) in *in-vitro* assays. These proteins have been demonstrated to play a direct role in neurotransmitter release. Other candidate proteins putatively



regulated by ZENK include neurotransmitter-gated ion channels, the monoamine oxidase B gene, the alpha-7 subunit of the nicotinic acetylcholine receptor, neurofilament and the adenosine 5'-triphosphate binding cassette, sub-family A, transporter 2 (ABCA2), to name a few (Pospelov et al., 1994; Carrasco-Serrano et al., 2000; Wong et al., 2002; Davis et al., 2003; Mello et al., 2004). Thus, ZENK is well positioned to affect the expression of genes that are involved not only in neurotransmitter release and membrane transport, but also other fundamental neuronal functions such as excitability. Moreover, *zenk* is well positioned to integrate activity-dependent changes in the cell surface with the genomic responses thought to underlie the physical correlates of experience-dependent circuitry modifications (Pinaud, 2004, 2005).

### **Activity-Dependent *zenk* Expression Reveals Functional Properties of the Songbird Auditory Telencephalon**

Despite significant effort directed at identifying the specific roles of ZENK in normal neuronal physiology, its activity-dependent expression has been used for over 10 years as a mapping tool for neuronal activation (reviewed in Kaczmarek and Robertson, 2002). One of the main advantages of this methodology is that it can assess neural activity in freely-behaving, awake and unanesthetized animals. In addition, the use of IEGs, including *zenk*, as a mapping tool can reveal large-scale, full brain activity maps with single-cell resolution (reviewed in Chaudhuri, 1997; Kaczmarek and Robertson, 2002).

The first experiment that investigated *zenk* expression in the songbird brain revealed that playbacks of conspecific songs elicited a robust induction of this IEG in auditory areas, with highest expression detected in NCM (Mello et al., 1992). Subsequent, more detailed studies revealed that song playbacks triggered a significant induction of the IEG *zenk* in several auditory stations including field L (subfields L1 and L3), CMM, the cup region of song nucleus RA and the shelf region underlying HVC (reviewed in Mello, 2002b; Mello et al., 2004). *zenk* expression that resulted from song playback presentation was observed in males that did not sing, as well as female songbirds that typically do not sing. These data are useful to suggest that *zenk* induction is associated with auditory experience, rather than singing behavior (Mello et al., 1992; Jarvis et al., 1998; Mello and Ribeiro, 1998; Mello, 2002a, b) (Fig. 4A). In addition, song-driven *zenk* expression has been demonstrated in telencephalic auditory stations of a number of songbirds, as well as non-oscine species that do not sing (Mello et al., 1992; Mello and Ribeiro, 1998; Ribeiro et al., 1998; Jarvis and Mello, 2000; Jarvis et al., 2000; Gentner et al., 2001). Finally, *zenk* expression induced by song presentation was shown to be greatly suppressed in animals that were maintained in acoustic isolation overnight, as well as for animals that were deafened by cochlear lesioning (Mello et al., 1992; Mello and Ribeiro, 1998; reviewed in Mello, 2002a, b) (Fig. 4B).

Important functional properties of the songbird NCM have been ascertained by studying patterns of *zenk* expression in conjunction with various experimental auditory stimulation and behavioral paradigms. For example, many studies from the Mello group have shown that *zenk* induction is highest for conspecific, as opposed to

heterospecific or artificial stimuli (Mello et al., 1992; Mello and Clayton, 1994; Mello et al., 1995; reviewed in Mello, 2002b). This observation is in agreement with electrophysiological reports that demonstrated that NCM units exhibit preference for conspecific auditory stimuli, as compared to non-species specific stimuli (Chew et al., 1996).

Induction of *zenk* has also been useful to demonstrate the tonotopic organization of the canary NCM (Ribeiro et al., 1998). In this species, stimulation with low frequency conspecific syllables activated clusters of cells that were located in the dorsal NCM, while high frequency syllables activated a population of neurons that was represented in the ventral aspect of this nucleus (Fig. 5). The activation patterns of NCM that result from stimulation with particular frequencies of the canary song differed significantly from that revealed in animals that were stimulated with computer-generated frequencies, that displayed the same amplitude envelope of the normal song syllables, or same frequency guitar notes (Ribeiro et al., 1998) (Fig. 6). These findings suggest that the tonotopic activation of NCM cells relies not only on frequency information, but also on fine acoustic features contained in the conspecific syllable stimulus, that are not present in artificial stimuli.

Activation patterns and properties of song-control nuclei have also been revealed by *zenk* expression. For example, this methodology has been used to reveal singing-induced activity across the anterior forebrain pathway (Jarvis and Nottebohm, 1997). In addition, context-dependent *zenk* expression has been shown in area X, whereby undirected singing (male to male) triggers a robust *zenk* induction in this song control nucleus, whereas directed singing (male to female) does not evoke a

detectable gene expression (Jarvis et al., 1998) (Fig. 7). Together, these data attest to the usefulness of *zenk* activity maps to reveal the distribution of patterns of activity that result from sensory or motor experience across large neuronal ensembles in the songbird brain.

Finally, *zenk* expression appears to correlate with song learning in auditory stations. Bolhuis and colleagues have demonstrated increased numbers of ZENK-expressing cells in the NCM of adult animals that exhibited a higher degree of incorporation of tutor song syllables within their own songs (Bolhuis et al., 2000). These data have been interpreted to suggest that the number of ZENK-positive cells in NCM correlates strongly and positively with the number of syllables that were copied from the tutor songs. To date, no experiments have directly tested the specific role of *zenk* in song-learning or maintenance in songbirds, however, some of these issues are discussed further in Chapter 6.

### **GABA and Inhibition in Birdsong Auditory Processing**

My interest in characterizing inhibitory function and the GABAergic system in songbirds motivated my move to Portland. In the year before my acceptance at OHSU I was involved in a project that explored the contributions of disinhibition to a cognitive process named, “perceptual filling-in” and to attentional processing in the primate visual system with Peter De Weerd, at the University of Arizona. While researching these subjects I was exposed to primary literature that significantly changed my view of the role of GABAergic transmission in sensory processing. These papers made it clear to me that GABAergic transmission did much more than

to set action potentiation thresholds or contain the lateral spread of excitation across sensory-driven networks. I learned that GABA also plays significant roles in regulating and/or generating receptive field (RF) properties, as well as some forms of experience-dependent plasticity for sensory systems of various modalities, including the visual and auditory systems. There was, in my view, a perfect fit between my research interests in GABAergic transmission and a void within the songbird field regarding a systematic characterization of the anatomical organization and functional roles of GABAergic circuits in auditory stations, in particular, in nucleus NCM. In reference to the GABAergic system, very few studies had addressed its contribution to the physiology of some song control nuclei, including nucleus RA (Spiro et al., 1999), while no studies had been conducted within the auditory system of any songbird species. This completely open niche was both attractive and intimidating. Attractive in the sense that any naïve curiosity was novel and necessary to further our understanding on the organization of NCM, and intimidating given that my work could not be assembled and extended on top of any previous work, thereby increasing the likelihood that I would march on a potentially meaningful path. After some inner searching, I became convinced that a combination of attractiveness and intimidation was just the perfect recipe for a doctoral work!

In the following paragraphs I will provide a brief background that details some generalities of the GABAergic system with an emphasis on those studies that are most relevant to discuss the results obtained in this thesis. Finally, I will outline some of the general questions tackled in this thesis in hopes to foreshadow the topics that will be addressed in subsequent chapters.

## **GABA Neurotransmission**

GABA is the principal inhibitory neurotransmitter in the CNS. Neurons that release GABA were once believed to act on the cortex in a broad fashion commonly described as inhibitory tone. In general terms, inhibitory tone can be thought of as a cortex-wide mechanism for lowering the gain on all on-going activity without strong temporal or spatial relationships to processing. Subsequently, it was reported that cells in a number of mammalian sensory systems exhibit spatially overlapping excitatory RFs, as well as inhibitory RFs that compete for functional expression in response to an adequate sensory stimulus (Benevento et al., 1972; Blakemore and Tobin, 1972; Creutzfeldt et al., 1974; Chen and Jen, 2000; Tremere et al., 2001a). More contemporary views of GABAergic transmission are that these inhibitory mechanisms are activated in parallel with excitation as part of sensory processing. Furthermore, balances of inhibition and excitation may be critical in determining if a cell moves towards a state of heightened plasticity or becomes more functionally rigid (reviewed in Tremere et al., 2003).

GABAergic neurons represent between 25-30% of the overall neuronal population in sensory cortices (Jones, 1993). Horizontally, the distribution of GABAergic neurons appears to be uniform within the same sensory areas, as defined by cytoarchitectonic features. There is, however, considerable variation in the proportion of GABAergic neurons when comparisons are made for cortical layers. Highest density of GABAergic cells appear to be found in layers II/III (supragranular layers), as well as the thalamo-recipient layer IV (Peters and Jones, 1984; Gabbott

and Somogyi, 1986; Akhtar and Land, 1991; Doetsch et al., 1993; Jones, 1993; Prieto et al., 1994a, b; Tremere et al., 2003). Conversely, significantly smaller numbers of GABAergic neurons are found in the infragranular layers of the mammalian sensory cortices (Peters and Jones, 1984; Gabbott and Somogyi, 1986; Hendry et al., 1987; Hendry et al., 1990; Akhtar and Land, 1991; Doetsch et al., 1993; Prieto et al., 1994a, b). This differential distribution of GABAergic neurons in the vertical organization of the mammalian cortex has been suggested to be important in defining the response range for individual cells during sensory stimulation.

### **GABAergic Receptors**

The effects of GABA are mediated by three classes of GABA receptors: the GABA-A, GABA-B and GABA-C receptors. GABA-A is the dominant and by far most studied class of receptor expressed in the vertebrate CNS. It has been proposed that GABA-A receptors are typically composed of 5 subunits (heteropentameric) of four different subunit families: alpha, beta, gamma, and delta (Macdonald and Olsen, 1994; Luddens et al., 1995). The most commonly reported assembly for GABA-A receptors is 2 alpha subunits, 1 beta and 2 gamma subunits (Barnard, 1995). GABA-A mediated transmission has been shown to constitute the principal source of fast acting cortical inhibition in the vertebrate brain (Krnjevic, 1984; Hendry et al., 1990; Jones, 1993; Macdonald and Olsen, 1994). Binding of GABA at GABA-A receptors immediately enables an inward chloride conductance that hyperpolarizes the post-synaptic cell, removing it farther from the threshold of action potential firing (Macdonald and Olsen, 1994).

The second type of GABAergic receptor is the metabotropic GABA-B receptor, which is less prevalent in mammalian sensory cortices and often located anatomically within the terminals of the thalamic afferents (Princivalle et al., 2000; Munoz et al., 2001). The kinetics of this receptor is slower as compared to GABA-A and GABA-C receptors given that they are a G-protein-coupled receptor (Mody et al., 1994). Pre-synaptically, the main action of GABA-B is to inhibit high voltage-gated calcium channel activity, which in turn decreases synaptic neurotransmitter release. Activation of GABA-B receptors post-synaptically has been shown to increase an inwardly rectifying potassium conductance, via Kir3 channels, which leads to membrane hyperpolarization. In addition, receptor activation post-synaptically has been shown to inhibit adenylate cyclase, thus decreasing cAMP levels (Gahwiler and Brown, 1985; Misgeld et al., 1995; Luscher et al., 1997; Jones et al., 1998; Kaupmann et al., 1998; White et al., 1998; Kuner et al., 1999).

The third type of receptor, GABA-C, shares many features with the GABA-A receptors. For example, it is a ligand-gated ionotropic receptor that allows for a chloride conductance upon activation (Qian et al., 2005). GABA-C receptors differ from GABA-A receptors by the presence of rho subunits in their structures; the earliest reports on this receptor resulted from experiments conducted in the retina, however, it is still a question of debate whether brain GABA-C receptors are homomeric and whether their molecular composition in cortical structures is identical to those found in the retina (for review see Zhang et al., 2001).



## **Sources of GABAergic Input**

In the mammalian, and possibly in the vertebrate CNS, there are two main sources of GABAergic input to sensory cortices. The majority of cortical GABAergic synapses belong to local inhibitory interneurons of which there are several morphologically classified types (Jones, 1993). GABAergic cells can also be further sub-divided based on their expression of the calcium-binding proteins calbindin, parvalbumin and calretinin. These calcium-binding proteins are expressed, with very few exceptions, in non-overlapping populations of GABAergic cells, and together they account for virtually all GABAergic cells within the CNS (Hendry and Jones, 1991; Rogers, 1992; Jones, 1993; Markram et al., 2004). Certain GABAergic cells also co-express a number of peptides such as neuropeptide Y, cholecystokinin and vasoactive intestinal polypeptide (Hogan et al., 1992; Bubser et al., 1998; Gonzalez-Albo et al., 2001; Markram et al., 2004). GABAergic neurons and their relative positions in the main sensory cortices have been described in detail in many previous works and will not be discussed further here, mainly because there appears to be significant differences across sensory systems and across species (Somogyi et al., 1981; Fairen et al., 1984; Jones, 1993). However, as briefly mentioned above, an apparently consistent property of the GABAergic system is that the greatest numbers of cells per unit area are located within supragranular layers and layer IV (Peters and Jones, 1984; Gabbott and Somogyi, 1986; Akhtar and Land, 1991; Doetsch et al., 1993; Jones, 1993; Prieto et al., 1994a, b). The conservation of this general organizational scheme across sensory modalities suggests that inhibitory mechanisms

are a central part of sensory processing, particularly in computations occurring at the thalamo-recipient and intra- and inter-cortical levels.

A second source of GABAergic inputs to sensory cortical neurons are inhibitory projection neurons from the basal forebrain (Freund and Meskenaite, 1992; Gritti et al., 1993; Gritti et al., 2003). The basal forebrain region contains two populations of projection neurons: cholinergic and GABAergic cells, with some neurons expressing both neurotransmitters (Freund and Meskenaite, 1992). The basal forebrain has been repeatedly involved in a wide variety of arousal, attention and learning related paradigms, which have direct implications for the experience-dependent regulation of RF size and sensory processing.

Interestingly, it has been shown that over 25% of the population of inhibitory projection neurons synapses with local inhibitory interneurons in cortical areas. These target cells have been extensively characterized by immunocytochemical approaches directed against calcium binding proteins and specific peptides. Somatostatin- and parvalbumin-positive non-pyramidal cells have been shown to constitute the major targets of the GABAergic forebrain with few, if any, contacts with neuropeptide Y, calbindin or cholecystokinin immunoreactive cells (Freund and Meskenaite, 1992; Hicks et al., 1993). These findings indicate that inhibitory projection neurons from the basal forebrain may participate in disinhibitory effects in sensory cortices, which have been proposed to mediate some forms of plasticity in the visual and auditory systems, for example, neural interpolation and reorganization of auditory spatial maps, respectively (Zheng and Knudsen, 1999; Tremere et al., 2001b; Zheng and Knudsen, 2001; Tremere et al., 2003; De Weerd et al., 2005).

## **Roles of GABAergic Transmission in Sensory Processing**

The roles of GABA in sensory processing have been investigated in the visual and somatosensory systems and, to a lesser extent, in the auditory system. In order to remain within the scope of this thesis, I will not extensively review these findings, and instead, will briefly describe the main findings of key experiments.

One technique that has been used extensively to identify contributions of inhibitory inputs onto cortical neurons is microiontophoresis. Given that the dominant receptor sub-type of GABA in sensory cortices is the GABA-A, the majority of studies have characterized roles for GABA at primary sensory cells with bicuculline methiodide (BMI), a competitive antagonist for this receptor (Macdonald and Olsen, 1994). The effects of pharmacological antagonism of the GABA-A receptor have also been explored to a lesser degree using another, less specific, GABA-receptor antagonist, picrotoxin (PTX).

### a) GABA Regulation of RFs in the Somatosensory Cortex

In the somatosensory cortex, experiments that aimed at investigating the roles of GABA in sensory processing were primarily conducted in cats, raccoons and monkeys. Batuev and colleagues provided the first evidence that the functional organization of cutaneous RFs could be influenced by antagonism of GABA-A receptors (Batuev et al., 1982). These authors described that RF area of primary somatosensory cortical (S1) neurons was significantly increased upon local microiontophoretic application of PTX in cats (Batuev et al., 1982). Subsequent

studies conducted in the cat, raccoon and monkey S1 reported similar findings whereby blockade of normal GABAergic transmission led to marked expansions of RF area and decreased threshold for mechanical activation (Hicks and Dykes, 1983; Dykes et al., 1984; Alloway and Burton, 1986; Alloway et al., 1989; Alloway and Burton, 1991; Tremere et al., 2001a; Chowdhury and Rasmusson, 2003) (Fig. 8A). A second important finding in these studies was that BMI application not only simultaneously expanded RFs but, on some occasions, exposed previously masked, separate RFs (Hicks and Dykes, 1983; Dykes et al., 1984; Tremere et al., 2001b). Importantly, microiontophoretic application of both glutamate and BMI exhibited comparable effects of lowering the threshold to cutaneous stimulation for most neurons. However, glutamate did not trigger RF expansions at any cells recorded, indicating that the effects reported could not be explained through a simple reduction in the spiking threshold, but rather through a specific action of GABA on GABA-A receptors in cortical neurons. These findings provide clear evidence that intracortical GABAergic transmission plays a pivotal role in carving the full extent of the anatomical connectivity of any given S1 RF into a functionally expressed RF.

#### b) GABA Regulation of RFs in the Visual Cortex

The possibility that inhibitory mechanisms could be responsible for features of RFs of visual cortical neurons was first raised by Hubel and Wiesel (Hubel and Wiesel, 1962). This line of questioning was pursued more aggressively by Adam Sillito and colleagues, as well as other groups, starting in the early 1970's. In the following paragraphs I describe the main results of these experiments that detail the

role of intra-cortical GABAergic transmission in regulating RF properties in primary visual cortical (V1) neurons.

Local iontophoretic application of BMI prevented the action of GABA at primary visual cortical neurons in the cat. Similarly to the findings discussed above for the somatosensory cortex, this effect was demonstrated to be qualitatively different from that of increasing cell excitability with glutamate application (Sillito, 1975a, b), indicating that the effects of GABA do not merely reflect enhanced neuronal activity. Experiments that aimed at describing the roles of GABA in shaping RF properties in V1 neurons were focused in two functional classifications of cortical neurons in V1: simple and complex cells. Simple cells often exhibit small RFs with clear “on” and “off” domains, low baseline activity and sharp orientation preference. Conversely, complex cells are characterized by broader orientation preference curves, high baseline activity and the absence (in most cases) of clearly defined “on” and “off” RF domains (Hubel and Wiesel, 1962, 1968).

Intra-cortical microiontophoretic application of BMI markedly altered firing behavior of V1 simple cells. For example, under blockade of GABAergic transmission, simple cells in V1 tended to fire robustly at the onset and at the offset of stimulus presentation, but not during the interval between (thus classified as on-off responses), regardless of whether the stimulus was placed on the originally “on” or “off” subfields, or covered the full extent of the RF (Sillito, 1975b).

Antagonism of GABA-A receptors by local BMI treatment was also shown to significantly expand RF area in V1 neurons, suggesting that GABAergic transmission

contributes to the functional pruning of anatomical connections leaving only a subset of inputs expressed (Ramoal et al., 1988; Eysel et al., 1998).

The contributions of GABAergic transmission to orientation and directional selectivity in simple cells were also tested. As indicated above, simple cells exhibit sharp orientation and direction preferences. Blockade of GABA-A receptors by microiontophoretic application of BMI affected both properties (Fig. 8B). Orientation selectivity tended to become much broader, as compared to the pre-BMI conditions (Sillito, 1975b). Similar results were obtained by BMI delivery through micro-osmotic pumps (Ramoal et al., 1988). In some infrequent cases, under BMI treatment, responses could be obtained with stimuli oriented  $90^\circ$  from the originally optimal orientation (pre-BMI), although responses would significantly decrease after  $22.5^\circ$  (Sillito, 1975b). Likewise, directional selectivity was completely abolished during BMI application (Sillito, 1975b). Both directional and orientation selectivity were recovered once BMI infusion was stopped; cells tended, however, to exhibit decreased responsiveness for approximately half-hour after pharmacological treatment was interrupted.

BMI application also significantly affected RF properties in V1 complex cells. For example, orientation specificity was significantly decreased upon BMI treatment (Sillito, 1975b). In contrast to what was observed with simple cells, robust responses from complex cells were easily detectable at large angles (including  $90^\circ$ ) away from the preferred orientation. Interestingly, BMI treatment in this cell type rarely altered directional preference (Sillito, 1975b). Finally, as was observed for simple cells, recovery from BMI treatment was often accompanied by an overall decrease in

excitability in complex cells. In addition, application of glutamate failed to trigger the same modifications in RF properties, suggesting that enhanced excitability does not account for the results observed (Sillito, 1975b).

These findings provide clear evidence that normal GABAergic transmission regulates the expression of functional RFs (as opposed to anatomical RFs) and suggest that orientation selectivity at both simple and complex cells results from intra-cortical GABAergic transmission. In simple cells, normal GABAergic transmission might also play a role in the generation of stimulus directional preference.

#### c) GABA Regulation of RFs in the Auditory Cortex

Few experiments have investigated the role of GABA in auditory processing at the level of the primary auditory cortex (A1). Most studies have focused on lower order auditory stations such as the inferior colliculus and the medial geniculate nucleus. Given that the findings obtained in these subcortical stations will be discussed to some extent in the discussion section of most subsequent chapters, I will focus here on the few studies that have addressed the contributions of GABAergic transmission to the regulation of RF properties at the level of the A1.

Microiontophoretic application of GABA significantly affected the physiology of A1 neurons of the rat. GABA actions on these cortical neurons were three-fold. As expected, GABA decreased pure-tone evoked responses as well as spontaneous discharge rates. In addition, enhanced inhibitory action by GABA application led to a significant increase in the signal-to-noise ratio of the responses.

Finally, GABA tended to augment and sharpen frequency specificity, as compared to pre-GABA conditions (Manunta and Edeline, 1997). Recordings obtained from A1 of the big brown bat, *Eptesicus fuscus*, showed that iontophoretic application of BMI tended to decrease the spiking threshold and to decrease the signal-to-noise ratio of sound-evoked responses. In addition, stereotypical responses (1-2 or 3-7 spikes/stimulus) appeared to be facilitated by blockade of normal GABAergic transmission. In these experiments, BMI application also triggered significant frequency tuning curve expansions (Chen and Jen, 2000) (Fig. 8C). Similar results, particularly those relating to marked expansions of frequency tuning curves under BMI treatment, were also obtained in the cat and the chinchilla A1 (Schreiner and Mendelson, 1990; Ehret and Schreiner, 1997; Wang et al., 2000). Frequency tuning for units in the A1 of the cat normally appear to be sharper in supragranular layers and the thalamo-recipient layer IV (Schreiner and Mendelson, 1990; Ehret and Schreiner, 1997). Interestingly, it is these layers that show the highest densities of GABAergic neurons in sensory cortices (Gabbott and Somogyi, 1986; Jones, 1993). Thus, it appears that normal GABAergic transmission plays a role in enhancing the signal-to-noise ratio and narrowing frequency preference, thereby possibly increasing frequency discrimination, of neurons in the mammalian A1.

### **GABAergic Transmission and Auditory Processing in the Zebra Finch: Thesis Goals**

The findings discussed in the previous sections provide clear evidence that GABAergic mechanisms control not only the overall excitability of cortical circuits



but provide dynamic regulation of RF properties for cortical neurons from a variety of sensory systems in the mammalian CNS.

With respect to the auditory system, GABA has been reported to fine-tune auditory responses, putatively enhancing sound discrimination. Given that song learning and maintenance requires normal auditory processing, and since GABA regulates RF properties in the auditory system, I chose to study the GABAergic system in the zebra finch auditory system, with a particular focus in NCM, a telencephalic region that is analogous, if not homologous, to the mammalian A1 (Vates et al., 1996; Mello et al., 1998). As stated above, no studies to date have tackled the role of inhibition in birdsong auditory processing. Thus, the goals of this thesis included the following:

- 1) To provide a thorough anatomical description of the distribution of GABAergic neurons throughout the ascending auditory pathway of the adult zebra finch.
- 2) To investigate whether GABAergic neurons in NCM are directly activated by birdsong auditory stimulation.
- 3) To study the role of GABAergic inhibition in the physiology of NCM in awake animals during auditory processing.

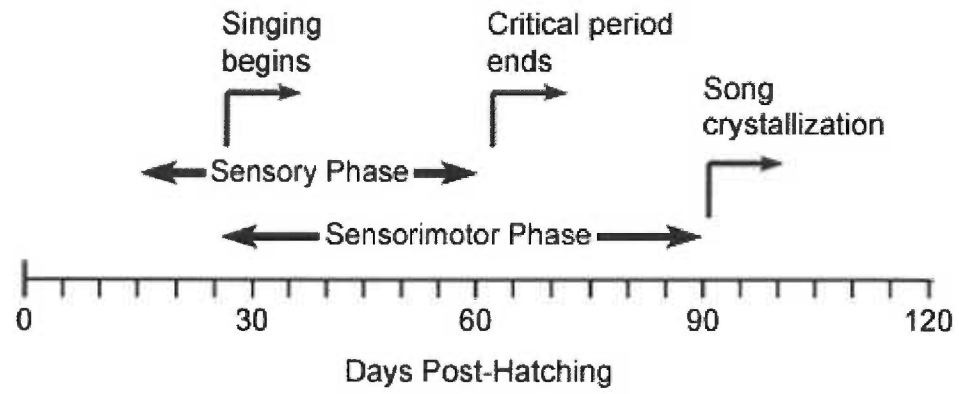
The subsequent chapters address these general questions and expand upon them. Chapter 2 provides an anatomical characterization of the distribution of GABAergic neurons through the ascending auditory pathway and song control nuclei of the zebra finch. Chapter 3 presents molecular biological evidence for the direct

participation of GABAergic neurons in the response of the caudomedial auditory lobe to song. This chapter also provides initial electrophysiological evidence for the role of GABA in the regulation of neuronal excitability in the zebra finch NCM. Chapter 4 further characterizes the contributions of GABAergic transmission to the regulation of excitability in NCM and provides electrophysiological evidence for a direct role of GABA in regulating the temporal dynamics of song- and tone-evoked responses in wake animals. Chapter 5 describes a further characterization on the neurochemical identity of inhibitory neurons in NCM. In this chapter, I discuss how an antibody that identifies the calcium-binding protein calbindin was used to localize a subpopulation of GABAergic neurons within this auditory area. The results reveal a sexual dimorphism in the calbindin-positive neuronal population in NCM, with males exhibiting twice as many cells as compared to females. Finally, in Chapter 6, it is my hope to integrate the data obtained in this thesis, as well as to further discuss key issues not addressed in the preceding chapters.

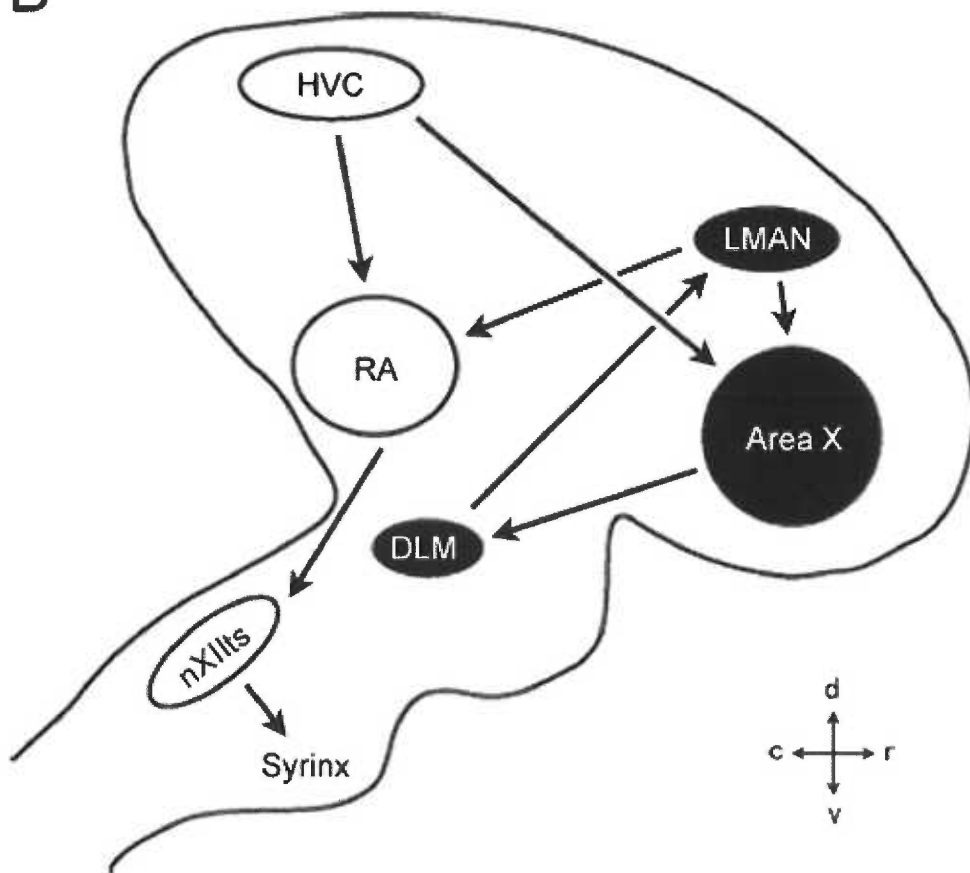
**Figure 1.1) Song learning and the song control system.**

(A) Schematic representation of the time frame and stages of song learning in zebra finches. In the early stages of the sensory phase, young birds acquire a memory of the tutor song; this memory will be used as a template during the sensorimotor phase, when young birds will use auditory feedback to correct and shape their own vocalizations. At the end of the sensorimotor phase the song “crystallizes” and will not change, under normal conditions, throughout the animal’s life. (B) Schematic drawing of a parasagittal section through the brain of a male zebra finch detailing the main connections of the song control system. Nuclei of the anterior forebrain pathway (AFP) are represented in black while nuclei that participate in the posterior forebrain pathway (PFP) are depicted in white. Projections from both AFP and PFP are originated in nucleus HVC. The AFP encompasses the following projections: HVC→area X→DLM→LMAN→RA and LMAN→area X. The PFP is composed by projections from HVC→RA→nXIIIts (see text for details and abbreviations).

A



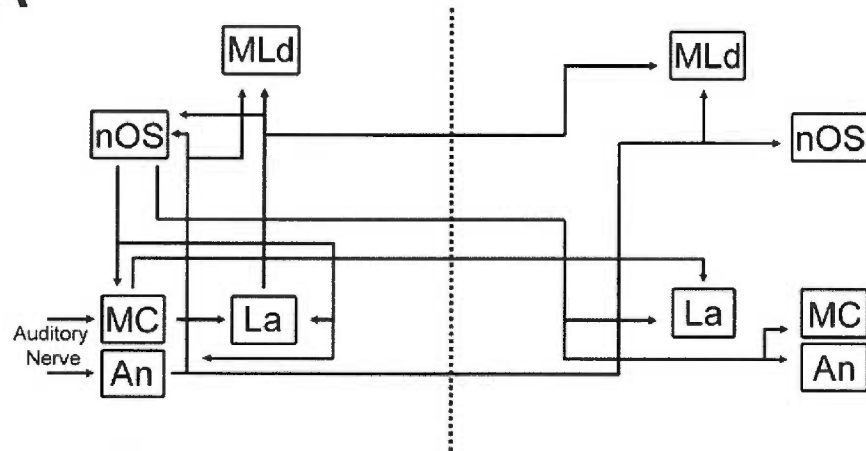
B



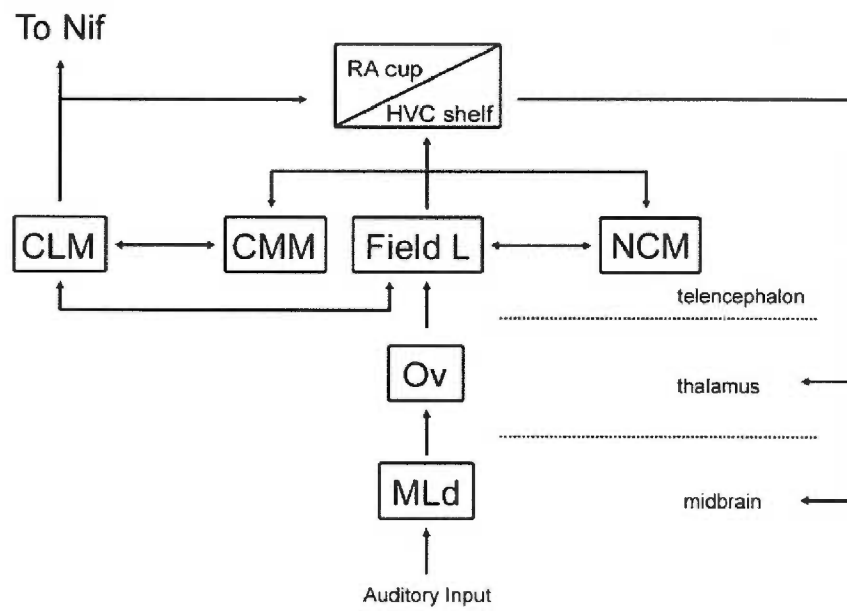
**Figure 1.2) The ascending and descending auditory pathways of songbirds. (A)**

Diagram of the main nuclei and connections of the auditory pathway, up to the midbrain. Dotted line represents the midline. This diagram is mostly based on work conducted in non-oscine species like chicks and the barn owl (Parks and Rubel, 1975; Rubel and Parks, 1975; Parks and Rubel, 1978; Takahashi and Konishi, 1988; Lachica et al., 1994; Levin et al., 1997). (B) Diagram of the auditory pathway from the midbrain to the telencephalon, intratelencephalic, and descending projections. For clarity, only the main nuclei and projections are shown in the diagrams, and only unilateral projections. This diagram is supported by data obtained in zebra finches and canaries, as well as non-oscine species like the pigeon, chicks and budgerigars (Karten, 1967, 1968; Parks and Rubel, 1975, 1978; Brauth et al., 1987).

A



B



**Figure 1.3) Main biochemical pathways involved in zenk expression integrate alterations in the cell membrane with the nuclear transcriptional machinery.**

Calcium influx either through NMDA receptor activation or via VSCC activates the MAPK/ERK pathway (left of schematics). Calcium activates Ras by recruiting specific GEFs (not pictured), which exchange GDP for GTP. This process triggers a kinase cascade. Ras-GTP recruits a kinase known as Raf. Activated Raf phosphorylates MEK, which phosphorylates, ERK. Phosphorylated ERK dimerizes and migrates to the nucleus where it will impact gene expression (below). Rises in cAMP through CaM modulation onto AC enhance kinase activity of PKA. PKA can phosphorylate RAP-1, which converges to the MAPK/ERK pathway by phosphorylating Raf. PKA can also directly impact transcriptional regulation by phosphorylating specific transcription factors, such as CREB.  $\text{Ca}^{2+}$ /CaM can also impact target proteins, such as CaMKII (right of schematics). Upon calcium-driven activation, CaMKII autophosphorylates and dissociates from actin filaments; it can then impact its target proteins, such as PSD 95. CaMKII might also contribute to phosphorylation of specific transcription factors, therefore directly influencing gene expression programs. These pathways integrate modifications in the cell surface to the cell's genome. Of particular interest to this thesis is the convergence of these biochemical pathways onto phosphorylation of the transcription factor CREB, which appears to integrate the activity of a population of inducible genes that contain the CRE element in their promoters (detailed in B). Abbreviations:  $\text{Ca}^{2+}$ , calcium; AC, adenylyl cyclase; ATP, adenosine triphosphate; cAMP, cyclic adenosine monophosphate;  $\text{Ca}^{2+}$ /CaM, calcium/calmodulin protein complex; CaM, calmodulin;

PKA, cAMP-dependent protein kinase; NMDA, N-methyl-D-aspartate; VSCC, voltage-sensitive calcium channel; CaMKII, calcium/calmodulin-dependent protein kinase II; PSD95, 95 KDa post-synaptic density protein; GEF, guanine nucleotide exchange factors; GTP, guanine triphosphate; GDP, guanine diphosphate; Raf, Raf proto-oncogene serine/threonine protein kinase; MAPK, mitogen-activated protein kinase; ERK, extracellular signal-regulated kinase; MEK, MAPK/ERK kinase; RAP-1, Ras-related protein 1; CREB, cAMP responsive element binding protein; CRE, cAMP responsive element.

(B) Several kinase pathways putatively regulate *zenk* expression and converge to CREB phosphorylation, which appears to play a critical role in *zenk* induction. A number of kinases, including ERK and PKA are able to phosphorylate CREB at Ser133. At resting conditions, CREB is bound to the CRE. Upon its phosphorylation, CBP is recruited and the transcriptional machinery is activated thereby initiating the expression of genes that exhibit the CRE in their promoters. Among these genes are a number of IEGs, including *zenk*. *zenk* gene expression triggers the synthesis of a specific transcript that is transported to the cytoplasm where translation takes place. Zenk protein, a transcription factor, is then transported back to the nucleus where it will participate in the regulation of late gene expression. Abbreviations: ERK, extracellular signal-regulated kinase; PKA, cAMP-dependent protein kinase; CaMKII, calcium/calmodulin-dependent protein kinase II; CREB, cAMP responsive element binding protein; CRE, cAMP responsive element; CBP, CREB binding protein; IEG, immediate early gene; LG, late gene; mRNA, messenger ribonucleic acid; S133, serine 133.



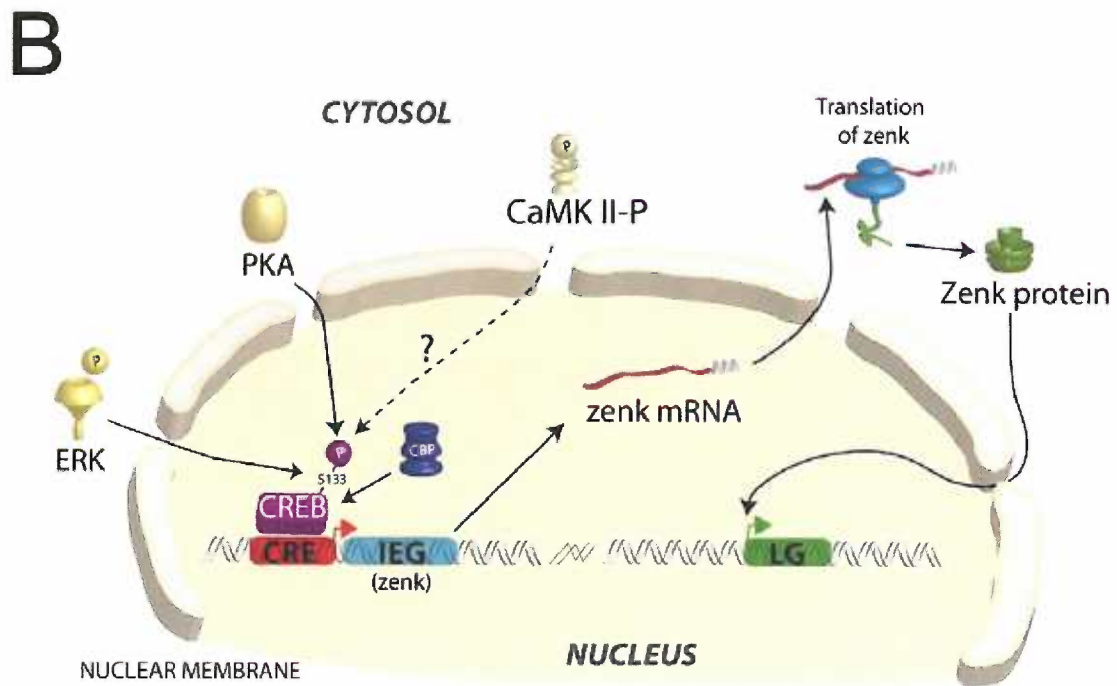
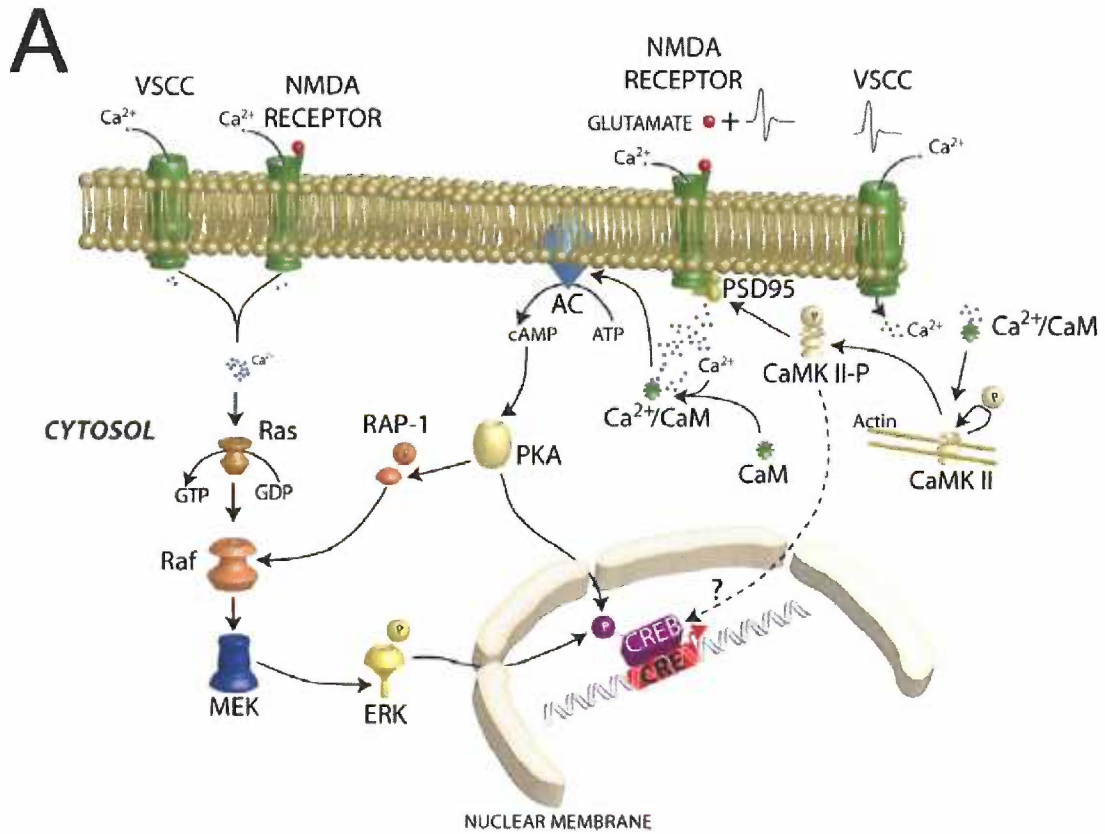


**Figure 1.4) Song-stimulation drives the *zenk* expression in NCM.** A brief episode of song stimulation (1 hr; song-stimulated) triggers a robust induction of Zenk protein in the zebra finch and canary NCM, while overnight acoustic isolation (silence) significantly reduces protein levels of this gene. (A and B) Immunocytochemical detection of Zenk-positive nuclei in a medial section through the NCM of song-stimulated (A) and isolated (B) zebra finches. (C and D) Density maps generated from raw immunocytochemical data depicting Zenk expression in a more lateral NCM level for both song-stimulated (C) and control (D) canaries. Hot colors indicate higher densities of Zenk-positive cells while cool colors represent lower densities of Zenk immunolabeled neurons. Figures A and B modified from (Mello and Ribeiro, 1998); Figures C and D modified from (Ribeiro et al., 1998).

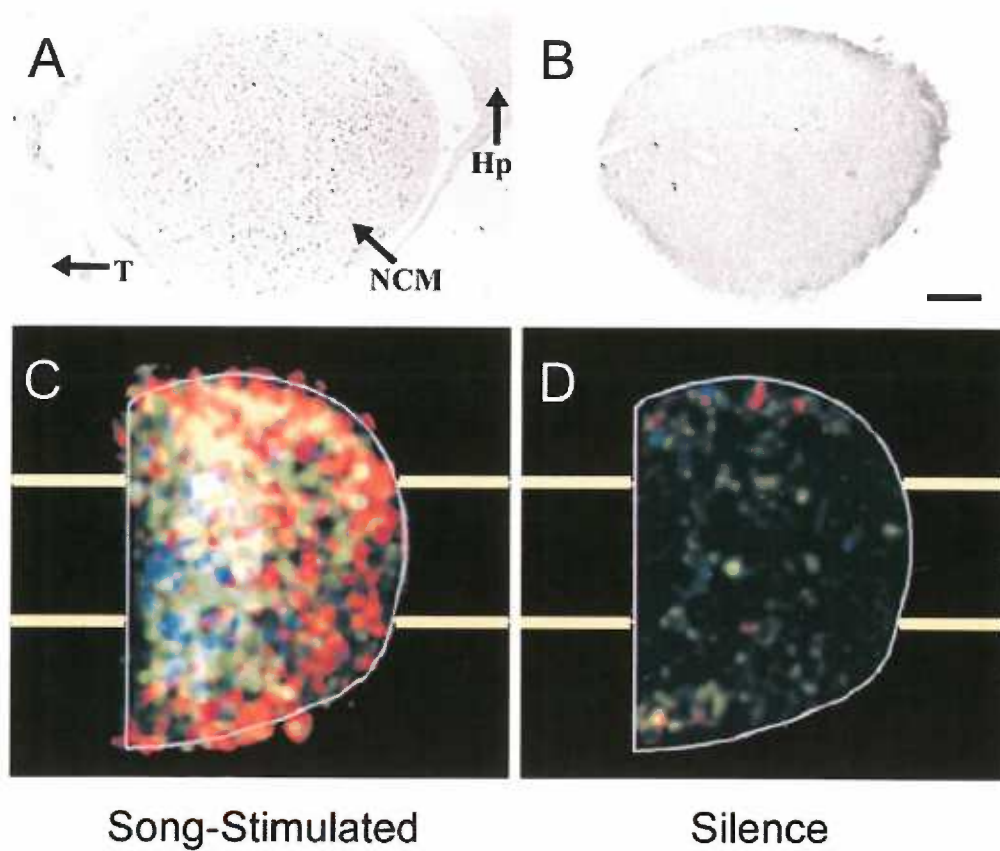


**Figure 1.5) Whistle-induced Zenk expression reveals the tonotopic organization of the canary NCM.** Pure tone-like canary song syllables were used to stimulate adult canaries. Sonograms of the stimuli used are represented on the top of each map. Density maps obtained from the raw immunocytochemical data for Zenk protein revealed that syllables of low frequencies preferentially activated cells clusters in dorsal NCM; increasingly higher frequencies tended to activate neuronal populations at levels that shifted towards more ventral domains within NCM. Modified from (Ribeiro et al., 1998).

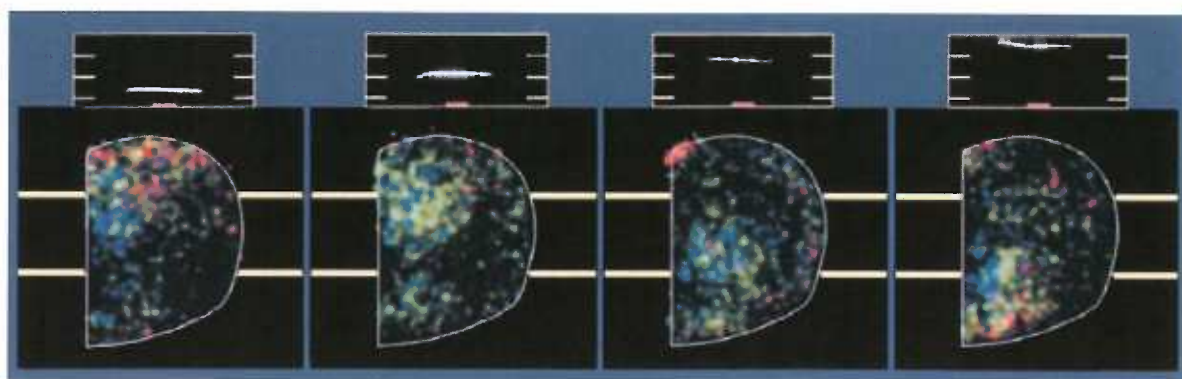


**Figure 1.6) Neuronal ensemble activation in NCM of the canary does not strictly depend on stimulus frequency.** Clusters of Zenk-positive cells are clearly defined when animals are stimulated with natural whistles (top panels). Synthetic whistles (middle panels) and guitar notes (bottom panels) of the same frequencies generate a different, more widespread, activation of neurons in the canary NCM. Modified from (Ribeiro et al., 1998).

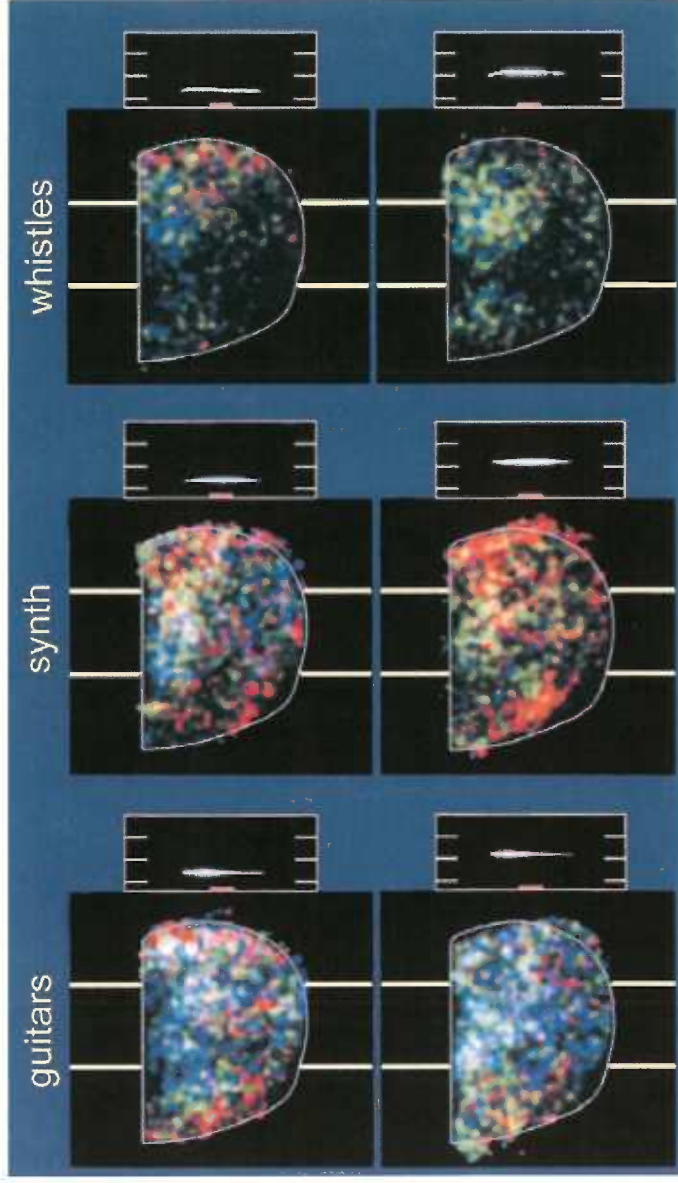
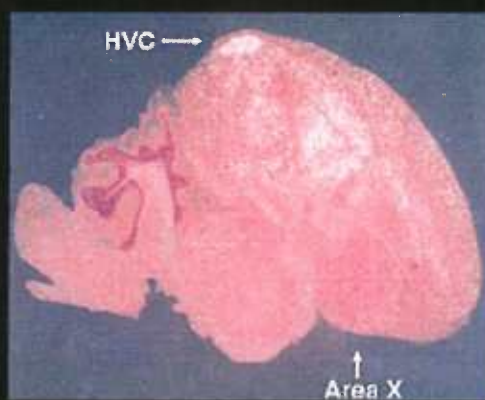


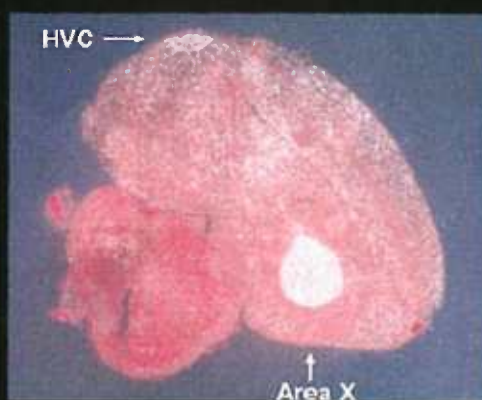
**Figure 1.7) *zenk* expression reveals context-dependent singing-induced activation of area X in male zebra finches.** In-situ hybridization targeting *zenk* mRNA reveals that directed singing (male to female; left column) does not involve the activation of song nucleus area X. Conversely, undirected singing (male to male, or solo context; right column) triggers a robust induction of *zenk*, and consequently neuronal activation in area X. Modified from (Jarvis et al., 1998).



**FEMALE CONTEXT**



**MALE CONTEXT**



**female-directed singing**

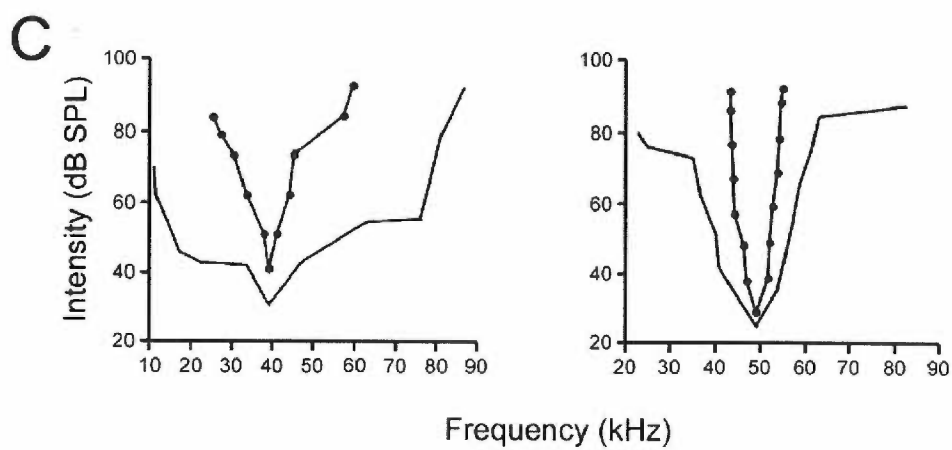
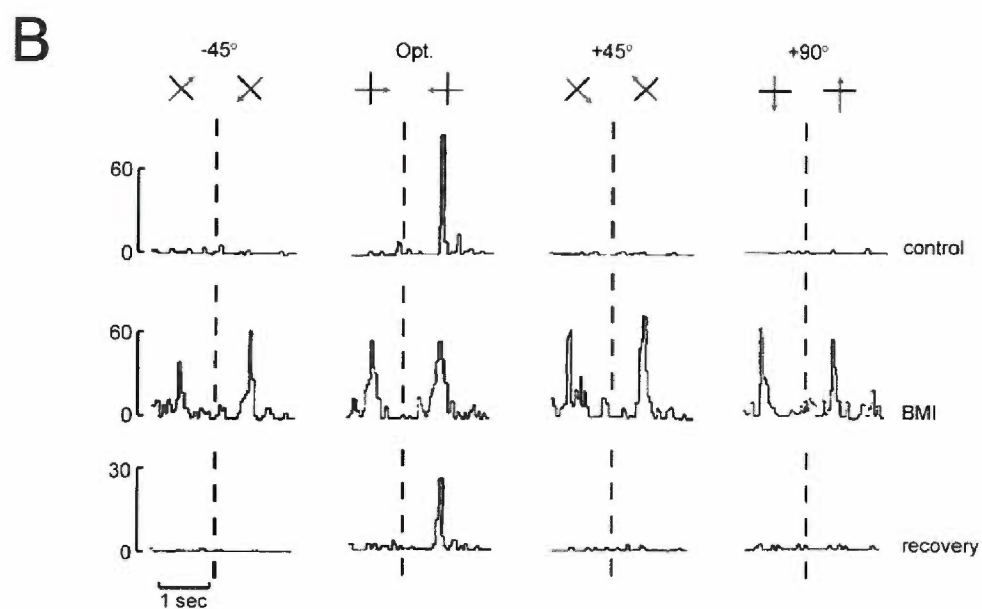
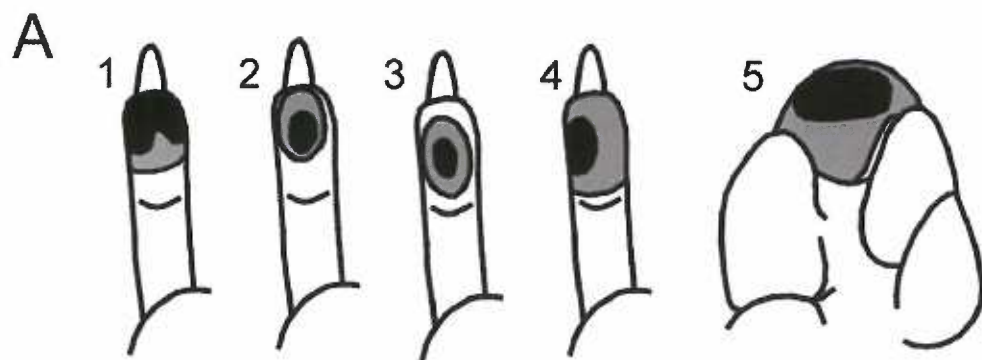


**undirected singing**

**Figure 1.8) GABAergic transmission regulates receptive field (RF) properties in a number of sensory systems of the vertebrate brain.** (A) In the primary somatosensory cortex (S1) of the raccoon, the area of cutaneous RFs (black area) are significantly expanded by local blockade of GABA-A receptors with selective antagonist bicuculline methiodide (BMI; grey area). 1-4 are representative RFs recorded from the fourth digit representation in the raccoon S1, while 5 shows BMI-induced expansion of RF in the palm representation.

(B) In the primary visual cortex (V1), simple cells exhibit direction and orientation preferences (top traces). Antagonism of GABA-A receptors by local infusion of BMI virtually abolishes directional and orientation selectivity (middle traces). Interruption of BMI infusion reinstates these properties within a few minutes (bottom traces)

(C) Frequency tuning curves of primary auditory cortical neurons in the big brown bat exhibit relatively sharp frequency tuning (lines and symbols). In these two representative examples, blockade of GABA-A receptors by local BMI iontophoresis triggers expansion of frequency tuning curves (solid lines). A, B and C modified from (Sillito et al., 1980; Chen and Jen, 2000; Tremere et al., 2001a)



## **CHAPTER 2**

### **GABA IMMUNOREACTIVITY IN AUDITORY AND SONG CONTROL BRAIN AREAS OF ZEBRA FINCHES**

## INTRODUCTION

Gamma-Aminobutyric acid (GABA) is the main inhibitory neurotransmitter in the vertebrate brain. GABA-mediated transmission has been implicated in the regulatory control of cellular properties such as the statistical likelihood of neuronal firing and of presynaptic neurotransmitter release (Chagnac-Amitai and Connors, 1989a, b; Morrisett et al., 1991; Isaacson et al., 1993; Scanziani et al., 1993; Thompson et al., 1993; Salin and Prince, 1996), as well as in complex network tasks such as the control of sensory receptive field properties (Sillito, 1977; Sillito and Versiani, 1977; Sillito, 1979; Bolz and Gilbert, 1986; Hata et al., 1988; Tremere et al., 2001a; Tremere et al., 2003) and experience-dependent modifications in cortical representation maps (Tremere et al., 2001b; Tremere et al., 2003). Thus, GABAergic transmission impacts the generation of appropriate neural codes required for CNS representations of sensory information about the environment, sensorimotor integration, and motor control programs (Bland and Oddie, 2001; Ziemann et al., 2001; Ramanathan et al., 2002; Werhahn et al., 2002). In most brain areas, GABAergic cells participate in local processing microcircuits, although long-range GABAergic projections have also been described in some systems (Ebner and Armstrong-James, 1990; Jones, 1993; Peruzzi et al., 1997; Luo and Perkel, 1999a, b; Bartlett et al., 2000; Sarter and Bruno, 2002).

We have been investigating the contribution of GABAergic transmission to central representations of vocal communication signals in songbirds. Songbirds are one of the few animals groups that evolved the ability to learn vocalizations based on

an auditory model (Marler et al., 1972; Marler and Waser, 1977). During the sensory acquisition phase of the song learning process, the juvenile hears and memorizes the adult song. During the sensorimotor phase, the bird changes its own vocalizations to match the acquired song template. Intact hearing is crucial for both phases: birds raised in acoustic isolation or deafened fail to develop normal song structure (Konishi, 1965a, b; for recent reviews see Zeigler and Marler, 2004), although some exceptions have been noted (Kroodsma et al., 1997; Leitner et al., 2002). Research in zebra finches and canaries have led to major insights into the neuronal basis of vocal learning, in large part because telencephalic areas involved in song auditory processing, production and learning have been identified and their connections mapped in detail (Nottebohm and Arnold, 1976; Nottebohm et al., 1976; Kelley and Nottebohm, 1979; Nottebohm and Arnold, 1979; Nottebohm et al., 1982; Bottjer et al., 1984; Scharff and Nottebohm, 1991; Vates et al., 1996; Mello et al., 1998). As occurs in other avian species and vertebrate groups, the ascending auditory pathway of songbirds is thought to consist of a series of pontine, mesencephalic and thalamic nuclei that convey auditory information from the cochlea to telencephalic centers, although the detailed connectivity of this pathway up to the midbrain has not yet been determined in songbirds (Fig. 1A and B). At the level of the telencephalon, several auditory areas are located within a prominent caudomedial bulge, or lobule (Vates et al., 1996; Mello et al., 1998). These areas include the primary auditory thalamo-recipient zone field L as well as major field L targets, namely the caudomedial nidopallium (NCM) and the caudomedial and caudolateral mesopallium (CMM and CLM, respectively; we use here the revised avian brain nomenclature, as detailed in

(Reiner et al., 2004). From field L and these primary targets, auditory inputs reach other telencephalic areas (Fig. 1B). Although the specific role of individual constituent nuclei or areas has not been clearly established, these central auditory pathways are thought to be crucial for song auditory processing, perception, and possibly the song memorization required for perceptual discrimination and vocal learning (for review, see Mello et al., 2004).

Songbirds also possess a set of interconnected forebrain nuclei known as the song control system that can be subdivided into two main pathways (Fig. 1C). The direct motor pathway is essential for the production of learned vocalizations and includes nidopallial nucleus HVC, the robust nucleus of the arcopallium (RA), and the descending projections of the latter onto the dorsomedial nucleus of the intercollicular complex (DM), the tracheosyringeal component of the hypoglossal nerve (nXIIts), which innervates muscles from the vocal organ (syrinx), and medullary respiratory control centers. The anterior forebrain pathway is essential for song learning and consists of area X of the medial striatum, the dorsal mediolateral nucleus of the thalamus (DLM), and the lateral magnocellular nucleus of the anterior nidopallium (LMAN), which are connected in a circuit organization analogous to mammalian cortico-basal ganglia-thalamo-cortical loops (Nottebohm et al., 1976; Nottebohm et al., 1982; Bottjer et al., 1989; for recent reviews, see Zeigler and Marler, 2004).

GABAergic transmission has been implicated in the physiology of areas involved in both auditory and motor processing of vocalizations in songbirds. For example, GABA antagonism affects synchronized firing within song control nucleus

RA and spike properties of projection neurons in nucleus LMAN (Bottjer et al., 1998; Spiro et al., 1999). We have recently used molecular and electrophysiological methods to show that GABAergic cells and synapses are prevalent in telencephalic auditory areas, and that GABAergic neurons induce the expression of the activity-dependent gene *zenk* in response to song auditory stimulation (Pinaud et al., 2004). Thus, inhibitory mechanisms involving GABA appear to participate in the auditory processing, production, and potentially learning of birdsong.

In the present work, we have used an anti-GABA antibody for a detailed characterization of GABAergic elements in auditory and song control areas of the zebra finch brain, to gain further understanding of the neurochemical organization of circuits involved in vocal communication and learning in songbirds. We demonstrate that GABAergic cells and processes are prevalent at several levels of the auditory pathway as well as within song control nuclei. Our observations are consistent with a prominent role of inhibitory mechanisms in the physiology of brain areas that participate in song auditory processing, learning and production in songbirds.



## MATERIAL AND METHODS

**Animals:** We used a total of 22 adult zebra finches (*Taeniopygia guttata* - 8 females; 14 males) purchased from a breeder and maintained in our local aviary. Experimental protocols utilized in this study were approved by OHSU's Institutional Animal Care and Use Committee (IACUC) and are in accordance with NIH guidelines. A subset of birds (6 females and 10 males) was maintained overnight in a sound-proof box. The next day, birds were stimulated with a playback of a medley of conspecific songs for 30 minutes, followed by 1 hr of silence (as in (Mello and Ribeiro, 1998)). All other birds were directly removed from our aviary and immediately sacrificed.

All birds received an overdose of Nembutal and were quickly perfused transcardially with 10 ml of phosphate-buffered saline (PBS; pH 7.4) followed by 60 ml of a solution containing 1% paraformaldehyde and 2% glutaraldehyde in 0.1M PB. A fast and efficient perfusion with saline prior to the fixative was critical for preventing GABA signal from being washed off the tissue. Brains were then dissected out of the skulls, cryoprotected by equilibration in a 30% sucrose solution., included in embedding medium (Tissue-Tek; Sakura Finetek, Torrance, CA), frozen in a dry-ice/propanol bath, cut on a cryostat (20 $\mu$ m thick sections), mounted on glass slides (Fisherbrand Superfrost Plus; Fisher Scientific, Pittsburgh, PA), and stored at -80°C.

**Immunocytochemistry (ICC):** We used a commercial rabbit anti-GABA polyclonal antibody (Chemicon International, Temecula, CA; catalog # AB141, immunogen

KLH-GABA). Slides were removed from the  $-80^{\circ}\text{C}$  freezer and allowed to dry at room temperature (RT) for 30 min. Slides were then immersed in PB and hydrated for 30 min, followed by incubation for 2 hr at RT in a blocking buffer (BB) that consisted of 0.5% albumin and 0.3% Triton X-100 in 0.1M PB. Sections were then washed for 30 min (3 x 10 min washes) in PB and incubated overnight at  $4^{\circ}\text{C}$  with the anti-GABA antibody (1:200 dil in BB), in a humid chamber. The slides were then washed for 30 min (3 x 10 min) in PB and incubated for 2 hr at RT with a biotinylated goat anti-rabbit antibody (1:200 dil in BB; Vector Laboratories, Burlingame, CA). Sections were then washed for 30 min in PB and incubated for 2 hr at RT in avidin-biotin complex (1:100 dil in PB; ABC Elite kit, Vector Laboratories, Burlingame, CA). The slides were then washed for 30 min (3 x 10 min) in PB and incubated in a filtered solution containing 0.03% diaminobenzidine, 0.15% Nickel sulfate and 0.001% hydrogen peroxide in PB. Sections were periodically monitored for signal under a microscope and reaction was stopped by immersion in PB. The sections were then dehydrated in a standard series of alcohols, delipidized in xylene, and coverslipped.

**Specificity Controls:** Omission of the primary antibody resulted in absence of cellular staining, demonstrating the specificity of our ICC detection system (secondary antibody plus ABC reagent). As discussed previously (Grisham and Arnold, 1994), preabsorption of the primary anti-GABA antibody with GABA alone does not block the immunoreactive product detected with this antibody. Rather, to determine the specificity of this antibody, it is necessary to pre-absorb it with GABA

conjugated to a carrier protein, analogous to the immunizing molecule used to generate this antibody. We therefore generated a GABA-BSA conjugate as described previously (Walrond et al., 1993), with modifications. We first cross-linked GABA (5mM) with BSA (5mg/ml) using glutaraldehyde (at 1% in 0.1M PB) for 1 hr at RT, under stirring. This solution was then dialyzed against 30 volumes of cold 0.01M PB (10 volumes/day for 3 days, at 4°C). To pre-absorb the anti-GABA antibody with the conjugate, we incubated the antibody at its working dilution with various concentrations of the post-dialysis conjugate overnight at 4°C under agitation. The pre-absorbed antibody was then used in the ICC procedure. We found that pre-absorption with both 10μM and 50μM (but not 1μM) of the GABA-BSA conjugate successfully and completely abolished GABA-like immunoreactivity in brain sections (Fig. 2B). Further pre-absorption controls using unbound BSA at the same concentrations as for the GABA-BSA conjugate did not alter GABA-like immunoreactivity in our preparations (Fig. 2A). These pre-absorption procedures are in accordance with the J. Comp. Neurol. recommendations for determining antibody specificity (Saper and Sawchenko, 2003).

**Imaging and Analysis:** We used a Nikon E-600 microscope equipped with a motorized stage drive (LEP Mac5000), and coupled to a PC containing the Neurolucida software (Microbrightfield Inc., Colchester, VT) through the Lucivid system for morphometry, or through a digital camera (DVC, Austin, TX) for photomicrograph acquisition. Acquired photomicrographs were transferred to Adobe Photoshop software, where levels were adjusted and illustration plates assembled.

To generate estimates of local densities of labeled cells, a regular grid containing squares of 100x100µm was superimposed on tissue sections containing areas of interest in sections processed for GABA ICC, or adjacent sections processed for cresyl violet staining. Five such fields were counted per area per bird for each staining. Nissl sections were used for estimates of the local neuronal cell density, using the inclusion criteria of large pale nucleus, usually with clear staining nucleolus, and prominent Nissl substance for neuronal cells, and the exclusion criteria of small cells with dark-, homogeneously-stained nuclei and scant cytoplasm. The results, expressed for each bird as the percentage of GABA-labeled cells relative to the density of neuronal cells, as defined by Nissl staining, were averaged across birds (n=3 birds per staining method; Table 1). We have chosen not to use stereological techniques, because the goal of our quantification was to compare the relative densities of labeled cells across different brain regions rather than to provide absolute numbers of GABAergic cells per structure in reconstructive analysis. Our methodology is in accordance with the recommendations and guidelines for the use of stereology in the J. Comp. Neurol. (Coggeshall and Lekan, 1996; Saper, 1996). In addition, the exact anatomical boundaries and, thus, the total size of several auditory telencephalic areas cannot be reliably defined, either by cytoarchitectonic or known histochemical criteria.

For cell size estimates, we measured the largest linear soma diameter of any given cell using Neurolucida's "Measurement" tool. For each area of interest, we randomly sampled a few hundreds neurons in non-overlapping fields throughout the areas investigated, across 3 birds. In Table 1, we represent the absolute values for the

largest and smallest soma diameter measured as “Cell Size Range” and the average diameters as “Average Size”.

## RESULTS

To reveal GABAergic cells in the zebra finch brain, we performed immunocytochemistry (ICC) with an anti-GABA antibody that has been previously used in this species (Grisham and Arnold, 1994). We could identify GABAergic cells in most brain areas examined. The majority of these cells were small, most likely representing inhibitory neurons that participate in local networks, as described in other systems. Several areas, however, also contained a small contingent of very large GABAergic cells that, at least in some cases, may correspond to projection neurons. Immunolabeled fibers and punctate staining were also observed in the majority of regions analyzed. The issue of specificity of the anti-GABA antibody we used was previously discussed (Grisham and Arnold, 1994). We have incorporated, however, critical pre-absorption controls (see Methods) to further establish the specificity of the staining patterns in our preparations. In addition, we examined the labeling in some populations of well-known GABAergic neurons (Gabbott et al., 1986; Batini et al., 1992; Sastry et al., 1997). In the cerebellum, we observed strongly labeled cells in the deep cerebellar nuclei (Fig. 3A-C). These cells were typically large with strongly-labeled triangular soma (Fig 3B and C; arrowheads). The Purkinje cells were probably the most heavily labeled cells in the brain (Fig. 3D and E). These cells were markedly large and relatively uniform in size across cerebellar folia. We observed strong immunoreactivity in the soma of virtually all Purkinje cells, and in most cases were able to discern negative cell nuclei (Fig. 3D, arrowheads). We also observed strong labeling over large extensions of the dendritic arborizations of Purkinje cells.

These processes could often be followed for a few hundred microns into the molecular layer, where they branched profusely, forming a dense immunoreactive network (Fig. 3D and E). The molecular layer also contained several smaller GABA-positive cells that based on the location, size and number, likely correspond to basket neurons (Fig. 3D and E, arrows).

GABAergic cells were also observed in the globus pallidus (GP). As is characteristic of this area (Smith et al., 1987; Smith and Bolam, 1990; Churchill and Kalivas, 1994), these neurons were very large and relatively sparse, with a predominantly triangular soma and a high density of immunostaining (Fig. 3F and G). Many labeled cells were lined up close to the border with the striatum (St), into which they extended prominent immunolabeled dendritic processes that were aligned with the dorso-ventral axis. Such processes were particularly visible in the caudal GP and caudal St (CSt; Fig. 3G, arrows). The dorsal border of the GP could be easily distinguished due to the markedly low density of GABAergic neurons in the CSt (Fig. 3F). The GP also contained a high density of uniformly distributed punctate staining.

Thus, known populations of GABAergic neurons are readily and reliably identified in our preparations, and their morphology and distribution are in accordance with previous studies. Below we describe the staining patterns we observed in the nuclei of the ascending auditory pathway, followed by auditory and vocal control areas of the telencephalon. The nuclei in the ascending auditory pathway were identified based on the published pigeon and canary brain atlases (Stokes et al., 1974); the lemniscal nuclei were not examined as they could not be

reliably identified in our preparations. All density estimates of GABA-positive cells are relative to the neuronal counts per area based on Nissl-stained adjacent sections.

### **Ascending Auditory Pathway**

#### *Nucleus magnocellularis (NM)*

We observed a high density of GABAergic cells (about 53% of the neuronal counts per area based on Nissl; Table 1) in this nucleus (Fig. 4C and D). These cells were evenly distributed and had predominantly round or ovoid labeled somata with no evident stained neurites. The cells were relatively large (18.2 $\mu$ m average diameter, 12.2 to 26.4 $\mu$ m range; Fig. 4D and Table 1), and the majority of them displayed high immunolabeling, suggesting the presence of high GABA contents (Fig. 4D). A moderate density of punctate staining could be observed, uniformly distributed throughout the extent of NM. It is worth noting that a low level of background staining persisted in this nucleus in the pre-absorption control. This is most likely due to an “edge-of-section” effect, as magnocellularis is located close to the (ventricular) border of the tissue. At any rate, the dramatic decrease in immunolabeling observed with the pre-absorption argues strongly for the GABAergic identity of the immunolabeled cells.

#### *Nucleus angularis (NA)*

Nucleus angularis had the lowest overall density of GABAergic cells compared to all other areas in the present study (19% of the neuronal counts per area; see Table 1). These cells had an asymmetric distribution, the lowest density occurring



laterally and the highest density medially (Fig. 4B), and were moderately small (11.1 $\mu$ m average diameter, 5.6 to 15.8 $\mu$ m range; Table 1). The soma morphology varied from round and oval to elongated (Fig. 4F). In addition, immunostaining was mostly confined to the soma but in some cases proximal neurites could be seen (Fig. 4F; arrowhead). Strong punctate staining could also be observed in NA, apparently over the somata of unlabeled cells (Fig. 4F).

#### *Nucleus laminaris (NL)*

Slightly lateral to NM, nucleus laminaris (NL) displayed a moderate density of GABAergic cells (20% of the neuronal counts per area). These cells had an asymmetric distribution, a higher density of immunolabeling perykaria seen laterally and a lower density ventromedially (Fig. 4C). The majority of labeled neurons had ellipsoid and moderately to strongly labeled somata (Fig. 4E, arrows), with no apparent labeled neurites. These cells were relatively small (9.7 $\mu$ m average diameter, 5.7 to 13.7 $\mu$ m range; Table 1). We also observed several clusters of coarse labeled puncta over what may represent unlabeled somata (Fig. 4E, arrowheads), suggesting that non-GABAergic cells in this nucleus receive a strong GABAergic input.

#### *Superior olivary nucleus (SON)*

A moderate overall density of GABAergic neurons (about 35% of the neuronal counts per area) was detected in this nucleus. Their somata were mostly small (7.6 $\mu$ m average diameter, 3.9 to 12.4 $\mu$ m range; Table 1) and their shape varied from round or ovoid to triangular and pyramidal-like (Fig. 5B and C). The cells had

moderate staining, but presented strongly labeled and coarse puncta over the soma (Fig. 5C). Such puncta were also distributed over the entire extent of the SON. Larger and more strongly labeled cells were more evident ventrally (Fig. 5B).

*Nucleus mesencephalicus lateralis, pars dorsalis (MLd)*

A high density of GABA-stained cells (approximately 32% relative to neuronal counts per area) was observed in this nucleus (Fig. 6B). They had a wide size range (6.7 to 28.4µm in diameter; Table 1) and marked variation in morphology. Both large neurons with varied soma shapes and small neurons with predominantly round soma were seen (Fig. 6C). Interestingly, the strongest staining in both cell types was nuclear, with a more modest labeling seen in the soma (Fig. 6C; arrows). Both cell types often exhibited immunopositive neurites that extended from the soma (Fig. 6C; arrowheads) and branched, forming a dense network of labeled processes and punctate staining with a reticular aspect throughout MLd.

*Nucleus ovoidalis (Ov)*

GABA-labeled cells comprised a high percentage (40% of the neuronal counts per area) in this thalamic nucleus and were present both in the core and shell regions (Fig. 7B). Most of these cells had predominantly round or ellipsoid soma that were strongly labeled (Fig. 7C), and had the smallest soma size compared to all other auditory areas examined (6.7µm average; Table 1). GABA-positive neurites were rarely seen, except for occasional moderately-stained processes in non-spherical

neurons (Fig. 7C, arrowheads). A moderate density of punctate staining was seen throughout the extent of Ov.

## **Auditory Areas in the Telencephalon**

### *Field L (L1, L2 and L3)*

Field L is a large structure, occupying an extensive area of the caudal telencephalon and consisting of several subdivisions. Most of our analysis, including morphometry, was carried out in parasagittal sections approximately 0.9 to 1.0 mm lateral to the midline, where the major field L subdivisions L1, L2a and L3 could be clearly identified based on cytoarchitectonic criteria seen on Nissl-stained sections adjacent to those reacted for GABA ICC. In addition, the boundaries of L2a could also be defined in GABA immunostained material itself, as labeled cells in this area were organized in a distinct string-like fashion along the dorso-ventral axis. For lack of reliable boundaries in our sections, we did not examine subfield L2b. The caudal boundary of L1 and the rostral boundary of L3 could be easily identified based on the intersection of L2a with the lamina pallialis subpallialis that separates field L from the adjacent CSt. However, the anterior boundary of L1 and the posterior boundary of L3 could not be identified either by Nissl or by ICC.

Very high densities of GABAergic neurons were detected in L1, L2a and L3 (39, 54 and 45% of the neuronal counts per area, respectively; Table 1). These cells had a mostly homogeneous distribution at this level of the brain (Fig. 8A). The labeled cells were predominantly round and had a wide size range (4 to 22  $\mu\text{m}$  in diameter; Table 1), but tended to be slightly larger in L2a (13.2 $\mu\text{m}$  average diameter)

than in L1 and L3, (9.4 and 10.8 $\mu$ m average diameter, respectively; Table 1). Cells in all subdivisions had moderately high soma staining; however, very few immunostained processes and puncta were seen. The medial-most part of subdivision L2a could be clearly seen in medial parasagittal sections that also contained NCM and CMM (Fig. 9C). At this level, the large cells in L2a were very strongly labeled, but numerous smaller cells could also be seen.

#### *Caudomedial Nidopallium (NCM)*

This field L target is also a large and complex area. Our analysis focused on medial parasagittal sections (between 0.7 and 1.0mm lateral to the midline), where the boundaries of NCM are very distinct (the ventricular zone dorsally, caudally and ventrally, and the lamina mesopallialis, or LaM, and field L2a rostrally). GABA-labeled cells were highly prevalent in NCM (52% of the neuronal counts per area). GABAergic neurons in NCM were mostly evenly distributed (Fig. 9B), with relatively few clusters of 2-4 cells observed (Fig. 9E, arrowhead). Immunoreactive neurons tended to be round or ellipsoid, with strongly stained soma and occasional labeled neurites (Fig. 9F and G). These cells also displayed high variation in diameter and a relatively small average size (Table 1). Qualitatively, these GABAergic cells appeared to fall into two predominant types. The first exhibited small soma (3.3-10  $\mu$ m diameter range) with varied shapes and pronounced processes (Fig. 9F and G; arrowheads). The second had a larger soma (15-20.8 $\mu$ m diameter range) with round shape and few processes (Fig. 9F and G; arrows). Both types were present throughout NCM, but the smaller cell type was more prevalent. The larger type was comparable

to that seen in adjacent field L2a (Fig. 9C; arrowheads). No apparent punctate staining could be observed in NCM.

#### *Caudomedial Mesopallium (CMM)*

A high density of GABA-labeled cells (52% of the neuronal cells detected by Nissl; Table 1) could be identified in CMM (Fig. 9D). They were distributed throughout this area, and had a tendency to group into clusters of 3-5 cells. Such clusters are typical of CMM, and can be readily identified in sections counterstained for Nissl. GABA-labeled cells in CMM were mainly round or oval and had a wide size range (~4µm to 19µm in diameter). The majority of these cells appeared to be small (7µm average diameter, 4-12µm range; Table 1), although some larger neurons (15-19µm diameter range) could also be observed. Immunolabeled cells had relatively high and uniform soma staining, and labeled neurites and punctate staining were rarely seen.

#### *Nidopallial shelf area*

The dorsal boundary of this field L target corresponds to the ventral boundary of HVC, but its ventral boundary can only be identified with tract-tracing (Vates et al., 1996). Our current analysis was restricted to a 200µm thick domain immediately ventral to HVC. A modest density of GABAergic cells (30% of the neuronal counts per area) could be identified in this region. These cells were distributed along the shelf (Fig. 10D), with no apparent clusters, and had round to ellipsoid somata with strong and homogeneous labeling (Fig. 10D). They tended to be slightly smaller

(8.9 $\mu$ m average diameter; Table 1) compared to the adjacent HVC. Very few neurites were immunolabeled and those did not extend far from the soma. Only low levels of punctate staining were observed.

#### *Arcopallial cup area*

The internal boundary of the cup area adjacent to song nucleus RA is defined by RA itself, but the external boundary does not exhibit any distinct cytoarchitectonic features and can only be defined by tract-tracing (Mello et al., 1998). Based on the latter, the cup region extends rostroventrally for about 500 $\mu$ m from the rostroventral boundary of RA. A relatively high density of GABA-positive cells (approximately 36% of the neuronal counts per area, assessed within 200 $\mu$ m from the RA boundary) was observed in this region (Fig. 11E and F). These cells were mostly small (7 $\mu$ m average diameter), had a narrow size range (4.4 to 10.5 $\mu$ m; Table 1), and tended to segregate into groups, but not in clusters (Fig. 11F; arrows). The majority displayed a round or ovoid soma that was heavily stained, with no apparent immunolabeled processes (Fig. 11F). Some cells, though, particularly those with moderate staining, had more varied shapes and immunopositive proximal neurites. The cup region also contained lightly immunolabeled processes that formed a modest mesh, as well as a moderately high density of punctate staining.

### **Telencephalic Song Control Nuclei**

#### *Nucleus Interfacialis (NI<sub>f</sub>)*

NIf could be identified in some of our GABA ICC preparations as a small domain embedded between L1, L2a and CSt (Fig. 8A). Compared to the adjacent L1 and L2a, GABAergic cells in nucleus NIf were relatively large (9.4µm average diameter; 3.4 to 16.7µm range; Table 1). They exhibited relatively strong and uniform soma staining, were uniformly distributed, with no apparent clusters, and had a predominantly round or ovoid soma, although some cells were more elongated (Fig. 8B). Very few processes and little punctate staining could be seen. Due to the difficulty in reliably identifying NIf in Nissl-stained sections and in some of our ICC preparations, we did not attempt to quantify the density of GABAergic neurons in this structure.

#### *Lateral magnocellular nucleus of the anterior nidopallium (LMAN)*

LMAN boundaries could easily be identified based on GABA ICC staining due to the marked difference in labeled cell sizes between LMAN and the surrounding nidopallium (Fig. 12B). A modest density of GABAergic cells could be detected in LMAN (about 29% of the neuronal counts per area). These cells were evenly distributed, with no apparent cell clusters (Fig. 12B). Although labeled cells in LMAN tended to be large (12µm average diameter), several small labeled neurons could also be seen (5 to 23.8µm diameter range; Table 1). These cells tended to have more rounded somata compared to the larger cells (Fig. 12C, arrows). The larger cell type displayed highly variable shapes that ranged from oval to more complex types (Fig. 12C, black arrowheads). Most labeled cells exhibited strong immunostaining in the soma and moderate staining of their proximal dendrites (Fig. 12C, white

arrowheads). Punctate staining was modest, but more marked in the vicinity of the larger cells.

#### *Area X of the striatum*

The boundaries of this song nucleus could be easily defined based on the different densities of immunolabeled cells between this region and the surrounding striatum (Figure 13B). A very high density of GABAergic cells was detected in area X (about 49% of neuronal counts per area). They were evenly distributed, although a few occasional clusters were seen, and were predominantly small (average diameter 7µm; range 3.6 to 22.6µm; Table 1). A qualitative evaluation indicated that immunolabeled cells fell into one of two groups: 1) small cells that tended to have a round or slightly oval soma (Fig. 13C, arrowheads), and sometimes an associated labeled neurite; and 2) large cells (3 to 5 times larger diameter than the smaller cells) that had mostly round somata (Figure 13C, arrows). The majority were of the smaller type, while cells of the larger type were much fewer. Both types exhibited strong cytoplasmic staining and were evenly distributed. We observed few immunolabeled puncta that were uniformly distributed.

#### *Nucleus HVC of the nidopallium*

A high density of GABAergic cells (about 40% of neuronal counts per area) was detected in HVC (Fig. 10B). These cells tended exhibit moderate size (10.7µm average diameter, 6.7 to 14.3µm range; Table 1), with a round- or oval-shaped soma (Fig. 10E) and a relatively homogeneous distribution throughout HVC (Fig. 10C and



E), instead of being organized into clusters. They displayed strong and homogeneous somatic staining, with very few labeled processes evident. No punctate staining was detected in HVC.

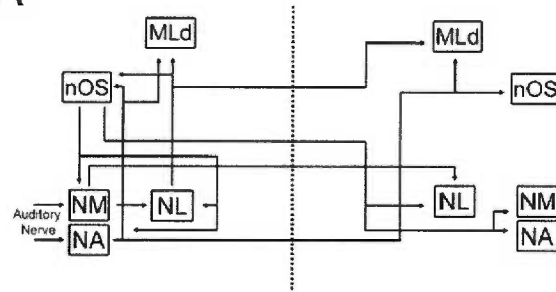
*Robust nucleus of the arcopallium (RA)*

The borders of RA could be easily identified in our preparations because the morphology and size of GABA-labeled cells in RA differed markedly from those in the surrounding arcopallium, and because of a low signal zone demarcating the boundary between RA and the neighboring arcopallium (Fig. 11B, C and E). A high density of GABAergic cells (about 47% of neuronal counts per area) was observed in RA. These cells tended to be large (14.3µm average diameter) but had a broad size range (6.4-28.5µm diameter; Table 1) and were uniformly distributed. Their morphology ranged from cells with round- or oval-shaped somata to pyramidal- and multipolar-like cells (Fig. 11D) and they typically exhibited heavy somatic immunostaining and a negative nucleus (Fig. 11D). Most cells had pronounced labeled processes that extended from the soma and then branched extensively, forming an intricate network throughout RA (Fig. 11D). Despite high neuritic labeling, little punctate staining was observed.

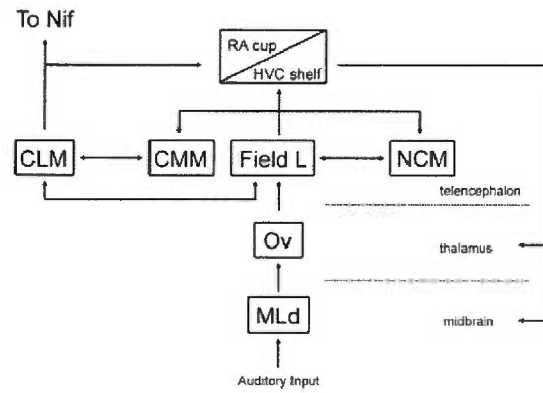
**Figure 2.1) The ascending auditory pathway and the song control system of songbirds**

(A) Diagram of the main nuclei and connections of the auditory pathway, up to the midbrain. Dotted line represents the midline. (B) Diagram of the auditory pathway from the midbrain to the telencephalon, and intratelencephalic projections. (C) Diagram of the song control system. For clarity, only the main nuclei and projections are shown in all diagrams, and only unilateral projections in (B) and (C). (A) is mostly based on work conducted in non-oscine species like chicks and the barn owl (Parks and Rubel, 1975; Rubel and Parks, 1975; Parks and Rubel, 1978; Takahashi and Konishi, 1988; Lachica et al., 1994; Levin et al., 1997), whereas (B) and (C) is supported by data obtained in zebra finches and canaries, as well as non-oscine species like the pigeon, chicks and budgerigars (Karten, 1967, 1968; Parks and Rubel, 1975; Nottebohm et al., 1976; Parks and Rubel, 1978; Bottjer et al., 1984; Brauth et al., 1987). For abbreviations, see list.

A



B



C

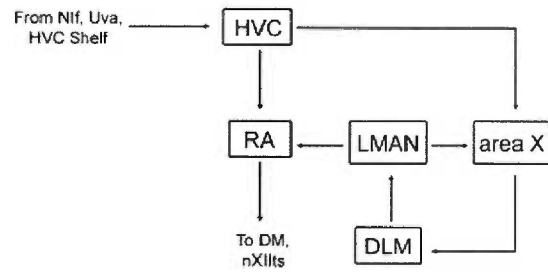


**Figure 2.2) Specificity of GABA-immunoreactivity in the zebra finch brain**

(A) Low power photomicrograph depicting GABA-like immunoreactivity in the nidopallium of a male zebra finch. This section was incubated with the anti-GABA antibody that was pre-absorbed with 50 $\mu$ M of unbound BSA. (B) Photomicrograph of a section incubated with the anti-GABA antibody pre-absorbed with 50 $\mu$ M of the GABA-BSA conjugate (see Material and Methods). Note that GABA-like immunoreactivity was completely abolished after the pre-absorption with the GABA-BSA conjugate. Scale bar = 100 $\mu$ m.

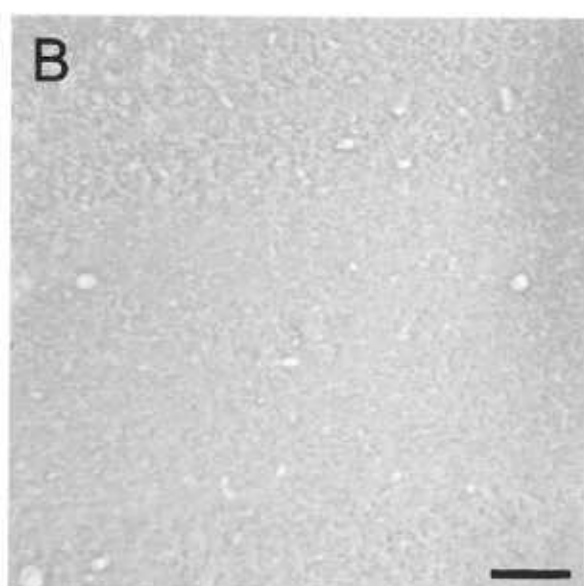
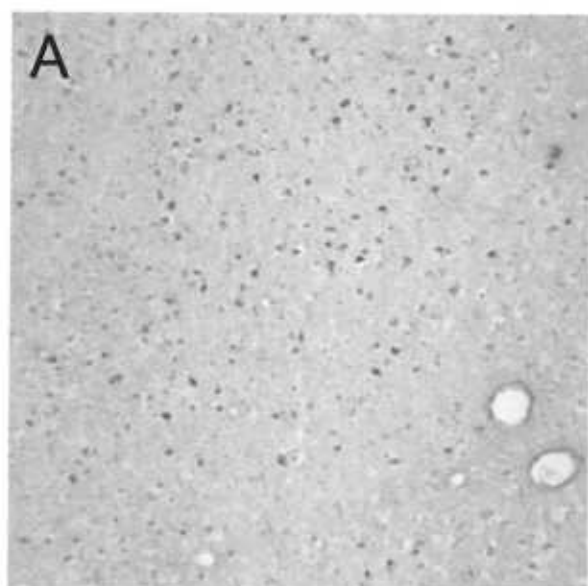


**Figure 2.3) GABA immunoreactivity in known GABAergic neurons in zebra finches**

(A) Low power view of a frontal section depicting strongly labeled GABAergic neurons in the deep cerebellar nuclei. Rectangles illustrate where photomicrographs in B and C were taken from. (B) and (C) Detailed views of middle and lateral cerebellar nuclei depicting a moderate density of strongly immunolabeled cells. Arrowheads indicate examples of cells with triangular and elongated somata. Inset in C shows a high power view of one labeled neuron. (D) Low power view of part of a cerebellar folium, depicting labeling of Purkinje cells; arrowheads indicate examples of immunopositive cells with clear immunonegative nucleus. Arrows depict small labeled cells in the molecular layer. (E) High power view of cerebellar Purkinje cells and respective dendritic arborizations. Arrow depicts putative basket cell in the molecular layer. (F) Low power photomicrograph of the transition between the GP and CSt. Note that GABAergic cells are strongly labeled and highly concentrated in the dorsal aspect of the GP, but are found at very low densities in the CSt. (G) High power view of GP depicting somata of labeled cells and respective dendrites extending into the CSt (arrows). Scale bars (in  $\mu\text{m}$ ): 250 (A); 100 (B-C); 12.5 (inset C); 50 (D); 25 (E); 100 (F); 25 (G). For abbreviations, see list.

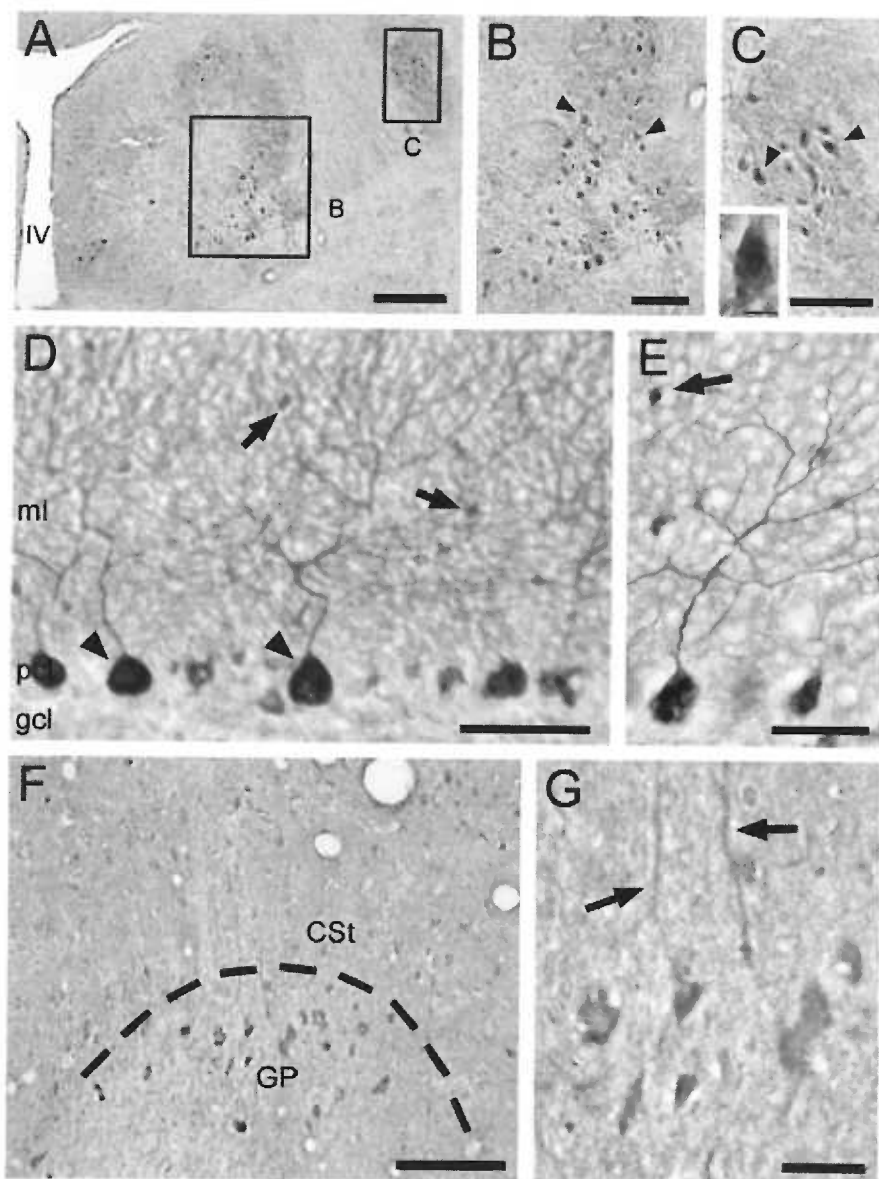


**Figure 2.4) GABA immunoreactivity in cochlear nuclei and nucleus laminaris**

(A) Camera lucida drawing of right half of a frontal section indicating the location of cochlear nuclei. (B) Low power photomicrograph depicting GABA immunoreactivity in NA. Note that GABAergic neurons are more prominent medially. Prominently labeled cells can also be observed in the adjacent VeL. (C) Low power photomicrograph depicting GABA immunolabeled neurons in NM and NL. (D-F) High power photomicrographs of NM, NL and NA, respectively, depicting the pattern of GABA staining in these nuclei. Arrows in E indicate immunopositive cells, while arrowheads indicate coarse punctate staining over immunonegative cells. Arrowhead in F indicates immunolabeled process extending from a GABA-positive soma. Scale bars (in  $\mu\text{m}$ ): 250 (B-C); 25 (D-F).



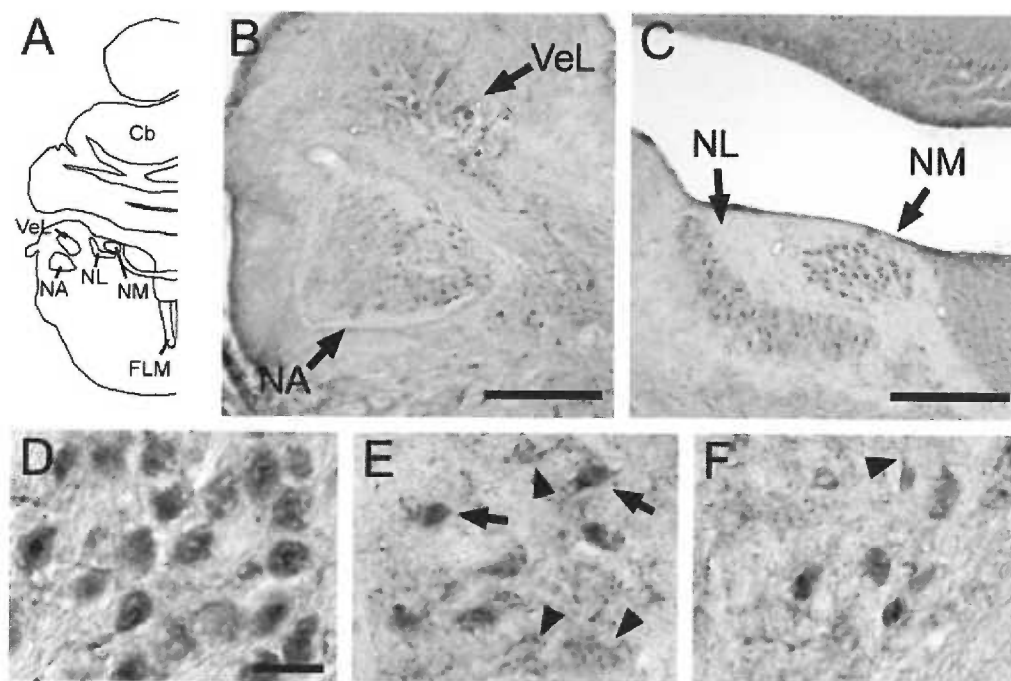
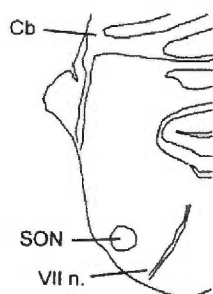


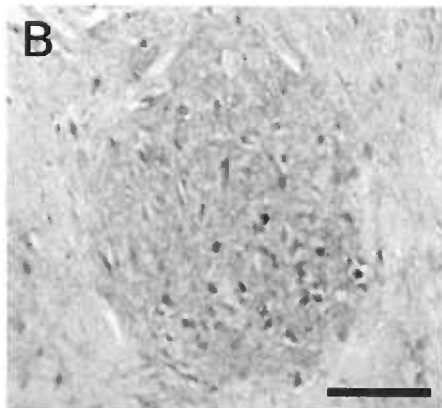
**Figure 2.5) GABA-positive neurons in the SON**

(A) Camera lucida reconstruction of frontal section at the level of the superior olivary nucleus, where photomicrographs B and C were obtained from. (B) Low power photomicrograph depicting the distribution pattern of GABAergic neurons in SON. Note that GABAergic neurons are found at a higher density ventrally. (C) High power photomicrograph illustrating GABA-immunopositive neurons and puncta. Scale bars (in  $\mu\text{m}$ ): 100 (B); 25 (C).

**A**



**B**



**C**

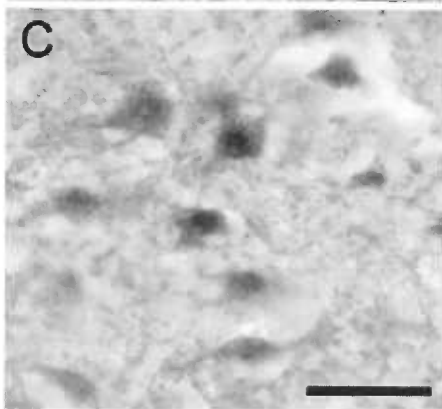


**Figure 2.6) GABA immunoreactive neurons in MLd**

(A) Camera lucida reconstruction of the right half of a frontal section depicting nucleus MLd and adjacent brain areas. Box represents the location where photomicrograph in B was taken. (B) Low power photomicrograph depicting the distribution of GABAergic cells in MLd. (C) High power image showing GABA immunolabeled cells in this nucleus. Arrows show typical examples of cells that exhibit high immunostaining over the nucleus and less intense cytoplasmic labeling. Arrowheads indicate processes that often extend from these neurons to form an intricate neuritic network. Scale bars (in  $\mu\text{m}$ ): 250 (B); 25 (C).

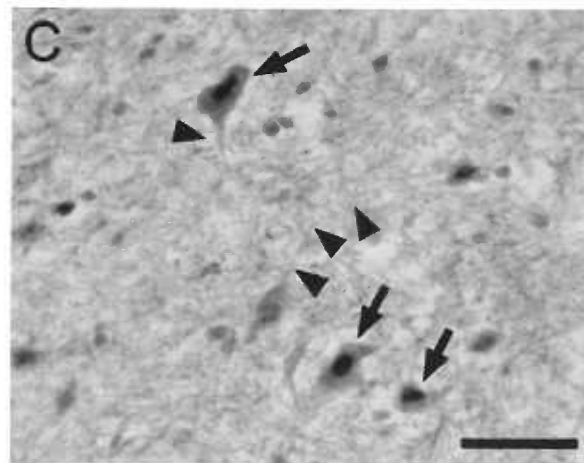
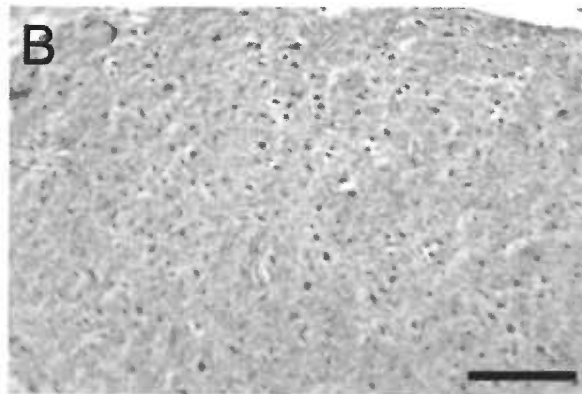
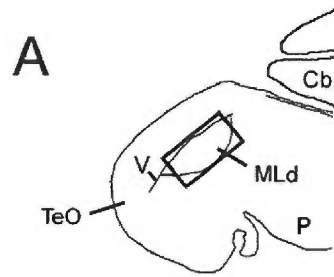


**Figure 2.7) GABA immunoreactivity in Ov**

(A) Camera lucida reconstruction of parasagittal section through nucleus Ov depicting its position relative to adjacent brain structures. Box illustrates where photomicrograph B was taken from. (B) Low power photomicrograph illustrating the distribution of GABA-immunolabeled neurons in core and shell regions (arrows) of Ov. (C) High power photomicrograph obtained in the core Ov depicting immunolabeled cells in this nucleus. Arrowheads indicate immunolabeled processes that extended from strongly labeled cells. Scale bars (in  $\mu\text{m}$ ): 100 (B); 25 (C).

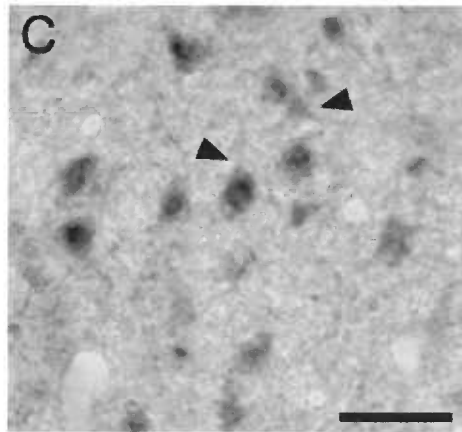
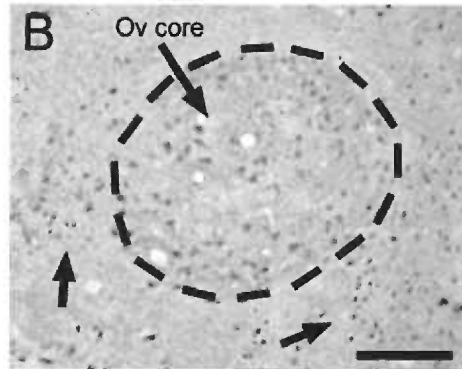
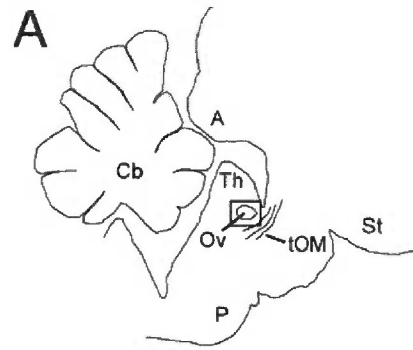


**Figure 2.8) GABA-immunolabeled neurons in field L and NIf**

(A) Low power photomicrograph depicting GABA-immunoreactivity in all field L subdivisions (L1, L2a and L3) and NIf. Note that the ventral border of these regions can be clearly defined by the very low density of GABAergic cells in the CSt. (B) Photomicrograph showing detailed view of GABA-immunolabeled cells in NIf. Scale bars (in  $\mu\text{m}$ ): 250 (A); 100 (B).



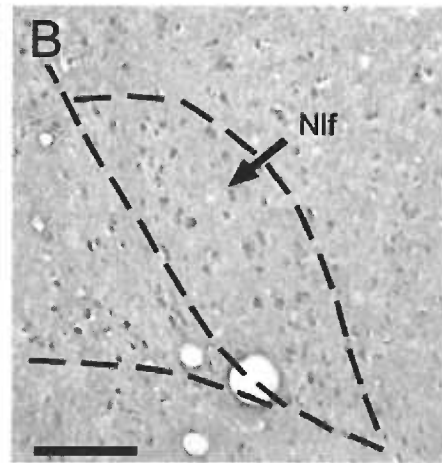
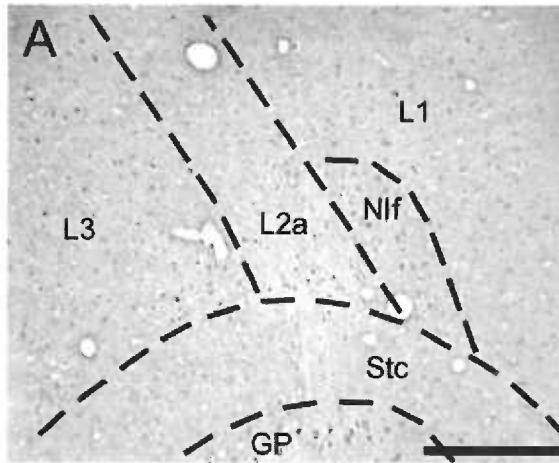


**Figure 2.9) GABA immunoreactivity in auditory areas of the caudomedial telencephalon**

(A) Camera lucida drawing of medial parasagittal section through auditory areas in the caudomedial telencephalon. Boxes indicate the locations of areas shown in panels B-D. (B-D) Low power views depicting GABA-labeled cells in (B) NCM, (C) field L2a, and (D) CMM; dashed lines indicate approximate borders of field L2a based on Nissl counterstaining of adjacent section. Arrowheads in (C) indicate some of the large GABAergic neurons in L2a; arrowheads in (D) indicate some GABAergic cell clusters in CMM. (E) Detailed view depicting heterogeneity of size and shapes of GABA-labeled cells in NCM, and cluster of GABAergic cells (arrowhead). (F-G) High power photomicrographs depicting large (arrows) and small (arrowheads) GABAergic cells in NCM. Scale bars (in  $\mu\text{m}$ ): 50 (B-D); 25 (E); 50 (F-G).

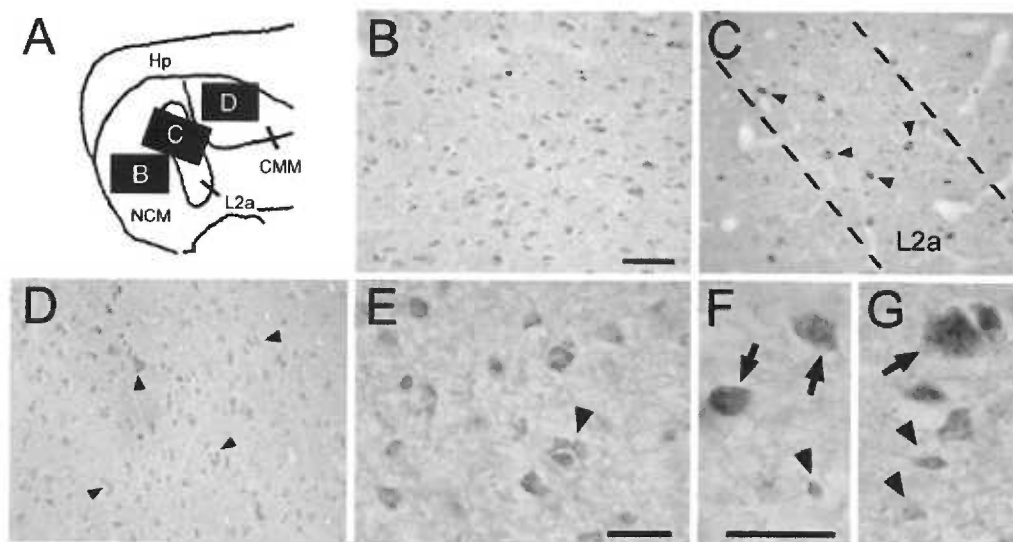


**Figure 2.10) GABA-immunolabeling in HVC and the nidopallial shelf area**

(A) Camera lucida drawing of parasagittal section depicting the location of HVC and the adjacent shelf area. Box shows the area where photomicrograph in B was taken. (B) Low power photomicrograph depicting the distribution of GABAergic cells in HVC and the shelf area. (C) Detail view of the distribution of GABA-immunoreactive neurons in HVC. (D-E) High power photomicrographs depicting labeled cells in the shelf area and HVC, respectively, detailing the morphology and staining patterns of GABAergic cells in these areas. Scale bars (in  $\mu\text{m}$ ): 250 (B); 100 (C); 25 (D-E).

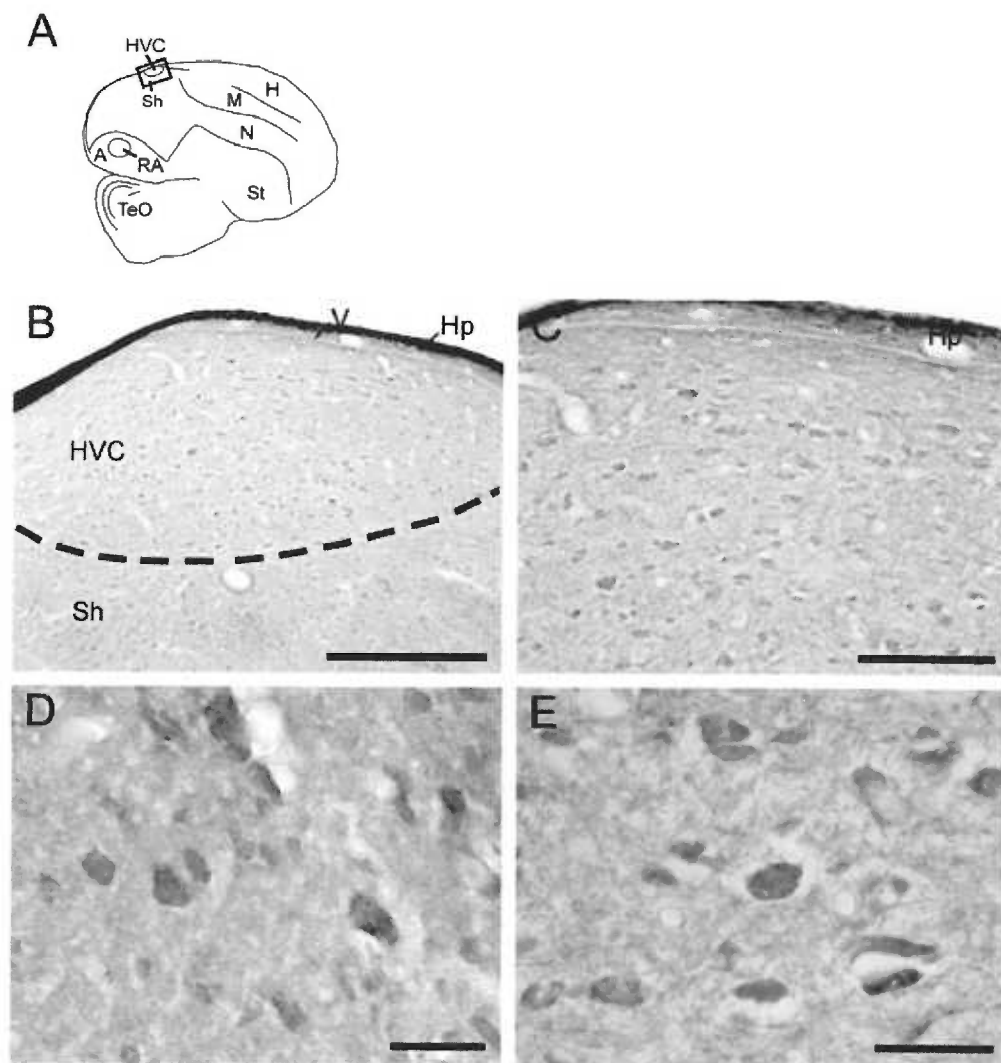


**Figure 2.11) GABA immunoreactivity in RA and the arcopallial cup area**

(A) Camera lucida drawing of parasagittal section illustrating the relative position of RA and adjacent structures. The box indicates where the picture in B was taken. (B) Low power photomicrograph illustrating the general distribution of GABAergic neurons in nucleus RA. Note the lower density of labeled cells in the surrounding tissue. (C) Detail view of GABAergic cells in RA and adjacent arcopallium. Dashed line indicates the boundary of RA based on Nissl counterstaining. (D) High power photomicrograph of GABA-labeled cells within RA. Arrowheads indicate immunolabeled processes that extend from labeled cells, branch, and form an intricate fiber network. (E) Low power photomicrograph depicting GABA-positive cells in the cup region, adjacent to RA. Dashed line indicates the rostral boundary of RA, as defined by Nissl counterstaining. (F) High power photomicrograph depicting uneven distribution of GABAergic cells in the cup region. Arrows indicate example of a loose group of cells. Scale bars (in  $\mu\text{m}$ ): 250 (B); 50 (C); 25 (D); 100 (E); 25 (F).

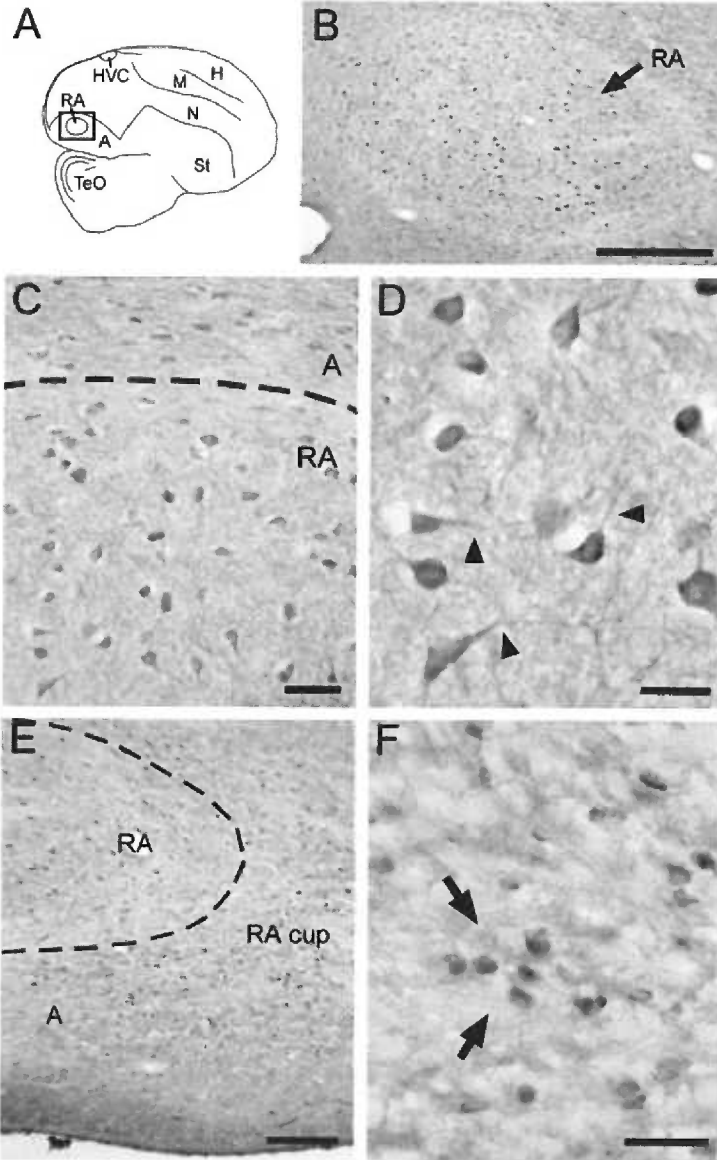


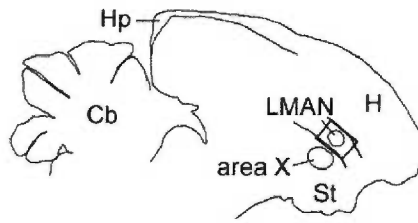
**Figure 2.12) GABA immunoreactivity in LMAN**

(A) Camera lucida drawing of parasagittal section indicating the relative position of LMAN and adjacent structures. Box indicates location where picture in B was taken.

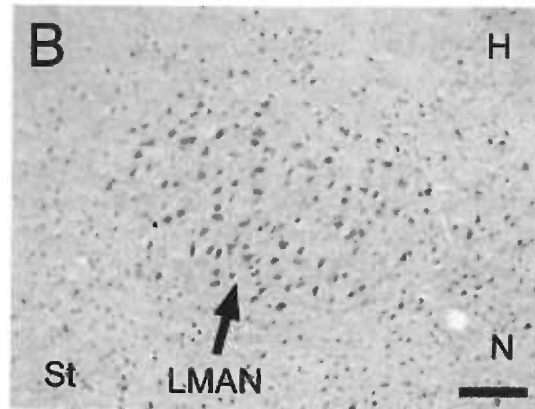
(B) Low power photomicrograph depicting the distribution of GABAergic cells in LMAN. Note the marked difference in cell size and labeling in LMAN compared to adjacent regions. (C) High power photomicrograph of GABA-immunolabeled cells in LMAN. Large cells (black arrowheads) were more abundant and varied in shape than small cells (arrows). Immunolabeled processes (white arrowheads) were primarily associated with larger neurons. Scale bars (in  $\mu\text{m}$ ): 100 (B); 25 (C).



A



B



C

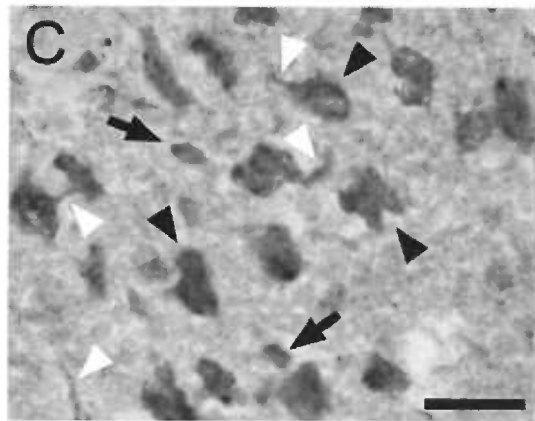
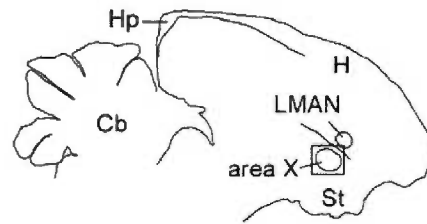


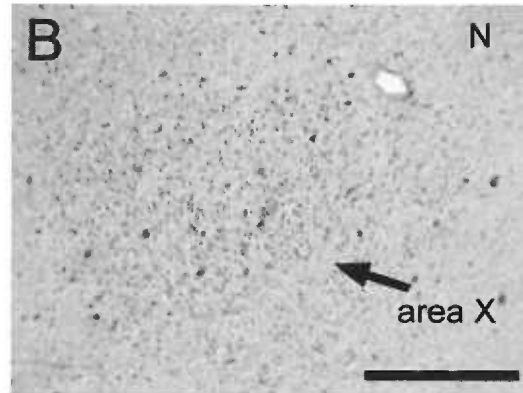
**Figure 2.13) GABAergic immunopositive cells in area X**

(A) Camera lucida drawing of parasagittal section illustrating the position of area X and adjacent brain areas. (B) Low power photomicrograph depicting the overall distribution of GABAergic neurons in area X. Note the higher density of GABAergic cells compared to the adjacent regions. (C) High power photomicrograph depicting the smaller (arrowheads) and larger (arrows) GABAergic cells in area X. Both types were evenly distributed throughout this nucleus. Scale bars (in  $\mu\text{m}$ ): 250 (B); 25 (C).

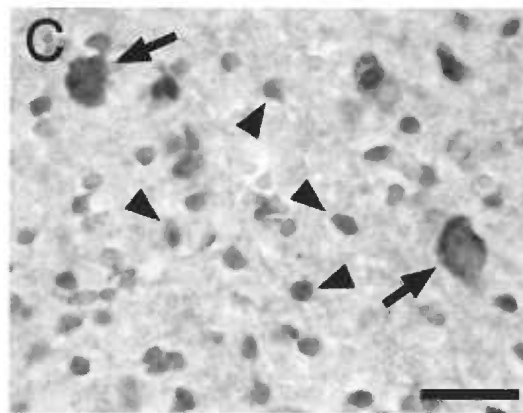
A



B



C



	Average Cell Size ( $\pm$ S.E.)	Range of Cell Sizes ( $\mu$ m)	Percentage of GABAergic Neurons ( $\pm$ S.E.)
NA	11.1 $\pm$ 0.6	5.6-15.8	19.3 $\pm$ 1.5
NL	9.7 $\pm$ 0.3	5.7-13.7	20.1 $\pm$ 1.2
NM	18.2 $\pm$ 0.5	12.2-26.4	53.2 $\pm$ 0.8
SON	7.6 $\pm$ 0.3	3.9-12.4	34.7 $\pm$ 2.0
MLd	16.0 $\pm$ 0.9	6.7-28.4	32.5 $\pm$ 0.5
Ov	6.7 $\pm$ 0.2	3.7-9.2	40.4 $\pm$ 0.5
Field L1	9.4 $\pm$ 0.3	4.1-15.1	39.7 $\pm$ 0.7
Field L2	13.2 $\pm$ 0.4	5.2-21.8	54.9 $\pm$ 2.0
Field L3	10.8 $\pm$ 0.4	4.9-18.6	45.9 $\pm$ 0.7
NCM	9.2 $\pm$ 0.6	3.3-20.8	51.9 $\pm$ 1.4
CMM	7.0 $\pm$ 0.5	3.9-19.3	51.8 $\pm$ 1.4
NIf	9.4 $\pm$ 0.5	3.4-16.7	
RA cup	7.1 $\pm$ 0.2	4.4-10.5	36.4 $\pm$ 0.3
HVC shelf	8.9 $\pm$ 0.5	3.4-16.0	29.7 $\pm$ 0.6
HVC	10.7 $\pm$ 0.4	6.7-14.3	39.9 $\pm$ 0.8
LMAN	12.5 $\pm$ 0.5	5.0-23.8	29.2 $\pm$ 0.3
RA	14.3 $\pm$ 0.7	6.4-28.5	47.1 $\pm$ 0.2
Area X	7.1 $\pm$ 0.5	3.6-22.6	48.6 $\pm$ 0.4

## **DISCUSSION**

We provide here a detailed account of the distribution of GABAergic elements in auditory processing areas and song control nuclei in the brain of zebra finches. We found that GABA-positive cells are prevalent in several of the examined nuclei of the ascending auditory pathway, in auditory telencephalic areas, and in nuclei of both the anterior and posterior forebrain pathways within the song control system. In addition, GABAergic processes and puncta, presumably corresponding to GABAergic terminals, were observed in a number of these areas. These observations are consistent with the view that GABA plays a significant role in various aspects of birdsong representation, such as song perceptual processing and memorization, motor control of song production, and vocal learning. Below we discuss the implications of these findings.

### **GABAergic Elements in the Ascending Auditory Pathway**

The avian ascending auditory pathway has been most extensively investigated in the barn owl, in the context of sound localization, and in chicks, in relation to general auditory physiology. Studies on nuclei angularis (NA) and magnocellularis (NM), which together comprise the avian cochlear nuclei, and nucleus laminaris (NL), thought to correspond to the mammalian medial superior olive (Boord, 1968), have demonstrated a prominent role of GABAergic mechanisms in auditory stimulus processing and encoding. NA encodes the intensity of sound in a series of spike trains, while NM is primarily concerned with temporal properties of the stimulus

(Young and Rubel, 1983; Sullivan and Konishi, 1984; Takahashi et al., 1984; Warchol and Dallos, 1990; Monsivais and Rubel, 2001; Fukui and Ohmori, 2004). Projections from NM primarily target NL, where interaural time differences (ITDs) required for sound localization are computed (Young and Rubel, 1983; Carr and Konishi, 1990; Overholt et al., 1992). Patch-clamp recordings in NL have shown that GABAergic inhibition increases coincidence detection of excitatory projections (Funabiki et al., 1998). In addition, the strength of GABA transmission may allow for either an increase or decrease in neuronal excitability in NL (Bruckner and Hyson, 1998). Electrophysiological recordings in the chick, though, indicate that NM is not the primary source of inhibitory input to NL (Zhou and Parks, 1991). Indeed, a GABAergic projection from NM to NL appears to be absent in this species (Bruckner and Hyson, 1998). Robust GABAergic projections in the chick have been described from the superior olivary nucleus (SON) to both NL and NM (Lachica et al., 1994; Yang et al., 1999; Monsivais et al., 2000), the latter regulating the fidelity of phase-locking of auditory signals (Monsivais et al., 2000). Feedback inhibition from SON onto NL contributes to the temporal integration and coincidence detection required for ITD computations (Yang et al., 1999). Feedback networks that affect auditory processing in NL and NM via the GABAergic projections from SON have been proposed to arise from NA projections to SON, but the neurochemical identity of the latter is not clear (Knudsen and Konishi, 1978; Brainard et al., 1992). In sum, GABAergic influence early in the auditory pathway regulates both gain control and the representation of temporal auditory cues in the cochlear nuclei of non-oscines.

Our findings in the zebra finch are consistent with a prominent role of GABA-mediated inhibition at early stages of the ascending auditory pathway of songbirds. The moderately high density of GABA-positive puncta and neuropil we observed in NM and NL could correspond to the innervation arising from SON. Indeed, relatively large GABAergic cells exist within SON that could correspond to inhibitory projection neurons. Thus, some basic aspects of GABAergic inhibition at the level of cochlear nuclei may be conserved between songbirds and chicks. Our results, however, also provide evidence for the presence of GABAergic cells in both the NM and NL of zebra finches. This finding contrasts with previous reports of very low numbers of such cells in the NM and NL of the chick and barn owl. Further studies with other GABAergic cell markers in both species would be helpful to further investigate this apparent species difference and to determine its potential impact on the physiology of these nuclei in songbirds. At any rate, significant species differences in the organization and development of the ascending auditory pathways have been previously described in birds. Such differences have been suggested to relate to specializations in auditory processing capabilities and strategies (Kubke and Carr, 2000; Kubke et al., 2004). By analogy, different evolutionary pressures might have contributed to a significantly larger GABAergic influence in the auditory brainstem of songbirds, as compared to other avian species. This neurochemical difference could thus be related to aspects of auditory processing that are of relevance to vocal learning, a behavior not found in the chick and barn owl, the main experimental avian models of brainstem auditory physiology.

GABAergic elements and GABA-mediated inhibition are also prominent at higher levels of the avian ascending auditory pathway. Nucleus MLd in the intercollicular complex (ICo) receives direct projections from SON and from cochlear nuclei, and is considered homologous to the mammalian inferior colliculus (IC) (Conlee and Parks, 1986). Research in both mammals and birds has shown that GABAergic transmission in the IC controls several aspects of auditory information coding, including the representation of sound intensity and location (Zheng and Knudsen, 1999; Knudsen et al., 2000; Pollak et al., 2003; Sivaramakrishnan et al., 2004). Inhibition through the GABA-A receptor has been shown to participate in the sharpening of auditory tuning-curves in the IC and at other sites along the ascending auditory pathway in both mammals and birds (Yang et al., 1992; Suga et al., 1997; Chen and Jen, 2000). Numerous GABAergic neurons are also present in the medial geniculate body (MGN), the main auditory nucleus of the mammalian thalamus, with significant species differences occurring in the number of such cells (Winer and Larue, 1996). Indeed, it has been suggested that an increase in inhibitory influence in the auditory thalamus across species might correlate with the complex processing required for speech-like communication signals (Winer and Larue, 1996).

Our data demonstrate that numerous GABAergic cells are present in the MLd of zebra finches, and suggest the existence of distinct GABAergic cell types, including small and more numerous cells that likely correspond to local inhibitory interneurons, as well as much larger cells. Interestingly, recent studies have revealed a significant inhibitory projection from the inferior colliculus to the medial geniculate nucleus (MGN) in mammals (Winer et al., 1995; Winer et al., 1996; Peruzzi et al., 1997;



Bartlett et al., 2000). In avian species, the equivalent circuitry consists in the projection from MLd to thalamic nucleus Ov, the avian equivalent of the mammalian MGN (Karten, 1967; Brauth et al., 1987). While this projection is likely to be predominantly excitatory, it could also contain an inhibitory component originating from putative GABAergic projection neurons in MLd. Consistent with this possibility is our observation that Ov displays a moderate level of GABAergic terminals. Alternatively, such terminals could arise from local connections, or from descending inhibitory projections targeting Ov. We also observed a high density of GABAergic neurons in Ov, consistent with the possibility that the density of such cells in the auditory thalamus may correlate with the complexity of thalamic auditory processing required for vocal communication (Winer and Larue, 1996).

Songbirds rely on the auditory processing of complex stimuli for the individual recognition that underlies behaviors such as territoriality, mate selection and courtship (Catchpole and Slater, 1995), as well as for song learning and for the maintenance of the stereotyped adult song (Konishi, 1965a; Nordeen and Nordeen, 1992; Leonardo and Konishi, 1999). Appropriately tuned auditory responses along the auditory pathway likely correlate with the perceptual processing of acoustic features of song. Based on the precedent in mammals (Suga et al., 1997; Ferragamo et al., 1998; Wenstrup, 1999; Ehret et al., 2003; Poirier et al., 2003), we suggest that MLd and Ov in songbirds participate in the shaping of auditory response properties that are relevant to birdsong representation, such as frequency tuning. Songbirds, including zebra finches, can discriminate frequencies with reasonable accuracy, as evidenced by their ability to match their own vocalizations to the tutor's song in the

context of vocal learning. More specifically, juveniles gradually shift the fundamental frequency of some syllables to maximize imitation (Tchernichovski et al., 2001). Such a process likely requires plastic changes in brain representations of song and could involve the dense GABAergic networks at the level of MLd and Ov. Although GABAergic inhibition has not been studied in the ascending auditory pathway of songbirds, the high prevalence of GABAergic elements in zebra finches is consistent with a key role of inhibition in the physiology of this pathway and, thus, in the auditory coding of birdsong.

### **GABAergic Elements in Auditory Telencephalic Areas**

GABAergic cells were highly abundant in auditory areas of the zebra finch telencephalon and appear to consist of distinct populations of inhibitory neurons. While the smaller cells most likely participate in local circuits, at least some of the large cells could represent inhibitory projection neurons, as seen in striatal song nucleus area X (Luo and Perkel, 1999a, b). Interestingly, the distribution of large versus small GABAergic cells in the auditory telencephalon was not symmetric. The majority of GABA-positive neurons in field L subfields L1 and L3 belonged to the smaller type, whereas in the thalamorecipient field L2a, particularly in its medial portion, the larger GABAergic cells were more prevalent. These findings are in accordance with the mRNA distribution of the zebra finch homologue of the 65 kD glutamic-acid decarboxylase (GAD65), the synthetic enzyme for GABA, in auditory areas of zebra finches (Pinaud et al., 2004). zGAD65-positive cells also segregate into two populations based on soma size and expression levels of zGAD65. While small

cells with relatively low zGAD65 levels are found throughout subfields L1 and L3 and the adjacent NCM and CMM, large neurons with high zGAD65 levels are found mostly in field L2a, where they are the predominant GABAergic cell type (Pinaud et al., 2004). Further studies are required to determine whether any of the large GABAergic cells in these early auditory telencephalic areas are projection neurons.

Higher-order auditory areas of the telencephalon are also involved in the auditory processing of birdsong and may play an important role in the formation of song auditory memories (Mello, 2002a; Mello et al., 2004). In particular, the caudomedial nidopallium (NCM) and mesopallium (CMM) display robust responses to birdsong auditory stimulation, as revealed by electrophysiological recordings and expression analysis of the activity-dependent gene *zenk* (Mello et al., 1992; Chew et al., 1995; Mello and Ribeiro, 1998; Gentner and Margoliash, 2003; Mello et al., 2004). Until recently, however, very little was known about inhibitory elements in these areas. Based on in-situ hybridization for zGAD65, we have recently estimated that 36-43% of the neuronal cells in caudomedial auditory structures are GABAergic (Pinaud et al., 2004). Our present estimates for the same areas based on GABA immunoreactivity are significantly higher (40-55% range). A likely explanation for this discrepancy is that GABAergic cells expressing only the 67kD isoform of GAD were not detected with the GAD65 probe, but clarifying this issue awaits molecular probes specific for GAD67. Nonetheless, double *in situ* hybridization for zGAD65 and *zenk* showed that about 42% of the cells that express *zenk* in response to song stimulation are GABAergic (Pinaud et al., 2004). Altogether, these findings provide clear evidence that GABAergic neurons participate in the auditory response to

birdsong and suggest that they might contribute to the perceptual processing that underlies song memory formation and vocal-learning.

An intriguing finding of the present work is the high density of GABA-positive neurons in various auditory areas of the songbird telencephalon (39-52%) compared to mammalian auditory areas, where GABAergic cells have been estimated to represent 25-30% of the overall neuronal population, being primarily concentrated in cortical layers 2-4 (Gabbott and Somogyi, 1986; Jones, 1993). It has been proposed that the avian brain, even though lacking for the most part a cortical laminar organization, contains neuronal populations that are comparable to those in various layers of the mammalian cortex (Karten, 1991; Mello et al., 1998; Reiner et al., 2004). Although great caution should be exercised in such a comparison, the various areas that compose the auditory system may correspond to some extent to the neuronal populations of different layers of the mammalian auditory cortex (Wild et al., 1993; Vates et al., 1996; Mello et al., 1998). For instance, subfield L2a might correspond to the auditory cortical layer 4, given that it is the main recipient of direct thalamic auditory projections. L2a targets including NCM and CMM might correspond in part to supragranular layers of auditory cortical areas and arcopallial cells (i.e., cells in the cup region) that originate long descending projections to auditory nuclei would correspond to infragranular layers. Thus, the caudomedial lobe that encompasses medial field L2a, NCM and CMM may contain an over-representation of cell populations (e.g. GABAergic cells) seen in granular and supragranular layers of the mammalian auditory cortex, should such a correspondence prove correct.

Only vocal learning birds possess telencephalic vocal control nuclei. While the reason may primarily be that vocal learning requires vocal motor representations within telencephalic circuits (see below), it is also possible that vocal control circuits in song learners need to have direct access to information processed in telencephalic auditory areas. Our current data attest to the prominence of GABAergic elements in the latter areas in zebra finches. In addition, experience-dependent plasticity has been described in auditory telencephalic areas, namely song-specific habituation in NCM and experience-dependent changes in unit selectivity in CMM (Chew et al., 1995; Gentner and Margoliash, 2003). Although not directly tested, GABAergic mechanisms could be involved in regulating plasticity and other basic aspects of the physiology of these areas. In fact, patch-clamp recordings of NCM slices have given indication that NCM is under the influence of a powerful inhibitory network at rest, whose action may prevent NCM from runaway excitation upon its activation (Pinaud et al., 2004). Further studies are required to test whether GABAergic influence at this level of the brain can affect perceptual aspects of vocal learning such as the acquisition of song auditory memories or the feedback evaluation of song.

### **GABAergic Elements in the Song Control System**

The relatively high densities of GABAergic neurons we observed in all song control nuclei suggests that inhibitory transmission is key to the physiology of the song control system. In general, these observations are consistent with the high incidence of GABAergic cells in mammalian pallial and striatal areas, where they provide the major inhibitory component of local processing networks (Smith et al.,

1987; Gerfen, 1988; Smith and Bolam, 1990). As in auditory areas, the marked variability we saw in GABAergic soma size in all song nuclei suggests the possible existence of distinct subpopulations of inhibitory cells.

The high density of GABAergic cells in the zebra finch equivalent of the basal ganglia, including song nucleus area X, is consistent with the prevalence of GABAergic neurons in the basal ganglia in mammals. Interestingly, area X has mixed striatal and pallidal features, the latter consisting of GABAergic cells that project to thalamic nucleus DLM (Luo and Perkel, 1999a, b). It seems reasonable to suggest that the large GABAergic cells in area X, which were relatively few and sparse, could correspond to the inhibitory neurons that participate in the area X to DLM projection. Both area X and DLM are components of the song system's anterior forebrain pathway, which is implicated in song learning but not in the motor control of song production (Bottjer et al., 1984; Sohrabji et al., 1990; Scharff and Nottebohm, 1991). This pathway is equivalent to mammalian basal ganglia-thalamocortical loops that are involved, among other things, in the learning and performance of movement sequences that require complex sensory-motor integration (Simpson and Vicario, 1990; Jarvis and Nottebohm, 1997; Jarvis et al., 1998). We also observed that area X contains a high density of small GABAergic cells. They presumably correspond to GAD-positive cells that do not participate in the X-to-DLM projection (Luo and Perkel, 1999a) and that are thought to be part of local processing networks within area X.

The pallial song control nuclei (LMAN, HVC and RA) also contain several small GABAergic neurons that are most likely local inhibitory cells. Our measurements,

however, give indication that GABAergic cell size is predominantly large in all pallial song nuclei. To some extent, this may reflect the generally larger neuronal size in these nuclei as compared with adjacent areas. It is possible, however, that long-range inhibitory projections are not specific to the anterior forebrain pathway and that at least some of the large GABAergic cells in pallial song nuclei are projection neurons. In RA, for instance, some neurons that project to nXIIts are immunopositive for the calcium-binding protein parvalbumin (PV) (Wild et al., 2001). Because PV-positive cells are thought to represent a subpopulation of GABAergic neurons (Reynolds et al., 2001; Reynolds et al., 2004), it appears that the RA-to-nXIIts projection is partly GABAergic and may thus exert a partly inhibitory effect on this medullary RA target (Wild et al., 2001). In contrast, recent evidence indicates that the HVC neurons that project to either area X or to RA do not co-express parvalbumin, calbindin or calretinin (Wild et al., 2005). Rather, these calcium-binding proteins appear to define populations of HVC interneurons. Because the three proteins co-localize highly with GABA and together are thought to comprise most or all GABAergic neurons (DeFelipe, 1997), we conclude that the GABAergic cells in HVC are very likely interneurons and not projection neurons.

GABAergic transmission in RA plays a significant role in the generation of appropriate song structure, and has been proposed to regulate the initiation and control of vocal output (Vicario and Raksin, 2000). In addition, the synchronous output from RA projection neurons is thought to be controlled by the activation of local GABAergic interneurons (Spiro et al., 1999). Interestingly, PV-positive cells in the rodent hippocampus have been reported to reliably display fast-firing behavior,

while GABAergic cells that express other calcium-binding proteins, namely calbindin and calretinin, do not exhibit consistent firing behavior (Kawaguchi et al., 1987). These observations are of potential relevance to RA physiology, where the fast neuronal firing required to reliably generate song structure could be related to the prominent local GABAergic network described here and to the high density of PV-positive cells (Wild et al., 2001). Similar roles for GABAergic transmission, mediated through GABA-A receptors, have been shown for song nucleus LMAN, where firing behavior is controlled by inhibitory interneurons (Bottjer et al., 1998). Altogether, our current data and the physiological studies discussed above indicate that GABAergic elements are present and quite prevalent in song control nuclei, and that inhibition plays a significant role in the normal physiology of the song system.

In sum, our data have provided a detailed characterization of GABAergic elements throughout the ascending auditory pathway and song control nuclei of the zebra finch brain. These findings should help in the interpretation of previous anatomical and physiological studies in zebra finches, as well as stimulate future investigations on the properties of inhibitory networks within the songbird brain.



## **CHAPTER 3**

### **GABAERGIC NEURONS PARTICIPATE IN THE BRAIN'S RESPONSE TO BIRDSONG AUDITORY STIMULATION**

## INTRODUCTION

The study of learned vocalizations in oscines has contributed extensively to our understanding of the neuronal basis of vocal communication and vocal learning. The learning and production of song and of certain calls depend on the integrity of a set of interconnected telencephalic nuclei known as the song control system (see reviews in (Brenowitz, 1997). Both the acquisition of learned song and the maintenance of song structure after learning require auditory feedback and, thus, depend on intact hearing (Nordeen and Nordeen, 1992; Leonardo and Konishi, 1999). In addition, the auditory processing of birdsong is required for song perception and discrimination, and is essential for behaviors such as territorial defense and mate selection (Catchpole and Slater, 1995; Kroodsma and Miller, 1996).

The caudomedial mesopallium (CMM; formerly known as the caudomedial hyperstriatum ventrale, or CMHV) and the caudomedial nidopallium (NCM; formerly known as the caudomedial neostriatum - we use here the new avian brain nomenclature described in Reiner et al., 2004) have been implicated in the auditory processing, discrimination and perception of birdsong. These structures receive direct or indirect input from the primary telencephalic auditory zone, field L, are reciprocally connected, and project mainly to other central auditory areas (Vates et al., 1996). Altogether, these telencephalic auditory areas have been postulated to comprise the avian homologue of the mammalian primary auditory cortex. According to this view, thalamo-recipient field L2 would correspond to the granular layer, while NCM and CMM would correspond to supragranular layers of the auditory cortex

(Karten and Shimizu, 1989; Wild et al., 1993; Mello et al., 1998; Reiner et al., 2004). NCM and CMM show evoked electrophysiological responses to song auditory stimulation that have longer latency and are more selective towards complex stimuli than those in field L (Chew et al., 1995; Sen et al., 2001; Gentner and Margoliash, 2003). In NCM, the electrophysiological responses to song show a rapid decrease, or habituation, upon repeated presentations of the same song (Chew et al., 1995). This “habituation” is song-specific, as a full response can be reinstated upon presentation of a novel song, suggesting a possible contributing mechanism for auditory discrimination of birdsong.

Importantly, NCM and CMM show robust induction of the immediate early gene *zenk* (we use *zenk* for the gene and ZENK for the protein) in response to auditory stimulation with conspecific song (Mello et al., 1992; Mello and Clayton, 1994). Expression of *zenk* (a.k.a. *zif-268*, *egr-1*, *NGFI-A*, and *krox-24*) is activity-dependent and is, thus, useful to identify cells that respond to specific stimuli or behavioral contexts (reviewed in Chaudhuri, 1997). *zenk* expression has revealed brain areas involved in the response to song auditory stimulation (including NCM and CMM; reviewed in Mello, 2002b) or in the motor control of song production (Jarvis and Nottebohm, 1997; Jarvis and Mello, 2000; Jarvis et al., 2000) in awake, unrestrained animals, without interference with natural behaviors (Jarvis et al., 1997). *zenk* expression analysis has also been invaluable to study the functional organization of song-responsive areas. For example, the *zenk* response in NCM is highest for conspecific song than for other stimuli, and it shows a song-specific decrease, or habituation, upon repeated presentations of the same song (Mello et al., 1995). In

canaries, *zenk* expression patterns in NCM resulting from stimulation with song syllables have a topographical organization based on frequency and tuned to features present in natural vocalizations (Ribeiro et al., 1998). Regional variations of the *zenk* response in NCM that correlate with acoustic properties of the song stimulus have also been described in starlings (Gentner et al., 2001). These observations indicate that the *zenk* response in NCM reflects the acoustic properties of the song stimulus, and that NCM participates in song auditory processing and discrimination. *zenk* expression in NCM may also be linked with aspects of song auditory memory. For example, ZENK levels in adult NCM correlate with the degree to which the bird copied the song used as a stimulus during the vocal learning period (Bolhuis et al., 2000; Bolhuis et al., 2001). In addition, the initiation of *zenk* inducibility by song in NCM correlates with the beginning of the sensory acquisition period for song in zebra finches (Jin and Clayton, 1997).

GABAergic mechanisms play a pivotal role in the processing of auditory stimuli, particularly in species that depend heavily on the auditory system for normal behavior (Fujita and Konishi, 1991; Yang et al., 1992; Suga et al., 1997; Zheng and Knudsen, 1999; Chen and Jen, 2000; Zheng and Knudsen, 2001). The GABAergic system has also been implicated in mediating some aspects of experience-dependent plasticity in a number of sensory modalities (Zheng and Knudsen, 1999; Tremere et al., 2001b; Morales et al., 2002). Here we used molecular, cellular and electrophysiological approaches to study the contribution of GABAergic mechanisms to birdsong auditory processing. We found a high incidence of GABAergic cells and a prevalence of GABAergic synapses in telencephalic auditory regions. Moreover, we

found that a large proportion of GABAergic cells participate in the brain's response to song stimulation. We conclude that GABAergic mechanisms participate in the physiology of brain areas that contribute to song auditory processing, perception and possibly song memory formation.

## **MATERIAL AND METHODS**

**Animals:** We used 30 adult zebra finches (*Taeniopygia guttata* - 14 females; 16 males). Animals were purchased from a breeder and maintained in our local aviary. Experimental protocols utilized in this study were approved by OHSU's Institutional Animal Care and Use Committee and are in accordance with NIH guidelines.

**zGAD65 cloning:** Genbank GAD65 sequences from several species were aligned and a pair of primers (forward: ccttcacatctgaacacagtc; reverse: accagaagcagacgtttgtgtg) designed to amplify a fragment spanning exons 3 to 9 of the mouse cDNA sequence (Figure 1A) from a zebra finch brain cDNA library. This library has been screened successfully for several genes expressed in the brain of zebra finches (Holzenberger et al., 1997; Denisenko-Nehrbass et al., 2000). We performed 30 PCR cycles, each consisting of 95°C for 45 sec, 44.2°C for 1 min and 72°C for 45 sec, using Taq polymerase and standard PCR buffer. The resulting band was cloned in Bluescript and its identity was confirmed by sequencing.

**Northern-Blot Analysis:** Total RNA from the telencephalon of an adult male zebra finch was extracted according to Chomczynski and Sacchi (1987). Ten micrograms of total RNA were run on a MOPS/formaldehyde gel and blotted onto a nylon filter according to standard protocols (Sambrook et al., 1989). The filter was hybridized to a <sup>33</sup>P-labeled antisense riboprobe for zGAD65 using established protocols, as described in Clayton et al. (1988), with modifications (detailed in Mello et al., 1997).

**Song Stimulation:** Birds were taken from the aviary and placed overnight individually in small soundproof boxes (30x12x11 inches), under a 12/12hr light/dark cycle (lights on at 7 am). The day following isolation, stimulated birds (n=25) were presented for 30 min with playbacks of a medley of novel conspecific songs (70dB mean SPL), while control birds were not stimulated. The stimulation paradigm used is known to induce a robust induction of the *zenk* gene in auditory areas of the zebra finch brain (Mello et al., 1992; Mello and Clayton, 1994). Unstimulated birds (n=5) were used to ascertain the effectiveness of song stimulation and were not included in the quantifications. Birds used for *in-situ* hybridization were sacrificed, immediately following the end of stimulation, while birds used for ICC were maintained in the soundproof boxes for an additional hour, and then sacrificed.

**Tissue Preparation:** For in-situ hybridization, birds (n=19 song-stimulated and 3 unstimulated) were sacrificed by decapitation and brains were quickly dissected, frozen in a dry-ice/propanol bath in embedding medium (Tissue-Tek; Sakura Finetek, Torrance, CA), and cut parasagittally on a cryostat, at 10µm. For ICC, birds (n=5 song-stimulated and 3 unstimulated) were sacrificed with an overdose of Nembutal and perfused transcardially with 20 ml of 0.1M phosphate buffer (PB; pH=7.4) followed by 60 ml of a 1% paraformaldehyde and 2% glutaraldehyde in PB solution. Brains were then dissected and cryoprotected by immersion in a 30% sucrose solution at 4°C until equilibrated. Brains were then frozen as for *in-situs*, sectioned parasagittally or coronally on a cryostat at 16µm, and thaw-mounted on Superfrost

Plus slides (Fischer Scientific, Pittsburgh, PA). Sections were then dried and stored at  $-80^{\circ}\text{C}$  until further processing.

**Labeling of zGAD65 Riboprobes:** Bluescript plasmids containing zGAD65 and *zenk* were isolated from bacteria using Qiagen miniprep kit (Qiagen Inc., Valencia, CA), linearized with the appropriate restriction enzymes, and purified using Qiagen PCR purification kit (Qiagen Inc., Valencia, CA).  $^{33}\text{P}$ -labeled sense and antisense riboprobes were generated and purified as previously described in detail (Mello et al., 1997), and used for Northern and in situ hybridization analysis.

**Radioactive In-situ Hybridization:** We used a previously described protocol (detailed in Mello et al., 1997). Briefly, glass-mounted sections were fixed in a 3% paraformaldehyde solution for 5 minutes, rinsed in 0.1M PBS, and dehydrated in a standard series of alcohols. Sections were then acetylated for 10 minutes in a solution containing 1.35% triethanolamine and 0.25% acetic anhydride in water, rinsed 3 times with 2X SSPE, dehydrated in the alcohol series and air-dried. After addition of hybridization solution containing the zGAD65 probe (16  $\mu\text{l}$  per section of solution containing formamide 50%, 2X SSPE, 2  $\mu\text{g}/\mu\text{l}$  tRNA, 1  $\mu\text{g}/\mu\text{l}$  BSA, 1  $\mu\text{g}/\mu\text{l}$  poly-A in DEPC-treated water and  $5 \times 10^5$  cpm of labeled probe), sections were coverslipped, sealed by immersion in mineral oil, and incubated overnight at  $65^{\circ}\text{C}$ . Sections were then rinsed twice in chloroform, decoverslipped in 2X SSPE, and washed by incubating sequentially for 1 hr at room temperature (RT) in 2X SSPE, 1.5 hr at  $65^{\circ}\text{C}$  in 2X SSPE containing 50% formamide, and twice for 30 minutes at  $65^{\circ}\text{C}$  in 0.1X



SSPE. Sections were then dehydrated in a series of alcohols and analyzed by phosphorimager autoradiography and/or processed for emulsion autoradiography, followed by cresyl violet counterstaining. Radioactive in-situ hybridization was used to investigate the overall brain distribution of zGAD65 at low-power magnification (phosphorimager autoradiograms) and for an assessment of cell types based on cytoarchitectonics (emulsion combined with Nissl-counterstaining).

**Fluorescence In-Situ Hybridization (FISH):** Sense and antisense zGAD65 probes were labeled using digoxigenin (DIG)-labeled UTP (as in Mello et al., 1997), adding a DIG nucleotide labeling mix (Roche Diagnostics Corp.) to our standard probe labeling buffer. The resulting products were purified in G-50 columns and evaluated for size and yield by agarose gel electrophoresis. One  $\mu$ l of the final purified reaction (added to the 16 $\mu$ l of hybridization solution) was used per section. Hybridization and washing steps were as above for radioactive in-situs, except that after the final wash sections were processed for detection of the DIG-labeled probes using tyramide signal amplification (TSA). Briefly, sections were incubated in 0.3% hydrogen peroxide in TNT buffer (0.1M Tris HCl, pH=7.2-7.4, 5M NaCl, and 0.05% Triton-X 100 in DEPC-treated water) for 10 minutes to inactivate endogenous peroxidase. Sections were then washed in TNT buffer (3 x 5 mins) and incubated for 30 mins in a blocking solution (TNB) consisting of TNT buffer containing 2 mg/ml of bovine serum albumine. Next, sections were incubated for 2 hr at RT with a peroxidase-conjugated anti-DIG antibody (1:100 dilution in TNB buffer; Roche Diagnostics Corp., Indianapolis, IN), followed by washes (3 x 5 mins) in TNT buffer. The

sections were then incubated for 2 hr in a solution containing tyramide conjugated with a fluorophore (Alexa 488 or Alexa 594; Molecular Probes, Eugene, OR). The dilution used was 1:100 in amplification buffer provided by the manufacturer.

Sections were then washed (3 x 5 mins) in TNT buffer, counterstained in Hoechst, washed in TNT (3 x 5 mins) and coverslipped with aquamount. SlowFade Light Antifade kit (Molecular Probes, Eugene, OR) was used in sections analyzed by confocal microscopy. To control for the specificity of the label, the same procedure was performed with omission of the anti-DIG antibody. FISH was used for a high resolution definition of cellular morphology in the analysis of zGAD65 expression.

**Double Fluorescence In-Situ Hybridization (dFISH):** dFISH was used for double-labeling analysis of zGAD65 and *zenk* expression. First, sections were hybridized simultaneously with the antisense probes for zGAD65 (DIG-labeled) and for *zenk* (biotin-labeled), as described above for FISH. After hybridization and washes, sections were developed for zGAD65 labeling, as described above for FISH, using a peroxidase-conjugated anti-DIG antibody followed by incubation for 2 hr in TNT containing tyramide coupled with Alexa 594 (1:500 dilution in TNT). Sections were then incubated in 0.3% hydrogen peroxide for 10 mins to inactivate any remaining peroxidase. The biotinylated-*zenk* probe was then detected by first incubating the sections for 2 hr with a peroxidase-conjugated anti-biotin antibody (Vector Laboratories, Burlingame, CA; 1:500 dilution in TNT). Sections were then incubated for 2 hr in Alexa 488-coupled tyramide (1:500 diluted in TNT), washed (3 x 5 mins) in TNT, counterstained with Hoechst and washed further (3 x 5 mins) in TNT.

Sections were then coverslipped with antifade solution. We also performed the entire procedure above with biotin-labeled zGAD65 and DIG-labeled *zenk* probes, and with the reverse combination of tyramide reagents. To control for the effectiveness of the peroxidase inactivation between labels, we performed additional dFISH reactions omitting the anti-DIG antibody, in which case, signal could only be observed in the appropriate filter. We also ran additional controls omitting the anti-biotin to control for the specificity of the biotin labeling.

**Double-Label Immunocytochemistry (dICC):** Sections were removed from the – 80°C freezer and air-dried at RT for 30 mins. Slides were then immersed in PB for 30 mins, followed by incubation for 2 hr at RT in a blocking buffer (BB) that consisted of 0.5% albumin and 0.3% Triton X-100 in 0.1M PB. Next, sections were incubated overnight at 4°C with a rabbit anti-egr-1 polyclonal antibody (Santa Cruz Biotechnology, Santa Cruz, CA), that recognizes ZENK protein in songbird brain tissue (Mello and Ribeiro, 1998) in a humidified chamber followed by a 2 hr incubation with a goat anti-rabbit biotinylated antibody (Vector Laboratories, Burlingame, CA; 1:200 dilution in BB) at RT. Sections were then incubated for 2 hr at RT with ABC (Vector Laboratories, Burlingame, CA). Finally, tissue was incubated in a filtered solution containing 0.03% diaminobenzidine (DAB), 0.15% Nickel sulfate and 0.001% hydrogen peroxide in PB. After 8-15 minutes, the reaction was stopped by immersion in PB. Each of the steps above was separated by washes (3 x 10 min each) in PB. After signal was developed in the DAB incubation step, sections were washed (3x10 min) in PB and incubated in a 0.3% hydrogen peroxide

solution for 20 min, to inactivate any peroxidase activity. Sections were then washed in PB, followed by another series of incubations using the anti-GABA antibody (Chemicon International, Temecula, CA; 1:200 dilution in BB) essentially as detailed above for ZENK ICC, except that nickel sulfate was not added to the DAB solution. The use of fluorescence ICC was not possible due to the high tissue auto-fluorescence when using the glutaraldehyde perfusion required GABA fixation. Sections were then dehydrated in a standard series of alcohols, delipidized in xylene and coverslipped with Krystalon (EM Science, Gibbstown, NJ).

**Cell Counts:** We used a Nikon Eclipse E-600 microscope equipped with a motorized stage drive and the Lucivid system, and conducted the mapping analysis with Neurolucida software (Microbrightfield Inc., Colchester, VT) installed in a PC. To estimate local densities of labeled cells, a regular grid of 100x100 $\mu$ m squares was superimposed on sections containing NCM after processing for FISH, dFISH, or Nissl staining. For FISH and dFISH, five such fields over rostral and caudal NCM each were counted per bird for cells labeled for zGAD65, *zenk*, or both mRNAs. Hoechst was used as a counterstaining method to identify and count all neurons within the same fields. In Hoechst-stained sections viewed under the proper fluorescence filter, neuronal cells typically exhibit lightly-, non-homogeneously-stained nuclei, often with prominent nucleoli, whereas glial cells usually have strongly-, homogeneously-stained nuclei; individual cells, even within clusters, can be readily identified. The relative density of zGAD65-labeled cells was calculated for each bird as the percentage of such cells relative to the neuronal cell estimates based

on Hoechst. The average results across fields were averaged across birds (n=3 birds per each staining method). For dFISH, *zenk*-positive only or double-labeled cells were mapped and counted as above by alternating the appropriate fluorescence filters in each grid area examined. The relative density of double-labeled cells was estimated as the percentage of such cells relative to the number of *zenk*-labeled cells in each field. Average results across fields were then averaged across birds. Our estimates of neuronal density in NCM using the Hoechst and Nissl methods yielded very similar results. Because all our estimates were of relative percentages of cells over sampled fields, rather than total number of cells within each class, we did not use stereological methods (as discussed in Coggeshall and Lekan, 1996; Saper, 1996). The dICC material was not amenable to quantification because a large number of cells displayed weak nuclear or cytoplasmic staining and thus double-labeled cells within the low intensity range of staining could not be reliably identified. In addition, cells with very high GABA content were often saturated in our preparations, thus possibly occluding the ZENK ICC signal.

**Imaging/Photomicrographs:** Photomicrographs were acquired with a Digital camera (DVC, Austin, TX) coupled to the microscope. We used Neurolucida software to acquire digital images, and Adobe Photoshop to assemble photomicrograph plates.

**Whole-Cell Patch-Clamp Electrophysiology:** Animals were decapitated after overnight isolation in a soundproof box. Brains were quickly dissected and placed in artificial cerebrospinal fluid (aCSF) solution for 10-20 minutes at 4°C, and 300µm

thick parasagittal sections (0.2mm lateral) containing NCM and adjacent areas (field L and CMM) were obtained on a vibratome (Leica Microsystems, Heerbrugg, Switzerland). We also prepared slices that contained NCM only by dissecting this structure from the surrounding tissue. Whole-cell patch-clamp recordings were performed in normal aCSF at RT. aCSF solution consisted of (mM): NaCl (125), KCl (2.5), NaHCO<sub>3</sub> (25), NaH<sub>2</sub>PO<sub>4</sub> (1.25), Glucose (25), CaCl<sub>2</sub> (2), MgCl<sub>2</sub> (1), ascorbic acid (0.4), sodium pyruvate (2), myo-inositol (3), pH 7.4 when bubbled with 95%CO<sub>2</sub>/5%O<sub>2</sub>. Soft, thin walled glass pipettes (WPI, Sarasota, FL) were pulled using a Narishige vertical puller (Narishige, East Meadow, NY). Resistance of the pipettes in the bath was in the 3-7 MΩ range. The internal solution consisted of (mM): Cs-methanesulfonate (90), CsCl (20), MgCl<sub>2</sub> (1), Na<sub>2</sub>-phosphocreatine (5), HEPES (40), TEA-Cl (10), EGTA (0.2), ATP-Mg (2), GTP (0.2), pH=7.3 with CsOH, 310 mOSM. To isolate spontaneous GABAergic post-synaptic currents, slices were perfused with 0.5μM tetrodotoxin (TTX) and glutamate receptor antagonists NBQX (5μM) and dl-AP5 (50μM). The holding potential was -70 or -80 mV. Bicuculline concentration used was 50μM. Data were collected using a double EPC-9 patch-clamp amplifier and HEKA software (HEKA, Germany). Signals were sampled between 10 and 50 μsec and filtered at 2.5kHz. All off-line analysis including the determination of the decay kinetics for the GABAergic minis was conducted with IgorPro software (Wavemetrics, Lake Oswego, OR).

## RESULTS

### Isolation of zGAD65

To clone the zebra finch homologue of the 65kD isoform of glutamic acid decarboxylase, we identified conserved domains in the gene by aligning the human, mouse and chicken sequences, and designed PCR primers to amplify a fragment of about 700 bp, extending from exon 3 to exon 9 of mouse GAD65 (Figure 1A). The predicted amino acid sequence of the resulting fragment spanned residues 276 to 507 of the mouse gene (nucleotides 824 to 1522; GenBank accession # BC018380; Figure 1B). The homologies with GAD65 of other species were 85% (mouse) and 93% (chicken) at the nucleotide level, and 95% (mouse) and 98% (chicken) at the amino acid level (Figure 1B). The homologies with GAD67, the gene encoding the 67kD GAD isoform, were lower (respectively 76% and 78% at the amino acid level with mouse and chicken GAD67). We named our clone zGAD65 (GenBank accession # AY364313).

Northern-blot analysis of total RNA from zebra finch telencephalon with an antisense zGAD65 riboprobe revealed a doublet (Figure 1C), whereas no band was detected with the sense probe (not shown). Although the significance of the doublet is unclear, the bands (4.1 and 4.4 Kb) are close to the expected size based on the chicken and mouse sequences. It seems unlikely that our probe cross-reacts with the GAD67 isoform, since that transcript is approximately 2Kb shorter in mice (Ahman et al., 1996).

### **zGAD65 Expression**

In-situ hybridization with an antisense riboprobe revealed the anatomical distribution of zGAD65 expression in zebra finches (Figure 2). In general, the results were in close accordance with the known distributions of GAD65 in mammals and non-songbird avian species (Veenman and Reiner, 1994; Bolam et al., 2000). For instance, zGAD65 expression was high in the striatum (Figure 2B) within the basal ganglia. Our probe also labeled well-known GABAergic cell populations such as cerebellar Purkinje cells (Figure 2H) and large neurons in the globus pallidus (Figure 2I). High zGAD65 expression was also found throughout pallial regions of the telencephalon (Figure 2B), including the caudomedial auditory areas field L2 (where expression was particularly high), NCM and CMM. The present study focuses on the latter three areas; a more detailed analysis will be presented elsewhere. Importantly, no signal was detected with a sense probe (Figure 2B, inset).

Emulsion autoradiography analysis revealed numerous zGAD65-expressing cells in NCM, field L2, and CMM (Figure 2 C-F). Based on a qualitative assessment (density of emulsion grains per cell), there appears to exist two types of zGAD65 positive neurons: cells with very high (Figure 2G; arrowhead) and cells with moderate to low zGAD65 expression (Figure 2G; arrow). The distribution of these two kinds of cells differs across areas (Figure 2D-F), with a higher density of the high expression cell type occurring in field L2 (Figure 2E, arrowheads), and the low-to-moderate expression type being most numerous in NCM (Figure 2D). The expression level of zGAD65 in the high-expression cell type (Figure 2G, arrowhead) is



comparable to that in Purkinje and pallidal cells (Figure 2H and I). No apparent qualitative differences in zGAD65 expression in telencephalic auditory areas were observed when comparing males versus females, or song-stimulated versus unstimulated birds (not shown).

We also used fluorescence in-situ hybridization (FISH) with digoxigenin (DIG)-labeled probes to study the expression of zGAD65 in field L2, NCM and CMM. Due to high spatial resolution, this method (with Hoechst counterstaining for nuclei) facilitates the identification of individual labeled neurons, particularly within cell clusters (Figure 3B). Numerous zGAD65-positive neurons were seen in NCM (Figure 3A), field L2, and CMM (not shown), whereas no signal was observed when the anti-DIG antibody was omitted. Our estimates of the density of GABAergic cells, expressed as the percentage of zGAD65-labeled cells relative to the total number of neurons per area (means + S.E., n= 3 birds), were  $39.7 \pm 0.2$  and  $38.2 \pm 1.4$  in caudal and rostral NCM respectively,  $35.8 \pm 1.1$  in field L2 and  $43.3 \pm 0.9$  in CMM, demonstrating the high incidence of GABAergic cells in telencephalic auditory areas. While most cells had comparable expression levels of zGAD65 based on a qualitative assessment of FISH sections, a small number of cells were very strongly labeled (Figure 3C; compare arrows and arrowheads). Cells of this latter type tended to be large and were more abundant in field L2 (not shown) than in NCM and CMM.

### **NCM Contains Active GABAergic Synapses**

To investigate the presence of active GABAergic synapses, we used whole-cell patch-clamp electrophysiology in slices, focusing on NCM (n = 12 cells from 7

birds). To isolate spontaneous GABAergic post-synaptic currents, slices were perfused with TTX and glutamate receptor antagonists. Under these conditions, we observed a number of miniature inhibitory post-synaptic events in all recorded cells (Figure 4A, top panel). The current magnitude of these events ranged between 8 and 40 pA. Furthermore, these GABAergic currents reverted around  $-39\text{mV}$ , which is in line with the predicted reversal potential for chloride. Importantly, application of bicuculline methiodide (BMI), a GABA-A receptor antagonist, blocked the occurrence of all miniature events (Figure 4A, bottom panel), indicating the existence of active GABAergic transmission in NCM, mediated by GABA-A receptors. The kinetics of these miniature inhibitory post-synaptic currents (mIPSCs) were further analyzed and presented an average decay time constant where  $\tau = 6.921$  milliseconds ( $n=4$  animals, 20 minis per cell) (Figure 4B). This time course agrees with previously documented time courses for GABA-A mediated mIPSCs in other preparations, in which the decay time constant can range from 4 to 11 milliseconds (Salin and Prince, 1996; Hollrigel and Soltesz, 1997; Smith et al., 2000). In TTX-free preparations, we also observed, upon BMI application, the appearance of bursts of large and asynchronous post-synaptic currents of putative excitatory origin (examples in Figure 4C). These bursts were observed in slices containing NCM and areas that provide input to NCM (field L and CMM), as well as in slices containing NCM only (not shown). Finally, the post-synaptic currents observed in the presence of BMI displayed a reversal potential of  $0\text{mV}$ , which suggests that these events are excitatory in nature. Altogether, our findings indicate that excitatory NCM neurons are tonically inhibited by local GABAergic networks.

### **Inhibitory Neurons in Auditory Processing Areas are Song-Responsive**

To test whether some of the numerous GABAergic neurons in NCM and CMM might directly respond to birdsong stimulation, we used song-induced *zenk* expression to reveal song-responsive neurons in these areas (field L2 was not included because it does not show song-induced *zenk* expression). We developed a double fluorescence in-situ hybridization (dFISH) procedure to detect *zenk* and zGAD65 mRNAs in the same brain sections from birds stimulated with conspecific birdsong. We found that several zGAD65-positive cells are also labeled for *zenk* mRNA and, thus, are song-responsive (Figure 5A, top two rows). Quantification of dFISH revealed that  $42.2\% \pm 2.2$  (mean  $\pm$  S.E., n=3 song-stimulated birds) of *zenk*-expressing cells in NCM are GABAergic, the remaining 57.8% presumably consisting of excitatory neurons. From the overall *zenk*-expressing population in CMM,  $33.8\% \pm 1.0$  co-expressed zGAD65 (mean  $\pm$  S.E., n=3 song-stimulated birds). We also found a considerable number of *zenk*-negative GABAergic cells (Figure 5A, third row), representing either GABAergic cells that are not song-responsive, or cells that respond to acoustic features that were absent in the song stimuli used. The three cell types above were found throughout NCM and CMM, without any obvious topographical distribution (Figure 5B). As expected, *zenk* expressing cells in unstimulated control birds were very few or absent and were not counted.

To independently test whether GABAergic neurons in NCM are song-responsive, we also developed a double-labeling ICC procedure for GABA and for ZENK protein. This procedure, due to the differential subcellular localization of the

antigens, revealed double-labeled cells with a dark-blue nuclear staining (ZENK) and a brown cytoplasmic staining (GABA). Several GABAergic neurons in NCM (Figure 6A and C) and CMM (not shown) of song-stimulated birds expressed ZENK protein in response to song auditory stimulation, confirming the existence of song-responsive GABAergic cells in these areas. In addition, several ZENK protein-expressing cells were negative for GABA and most likely represent excitatory song-responsive neurons (Figure 6D). Finally, several GABAergic cells did not express ZENK protein (Figure 6A, arrows; 6B). In unstimulated birds, ZENK-labeled cells were very few or absent and thus were not counted. These findings provide direct evidence that GABAergic cells participate in the physiological response to song auditory stimulation.

**Figure 3.1) zGAD65 cloning**

(A) Schematic diagram of the mouse GAD65 cDNA. Numbers indicate exons and arrows indicate the locations of the primers designed to amplify the zebra finch homologue (zGAD65).

(B) Alignment of the predicted aminoacid sequences of zGAD65 with those of the chicken (gGAD) and mouse (mGAD) homologues. Boxed regions indicate residue identity.

(C) Northern-blot of total telencephalic RNA from adult zebra finch probed with zGAD65. Arrows indicate two bands identified by probe (4.1 and 4.4 Kb in size).



**B**

zGAD65 FTSEHSHFSVKKGAAALGIGTDSVILRCDERGKMIPSDL  
 gGAD65 FTSEHSHFSVKKGAAALGIGTDSVILRCDERGKMIPSDL  
 mGAD65 FTSEHSHFSVKKGAAALGIGTDSVILRCDERGKMIPSDL 315

zGAD65 ERRIVEAKDKGLVPFLVSATAGTTVYGAFOPLIAIADICK  
 gGAD65 ERRILEAKDKGLVPFLVSATAGTTVYGAFOPLIAIADICK  
 mGAD65 ERRILEAKDKGLVPFLVSATAGTTVYGAFOPLIAIADICK 355

zGAD65 KYKIWMHVDGAWGGGLLSRKKKKWKLNGVERANSVTWNPH  
 gGAD65 KYKIWMHVDGAWGGGLLSRKKKKWKLNGVERANSVTWNPH  
 mGAD65 KYKIWMHVDGAWGGGLLSRKKKKWKLNGVERANSVTWNPH 395

zGAD65 KMMGVPLQCSALLVREEGLMOSCNQMHASYLFQDDKHYDL  
 gGAD65 KMMGVPLQCSALLVREEGLMOSCNQMHASYLFQDDKHYDL  
 mGAD65 KMMGVPLQCSALLVREEGLMOSCNQMHASYLFQDDKHYDL 435

zGAD65 SYDTGDKALQCGRHVDVFKLWLMWRAGTTGFETQIDKCL  
 gGAD65 SYDTGDKALQCGRHVDVFKLWLMWRAGTTGFETQIDKCL  
 mGAD65 SYDTGDKALQCGRHVDVFKLWLMWRAGTTGFETQIDKCL 475

zGAD65 ELAEVLYNKIKNREGYEMVFDGKPOHTNVCFW  
 gGAD65 ELAEVLYNKIKNREGYEMVFDGKPOHTNVCFW  
 mGAD65 ELAEVLYNKIKNREGYEMVFDGKPOHTNVCFW 507

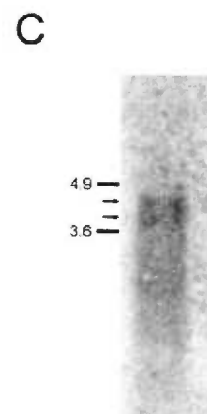


**Figure 3.2) Radioactive In-situ Hybridization of zGAD65 in the Zebra Finch Brain**

- (A) Schematics of a medial parasagittal section depicting regions within the auditory telencephalon. Scale bar = 4mm
- (B) Phosphorimager autoradiogram of a section at the level represented in (A), hybridized with zGAD65 antisense riboprobe. Inset depicts autoradiogram of sense probe hybridization. Scale bar = 4mm
- (C) Darkfield view of emulsion-dipped section (same level as in A) after hybridized with zGAD65, depicting labeled cells in NCM, field L2 and CMM.
- (D-F) Brightfield views of emulsion-dipped sections showing zGAD65-positive cells in auditory areas: (D) NCM, (E) field L2, (F) CMM; arrowheads indicate cells with high expression levels of zGAD65.
- (G) Detailed view of emulsion-dipped section showing differential accumulation of silver grains over cells in NCM; Arrowhead depicts a high-expression zGAD65-positive cell, arrow indicates a lower-expression zGAD65-labeled cell.
- (H) View of emulsion-dipped section showing zGAD65 expression in cerebellar Purkinje cells; ml: molecular layer; pcl: Purkinje cell layer; gcl: granule cell layer.
- (I) Detailed view of zGAD65 positive neurons in the pallidum.
- Scale bars (in  $\mu\text{m}$ ): 100 (C); 50 (D-F); 10 (G); 25 (H-I).

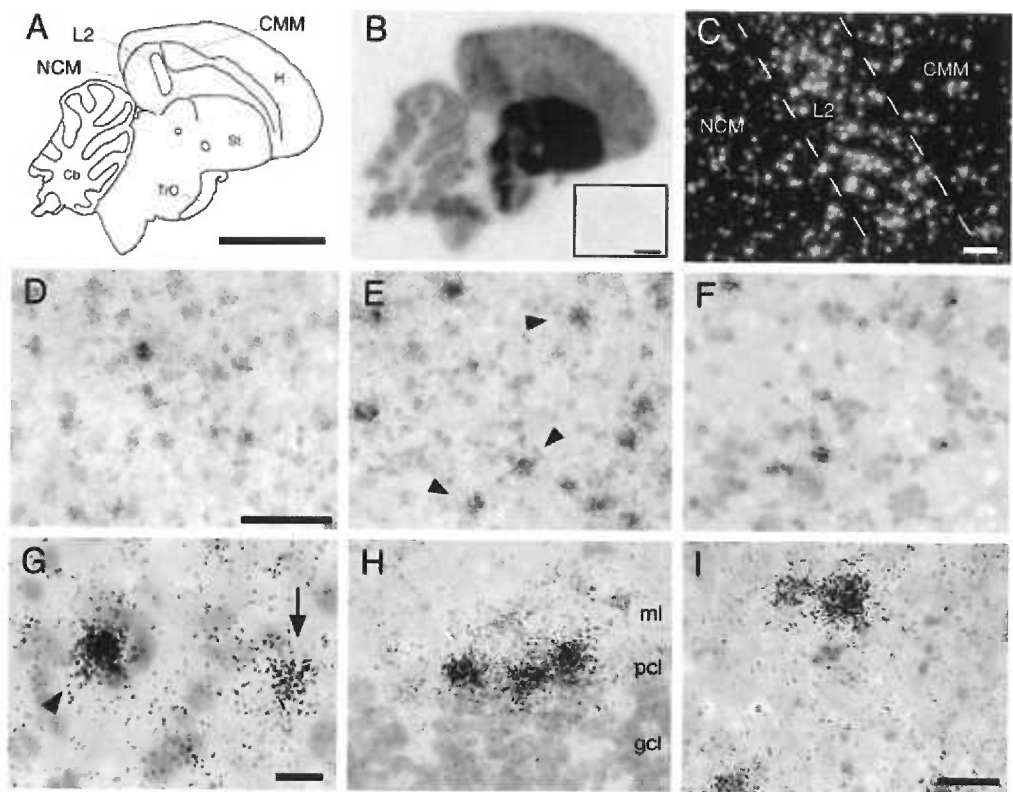




**Figure 3.3) Fluorescence In-situ Hybridization (FISH) for zGAD65**

(A) Low power photomicrograph of parasagittal section depicts zGAD65 expression in NCM using DIG-labeling.

(B) Same field as in (A), with superimposed image depicting Hoechst counterstaining for cell nuclei; the high cell density area in the upper right corresponds to the ventricular zone.

(C) High power photomicrograph showing detailed view of zGAD65 positive cells in NCM; arrowheads indicate examples of strongly-labeled cells with large soma size, arrows indicate cells with less intense labeling and smaller soma size.

Scale bars (in  $\mu\text{m}$ ): 50 (A-B); 25 (C)

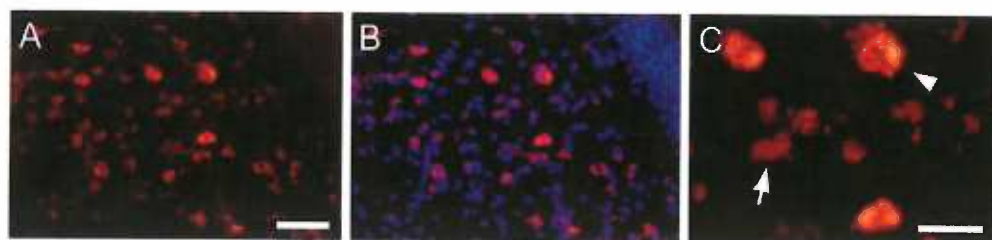


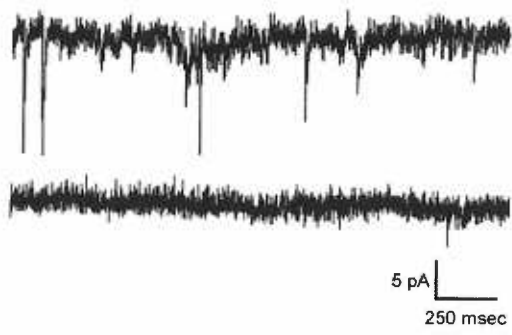
**Figure 3.4) Spontaneous miniature post-synaptic events are GABAergic and provide tonic inhibition to NCM neurons**

(A) Whole-cell patch clamp recordings of spontaneous events in an NCM neuron of a slice perfused with normal aCSF + TTX (top trace) and after the addition of bicuculline (bottom trace). Holding potential = -70 mV.

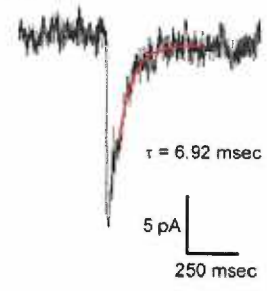
(B) Expanded view of a representative mIPSC recorded in an NCM neuron. The red line shows a single exponential fit of the decay time, demonstrating that these spontaneous miniature events are GABAergic.

(C) Whole-cell patch clamp recordings depicting examples of bicuculline-evoked post-synaptic currents in NCM neurons. The section was perfused with TTX-free aCSF; recordings from two representative neurons are shown.

A



B



C



**Figure 3.5) dFISH for zGAD65 and zenk Reveals Song-Responsive Inhibitory Neurons in NCM**

(A) Top two rows: Representative examples of neurons that co-express zGAD65 and zenk mRNAs in NCM of zebra finches stimulated with conspecific song. Third row: Representative example of zGAD65-positive cells that do not express zenk; section is the same as in top rows. Fourth row: Representative example of a zenk-positive cell that is negative for zGAD65 from the same section as in upper rows. All images were obtained with confocal microscopy. Scale bar = 5  $\mu$ m.

(B) Schematics depicting the areas in rostral and caudal NCM that were mapped for double labeled cells (black boxes on left image; not to scale). These maps are generated in Neurolucida software and allow for quantification and analysis of topographical distribution of zenk- (red circles) and zGAD65- (green crosses) positive cells. Each mapped field is 100 $\mu$ m by 100 $\mu$ m in size.

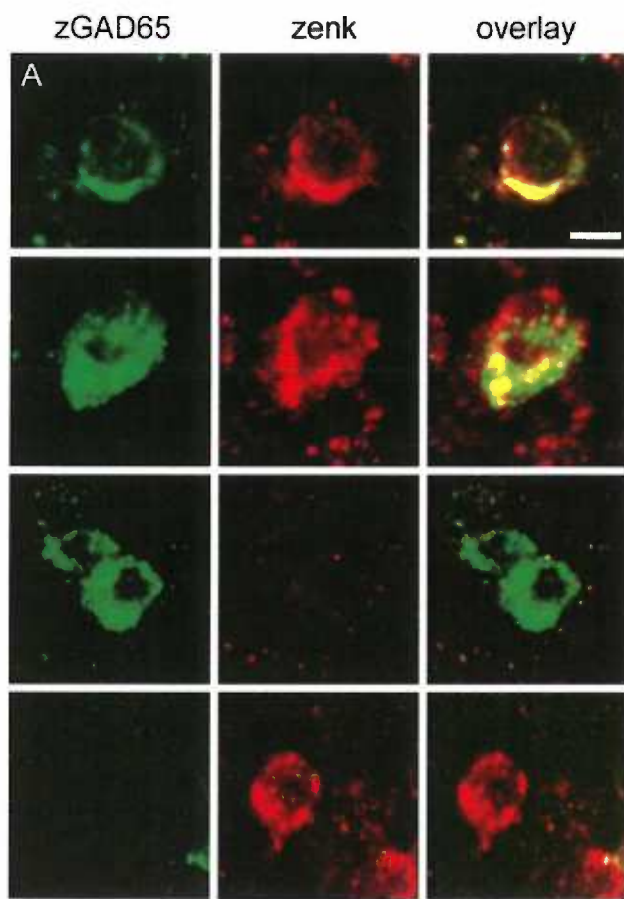


**Figure 3.6) Double-Immunocytochemistry Reveals Co-Localization of ZENK and GABA in NCM of Song-Stimulated Birds**

Shown are representative examples of different cell types from the same histological section.

(A) Cell double-labeled for ZENK (black nuclear staining) and GABA (brown cytoplasmic staining). Arrows depict GABAergic cells that do not express ZENK (cytoplasmic staining only).

(B) Large GABAergic cell that does not express ZENK (cytoplasmic staining only).

(C) Another example of a GABAergic cell (cytoplasmic staining) that expresses ZENK (nuclear staining).

(D) Example of non-GABAergic ZENK-positive cell (nuclear staining only); arrow depicts a small GABAergic cell that does not express ZENK.

Scale bar = 25 $\mu$ m.

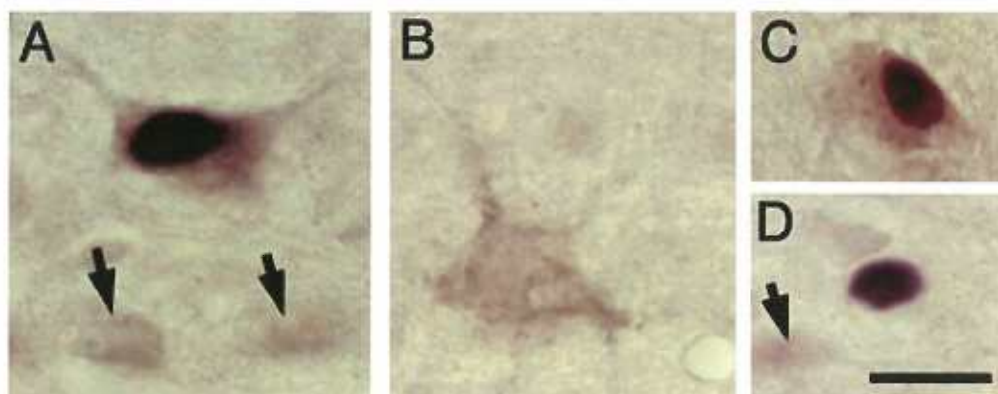




**Figure 3.7) Schematic Circuit Diagrams Indicating Putative Roles of Inhibitory Cells in NCM**

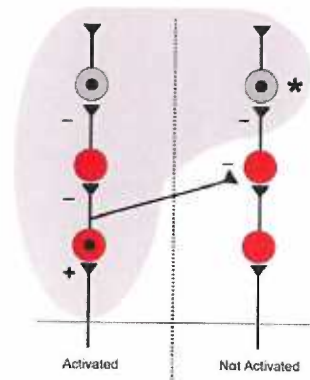
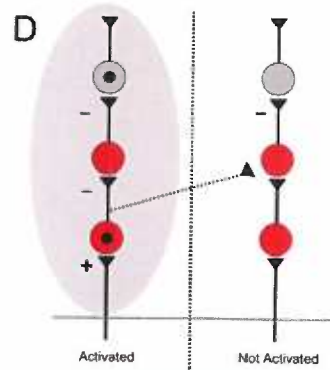
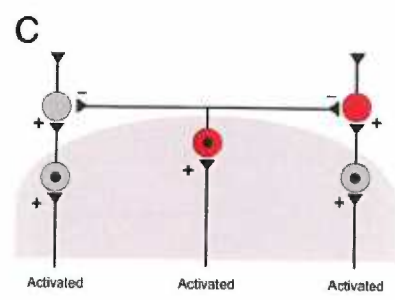
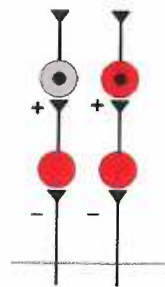
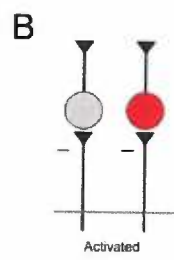
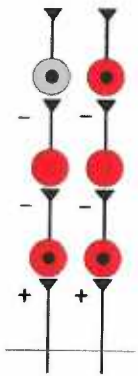
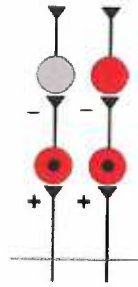
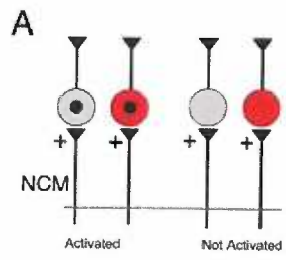
(A) Models illustrating how zenk expression in excitatory and inhibitory neurons in NCM may be determined by the excitatory drive from external inputs.

In this and all other panels, excitatory neurons are indicated in grey, inhibitory neurons are indicated in red, zenk-expressing/activated neurons are indicated by a black dot, and the NCM border indicated by a grey horizontal line.

(B) Models illustrating how zenk expression in excitatory and inhibitory neurons in NCM may be determined by inhibitory drive from external inputs to NCM.

(C) Model illustrating how functional domains within NCM may be sharpened by GABAergic cells.

(D) Proposed mechanism for experience-dependent plasticity in NCM mediated by inhibitory neurons. Under normal conditions (top panel), GABAergic interneurons would participate in local inhibitory processes within activated domains (shadowed region). Under conditions of reorganizational pressure (bottom panel), GABAergic cells would mediate disinhibition of domains that are not directly activated by auditory input (expanded shadowed region). The latter domains would become functionally coupled to the activated domain. The induction of plasticity-related activity-dependent genes (asterisk) might result in long-lasting circuit reorganization.



## DISCUSSION

We have demonstrated a high incidence of GABAergic cells and a prevalence of active GABAergic synapses in auditory areas of the zebra finch telencephalon, and that a large proportion of these cells respond to birdsong stimulation. We discuss below the relevance of our findings with respect to birdsong auditory processing and experience-dependent plasticity.

### **zGAD65 Cloning**

To identify and characterize GABAergic cells that might be involved in the auditory processing of birdsong, we cloned a songbird homologue of GAD65 and generated probes for in-situ hybridization. The two known glutamic acid decarboxylase isoforms, GAD65 and GAD67, are encoded by distinct genes and synthesize GABA efficiently. However, whereas GAD67 appears to preferentially synthesize cytoplasmic GABA for cellular respiration, GAD65 seems to catalyze GABA synthesis for vesicular release (Soghomonian and Martin, 1998). In addition, both genes show differential expression across brain regions (Soghomonian and Martin, 1998) that correlates with electrophysiological properties: while GAD67 is mainly expressed in neurons that fire tonically, GAD65 appears to preferentially locate to neurons whose activation relies on synaptic input (Soghomonian and Martin, 1998). Furthermore, while GAD65 is mostly targeted to the cellular membrane and nerve endings, GAD67 has a broader intracellular distribution (Ruppert et al., 1993; Soghomonian and Martin, 1998). We focused on GAD65 to reveal GABAergic cells

that are more likely involved in the synaptic response to birdsong. Our evidence demonstrates that we have isolated the zebra finch GAD65 homologue and that our probe identifies GABAergic cells.

### **zGAD65 in Telencephalic Auditory Processing Areas**

The caudomedial telencephalon is a bulging lobule that contains the thalamorecipient zone field L and the adjacent caudomedial nidopallium (NCM) and caudomedial mesopallium (CMM), all of which are part of the central auditory pathway, and display robust electrophysiological and inducible gene responses to auditory stimulation with birdsong (Mello, 2002a, b). We found that GABAergic cells are a major constituent of these areas. Given that zGAD65 is more tightly linked with the synaptic pool of GABA, our conservative estimate may represent a more accurate assessment of GABAergic neurons directly involved in the synaptic response to birdsong.

We observed heterogeneity in the size and relative labeling of GABAergic cells, suggesting the existence of two subpopulations with differential distribution. It is possible that the smaller and larger cells correspond to local interneurons and projection neurons, respectively. This hypothesis is suggested by previous studies of song control nucleus area X, where the fewer, large, GABAergic cells are projection neurons that constitute the basal-ganglia-thalamic projection of the anterior forebrain pathway required for song learning (Luo and Perkel, 1999a, b). Testing this hypothesis will require careful quantitative analysis of zGAD65 expression.

It is also interesting that the overall proportion of GABAergic neurons we observed in auditory pallial areas is high in comparison with primary sensory cortical areas in mammals, where the estimates range from 25% to 30% of neuronal cells for both visual and somatosensory cortices (Jones, 1993). In mammals, such cells are highly concentrated in the thalamorecipient cortical layer 4, as well as in layers 2 and 3 (Gabbott and Somogyi, 1986). It has been argued that the avian brain contains neuronal populations that are equivalent to those that form cortical circuits in mammals. In addition, basic aspects of their circuitry organization, such as thalamo-telencephalic reciprocity, are preserved. However, this organization is nuclear, rather than layered, (Karten and Shimizu, 1989). If NCM, CMM and field L are the functional equivalents of supragranular and granular layers of the mammalian auditory cortex (Vates et al., 1996; Mello et al., 1998), then sampling of inhibitory neurons in these nuclei may over-represent the general inhibitory influence in auditory areas.

### **Active GABAergic Synapses are Prevalent in NCM**

Our patch-clamp recordings showed that active GABAergic synapses are prevalent in NCM slices, indicating a prominent role of GABAergic transmission in this region. The high frequency of mIPSCs occurrence in NCM neurons suggests that these cells may be under tonic inhibition, possibly as a means to prevent runaway excitation. Consistent with this hypothesis, the pharmacological blockade of GABA-A receptors led to the firing of bursts of post-synaptic currents in NCM cells. Because inhibitory synapses could be detected in both slices containing NCM, CMM and field

L, as well as in more restrictive slices containing only NCM, the tonic inhibition of NCM is likely to be exerted by local inhibitory interneurons. It is also possible, though, that at least some GABAergic neurons in field L provide inhibitory input to target areas such as NCM and CMM. These putative inhibitory projection neurons would, upon their activation, shut-down GABAergic interneurons within NCM, relieving other NCM neurons from tonic inhibition. Consistent with this model, a number of NCM cells fire action potentials spontaneously in slices (not shown). In experiments where NCM was physically isolated, we still observed large spontaneous post-synaptic currents that corresponded to action potential-like events. Overall, our electrophysiological experiments implicate GABAergic cells in the normal physiology of auditory processing areas of the songbird brain.

### **Inhibitory Neurons in Auditory Processing Areas are Song-Responsive**

The use of *zenk* expression analysis by *in situ* hybridization or ICC to identify song-responsive cells within auditory structures is well-documented (Mello et al., 1992; Mello and Ribeiro, 1998). *zenk* expression in auditory and vocal control pathways depends on the previous activation of neuronal cells by birdsong stimulation or singing behavior (Jarvis and Nottebohm, 1997; Jarvis et al., 1998; Mello and Ribeiro, 1998). The expression of *zenk* in a given neuronal cell can be taken as clear indication of that neuron's activation by the stimulus presented (Chaudhuri, 1997; Mello, 2002a, b). Our double-labeling data demonstrate that GABAergic cells in NCM and CMM express *zenk* mRNA and protein in response to birdsong auditory stimulation, and that these cells represent a large proportion of the

overall *zenk*-expressing cell population. Thus, GABAergic cells in telencephalic auditory regions are activated by birdsong stimulation and thus participate in the auditory processing of song. Conversely, the several non-GABAergic *zenk*-expressing cells are most likely excitatory song-responsive neurons. Although caution is required in interpreting *zenk*-negative cells (for example, some specific regions do not show song-induced *zenk* expression - see Mello et al., 1995 - and neurons in NCM and CMM may exhibit habituation to repeated song stimulation - Chew et al., 1995, *zenk*-negative GABAergic and non-GABAergic cells most likely were not activated by the stimulation.

Several potential scenarios could account for the *zenk* expression patterns observed (see models in Figs. 7A and B). For example, excitatory inputs activated by song could act directly onto NCM neurons. Alternatively, song could act through a release of the local inhibitory tone. This possibility requires song activation of local inhibitory interneurons within NCM microcircuitry. Our present data show that GABAergic cells are indeed activated by song stimulation, and could be involved in local disinhibition. NCM anatomically occupies a position that corresponds to supragranular layers of the mammalian auditory cortex. In our models (Figure 7A), the excitatory input to NCM would, thus, be equivalent to drive to the supragranular layers of the mammalian sensory cortex from either granular or supragranular layers (the latter corresponding to cortico-cortical interactions). Alternatively, NCM could receive inhibitory inputs (Figure 7B) that might then release tonic inhibition, by acting on local GABAergic interneurons, within NCM (Figure 7B). This type of inhibitory interactions would be comparable to some forms of lateral inhibitory

connections described in the mammalian sensory cortex. Overall, the concepts diagrammed in our models could apply, in principle, to any area containing inhibitory interneurons, regardless of a layered (mammals) vs. non-layered (birds, reptiles) organization.

The neurochemical identity of *zenk*-expressing cells had not been previously studied. Our data demonstrates that *zenk* is induced by birdsong in GABAergic and non-GABAergic cells. Thus, the same activity-dependent gene can be induced by song in cells that play opposite roles in functional circuitry organization. Given that *zenk* encodes a transcriptional regulator (Christy and Nathans, 1989), identifying ZENK protein targets will be essential for establishing the significance of *zenk* induction. It will be important, however, to consider neuronal subtypes separately, as *zenk* targets and their regulation (up- or down-) may differ in excitatory and inhibitory cells. In-vitro studies have shown that ZENK regulates neuronal genes such as synapsins I and II (Thiel et al., 1994; Petersohn and Thiel, 1996). We have preliminary evidence that synapsin II is regulated by birdsong stimulation in NCM (Velho TAF, Pinaud R & Mello C.V., unpublished observations), but whether this induction is *zenk*-dependent or occurs in different neuronal types remains to be determined.

### **Roles for Inhibition in Auditory Processing, Plasticity and Learning**

GABAergic inhibition plays a significant role in shaping the response properties of sensory neurons. For instance, antagonism of the GABA-A receptor leads to expansions of the classical receptive fields of cells in the visual and



somatosensory cortices (Ramoia et al., 1988; Eysel et al., 1998; Kyriazi et al., 1998; Tremere et al., 2001a). In the auditory system, the sharpness and specificity of receptive fields are also dependent on GABAergic mechanisms. A clear example is the demonstration that the GABA-A receptor is involved in the sharpening of auditory tuning curves of neurons that participate in echolocation in the mustached bat (Yang et al., 1992; Suga et al., 1997; Chen and Jen, 2000). GABA-A receptors have also been implicated in the formation of exquisitely fine auditory spatial maps and in the generation of interaural time difference selectivity in mesencephalic neurons in the barn owl (Fujita and Konishi, 1991; Zheng and Knudsen, 1999, 2001). In the chicken telencephalon, local application of bicuculline to regions post-synaptic to the thalamorecipient field L2 enlarges isointensity-response areas (Muller and Scheich, 1988). By analogy, it is possible that GABAergic cells also mediate functional sharpening of receptive field properties in NCM neurons (see model in Figure 7C).

It has also been proposed that inhibition is pivotal in generating conditions that enable experience-dependent plasticity in a number of sensory systems (Gierdalski et al., 2001; Tremere et al., 2001b; Meredith et al., 2003). By inference, GABAergic mechanisms might also play a role in plasticity-related phenomena in a song-processing area such as NCM. For example, the electrophysiological responses of NCM neurons decrease (habituate) in consequence to repeated song presentations (Chew et al., 1995). This habituation is rapid (within seconds) and could be mediated by a fast-acting mechanism involving GABA and/or noradrenaline (the latter suggested by Ribeiro and Mello, 2000).

GABAergic mechanisms have also been implicated in activity-dependent functional reorganization of brain networks through disinhibition. Under conditions of reorganizational pressure (e.g. digit amputation, retinal lesions), GABAergic interneurons within activated brain domains may promote, through lateral inhibition, the shutting down of inhibitory interneurons within non-activated domains (Tremere et al., 2001b). Local GABAergic neurons may also mediate the functional properties and some forms of plastic changes in NCM. Preliminary evidence suggests that the NCM of canaries undergoes reorganization of its frequency-dependent representation of song syllables after prolonged exposure to frequency-shifted songs (Ribeiro, S and Mello, CV, unpublished observations). Auditory input from birdsong stimulation would normally activate only NCM cells that are anatomically positioned to receive that information (Figure 7D, shadowed area in top panel). Under conditions of reorganizational pressure (e.g., frequency-shifted songs), GABAergic interneurons within the activated domain would inhibit GABAergic neurons within non-activated domains. Cells in non-activated domains would, thus, be activated in the absence of direct auditory input through disinhibition, becoming functionally coupled to the activated domain (Figure 7D, extended shadowed area in bottom panel). Long-lasting physical changes in neuronal circuit organization might also ensue, mediated by the induction of activity-dependent genes associated with phenomena such as synaptic potentiation, neurite sprouting and changes in neuronal excitability (Figure 7D, asterisk in bottom panel). In mammals, this type of inhibition (GABAergic to GABAergic cell) is prominent in primary sensory cortical areas, and a likely anatomical substrate has been demonstrated (Winfield et al., 1981; McGuire et al.,

1991). Experimental testing of this model in songbirds should provide significant insights into the functional role of the GABAergic system in the perception and memorization of song.

The involvement of GABAergic transmission in some forms of learning has been previously demonstrated in birds. For example, the marked plastic changes in receptive field properties of auditory neurons that occur in the barn owl upon manipulations of the visual environment depend on an intact GABAergic system (Zheng and Knudsen, 1999; Knudsen et al., 2000). In addition, our data are consistent with the previous finding that an activity-dependent gene, namely *c-fos*, can be induced in activated GABAergic cells in the context of visual imprinting in chicks (Ambalavanar et al., 1999). That phenomenon was observed in the intermediate medial mesopallium, (IMM, formerly known as IMHV), an area required for visual imprinting. The induction of *c-fos* in the IMM has been associated with learning in this paradigm, rather than with sensory processing or locomotor activity per se (McCabe and Horn, 1994). Therefore, *c-fos* activation in GABAergic cells indicates that inhibitory neurons play a prominent role in visual imprinting (Ambalavanar et al., 1999; for a recent review see Horn, 2004). One of the auditory areas in the present study, the CMM, is located in the same telencephalic subdivision as the IMM and is involved in the auditory processing of vocalizations in various avian species (Bonke et al., 1979; Scheich et al., 1979; Muller and Leppelsack, 1985; Capsius and Leppelsack, 1999; Sen et al., 2001; Gentner and Margoliash, 2003). Interestingly, significant changes in song selectivity occur in CMM neurons as a result of exposure to song in the context of song recognition learning (Gentner and Margoliash, 2003).

Thus, it is possible that the song-responsive GABAergic neurons we identified in the CMM based on *zenk* induction play a role in neuronal selectivity changes associated with song perceptual learning.

Together with our current findings, the data discussed above indicate a prevalent participation of GABAergic neurons in the processing of behaviorally relevant sensory stimuli in birds (McCabe and Horn, 1994; Ambalavanar et al., 1999). A similar involvement may also occur in mammals, where GABAergic neurons play a major role in cortical physiology. Further studies in mammals, birds and other vertebrates should help determine whether the involvement of GABAergic mechanisms in brain function, as it relates to behavior, has been evolutionarily conserved.

## **CHAPTER 4**

### **A NOVEL MECHANISM FOR AUDITORY PROCESSING DYNAMICS INVOLVING DISINHIBITION IN THE SONGBIRD ANALOGUE OF THE AUDITORY CORTEX**

## INTRODUCTION

Songbirds have been used extensively as a model for vocal learning, which is the ability to learn vocalizations based on auditory input (Kroodsma and Miller, 1982; Catchpole and Slater, 1995; Kroodsma and Miller, 1996). Over the years, research in this area has clearly demonstrated that, like humans, songbirds rely on audition to generate auditory memories to be used as templates for the normal development of vocal behavior (Konishi, 1965a; for reviews see Nottebohm, 1999; Koppl et al., 2000; Marler and Doupe, 2000). Because vocal learning depends on auditory information, a great deal of effort has been directed at understanding the physiology of brain areas that process birdsong auditory information. A particular focus has been placed on the caudomedial nidopallium (NCM), a telencephalic auditory area equivalent to supragranular layers of the primary auditory cortex in mammals (Karten and Shimizu, 1989; Wild et al., 1993; Vates et al., 1996; Mello et al., 1998). NCM displays strong evoked electrophysiological auditory responses to song stimulation, which have longer latency and are more selective towards more complex stimuli, when compared to lower auditory areas such as field L (Chew et al., 1995; Chew et al., 1996; Sen et al., 2001). Interestingly, NCM's responses also present a preference for conspecific, rather than heterospecific songs or artificial stimuli (Chew et al., 1996), suggesting that this area contributes to auditory discrimination of birdsong.

It has been demonstrated in a number of sensory systems that GABAergic transmission, especially that mediated through GABA-A receptors, plays a pivotal role in the shaping of receptive field properties. For example, antagonism of GABA-

A receptors has been demonstrated to expand receptive fields in both primary somatosensory (S1) and visual (V1) cortices (Dykes et al., 1984; Ramoa et al., 1988; Eysel et al., 1998; Tremere et al., 2001a). In addition, complex response properties, such as directional and orientation selectivity in V1 neurons, is under the control of GABAergic transmission (Sillito, 1975b), suggesting that inhibitory influences not only regulate receptive field properties, but might also contribute to the generation of complex response properties of sensory neurons. In the auditory system, GABAergic transmission has also been demonstrated to contribute to both the regulation of sensory processing and some forms of experience-dependent plasticity, especially in animals that rely heavily on audition for normal behavior. For example, antagonism of GABA-A receptors has been demonstrated to lead to marked expansions in auditory tuning curves in central auditory neurons, including cortical neurons (Yang et al., 1992; Suga et al., 1997; Chen and Jen, 2000). In addition, GABAergic neurons have been shown to regulate experience-dependent plasticity of auditory spatial maps in barn-owls (Zheng and Knudsen, 1999; Knudsen et al., 2000; Zheng and Knudsen, 2001). Importantly, GABAergic transmission has been demonstrated to regulate integration dynamics in the time domain to influence the statistical probability and/or precise timing of action potential generation, postulated as behavioral mechanisms used by the cell to encode perception. For example, Chen and Jen (2000) have demonstrated in the big brown bat that auditory cortical neurons that respond to a narrowly defined phase range, hence “phasic” responders, can be converted into tonic responders through the antagonism of GABA-A receptors. The possibility that a neuron’s response type could undergo such a change suggests that during normal

auditory processing, GABA may act to suppress sustained excitatory drive in response to auditory stimulation (Chen and Jen, 2000). These data are in accordance with findings from primary areas of other sensory systems, the conversion of a phase locked response pattern to the tonic response, by virtue of antagonism of inhibition, enhances overall neuronal excitability (Sillito, 1975a, 1979).

Here we report a novel interaction between inhibitory networks in NCM of a songbird, a primary sensory area involved in birdsong auditory processing (reviewed in Mello, 2002a; Mello et al., 2004). Song-evoked auditory responses in awake animals, which are characterized by sustained firing between syllables, are converted functionally into highly synchronized phasic on/off-like responses with the application of bicuculline methiodide (BMI), a competitive GABA-A receptor antagonist. The loss of the tonic component during BMI application suggests that other inhibitory mechanisms in NCM are released from GABAergic control, through GABA-A receptors. Our findings suggest that GABA-A transmission contributes not only to excitability, but also regulates the timing of auditory responses in a primary auditory region. In addition, we present evidence for the first time, for the existence of components of neural circuitry in NCM that could utilize GABAergic transmission to regulate auditory processing through relief of a secondary inhibitory network (disinhibition) within NCM.



## MATERIAL AND METHODS

### Subjects and Procedures

20 adult zebra finches (*Taeniopygia guttata*) were used in the present experiments. Animals were raised in an aviary at Rutgers University or OHSU. In order to prepare for electrophysiological recording animals were anesthetized (Nembutal 50mg/kg, Abbot Laboratories, N. Chicago, Ill), placed in a stereotaxic device, and a metal head post was attached to the skull with dental cement (Dentsply Caulk, Milford DE). After a 48 h recovery period subjects were placed in an acoustically isolated booth for testing. The head post and a plastic body tube permitted immobilization of awake animals during recording and microinjections.

The skull and dura were opened and a landmark on the brain surface, bifurcation of the sagittal sinus, was used to position 7, 2-4 M ohm microelectrodes (Quartz-Platinum/Tungsten Type ESI2ec, Thomas Recording, Giessen, Germany) and a glass micropipette (Drummond Scientific Co. Broomall, PA) above NCM. 3 electrodes were then driven into the left hemisphere and 4 into the right by a calibrated electrode microdrive (Thomas Recording) and white noise stimuli were used to locate responsive sites. After playing pre-bicuculline auditory stimulus sets (described below) a glass micropipette was driven into the right hemisphere to approximately the same depth as the electrodes, and bicuculline (BMI) was administered by a microinjector (Narishige Scientific Instrument Labs, Tokyo, Japan). Doses were adjusted for each bird so that neural firing remained just below threshold for seizure-like activity. Subjects received an initial loading dose (6-10 nl),

followed 5-15 min later by maintenance doses (1-2 nl every 1-4 min) for the duration of the auditory stimulus trials.

### **Stimuli**

Stimuli included 4 conspecific song segments played in a pseudo-random order through a small speaker at an amplitude of 70 dB spl, under computer control (Spike2 version 5.05, Cambridge Electronic Design, Cambridge, UK). Each song segment was played 25 times before BMI injection and then repeated 25 times during BMI administration (stimulus durations: 1.18, 1.10, 1.48, and 1.12 s, inter stimulus interval: 8 s). A set of 20 sine wave stimuli was also played (duration: 260 ms, range: 250-5000 Hz, in 250 Hz increments, inter stimulus interval: 6 s) in a pseudo-random order 5 times before and 5 times after BMI.

### **Histology**

In order to histologically confirm recording locations, electrolytic lesions (10  $\mu$ A of current for 10 s, 3 lesions per hemisphere) were made in each brain. Animals were then sacrificed by nembutal overdose and perfused with saline followed by 4% paraformaldehyde. Fixed brains were removed and cut on a vibratome into 50 $\mu$ m parasagittal sections, and processed for Cresyl violet histology.

### **Whole-Cell Patch-Clamp Electrophysiology**

20 adult zebra finches (17 females and 3 males) were used in the *in vitro* experiments. Animals were decapitated and the brains were quickly dissected and placed in ice-

cold artificial cerebrospinal fluid solution (aCSF) modified for slicing consisted in mM: NaCl (87), NaHCO<sub>3</sub> (25), KCl (2.5), NaH<sub>2</sub>PO<sub>4</sub> (1.25), CaCl<sub>2</sub> (0.5), MgCl<sub>2</sub> (7), glucose (25), sucrose (75), ascorbic acid (0.4), sodium pyruvate (2), myo-inositol (3), 354 mOsm, pH 7.4 when bubbled with carbogen 95%O<sub>2</sub>/5%CO<sub>2</sub> , and 4 to 5 200µm thick parasagittal sections (medial to lateral) containing NCM and adjacent areas were obtained on a vibratome (Vibratome® Series 1000, Vibratome, St Louis, MO). Slices were stored in the same solution at 35°C for 45 minutes and thereafter at room temperature. For recordings, slices were transferred to a chamber mounted on a stage of a upright microscope and continuously perfused with normal aCSF which consisted of (mM): NaCl (125), KCl (2.5), NaHCO<sub>3</sub> (25), NaH<sub>2</sub>PO<sub>4</sub> (1.25), glucose (25), CaCl<sub>2</sub> (2), MgCl<sub>2</sub> (1), ascorbic acid (0.4), sodium pyruvate (2), myo-inositol (3), 295 mOsm, pH 7.4 when bubbled with 95%CO<sub>2</sub>/5%O<sub>2</sub>. Borosilicate glass pipettes (Sutter Instruments, Novato CA) were pulled using a P-97 horizontal puller (Sutter Instruments). Spontaneous post-synaptic currents (sPSCs) were recorded in whole cell voltage-clamp with an Axopatch 1-D amplifier (Axon Instruments, Foster City CA) in a membrane holding potential of -70 mV. For recording the pipettes were back-filled with the internal solution that consisted of (in mM) CsCl (140), EGTA (5), HEPES (10), ATP-Mg (4), phosphocreatine-Na (20), pH 7.3 with CsOH. Some cells were recorded with a low chloride internal solution (CsMeSO<sub>4</sub> 140 mM/CsCl 20 mM). Resistance of the pipettes in the bath was in the 3-10 MΩ range. Bicuculline concentration used was 20µM. Signals were sampled between 10 and 50 µsec and filtered at 5kHz. Clampex 6.0 (Axon Instruments) and the sPSCs analyzed using the mini analysis software (Synaptosoft, Decatur GA).

For the electrophysiology, birds were acoustically isolated 12 hours prior of the experiment (n=11 neurons) or taken direct from the aviary (n=17 neurons). No difference was observed in the frequency ( $3.4 \pm 0.7$  Hz. vs.  $3.1 \pm 0.4$  Hz) and the amplitude at  $-70$  mV in CsCl ( $49.4 \pm 7.7$  pA vs.  $46.9 \pm 4.3$  pA) of the GABAergic sPSCs. However the bicuculline-elicited glutamatergic events were seen more in cells from non-isolated animals (8 out of 11 cells) than in cells from isolated animals (3 out of 8 cells).

## RESULTS

### Spontaneous GABA Release Controls NCM Neuronal Excitatory Circuitry

In a previous work (Pinaud et al., 2004) we showed the presence of miniature inhibitory post-synaptic currents (mIPSCs) of GABAergic origin in the NCM, and putative excitatory events elicited by GABA-A receptor blockade. In order to further characterize the influence of the GABAergic input in the NCM we conducted a series of whole-cell patch-clamp recordings from slice preparations of NCM. The majority of NCM recorded neurons received a vast input revealed by the high-frequency of spontaneous post-synaptic currents (sPSCs) recorded in almost all cells (28 out of 31). Data analyzed from neurons from 20 birds revealed a mean frequency of appearance of sPSCs of  $3.23 \pm 0.4$  Hz ( $n=28$ ; Fig. 1A, top trace). When recorded with a high chloride internal solution at  $-70$  mV these events exhibited a mean amplitude and half-width of  $-52.19 \pm 3.9$  pA and  $7.9 \pm 0.7$  ms ( $n=19$ ; Table 1), respectively, and reverted around 0 mV. When a low chloride internal solution was used ( $n = 9$ ), the mean amplitude of sPSCs at  $-70$  mV was smaller ( $-32 \pm 9$  pA;  $n=6$ ) and reverted around  $-40$  mV, which indicates that these currents are carried by the chloride ion, and are inhibitory in nature. GABA and glycine are the inhibitory neurotransmitters in CNS that act primarily via ionotropic receptors; these can be easily identified by the use of specific pharmacological antagonists. Application of bicuculline, a classic GABA-A receptor antagonist, eliminated virtually all the sPSCs in all cells tested ( $n=19$ ; Fig. 1A, bottom trace). These findings show that the sPSCs in the NCM are

GABAergic and are the major source of active input to NCM slices at resting conditions.

We were able to observe in 11 out of 19 cells perfused with bicuculline, however, a second set of synaptic events that were not present in control conditions (Fig. 1B). These events were significantly larger than the sIPSCs previously observed (mean amplitude of  $232.5 \pm 37.6$  pA at  $-70$  mV and using CsCl internal solution;  $n=7$ ; Tables 2 and 3) but had a much lower frequency of appearance ( $0.08 \pm 0.01$  Hz.;  $n=7$ ) and were elicited in a seemingly rhythmic pattern (Fig. 1B, bottom trace). Application of DNQX ( $20$   $\mu$ M), an antagonist of the AMPA/kainate glutamate receptors, completely eliminated these large bicuculline-elicited events (not shown), confirming that these are originated from glutamatergic synapses that were originally inhibited by the spontaneous GABAergic transmission.

These results suggest that a putative function of the sIPSCs is to suppress excitatory components of NCM network that are active at resting conditions; these would only be allowed to be expressed under conditions where the spontaneously active GABAergic input is inhibited.

Interestingly the spontaneously active GABAergic synapses detected in NCM slices are driven by glutamatergic inputs. This was seen in 75% ( $n=3/4$ ) of cells, where application of DNQX to the recording bath dramatically decreased both the frequency and amplitude of the GABAergic events (Fig. 2 A and B). All the residual current not blocked by DNQX application was completely blocked by co-application of bicuculline (Fig. 2C). These findings suggest that excitatory glutamatergic inputs regulate the activity of those inhibitory neurons that participate in the generation of

sIPSCs. In summary, we interpret our patch-clamp data to suggest that tonic GABAergic input in NCM maintains most of excitatory network repressed at resting conditions. However, the strength and frequency of inhibitory input is driven by excitatory synapses.

### **GABA-A Receptors Regulate Temporal Dynamics of Information Processing: Disinhibitory Mechanisms**

Our whole-cell experiments indicate a role for GABAergic transmission in normal physiology of NCM in a slice preparation. In order to characterize the specific contributions of GABAergic transmission to birdsong auditory processing in NCM, we combined multielectrode extracellular recordings in wake, restrained adult zebra finches with local pharmacological interventions during playback of a randomized series of conspecific and heterospecific songs. Simultaneous multi-unit recordings were made bilaterally from multiple NCM sites before, during and after pressure injections of BMI into the right hemisphere (4 electrodes were placed in the right hemisphere). The left hemisphere, which contained 3 electrodes, was evaluated as an internal control, i.e. within the same experimental animal (Fig. 3). Before injection, song stimuli evoked responses in both hemispheres that were detectable across all channels. These responses consisted of phasic bursts of action potentials generated in response to most syllables with a pattern of sustained firing that appeared between those syllables (Fig. 4A). This pattern of activity was similar and consistently appeared for NCM regions in both hemispheres for all experimental animals studied.

The parallel and bilateral responsiveness of NCM was observed in response to both conspecific and heterospecific songs.

GABAergic influences in NCM neurons were blocked with either a selective competitive antagonist for the GABA-A receptor bicuculline methiodide (BMI), or the GABA-A and C receptor antagonist, picrotoxin (PTX). Both drugs were administered by micropipette pressure injection into the right hemisphere.

Sub-threshold application of BMI dramatically changed the firing properties of NCM neurons. First, tonic, pre-injection, responses could be converted to highly synchronized, phasic responses to display on/off-like firing (Fig. 4B). Other cells however, displayed on-only and off-only behavior in the presence of BMI (not shown). This BMI-induced phasic behavior was markedly increased during song presentation, especially in response to the first song syllable (Fig. 4B). Second, the sustained tonic firing between syllables was largely abolished by BMI application (Fig. 4B). Interestingly, quantification of this data demonstrated that the overall response amplitude was unchanged in conditions of antagonism of GABA-A receptors, as compared to responses obtained in the control hemisphere (Fig. 5). However, a considerable difference was obtained when comparing the standard deviation from song-evoked responses obtained in control hemispheres and those hemispheres that underwent pharmacological intervention (Fig. 5). These findings suggest that BMI application alters the temporal response properties of NCM neurons, rather than strictly affecting cell recruitment and/or lowering spiking threshold.



Our results also suggest that GABAergic transmission, via GABA-A receptors, regulates a secondary form of inhibition within NCM given that the removal of GABA-A-mediated inhibition by BMI application, leads to the disappearance of the tonic component of evoked responses, which is presumably suppressed by an active inhibitory mechanism.

Given that this phenomenon occurs in a fast time scale, metabotropic receptors are not likely involved. We therefore decided to investigate whether the ionotropic GABA-C receptors mediate the “secondary” inhibition. We reasoned that if GABA-C receptors were responsible for suppression of the tonic component of the song-evoked responses, concomitant blockade of GABA-A and GABA-C receptors would reinstate the tonic component. To test this prediction we conducted the same experiment as outlined above, except that picrotoxin (PTX), a non-specific GABA-A and GABA-C receptor antagonist, was used in the place of BMI. This experiment also led to dramatic changes in NCM cell firing behavior (Fig. 1C). Local PTX administration converted the sustained tonic responses, found in the pre-injection condition, to phasic on/off-like responses, as observed with BMI application (Fig. 1C). Quantitative analysis failed to reveal any statistically significant differences between BMI and PTX experiments, indicating that this secondary form of inhibitory transmission is not likely mediated through a second population of GABA receptors affected during PTX application, those being the GABA-C receptors. These findings suggest that it is a GABA-A-sensitive component in NCM that mediates the synchronization of firing and the repression of the tonic component of song-evoked responses in NCM. In addition, these results suggest an unconventional form of

information processing in the songbird NCM whereby ascending auditory input likely triggers a relief of inhibition tone, through GABA-A receptors, within NCM circuitry.

### **GABA-A Receptor Activation Regulates the Fidelity of Information Processing**

In the previous experiments, we have demonstrated that BMI application dramatically alters the temporal dynamics of song-evoked response properties of NCM neurons. To initiate an investigation of how blockade of GABA-A receptors could affect the fidelity of information transfer in NCM networks, we compared pre- and post-BMI spiking pattern of neurons in response to stimulation with the same songs (Fig. 6). As observed previously, NCM neurons tended to respond with phasic bursts to the majority of song syllables and sustained spiking activity in between syllables (Fig 6). As described above, BMI application led to high synchronization of spiking activity with the abolishment of the sustained component of the response (Fig. 6). A comparison of pre- and post-BMI conditions revealed that, under BMI influence, highly synchronized spikes could be evoked by presentation of certain syllables embedded within the complete song (Fig. 6, arrowhead). However, a number of syllables failed to trigger neuronal responses in NCM (Fig. 6, arrow). We interpret these findings to suggest that the BMI-induced alterations in firing behavior translated functionally into a decreased fidelity of information processing/transfer in NCM in response to natural auditory stimuli. This argument is based on our observations that certain sounds, under conditions of BMI application, failed to drive corresponding spike trains in NCM neurons and hence, those stimuli were apparently not encoded.

## **GABA-A Antagonism Does not Influence Frequency Tuning-Curve Shape in NCM**

In order to investigate whether BMI-induced reorganization of temporal response properties in NCM affected perceptual processing of auditory stimuli and sound discrimination, we conducted an analysis of frequency tuning for NCM cells. It has been shown in a number of experimental models, including bats, frogs and mice, that blockade of GABA-A receptors lead to marked expansion in frequency tuning curves and thus, a decrease in frequency discrimination capabilities (Yang et al., 1992; Suga et al., 1997; Chen and Jen, 2000). Frequency tuning curves were obtained for cells in both control and experimental hemispheres, before and after BMI application. Interestingly, contrary to what has been reported in auditory areas of other vertebrate species, frequency tuning curves in the zebra finch NCM were not significantly affected by GABA-A receptor antagonism (Fig. 7) suggesting that although firing patterns are markedly altered by GABAergic antagonism, frequency discrimination is still preserved within NCM circuitry. These findings also suggest that if normal GABAergic transmission is required to shape frequency information in the songbird auditory system, that this process takes place in stations that hierarchically precede NCM.

**Figure 4.1) sIPSCs in NCM are GABAergic and Maintain Stability of Intrinsic  
Excitatory Network**

A) Top Trace: Spontaneous synaptic events recorded at -70mV in an NCM neuron. Bottom Trace: Application of 20 $\mu$ M BMI completely abolishes the sPSC, indicating that they are GABAergic. B) Top trace: BMI application triggers the appearance of large spontaneous excitatory events (sensitive to DNQX; not shown), suggesting that sIPSCs prevent spontaneous firing of NCM's excitatory network. Bottom trace: Periodicity of large events can be observed with a larger time scale.

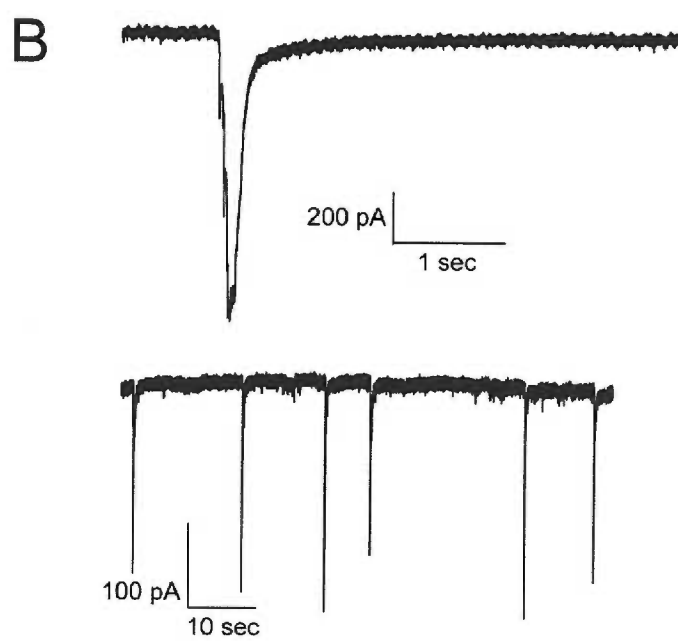
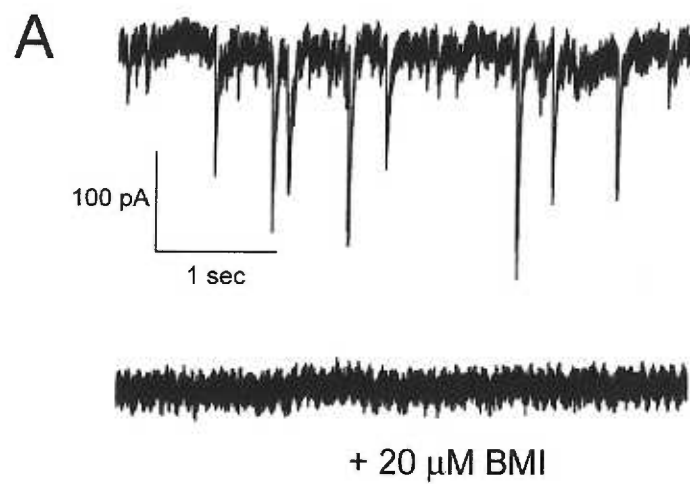
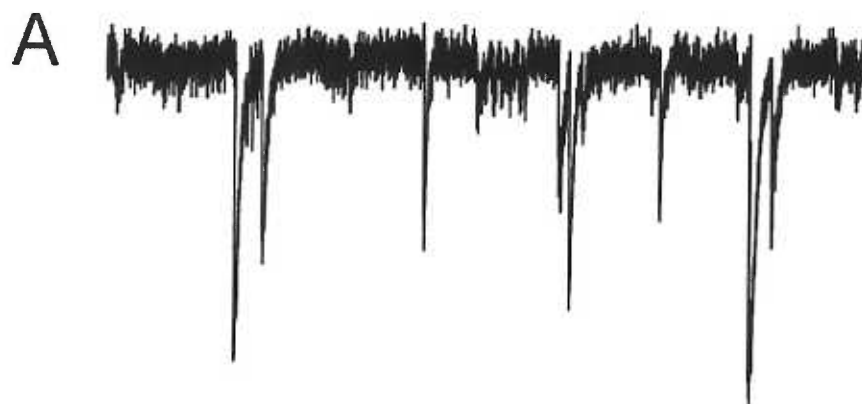
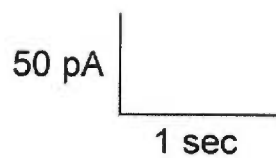


**Figure 4.2) Frequency and Amplitude of sIPSCs are Regulated by Excitatory Networks**

A) Spontaneous GABAergic events recorded in NCM neuron. B) Application of 20 $\mu$ M DNQX abolishes a large part of the spontaneous events. C) Remaining spontaneous events are blocked by addition of 20 $\mu$ M bicuculline to the bath.



+ 20  $\mu$ M DNQX



+ 20  $\mu$ M DNQX + 20  $\mu$ M BMI

### **Figure 4.3) Schematics of the Recording Setup**

A microdrive is used to lower three electrodes in the left hemisphere (control hemisphere) and four electrodes in the right hemisphere (experimental hemisphere).

A glass pipette is used to deliver drugs in the vicinity of the electrodes placed in the right hemisphere.



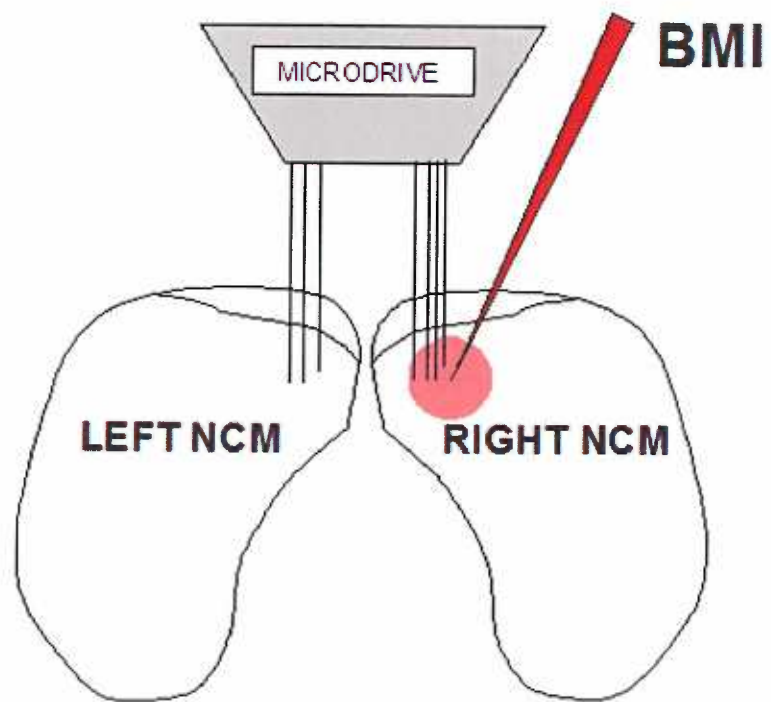


**Figure 4.4) Local BMI and PTX Application Dramatically Changes Song-Induced Firing Temporal Responses in NCM Units**

A) Raw traces depicting multi-unit activity from representative electrodes located in both control and experimental hemispheres prior to drug application. Note that responses are in phase with the song stimulus and sustained responses are detected throughout its full duration in both hemispheres. B) Application of BMI in the experimental hemisphere drastically changes in the response profile of units recorded with representative electrode. Note that responses become highly phasic and synchronized, particularly in relation to the first song syllable, and that sustained activity in between syllables is largely abolished. C) PTX treatment induces changes that are similar and not significantly different from those observed with BMI treatment.

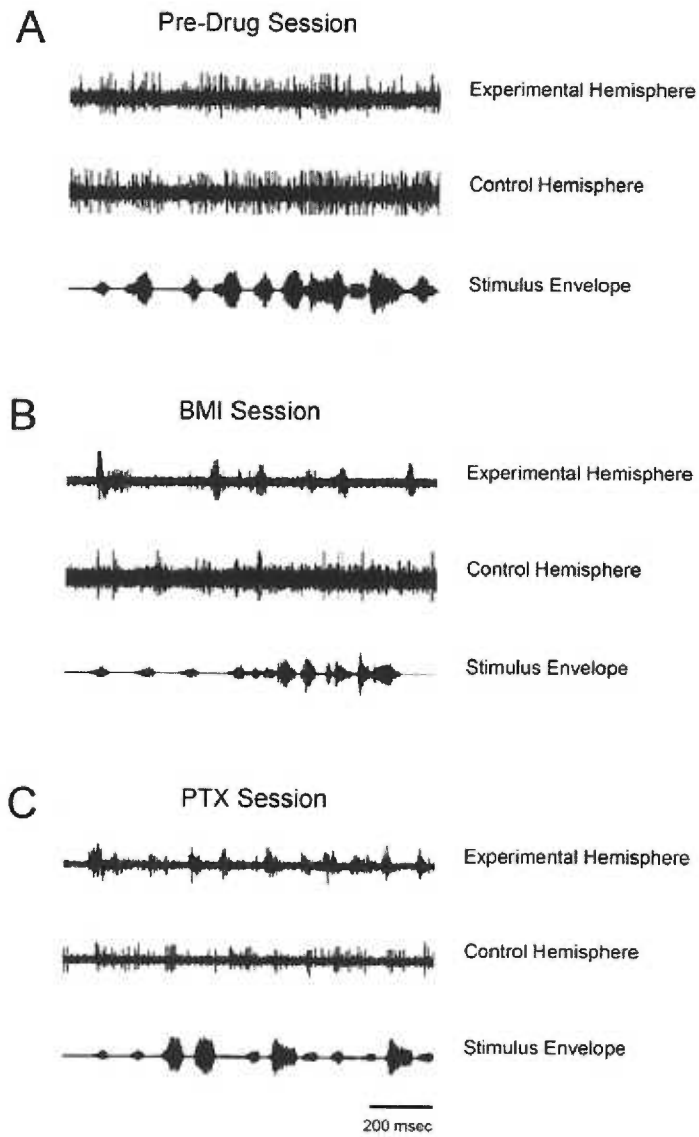


**Figure 4.5) BMI Application Affects Temporal Response Properties, but Not Response Amplitude in Song-Stimulated Awake Birds**

A) Total response amplitude for 4 conspecific songs was quantified as the rms over the response period (stimulus duration + 100ms). The total response amplitude post-BMI injection was divided by the total response amplitude pre-BMI to form a ratio. This post/pre amplitude ratio does not differ between BMI and Control hemispheres, indicating that the total neural activity is unaffected by BMI blockade of GABA-A receptors. The temporal structure of the response was quantified by computing the standard deviation of the response over the response period. The standard deviation post-BMI injection was divided by the standard deviation pre-BMI to form a ratio. This post/pre standard deviation ratio is significantly higher in the BMI hemisphere than in the Control hemisphere, indicating that variability has increased, and reflecting the more phasic character of the response.

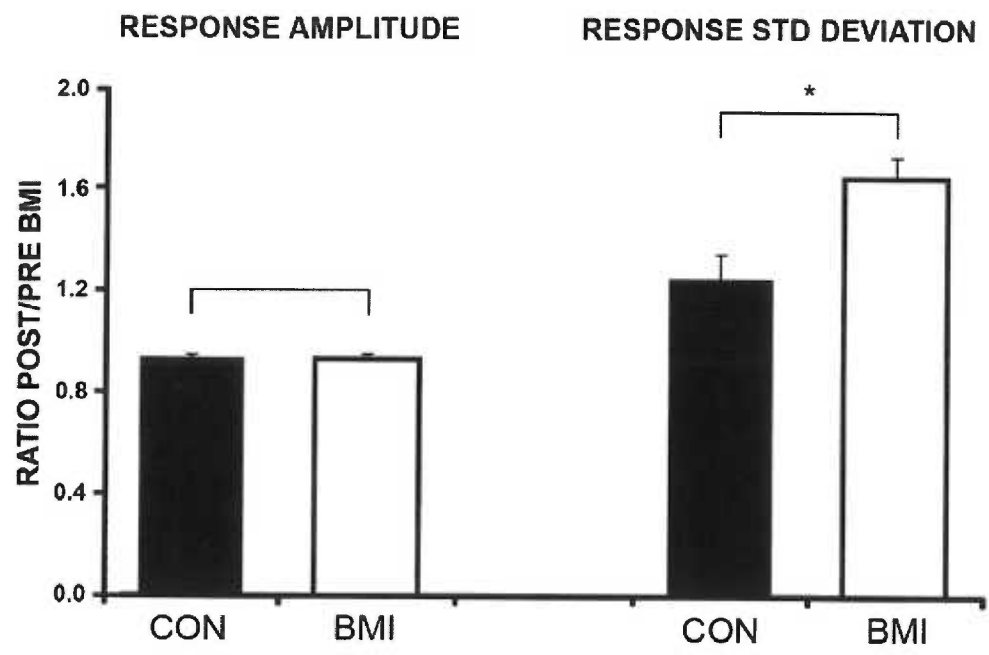
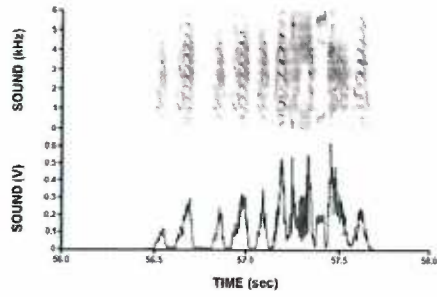


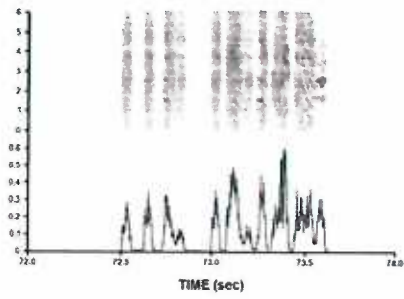
**Figure 4.6) Blockade of GABA-A Receptors Alters Temporal Dynamics of Song-  
Evoked Responses in NCM**

Averaged responses (n=50) to 2 conspecific songs at four sites (2 left-Control, 2 right-BMI) in NCM before (blue) and after (red) BMI injection. On the Control side, the response pattern is similar before and after BMI injection. Small changes reflect variability and habituation to the stimulus. On the BMI side, responses have become dramatically more phasic with a significant disappearance of sustained responses throughout stimulus.

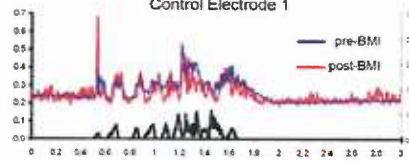
SONG 1



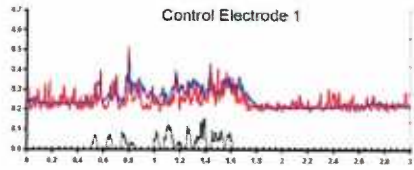
SONG 2



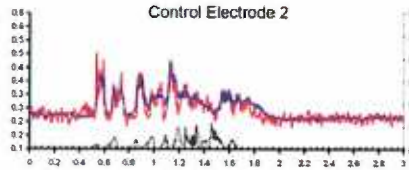
Control Electrode 1



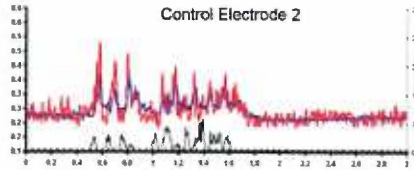
Control Electrode 1



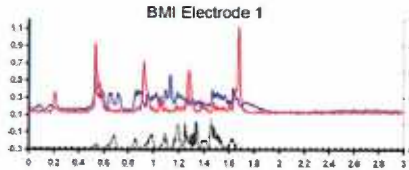
Control Electrode 2



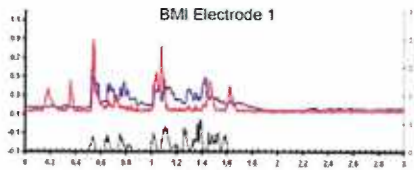
Control Electrode 2



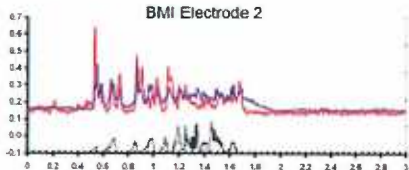
BMI Electrode 1



BMI Electrode 1



BMI Electrode 2



BMI Electrode 2

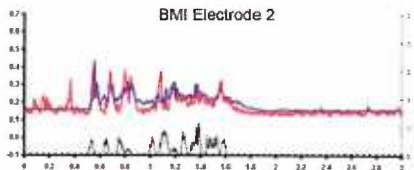


**Figure 4.7) GABAergic Transmission Does Not Participate in the Shaping of Frequency Tuning Curves in NCM**

Tuning functions based on normalized phasic (0-50 msec) responses to tone stimuli (250-5000Hz) before (blue) and after (red) BMI application at four recording sites (2 left-control; 2 right-BMI). Lower lines without markers show background levels.

Different sites show different best frequencies, but BMI does not cause any changes in the overall shape of the tuning functions.



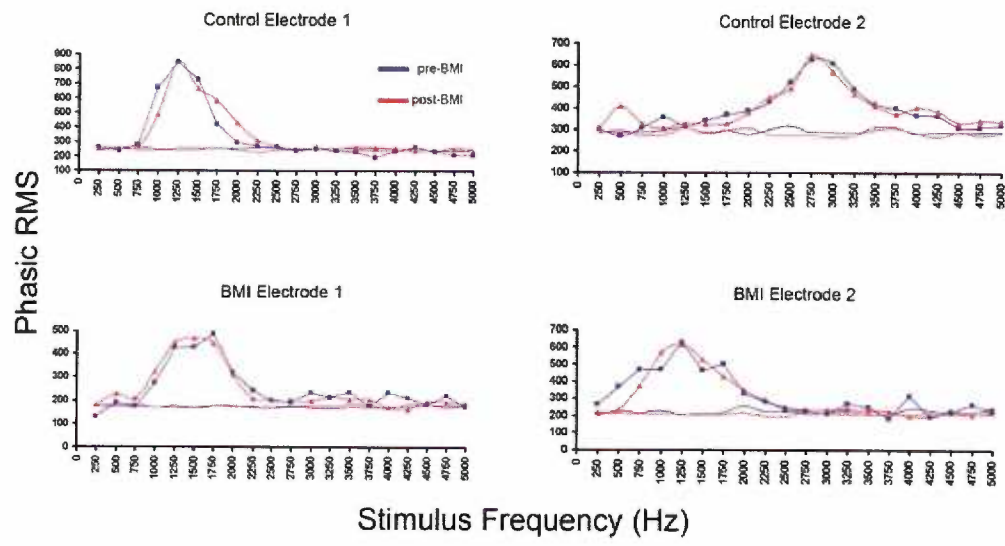
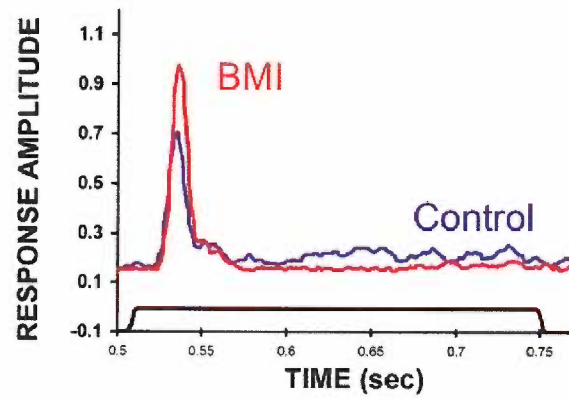


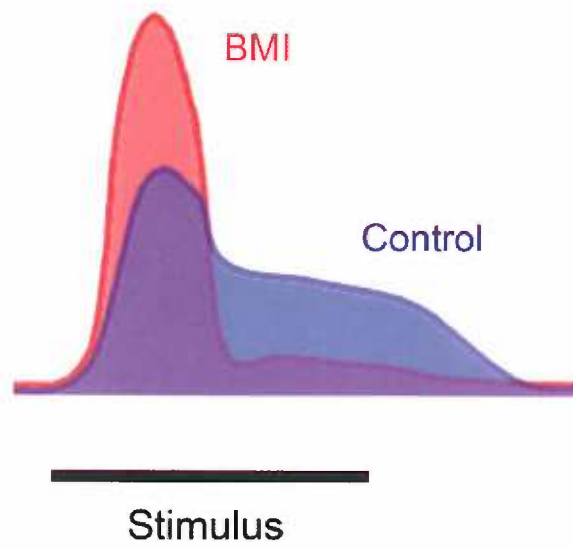
**Figure 4.8) Pure-Tone Evoked Responses Evidence Reorganization of Firing Temporal Dynamics**

A) Average response ( $n=5$ ) to a tone burst before (blue) and after (red) BMI application. Note that responses before BMI application are high to the onset of the stimulus and present a sustained response throughout the duration of the presentation. After BMI application, responses get highly synchronized, especially in response to the onset of the stimulus. However, the sustained response throughout the duration of the stimulus decreases significantly as compared to control levels. B) This cartoon compares the temporal pattern of response to a single song syllable with BMI (red) and without (blue), based on the data presented in (A). The BMI response has a higher phasic peak, followed by a lower tonic valley, corresponding to the higher variation seen with BMI. For the total areas under each curve to be equal, as the data show, the area of the difference between the two curves during the phasic period must be equal and opposite to the area of the difference between the two curves during the tonic period. This suggests that GABAergic mechanisms normally shape the temporal pattern of the response by shifting activity from the phasic period into the tonic period.

A



B



**Frequency of Spontaneous GABAergic Events (in Hz).**

<b>Frequency (in Hz)</b>		
Average	S.E.M.	n
4.74	0.6	7

\*20 $\mu$ M BMI blocks ~ 100% of events

**Effects of AMPA/Kainate Receptor Blockade on Frequency and Amplitude of GABAergic Spontaneous Events**

Frequency (in Hz)			
	Average	S.E.M.	n
Control	4.59	0.61	3
DNQX (20 $\mu$ M)	1.46	0.6	3

Amplitude (in pA)			
	Average	S.E.M.	n
Control	46.69	0.29	3
DNQX (20 $\mu$ M)	30.68	0.31	3

### Frequency and Amplitude of Bursts of Glutamatergic Events

Glutamatergic EPSCs			
	Mean	S.E.M.	n
Intraburst Interval (s)	13.79	2	4
Frequency (Hz)	0.079	0.01	4
Amplitude (pA)	359.22	84.4	4

## **DISCUSSION**

### **A Novel Mechanism for Auditory Information Coding**

The novel finding reported in present paper is that GABAergic transmission regulates, in an unconventional fashion, local inhibitory input during auditory processing of birdsong in NCM. By using extracellular electrophysiological recordings in awake restrained animals, we observed that blockade of GABA-A receptors leads to the release of a second form of inhibitory transmission in this auditory area. We showed that the song-evoked responses, which primarily exhibit a sustained firing behavior, undergo a dramatic shift to highly synchronized, phasic responses upon blockade of GABA-A receptors (Fig. 8). These findings are in sharp contrast to previous reports on the auditory system of other vertebrate experimental models, whereby BMI-induced shifts from phasic to tonic behavior were observed (Chen and Jen, 2000). This set of previous work did not report, however, tonic response profiles shifting into phasic responders for any of the cells studied, as were described in the present report. These earlier findings are not surprising given that antagonism of GABA-mediated transmission is expected to decrease the threshold for action potential generation and to generally increase excitability of neuronal networks; thus would be expected to account for the increase in stimulus-evoked firing and hence the frequency of those events, as was observed by Chen and Jen (2000). In fact, in other avian species, such as the barn owl, it has been reported that BMI application also led to a marked increase in firing behavior in motion-sensitive cells of the inferior colliculus (Kautz and Wagner, 1998). It thus appears that

GABAergic transmission in the majority of vertebrate species acts to contain both spatial and/or temporal excitatory activity occurring during sensory processing. Our results show that blockade of GABAergic transmission does not affect the overall firing rate of NCM neurons during birdsong auditory stimulation, but rather dramatically alters the temporal organization of their spiking behavior (Fig. 8).

These results indicate that the songbird auditory telencephalon appears to process information through mechanisms that are widely different from other vertebrates. What remains unclear is why songbirds would have evolved different auditory-processing network configurations, in telencephalic auditory stations, compared to other species. One possible explanation for such a disparity might reflect the fact that songbirds are among the very few species that exhibit vocal learning behavior. Just a few species exhibit vocal learning in addition to songbird including parrots, whales and dolphins (cetaceans) and humans (for recent reviews see Zeigler and Marler, 2004). Vocal learning involves a complex association between auditory information processing and the production of highly stereotyped motor patterns/programs involved in vocal output generation (for recent reviews see Zeigler and Marler, 2004). It has been proposed that GABAergic influences in auditory stations increased significantly throughout evolution to support the heightened complexity of computations required to regulate a growing set of behaviors related to auditory processing and vocal communication (Winer and Larue, 1996). This proposal has been forwarded based on observations conducted in the medial geniculate nucleus (MGN), whereby an increase in complexity in the phylogenetic scale is paralleled by an increase in the numbers of MGN GABAergic cells, but not in



other thalamic stations such as the lateral geniculate nucleus (Winer and Larue, 1996). This increase in inhibitory components is observed for the songbird MGN equivalent, nucleus Ov, where approximately 40% of the total neuronal population is GABAergic (Pinaud et al., 2005). This hypothesis is further strengthened by recent findings by our group demonstrating that essentially half of all neurons NCM are GABAergic (Pinaud et al., 2004; Pinaud et al., 2005), whereas in their mammalian equivalents only 25-30% of the neuronal population is inhibitory (Jones, 1993). Interestingly, a large proportion of song-activated cells in NCM is GABAergic (Pinaud et al., 2004), further indicating that these inhibitory neurons likely play prominent roles in the processing of birdsong in this telencephalic region.

Should the hypothesis that elaborated inhibitory processing is required to encode and process complex auditory events (Winer and Larue, 1996), like those involved in vocal learning behavior, be correct, and that such a situation applies to songbird telencephalic auditory stations, then the present results could be interpreted to mean that the organization of the GABAergic circuit in songbirds divergently or independently evolved in response to behavioral and/or evolutionary pressures.

### **A Disinhibitory Circuit**

Our experiments demonstrate that BMI application largely abolishes the sustained firing of NCM neurons that is commonly observed during birdsong auditory stimulation in awake animals. These results are counter-intuitive in the sense that BMI application enhances network excitability by blocking GABA-mediated inhibition. Instead, blockade of GABA-A receptors leads to a suppression of song-

evoked firing behavior in response to some song syllables, as shown in the present work. One interpretation of these results is that with BMI-induced neuronal synchronization, sustained responses are not observed because the refractory period that is associated with neuronal firing falls within the same temporal window. Such temporal proximity could prevent action potentials for the period that corresponds to the refractory events. I argue however, that this interpretation is unlikely given that song-induced synchronized bursts of activity were often interspersed for periods that exceeded 500 milliseconds, a time frame that greatly surpasses the minimal time required for recovery of inactivation, which tends to last a few milliseconds in a wide variety of preparations.

Another possibility suggested by these results, however, is that following BMI treatment, a secondary inhibitory network is “released” from GABA-A control and can then act to suppress the sustained component of auditory responses. We conducted experiments with PTX in order to investigate whether the “secondary” NCM inhibition was mediated through GABA-C receptors. Our results however, have indicated that this possibility is not likely to be valid given that no differences were observed when comparing the results obtained by BMI and PTX treatment. Furthermore, these results suggest that GABA-A receptors are the first and foremost mechanism of inhibition within NCM microcircuitry. Overall, our data indicate that during normal auditory processing in NCM, GABA-A mediated inhibition suppresses a likely spontaneously active GABAergic cell population thereby allowing for the excitatory network to be expressed and appropriately encode auditory information. Our patch-clamp results lend further support to this hypothesis, that a population of

GABAergic neurons provides inhibition through spontaneous quantal release at rest conditions (in the absence of song-evoked auditory responses). These data, however, indicate that the spontaneous inhibitory transmission acts only via GABA-A receptors since BMI completely abolishes the sIPSCs. It remains to be investigated whether BMI affects different populations of GABAergic neurons in dissimilar manners, or whether a mechanism not involving GABA-A and GABA-C receptors could be under the control of GABA-A mediated inhibition during auditory processing in NCM, such the activation of metabotropic glutamate receptors (Fiorillo and Williams, 1998).

### **Fidelity of Information Processing is Regulated by GABA**

We show here that altering GABAergic transmission by blocking GABA-A receptors markedly decreases the fidelity of auditory information processing in NCM neurons. The lack of responses to certain syllables might be related to the dramatic synchronization of neuronal firing during BMI treatment. One possibility for the decrease in fidelity is that synchronization generates windows of synchronized refractory periods during which neurons would be unable to fire in response to sensory drive. Under normal conditions, the refractory period of a neuron or linked population of cells could become irrelevant should the circuit have mechanisms for sampling auditory inputs across multiple parallel channels and/or have neurons specifically activated by exact and different acoustic features at different latencies. However, under conditions of synchronization, the refractory behavior of neurons would significantly overlap, possibly accounting for the observation that the encoding of certain syllables was prevented.

A second possibility that could account for the marked decrease in the fidelity of processing could be related to a decreased discrimination ability of NCM units. It has been previously demonstrated in a number of experimental models that antagonism of GABA-A receptors generates marked expansions in frequency-tuning curves in several stations of the vertebrate ascending auditory pathway (Yang et al., 1992; Suga et al., 1997; Chen and Jen, 2000). This is clear evidence for decreased neuronal discrimination ability. In our experiments, however, frequency tuning curves were found to be unaffected by BMI treatment, suggesting that frequency discrimination of NCM cells is likely unaffected by this pharmacological agent. Overall these results suggest that the songbird auditory telencephalon exhibits a dramatically different functional organization as compared to other vertebrate species commonly studied in auditory physiology paradigms. These differences might be key in understanding how vocal learning behavior, particularly with regards to the formation of auditory memories, is encoded in neural networks of vocal learners, including humans. This possibility highlights the potential of songbirds as a powerful model to investigate auditory processing in vocal learners.

The data presented here, to the best of our knowledge, is the first description of a primarily disinhibitory circuit in a primary sensory region of a vertebrate species. In future experiments we will characterize and separate contributions of individual inhibitory components of this circuit and relate them to the process of auditory information processing.

## **CHAPTER 5**

### **CALBINDIN-POSITIVE NEURONS REVEAL A SEXUAL DIMORPHISM WITHIN THE SONGBIRD ANALOGUE OF THE MAMMALIAN AUDITORY CORTEX**

## INTRODUCTION

Various areas of the vertebrate brain are known to be sexually dimorphic. Most such areas reside in the hypothalamus and limbic system and include the sexually dimorphic nucleus of the preoptic area (SDN-POA), the bed nucleus of the stria terminalis (BNST), parts of the amygdala, and discrete regions of the basal forebrain (see reviews in Cooke et al., 1998; Stefanova and Ovtcharoff, 2000; Simerly, 2002). These brain sex differences range from marked dimorphism in overall size and shape of entire areas or nuclei, to more subtle differences in the densities of neurochemically-distinct cell populations, such as enkephalin- and parvalbumin-expressing cells of the BNST and amygdala or calbindin-positive neurons of the SDN-POA, to differences in neuronal density, size and morphology, as described for dentate granule cells (Wimer and Wimer, 1985; Roof, 1993; Cooke et al., 1998; Brager et al., 2000; Sickel and McCarthy, 2000; Stefanova and Ovtcharoff, 2000). Sexual dimorphism has also been well characterized in the accessory olfactory system, which is involved in the detection and encoding of pheromones. For example, the vomeronasal organ (VNO) has sexually dimorphic patterns of pheromone receptor expression and bipolar neuronal numbers, the accessory olfactory bulb (AOB) contains significantly fewer neurons in females, and the part of the amygdala thought to integrate inputs from the AOB is significantly larger and contains larger neurons in males (Segovia and Guillaumon, 1982; Mizukami et al., 1983; Segovia and Guillaumon, 1993; Herrada and Dulac, 1997; Cooke et al., 1998).

A striking example of brain sexual dimorphism is the song control system of songbirds, an interconnected set of brain nuclei that play critical roles in vocal production and learning (Nottebohm and Arnold, 1976; for recent reviews, see Zeigler and Marler, 2004). This system is typically more developed in males, where song nuclei contain more and larger neurons as compared to females. As in mammals, the development and maintenance of this gender difference is regulated by gonadal steroids, although some evidence suggests that sex-specific brain-expressed genes may also play a role (for reviews, see (Simerly, 1998; Arnold, 2004; Ball et al., 2004). The dimorphism of the song system correlates well with sexual dimorphism in singing behavior, being most pronounced in species that present dramatic gender differences in singing behavior (usually males, but not females, sing), but less pronounced or absent in species where both sexes sing (Brenowitz and Arnold, 1985; Brenowitz et al., 1985; Brenowitz, 1997). Importantly, gender differences have also been described in the perceptual processing of song and calls (Williams, 1985; Cynx and Nottebohm, 1992a, b; Del Negro et al., 2000; Del Negro and Edeline, 2001, 2002; Vicario et al., 2002). Although these sex differences in perception have been associated with the dimorphism of the song control system, no studies have investigated the existence of dimorphism in sensory areas directly involved in the auditory processing of birdsong.

We have been studying the role of GABAergic inhibition in song-processing auditory circuits in the zebra finch telencephalon, with emphasis on the caudomedial nidopallium (NCM; we use the revised avian brain nomenclature, as in Reiner et al., 2004), a component of the central auditory pathway of songbirds implicated in the

perceptual processing of song (Mello et al., 2004; Pinaud et al., 2004). Based on connectivity studies, NCM has been suggested to be analogous to the supragranular layers of the mammalian auditory cortex (Vates et al., 1996). NCM exhibits robust song-evoked electrophysiological responses (Chew et al., 1995), as well as induced expression of the activity-dependent gene *zenk* in response to song stimulation (Mello et al., 1992; Mello and Ribeiro, 1998; Mello et al., 2004). In addition, we have recently demonstrated that almost half of the song-activated NCM cells are GABAergic, indicating that inhibitory neurons may play a critical role in the auditory processing of birdsong in this area (Pinaud et al., 2004). We report here that cells positive for the calcium-binding protein calbindin constitute a subpopulation of GABAergic neurons primarily localized to caudal NCM and are almost twice as numerous in males as in females. This difference is not explained by differences in the overall density of neuronal or of GABAergic cells in NCM. In addition, calbindin-positive neurons in NCM do not present song-induced ZENK expression and are, therefore, a distinct GABAergic cell population compared to that detected in our previous work (Pinaud et al., 2004). We also report that the caudal NCM domain that is enriched in calbindin-positive neurons expresses high levels of aromatase, a key enzyme catalyzing the conversion of testosterone into estrogen. We found, however, that neither the mRNA levels nor the distribution of aromatase expression was influenced by sex. Short-term auditory stimulation with song also did not alter the overall density of calbindin-positive neurons in either sex. Together, these findings provide clear evidence for a sexual dimorphism in a “cortical-like” auditory



area and suggest that local sex steroids might impact auditory processing circuits in the adult vertebrate brain.

## **MATERIAL AND METHODS**

### **Animals and Tissue Preparation**

We used a total of 48 adult zebra finches (*Taeniopygia guttata*; 24 females; 24 males), maintained in a 12h/12h light/dark cycle with access to food and water ad libitum. For calbindin immunocytochemistry (ICC), birds (n= 5 males and 5 females) were sacrificed with an overdose of Nembutal and transcardially perfused with 20 ml of 0.1M phosphate buffer (PB; pH=7.4) followed by 60 ml of a solution of 4% paraformaldehyde in PB. To allow for the analysis of calbindin and ZENK co-expression and to characterize the effects of birdsong auditory stimulation on the number of calbindin-positive neurons, a subset of these birds (n=4 males and 4 females; sound stimulated subset) was sacrificed immediately after stimulation for 1 hr with a medley of 3 conspecific songs following overnight housing in sound-proof boxes (as detailed in (Mello et al., 1992; Mello and Ribeiro, 1998); the remaining birds were killed after overnight sound isolation but without song stimulation (unstimulated subset). For GABA ICC and for double ICC for GABA and calbindin (n= 5 males and 5 females), the perfusion was conducted as described above for calbindin, except that the fixative was a cocktail of 1% paraformaldehyde and 2% glutaraldehyde in PB. The brains were then dissected out and cryoprotected in 30% sucrose, dried, split at the mid-sagittal plane, included in embedding medium (Tissue-Tek; Sakura Finetek, Torrance, CA), frozen in a dry-ice/isopropanol bath, sectioned

parasagittally on a cryostat (20 $\mu$ m), mounted directly onto glass slides (Fisherbrand Superfrost Plus), dried at RT and stored at  $-80^{\circ}\text{C}$ .

In order to investigate possible gender differences in the expression of aromatase mRNA in the caudal part of NCM, an additional set of 18 birds (9 males, and 9 females) was first exposed to either 30-min of novel conspecific song (n=8; using a song medley identical to that described above) or silence (n=10). Following song exposure, birds were sacrificed by decapitation, their brains were quickly dissected, and individual hemispheres were embedded in Tissue-Tek and flash frozen in a dry-ice/isopropanol bath. The hemispheres were sectioned parasagittally on a cryostat (at 10  $\mu$ m) and stored at  $-80^{\circ}\text{C}$ . All animal protocols were approved by OHSU's IACUC committee and are in accordance with NIH guidelines.

### **Immunocytochemistry (ICC)**

We used a commercial anti-calbindin D-28K monoclonal antibody (Sigma, St.Louis, MO). Calbindin is a highly conserved protein, the avian (chicken) homologue presenting 93% identity at the aminoacid level with rat calbindin (Hunziker and Schrickel, 1988). It has been shown, through western blot analysis, that pigeon and rat brain calbindin are recognized as single bands and that pre-absorption of the monoclonal antibody with the immunizing peptide completely abolishes calbindin immunostaining in the pigeon brain (Pasteels et al., 1987). The immunoreactivity pattern we detected in our birds for song control nuclei HVC and RA (not shown) is in agreement with the patterns previously reported for these nuclei in zebra finches using an antibody raised against the chicken calbindin (no longer available) (Wild et

al., 2001; Wild et al., 2005). We used an ICC protocol that has been previously described in detail (Pinaud et al., 2004), with minor modifications. Briefly, the sections were removed from the freezer, hydrated in PB for 30 min, followed by a 20 min incubation in a blocking buffer (BB; 0.5% albumin and 0.3% Triton X-100 in 0.1M PB). The sections were then briefly washed in PB, incubated overnight at 4°C with the anti-calbindin antibody (1:3000 dil in BB) in a humid chamber, incubated for 2 hr at room temperature (RT) with a biotinylated secondary antibody (1:200 dil in BB; Vector Laboratories, Burlingame, CA), and incubated for 2 hr at RT with ABC reagent (1:100 dil in PB; Vector Laboratories, Burlingame, CA). Sections were developed by incubation in a solution containing 0.03% diaminobenzidine, 0.15% Nickel sulfate and 0.001% hydrogen peroxide, in PB. All steps above were separated by PB washes (3 x 10 min each). The sections were then dehydrated in a standard series of alcohols and immersed for 30 min in xylenes. Omission of primary antiserum resulted in complete absence of immunolabeling. For GABA ICC we used a commercially available rabbit antibody (1:200 dil in BB; Chemicon International, Temecula, CA) and the same protocol as for calbindin. The immunostaining pattern seen for GABA was abolished when the antiserum was pre-absorbed with a GABA-BSA conjugate. The sections from all males and females were processed together in a single immunocytochemical batch, to minimize procedural variability in the resulting staining patterns.

### **Double-ICC**

For ZENK and calbindin double-ICC, we first reacted sections for calbindin as described above, except that a goat-anti-mouse secondary antibody coupled to Alexa-488 was used (1:200 dil; Molecular Probes, Eugene, OR). After incubation with this secondary antibody (2 hr at RT) sections were washed in 0.1 PB (3 x 10min), incubated overnight with a rabbit anti-egr-1 antibody (1:500 dil; Santa Cruz Biotechnology, Santa Cruz, CA), washed in PB (3 x 10min) and incubated for 2 hr at RT with a goat-anti-rabbit secondary antibody coupled to Alexa-594 (Molecular Probes, Eugene, OR). A similar protocol was used for double-ICC for GABA and calbindin. Briefly, sections were first exposed to UV light under a fluorescence microscope to quench the excess autofluorescence resulting from glutaraldehyde fixation. The sections were then reacted for calbindin using the fluorescence procedure described above. Subsequently, sections were washed in PB 0.1M for 30 min and incubated overnight with the anti-GABA antibody (1:100 dil in BB; Chemicon International, Temecula, CA). Sections were then incubated for 2 hr at RT with a goat-anti-rabbit secondary antibody coupled to Alexa-594 (Molecular Probes, Eugene, OR). After a final series of washes, all sections were coverslipped with Aquamount (Lerner Labs, Pittsburgh, PA).

### **Aromatase *In situ* Hybridization**

Plasmids containing the cloned zebra finch aromatase cDNA (a generous gift from Dr. C. Saldanha, Lehigh Univ.) were isolated from bacterial stock using the Qiagen miniprep kit (Qiagen Inc., Valencia, CA), linearized with the appropriate restriction enzymes, and purified using Qiagen PCR purification kit (Qiagen Inc., Valencia,

CA).  $^{33}\text{P}$ -labeled antisense riboprobes were generated, purified, and used for *in situ* hybridization according to previously described protocols (Mello et al., 1997; Pinaud et al., 2004). Briefly, sections were fixed in a 3% saline-buffered paraformaldehyde solution for 5 minutes, rinsed twice in 0.1M PBS, and dehydrated in an alcohols series. Sections were then incubated for 10 min in acetylation solution (1.35% triethanolamine and 0.25% acetic anhydride in water), rinsed 3 times with 2X SSPE, dehydrated in the alcohol series and air-dried. A hybridization solution (16 $\mu\text{l}$ ) containing 50% deionized formamide, 2X SSPE, 2 $\mu\text{g}/\mu\text{l}$  tRNA, 1  $\mu\text{g}/\mu\text{l}$  BSA, 1  $\mu\text{g}/\mu\text{l}$  poly-A in DEPC-treated water, and  $5 \times 10^5$  cpm of antisense aromatase riboprobe was then added to each section. The slides were coverslipped, sealed by immersion in mineral oil, and incubated at 65°C overnight. Sections were then rinsed in chloroform, de-coverslipped in 2X SSPE, and washed by incubating sequentially for 1 hr at room temperature (RT) in 2X SSPE, for 1.5 hr at 65°C in 2X SSPE containing 50% formamide, and twice for 30 min at 65°C in 0.1X SSPE. Sections were then dehydrated in an alcohol series and analyzed by either X-ray film or phosphorimager autoradiography with a low energy screen and a Typhoon scanner (Molecular Dynamics). Sections were counterstained with cresyl violet for microscopic analysis.

### **Section Mapping, Analysis and Photomicrography**

Stained sections were examined and mapped using the Neurolucida software package integrated with a Nikon E-600 microscope equipped with a motorized stage drive (LEP Mac5000) and coupled to a PC through a Lucivid system (Microbrightfield; Colchester, VT). For calbindin ICC experiments, three parasagittal planes were

examined (approximately 0.1, 0.5 and 0.9 mm from the midline), and the number of calbindin-labeled cells in NCM in each section was mapped, counted, and averaged across birds according to gender (n=5 males and 5 females). NCM boundaries consisted of the ventricle in its dorsal, caudal and ventral aspects, and the boundary with field L2 rostrally. Because of the highly uneven distribution of calbindin-positive cells in NCM, a random sampling method for density estimates would not have been adequate. To generate estimates of local densities of GABAergic cells, a grid containing squares of 100 x 100µm was superimposed on sections reacted for GABA ICC at the same planes as for calbindin ICC. A minimum of 15 such squares per stereotaxic level, per bird, evenly spaced through rostral and caudal NCM were used for counting labeled cells. Because no differences were detected for rostral and caudal NCM in relation to the overall neuronal and GABAergic cell populations, results were averaged for each of the three planes examined and across birds (n=5 males and 5 females). To estimate neuronal cell density, we counted the number of neurons per unit area in Nissl-stained adjacent sections of the same animals using the same sampling as above for GABA. The inclusion criteria for neurons were a large pale nucleus, usually with clear staining nucleolus, and prominent Nissl substance, while the exclusion criteria consisted of small cells with dark, homogeneously-stained nuclei and scant cytoplasm. For double-ICC experiments (calbindin/GABA and calbindin/ZENK), we examined the full extent of NCM in all reacted sections and quantified the proportions of double-labeled cells (about 900 calbindin-positive cells per male bird and 500 per female were examined). For all estimates above, we did not use stereology because: 1) our primary purpose was to verify relative gender

differences in the various cell counts, rather than to estimate the total number of counted cells in NCM in each gender; 2) the sections' thickness would be inappropriate for an adequate stereological analysis; and 3) the lateral boundary of NCM, as well as its rostral boundary at lateral levels, are not well defined, therefore it is not possible to generate an accurate estimate of the size of NCM.

For size estimates of calbindin-positive cells, we used NeuroLucida software to reconstruct the perimeters of individual neurons and to derive the largest soma diameter and area. We analyzed 50 neurons for each parasagittal plane in three randomly placed fields in caudal NCM that spanned the dorsal-to-ventral extent of this area. Because no differences were detected for cell sizes in dorsal vs. ventral and medial vs. lateral NCM comparisons (not shown), all data for soma diameter and area were combined for each animal. Data were then averaged across animals for each sex (n=5 per sex).

In order to compare the distribution and overall abundance of aromatase mRNA expression in the caudal NCM of males and females, we also performed a series of quantitative measurements over phosphorimager autoradiograms of *in situ* hybridized brain sections at two stereotaxic levels (0.1 and 0.5mm from the midline) using NIH Image software. For each section we first established a threshold defining a standardized aromatase expression contour, or band of high intensity aromatase expression greater than 6-fold above the tissue background intensity measured over the cerebellum. At each stereotaxic level, we then measured the total area ( $\mu\text{m}^2$ ) occupied by the aromatase expression contour. We also measured the average optical density over this area and over the cerebellum, subtracted nonspecific slide-glass



background from both measurements, and calculated the ratio (fold difference) between the NCM and cerebellar measurements. We repeated the above measurements for an additional set of contours inclusive of expression at least 8-, 10-, and 12-fold greater than the cerebellar levels. Photomicrographs were acquired with a Digital camera (DVC, Austin, TX) coupled to the microscope. Adobe Photoshop was used for final assembly of photomicrograph plates and of mapped sections.

### **Statistical Analysis**

A one-way analysis of variance (ANOVA) was used to examine gender differences in the various parameters (e.g. numbers of Nissl, GABA and calbindin-positive cells, average optical densities, total area, etc.) measured at each stereotaxic plane examined. In addition, three-way ANOVA was used to compare the overall neuronal, GABAergic and calbindin-cell densities across stereotaxic levels, genders and sampling location in NCM. The criterion for significance was set at  $P < 0.001$ .

## RESULTS

### **Calbindin-Positive Cells in NCM Represent a Distinct Population of GABAergic Cells**

We observed a discrete number of calbindin labeled cells (Fig. 1B) in comparison with the very high density of GABAergic cells present in this area (Pinaud et al., 2004). Calbindin-positive cells were relatively small and had strong staining in the soma, which tended to be round or ellipsoid. In some cases, immunolabeled neurons exhibited labeled neurites that extended for relatively long distances (Fig. 1C). Interestingly, labeled cells were not distributed homogeneously, but rather were more concentrated in caudal NCM and scarce rostrally (Figs. 1B and 3). This pattern was consistent along the medial-to-lateral extent of NCM as revealed by examining serial parasagittal sections (Supplementary Material, Fig. 1; an analysis of calbindin immunoreactivity in other brain areas will be presented elsewhere).

In most brain areas examined to date, including the auditory cortex, calbindin-positive neurons are thought to constitute a sub-population of GABAergic neurons (Hendry and Jones, 1991; Rogers, 1992; Reynolds et al., 2004). In order to investigate whether this is the case in the songbird NCM, we conducted double-ICC for GABA and calbindin. This experiment revealed that calbindin-positive cells in NCM are GABAergic (Fig. 2A-C). Extensive analysis showed that all calbindin-positive cells examined (approximately 900 cells per male and 500 cells per female) were also positive for GABA. Moreover, the majority of GABAergic neurons were calbindin-

negative, indicating that the calbindin-positive cells represent a distinct sub-population of GABAergic cells within NCM (Fig. 2C).

GABAergic neurons in NCM are known to express the activity-dependent gene *zenk* (both mRNA and protein) in response to birdsong auditory stimulation (Pinaud et al., 2004). Expression analysis of *zenk* has been extensively used to identify and map song-responsive cells in the songbird brain (reviewed in Mello, 2002b; Mello et al., 2004). To determine whether calbindin-expressing cells in NCM also respond to song by inducing *zenk* expression, we conducted a double-labeling immunocytochemical analysis for ZENK and calbindin proteins in 8 song-stimulated birds (n= 4 males and 4 females). Following a detailed examination (about 200 calbindin-positive cells per plane examined), we were unable to find cells in NCM that expressed both ZENK and calbindin, regardless of gender (Fig. 2D-F). These results indicate that calbindin-positive cells in NCM constitute a unique population of GABAergic neurons that lacks a ZENK response to song.

### **Calbindin Reveals a Sexually Dimorphic Neuronal Population in NCM**

Visual comparison of calbindin immunoreactivity patterns between males and females indicated a marked gender difference in the numbers of labeled cells in NCM, with males exhibiting more calbindin-positive cells than females. To quantify this phenomenon, we mapped and counted calbindin-positive neurons at three selected parasagittal planes (approximately 0.1, 0.5 and 0.9 mm from the midline) in males and females (Figs. 3 and 4). Because of the regional differences in labeled cell density (higher in caudal and lower in rostral NCM), we included in our analysis all

labeled cells within NCM for each plane examined. Males were found to have a significantly greater number of calbindin-positive cells than females at all levels examined (Fig. 4A), although the difference was most pronounced medially (~80, 74 and 42% more cells in males than females for 0.1, 0.5 and 0.9 mm planes, respectively).

To determine whether a general gender difference in neuronal cell density in NCM might account for this dimorphism, we quantified the overall neuronal density in Nissl-stained sections adjacent to those stained for calbindin. We found, however, that neuronal density in NCM is not significantly different across genders (Fig. 4B). Thus, a sex difference in neuronal density is not likely to account for the higher number of calbindin-positive cells in male zebra finches.

Given that calbindin is exclusively expressed in a subset of GABAergic neurons in NCM (Fig. 2A-C), another possibility for the dimorphism observed is that males have a greater density of GABAergic neurons in NCM, as compared to females. To investigate this possibility, we quantified the average numbers of GABAergic neurons per unit area in sections reacted for GABA ICC that were adjacent to those used to quantify calbindin expression. No significant differences in the density of GABAergic neurons were found in NCM between males and females (Fig. 4C), indicating that the gender difference in calbindin-positive cell numbers in NCM is not explained by a higher overall density of GABAergic cells in males.

### **Calbindin-Positive Neurons Are Enriched in an NCM Region That Has High Aromatase mRNA Expression**

Aromatase is a key enzyme in the estrogen synthesis pathway in the vertebrate brain (Schlinger, 1997). It has been previously reported that the expression levels of aromatase mRNA are higher in caudal than rostral NCM of the canary (Fusani et al., 2001), suggesting that the expression of aromatase and calbindin may be associated. To examine whether calbindin and aromatase have overlapping distributions, we performed *in situ* analysis of aromatase expression in parasagittal sections at levels comparable to those reacted for calbindin (Figs. 3 and 5A). We observed that aromatase mRNA expression varies along the rostro-caudal axis, being highest in caudal NCM and decreasing rostrally, apparently in a gradient fashion (Fig. 5B). As shown by the overlay in Fig. 5C, the pattern of aromatase expression and the distribution of calbindin-positive cells in NCM are strikingly similar, suggesting that the expression of these two proteins may be related.

To determine whether aromatase is also expressed in a sexually dimorphic fashion, we examined its expression in NCM by *in situ* hybridization of parasagittal sections comparable to the medial and intermediate levels examined for calbindin. We found that both males and females express high levels of aromatase in caudal NCM (Fig. 5D and E). A densitometric analysis revealed no significant differences in either the relative areas ( $1.85 \pm 0.23$  versus  $1.79 \pm 0.31 \text{ mm}^2$ ,  $p=0.88$ ;  $2.14 \pm 0.65$  versus  $2.63 \pm 0.18$ ,  $p=0.09$ ; for females versus males at 0.1 and 0.5mm from midline, respectively), or average signal intensities ( $11.6 \pm 0.56$  versus  $11.6 \pm 1.9$ ,  $p=0.99$ ;  $10.4 \pm 0.4$  versus  $11.2 \pm 0.6$ ;  $p=0.29$ ) for the high expression domain in NCM (6-fold above background) across genders. Similarly, comparisons of measurements obtained from more restricted aromatase contours (signal levels 8-, 10-, and 12-fold above

background) were also not significant. These results are consistent with previous assessments of the numbers of aromatase-positive cells in NCM across genders (Saldanha et al., 2000) and suggest that despite the similarities in the distribution of aromatase mRNA and calbindin-positive cells in NCM, relative levels of aromatase expression do not predict the observed calbindin sexual dimorphism.

Sex and hormone levels are known to significantly affect cell size and morphology in sexually dimorphic nuclei, including those of songbirds (for examples see DeVoogd and Nottebohm, 1981; Johnson and Bottjer, 1993; Adkins-Regan et al., 1994). To determine whether the calbindin-labeled cells themselves are sexually dimorphic, we reconstructed the perimeter of calbindin-positive neurons and compared the largest diameter and the area occupied by their soma in males and females. We found, however, that the average soma diameter ( $8.9\mu\text{m} \pm 0.2$  S.E. for males;  $8.7\mu\text{m} \pm 0.2$  S.E. for females) or soma area ( $39.6\mu\text{m}^2 \pm 1.4$  S.E. for males and  $35\mu\text{m}^2 \pm 2.1$  S.E. for females) is not significantly different between males ( $n=150$  cells per bird, in 5 birds) and females ( $n=150$  cells per bird, in 5 birds;  $F=5.317$ ;  $p=0.448$  and  $F=3.294$ ;  $p=0.107$ , for soma diameter and area, respectively).

The dimorphism observed could also be related to differential expression levels of calbindin in NCM cells between males and females. Upon close inspection, however, we did not observe a graded labeling for calbindin. Rather, calbindin-positive cells exhibited typically strong labeling in both sexes. In fact, a striking characteristic of calbindin immunoreactivity is that there is virtually no ambiguity in defining labeled cells in either sex (Supplementary Material, Fig. 2), regardless of the

detection method used for ICC (ABC plus DAB deposition or fluorescence-labeled antibodies).

### **The Density of Calbindin-Positive Neurons in NCM is Not Affected by Auditory Experience**

In order to investigate whether the density of calbindin-positive cells in NCM might be affected by song auditory experience, we compared the numbers of these cells per unit area in the NCM of song-stimulated versus unstimulated birds. We found that song auditory stimulation did not alter the average density of calbindin-positive cells in either gender at any level analyzed ( $F=0.459$ ,  $p=0.527$ ;  $F=0.149$ ,  $p=0.711$  and  $F=0.237$ ,  $p=0.642$ , for males, and  $F=0.126$ ,  $p=0.733$ ;  $F=0.088$ ,  $p=0.775$  and  $F=0.121$ ,  $p=0.739$ , for females, at 0.1, 0.5 and 0.9mm from the midline, respectively). Thus, short-term exposure to song does not seem to impact the density of calbindin-positive cells in NCM and, therefore, does not likely account for the sexual dimorphism in this GABAergic cell population.

**Figure 5.1) Calbindin-Positive Cells Are Located in Caudal NCM**

A) Camera lucida drawing of a representative parasagittal section through NCM and adjacent structures (~0.5mm from the midline). The rectangle represents the approximate location where the photomicrograph in (B) was taken. B) Low power view of section reacted for calbindin ICC depicting the distribution of immunoreactive cells in NCM. C) High power view of a representative calbindin-positive cell. Scale bars in  $\mu\text{m}$ : (B) 250; (C) 10. Abbreviations: CMM, caudomedial mesopallium; Hp, hippocampus; L2, field L, subfield L2; NCM, caudomedial nidopallium.



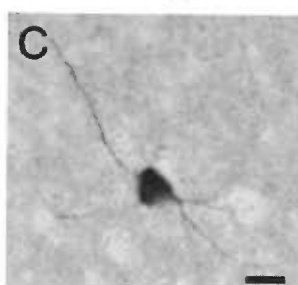
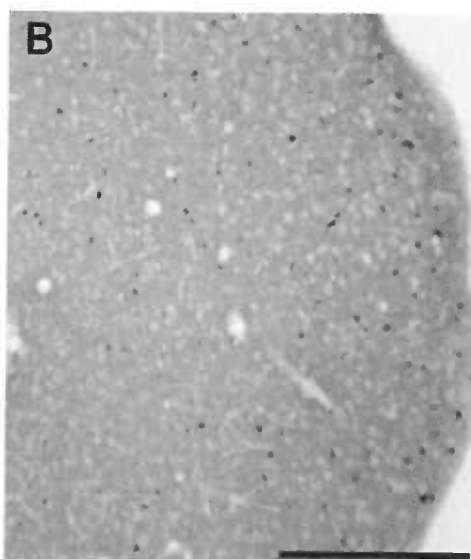
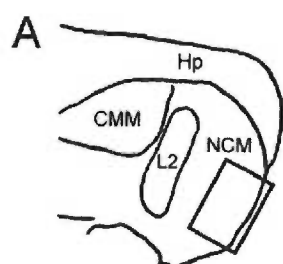


**Figure 5.2) Calbindin-Positive Cells Are GABAergic and Do Not Co-Localize ZENK in Song-Stimulated NCM**

Photomicrographs depicting double labeling experiments against GABA (A) and calbindin (B) in a single representative section through NCM of a male (females exhibit the same immunolabeling profile). C) Overlay of the two channels (GABA in red and calbindin in green) reveals that all calbindin-positive neurons are GABAergic. D-E) Representative photomicrographs from NCM of a stimulated female depicting ZENK (D) and calbindin (E) immunoreactivity. F) No co-localization was detected for either sex throughout this region. Scale bar=25 $\mu$ m.

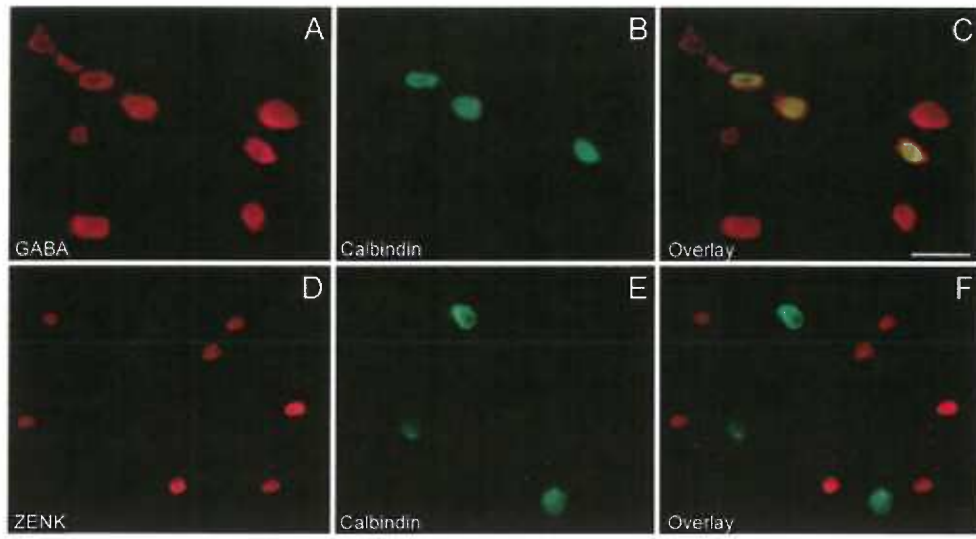


**Figure 5.3) Calbindin-Positive Cell Population in NCM is Sexually Dimorphic**

The camera lucida drawings on the left column are of serial parasagittal sections (0.1, 0.5 and 0.9 mm from midline) and depict the major brain structures present at each level examined. The middle and right columns are maps of calbindin positive cells (black dots) in a representative male and female zebra finch, respectively. Note that calbindin-positive cells are more concentrated in caudal than in rostral NCM. All labeled cells in NCM were plotted; these cells are more numerous in males at all levels examined. The rostral lamina that separates NCM from CMM and the boundaries of field L2 are indicated. A few labeled cells were present in L2 and CMM are not depicted. Scale bar = 1mm. Abbreviations: Cb, cerebellum; CMM, caudomedial mesopallium; H, hyperpallium; Hp, hippocampus; L2, field L, subfield L2; NCM, caudomedial nidopallium.

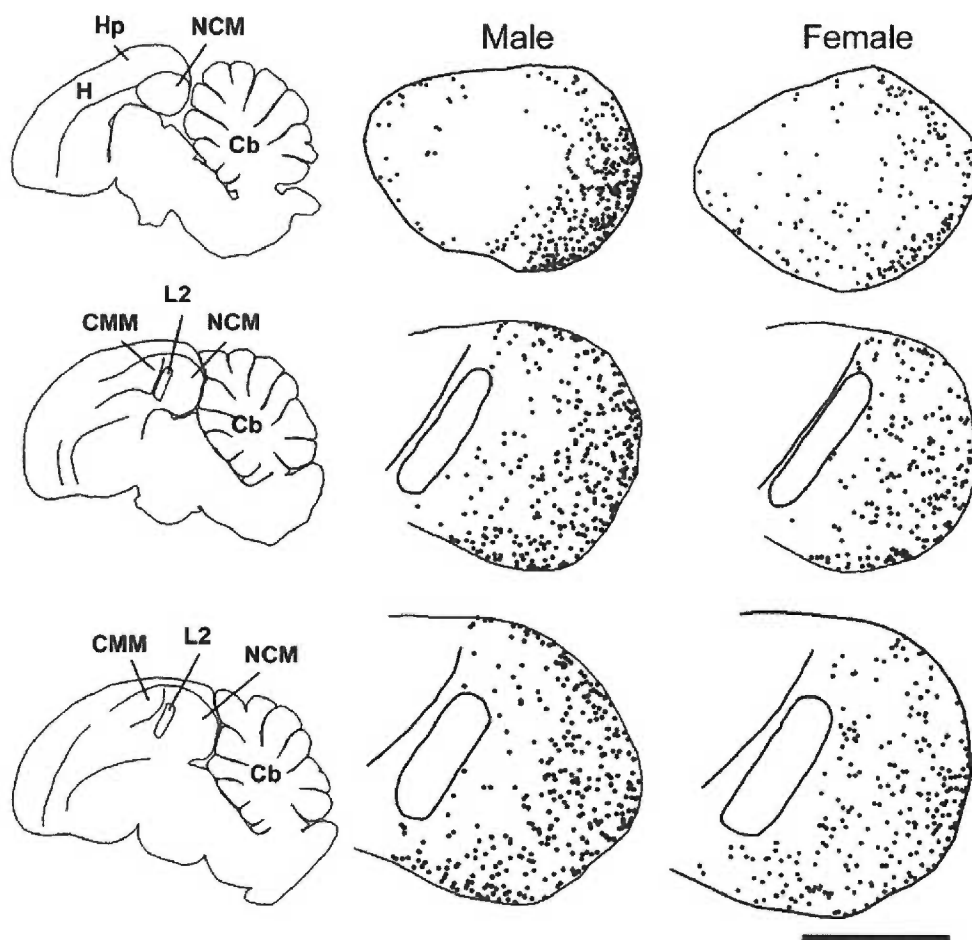


**Figure 5.4) Quantification of Sexual Dimorphism in Calbindin-Positive Cells in NCM**

Plotted are average counts ( $\pm$  S.E.M.;  $n=5$  birds per sex) of all calbindin-positive cells (A), neuronal cells based on Nissl (B), or GABAergic cells based on GABA ICC (C) at the three parasagittal planes examined (0.1, 0.5 and 0.9 mm from midline).

Significant gender differences were observed at all levels analyzed in the number of calbindin-positive cells ( $F=115.563$ ;  $p=1.33 \times 10^{-5}$  for 0.1mm;  $F=32.844$ ;  $p=0.0004$  for 0.5mm and  $F=36.358$ ;  $p=0.0003$  for 0.9 mm from midline, respectively), but not for neuronal density ( $F=0.130$ ;  $p=0.730$ ;  $F=0.090$ ;  $p=0.773$ ;  $F=0$ ;  $p=1$ , for 0.1, 0.5 and 0.9 mm from midline, respectively) or the density of GABAergic cells ( $F=0.834$ ;  $p=0.396$ ;  $F=1.744$ ;  $p=0.234$ ;  $F=0.234$ ;  $p=0.645$ , for 0.1, 0.5 and 0.9mm from midline, respectively).

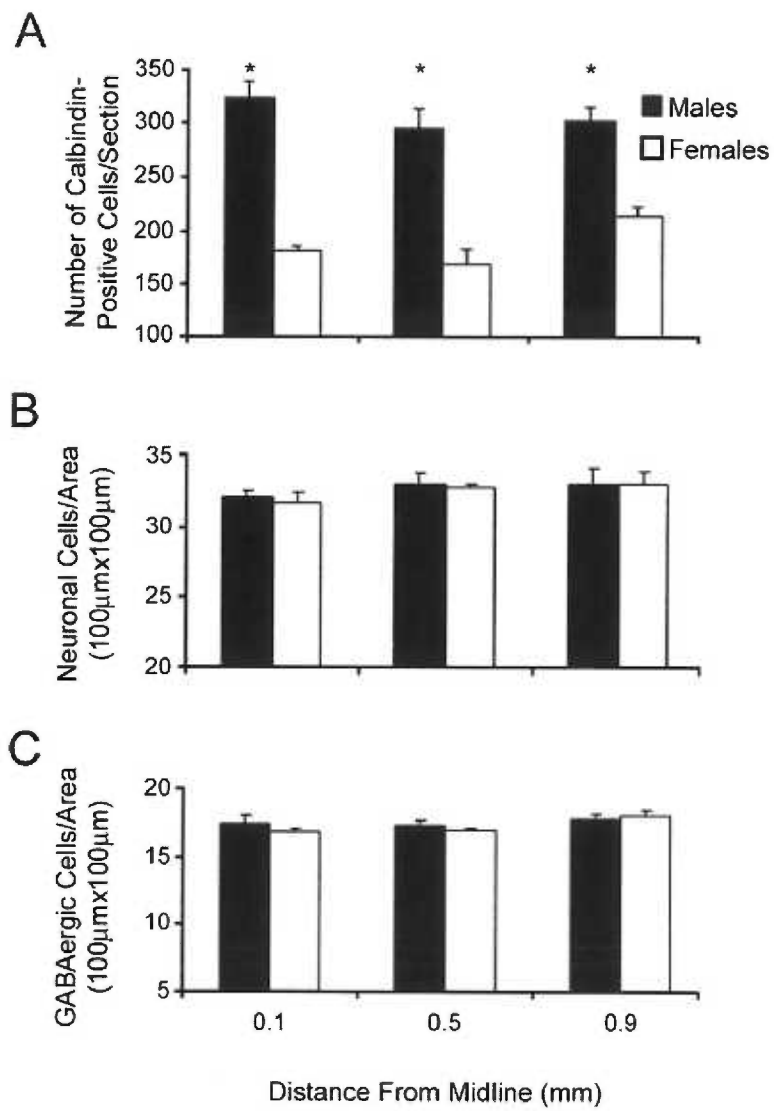
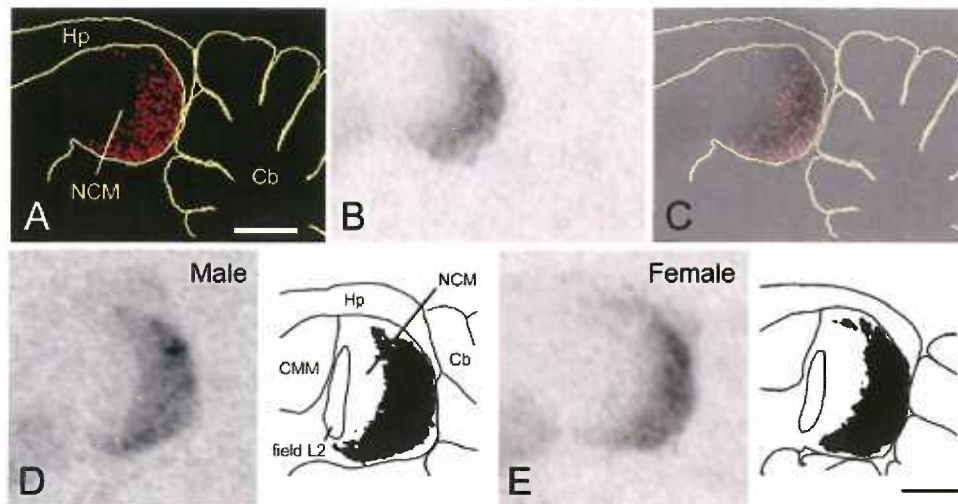


**Figure 5.5) Aromatase Expression Overlaps With Calbindin Distribution in Caudal NCM and Does Not Vary Across Genders**

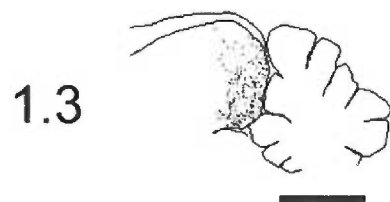
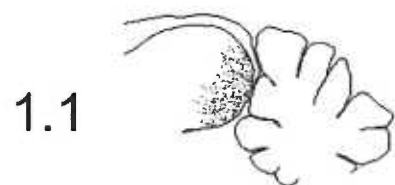
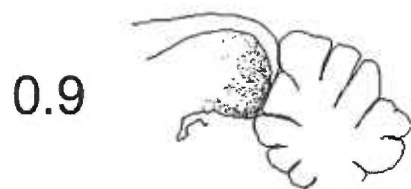
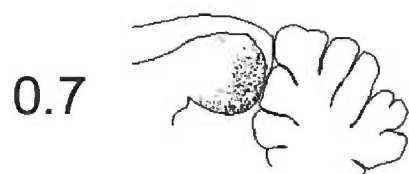
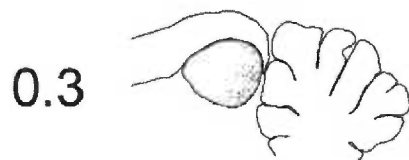
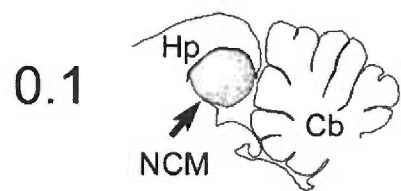
A) Map of the distribution of calbindin-positive cells (red dots) in NCM (0.7mm from the midline). B) In situ hybridization autoradiogram of parasagittal section (approximately the same level as the map in A) depicting the expression of aromatase mRNA throughout the caudal region of the NCM. C) An overlay of panels (A) and (B) determined by tissue boundaries and laminae, depicts a remarkable spatial overlap of aromatase mRNA and calbindin-positive neurons in caudal NCM. D-E) *In situ* hybridization autoradiograms of parasagittal sections depicting the pattern of aromatase transcripts within the caudal telencephalon (~0.5mm from the midline) of a representative male (D, left panel) and female (E, left panel) zebra finch. In NCM, aromatase expression is primarily restricted to a crescent shaped domain that lies upon the ventro-caudal margin of NCM. Camera lucida drawings of the sections whose autoradiograms are shown in D-E (left panels) illustrate a thresholded region of aromatase expression in NCM that is at least 6-fold greater than background for both male (D, right panel) and female (E, right panel) brains. Although aromatase transcripts are quite abundant throughout the caudal NCM in both sexes, no significant gender differences were detected in either the overall pattern of mRNA distribution or in the average intensity of expression over the caudal NCM. Abbreviations: Cb, cerebellum; Hp, hippocampus; NCM, caudomedial nidopallium; CMM, Caudomedial mesopallium. Scale bars: 1mm.





**Supplementary Material Figure 1) Calbindin-Positive Cells Are Primarily  
Localized to Caudal NCM**

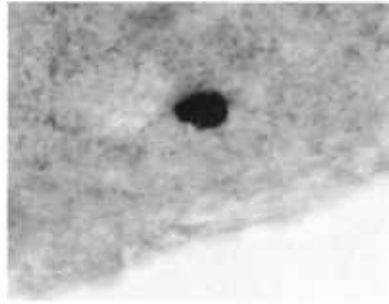
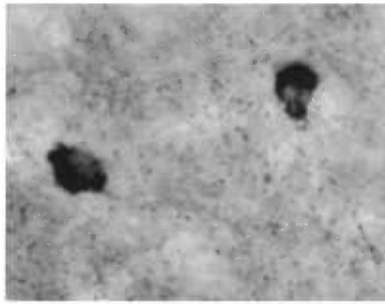
Representative serial parasagittal sections were used to map the distribution of calbindin-positive cells in the caudomedial telencephalon of a female bird (numbers on the left represent distance from midline in millimeters). Note that calbindin-positive cells are primarily located in a caudal crescent-shaped domain along the mediolateral extent of NCM. Scale bar = 2mm.



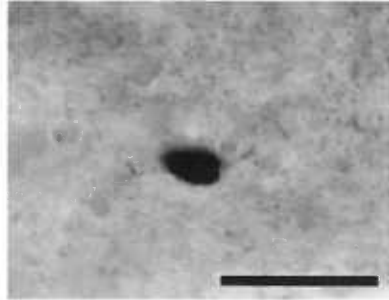
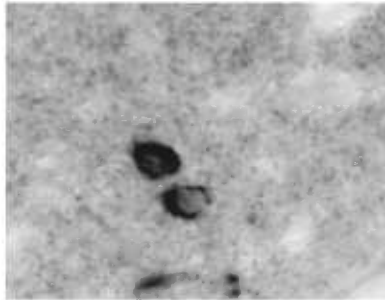
**Supplementary Material Figure 2) Calbindin-Expression Levels Area Similar  
Across Genders**

Representative photomicrographs of calbindin-labeled cells in the NCM of two males and females. All cells in both sexes exhibit strong immunolabeling, visualized either with DAB deposition (this Fig.) or fluorescent ICC (not shown), demonstrating the similarity in cellular staining across genders. Scale bar = 25um.

Males



Females



## DISCUSSION

### **Sexual Dimorphism in a Cortical-Like Auditory Area**

Our findings demonstrate a sexually dimorphic trait in a brain region primarily involved in the auditory processing of birdsong. Although sexual dimorphisms have previously been described at the level of the inner ear in various species such as the midshipman fish (Sisneros et al., 2004), *E. coqui* frogs (Narins and Capranica, 1976), and humans (Sato et al., 1991), our results indicate that dimorphisms may also occur in higher-order processing areas within the auditory system.

In songbirds, the previously described dimorphic song nuclei are part of the system involved in vocal motor production and learning. Because auditory stimulation is known to evoke responses in the song nuclei, it has been suggested that these primarily motor-related areas might also be involved in the perceptual processing of song (McCasland and Konishi, 1981; Margoliash, 1983; Williams and Nottebohm, 1985; Vicario and Yohay, 1993; Halle et al., 2002). Some support for this hypothesis has come from lesion studies targeting HVC (Brenowitz, 1991; Scharff et al., 1998; Halle et al., 2002), but such lesions are often large or include adjacent areas and fibers of passage that belong to the central auditory pathways proper (Vates et al., 1996; Mello et al., 1998). In addition, the evoked auditory responses in the song system are generally robust under anesthesia and during sleep, and reduced during wakefulness, when perceptual processing of song should be most active (Doupe and Konishi, 1991; Vicario and Yohay, 1993; Doupe, 1997; Dave et al., 1998; Schmidt

and Konishi, 1998; Cardin and Schmidt, 2003, 2004). These responses are highly selective towards the bird's own vocalizations and are likely a reflection of the vocal learning process (reviewed in Margoliash, 1997). However, the projections of the song system are akin to the cortico-basal ganglia-thalamo cortical loop and the descending cortical projections characteristic of mammalian motor control systems, and the final output of the song system is dedicated to vocal and respiratory control centers in the brainstem and medulla (see reviews in Zeigler and Marler, 2004). It is thus unclear what exact role song nuclei and related auditory responses might have in the sensory processing required for song perception and discrimination.

In contrast, NCM is a component part of the central auditory pathway in the pallial telencephalon. It receives a robust projection from the thalamorecipient zone field L2a and a less robust input from the auditory thalamus, and it is analogous (possibly homologous) to supragranular layers of the mammalian primary auditory cortex (Vates et al., 1996; Mello et al., 1998). Electrophysiological and gene expression studies have linked NCM to the perceptual processing of species-specific vocalizations and possibly to some aspects of the auditory memorization of song (Mello et al., 1992; Mello and Clayton, 1994; Chew et al., 1995; Chew et al., 1996). The dimorphism in the calbindin cell population in NCM is, thus, a clear example of a sexually dimorphic trait within a cortical-like area primarily involved in the auditory processing of a behaviorally relevant stimulus. We are unaware of previous reports of a sexual dimorphism at a comparable brain level. It also seems to us that a dimorphism in NCM, compared to song nuclei, offers a more conservative explanation for gender differences in the perceptual processing of birdsong. After

song information has been processed in NCM and related auditory areas, it can then potentially be passed on to other brain regions, including the song system and areas involved in non-vocal behaviors in response to song. For example, both spontaneous and evoked auditory responses in canary HVC, a sensorimotor nucleus in the telencephalic song system, differ markedly between males and females (Williams, 1985; Del Negro et al., 2000; Del Negro and Edeline, 2001, 2002). Although the origin of such a difference is presently unclear, it could derive from differential processing at the level of a preceding auditory area like NCM.

### **Calbindin-Expressing Cells Are a Distinct Population of GABAergic Cells**

The gender difference we observed is not a reflection of a dimorphism in the overall density of neuronal or GABAergic cells in NCM. Rather, it is restricted to calbindin-positive cells. Similar to parvalbumin and calretinin, calbindin is an intracellular calcium-binding protein thought to define a subset of inhibitory interneurons in most of the brain areas that have been examined, including the mammalian auditory cortex, although exceptions have been noted (e.g. the superior colliculus and the thalamic reticular nucleus) (Hendry and Jones, 1991; Rogers, 1992; Jones, 1993; Parent et al., 1995; DeFelipe, 1997; Reynolds et al., 2004). The double-ICC experiment conducted in the present work provides conclusive evidence that the calbindin-positive cells in the songbird NCM are GABAergic. Interestingly, calbindin has a particularly strong calcium buffering action (Heizmann, 1992), suggesting that some calcium-dependent processes may be downregulated or suppressed in calbindin-positive cells. Consistent with this view, although the general population of



GABAergic cells in NCM shows a *zenk* response to song (Pinaud et al., 2004), calbindin-positive cells lack such a response. This suggests that the coupling between neuronal activation and gene induction, a calcium-dependent process in mammals (Cole et al., 1989; Bading et al., 1993) and in songbird NCM (Cheng and Clayton, 2004), is absent in calbindin-positive cells. Alternatively, calbindin-positive cells could constitute a subset of GABAergic cells that are not directly activated by song. At any rate, the dimorphic calbindin-positive cell population likely represents a distinct subset of GABAergic cells with unique functional properties.

Although further analysis of morphology and of calbindin mRNA levels might be informative, we have found no evidence that the calbindin-positive cells themselves are dimorphic. To the extent that the action of sex steroids onto neurons usually results in marked changes in cell size and morphology, the apparent lack of a gender difference in the size of calbindin-positive cells suggests that these cells are not suffering the direct action of steroids in adult NCM. Rather, the dimorphism we observed was on the number of these cells, possibly the result of a developmental process. GABAergic cells in the pallium of both mammals and birds derive primarily from cells that migrate from the ganglionic eminences and invade the pallium during development (Zhu et al., 1999; Cobos et al., 2001). Although this process has not been directly investigated in zebra finches, immunolabeling for parvalbumin and calbindin in this species is high in the striatum but low or absent in most of the pallium in the early days post-hatch (Braun et al., 1991). The density of immunostaining in the nidopallium then undergoes a large increase and reaches adult levels after days 14 and 28 for calbindin and parvalbumin, respectively, likely due to

an invasion of the pallium by GABAergic cells. It is therefore possible that the adult gender difference in the number of calbindin cells in NCM results from local differences in cell migration and/or survival that occurred during this developmental period.

The consequences of a higher density of calbindin-positive cells in male NCM are unclear. It seems unlikely that the overall inhibitory tone in NCM is higher in males, as we observed no gender differences in the local density of GABAergic cells. Alternatively, due to a possibly higher calcium-buffering capacity, the auditory processing circuits in male NCM may be less prone to undergo calcium-dependent plasticity events (such as induced gene expression) or more resistant to calcium-related excitotoxicity than in females, but these possibilities remain to be tested experimentally.

### **NCM Subdomains, Aromatase and Sex Steroids: A Sex Dimorphism in Auditory Processing?**

Previous studies have identified the caudomedial telencephalon as a general area of high aromatase expression, both at the mRNA and protein levels (Shen et al., 1995; Saldanha et al., 2000), and suggested a regional difference in aromatase expression within NCM (Fusani et al., 2001). Our current study provides a more detailed analysis of aromatase expression in NCM. In particular, we show that the expression of aromatase mRNA in NCM is very similar to the distribution of calbindin-positive cells. These observations support previous data indicating that NCM might contain at least two distinct subdomains. For example, rostral and caudal

NCM appear to have different connectivities, rostral NCM receiving a more robust input from field L than caudal NCM (Vates et al., 1996). Electrophysiological recordings show that a song-specific habituation of the evoked auditory responses to song occurs in NCM; this habituation is prominent in caudal but not rostral NCM, and absent in the more rostral field L2a (Chew et al., 1995). In canaries, a frequency-dependent organization of the ZENK expression response to song syllables occurs in rostral, but not caudal NCM (Ribeiro et al., 1998). Regional differences in ZENK expression in response to song stimulation have also been described in starlings and zebra finches (Gentner et al., 2001; Terpstra et al., 2004). Our current observations provide neurochemical evidence for a rostral-to-caudal differentiation of NCM, highlighting the need to carefully consider the anatomical level of analysis in studies of NCM structure and function (see also Terpstra et al., 2004).

It is of particular interest that the distribution of calbindin-labeled cells coincides closely with the expression of aromatase. Aromatase is involved in the local production of estrogen in the brain (Schlinger, 1997), which potentially makes caudal NCM an area of high estrogen concentration. This could have important implications. For example, estrogens are known to modulate neuronal excitability by modifying the expression and subunit composition of neurotransmitter receptors (e.g. GABA-A and NMDA receptors) or the morphological and physiological characteristics of dendritic processes and synapses (Maggi and Perez, 1984; Schumacher et al., 1989; Gould et al., 1990; Woolley and McEwen, 1992; Herbison and Fenelon, 1995; Gazzaley et al., 1996; Herbison, 1997). If similar actions occurred in NCM, estrogen could have an impact on processing at this level of the auditory pathway, as suggested previously

(Schlinger, 1997; Saldanha et al., 1999), as well as regulate the differential properties of rostral versus caudal NCM. Although a clear dimorphism was not apparent in the pattern or level of aromatase mRNA expression in NCM, we cannot rule out the possibility that either aromatase activity, acting through the production of local estrogen, or the differential expression of estrogen receptors, might influence NCM function and the expression of calbindin. During development, a gender difference in local estrogen levels could lead to the differential survival or incorporation of calbindin cells into NCM circuits, in a manner analogous to the known effect of estrogen on neuronal survival in song control nuclei (for example, Adkins-Regan et al., 1994; Burek et al., 1995). Interestingly, a larger number of aromatase-positive fibers in the NCM of male zebra finches, as compared to females, has been reported previously. This sexual dimorphism, however, does not involve differences in the overall numbers of aromatase-positive cells (Saldanha et al., 2000).

Intriguingly, early reports indicated that the expression of the estrogen receptor ( $ER\alpha$ ) is very low or absent in most of NCM, except for a thin strip of tissue adjacent to the ventricle (Balthazart et al., 1992; Metzdorf et al., 1999). This apparent mismatch between aromatase and ER expression led to the suggestion that estrogen possibly generated in NCM might act at a distance, or through non-genomic mechanisms (Schlinger, 1997). However, the more recently identified estrogen receptor  $\beta$  ( $ER\beta$ ), is expressed in a broader domain in the NCM of starlings (Bernard et al., 1999). If  $ER\beta$  has a similar distribution in zebra finches, it would provide a target for local estrogen action in NCM of this species and could also be potentially dimorphic in expression.

It is presently unclear whether the dimorphism reported here in a cortical/pallial auditory region results in a gender difference in auditory processing. Interestingly, a gender difference in an auditory task involving spatial discrimination has been recently described in humans (Lewald, 2004). Although the brain level involved in such dimorphism is unclear, it has been suggested that auditory cortical areas related to the task are involved. Thus, the existence of gender differences in the auditory system is clearly not restricted to the periphery, but also includes neuronal populations at cortical-like levels. Based on these observations we suggest that sexual dimorphism in the vertebrate auditory system may be more common than originally suspected. Although the specific mechanisms likely differ in each case, gender emerges as an important modulator of the auditory system, and possibly of sensory systems in general.

## **CHAPTER 6**

### **SUMMARY AND CONCLUSIONS**

The main goal of this work was to characterize the anatomical organization and functional role of GABAergic transmission in telencephalic auditory areas of the zebra finch brain, that are thought to play important roles in auditory and possibly perceptual processing of birdsong. Using a combination of anatomical, molecular, cellular and electrophysiological approaches, I have characterized many of the basic organizational principles and functional roles for inhibitory transmission in the songbird NCM.

In lieu of a detailed discussion on the particulars of the data presented in this thesis, which has been done in the discussion section of each individual chapter, I have chosen to amalgamate the main conclusions of this work as a simplified model of the anatomical-functional organization of NCM. My objective in this last section is to present my view on how these findings could be integrated conceptually. For this section, it is also my hope to generate a framework that could be used by others who may wish to conduct their own investigations on the role of inhibition in the songbird NCM. In the following paragraphs I will introduce and discuss this operational model of NCM. Subsequently, I will discuss other issues related to our current understanding of NCM's intrinsic organization and its relation to the mammalian auditory cortex. Finally, I will discuss the use of *zenk* as a mapping tool for neuronal activity and its role in NCM's physiology. I will conclude this chapter by outlining open-ended questions that arise from my own contribution.

### **Summary of Key Contributions**

The major accomplishments of my work that are described in this thesis are:

- 1) The characterization of a highly prevalent and active GABAergic system in the songbird auditory telencephalon, in particular in NCM;
- 2) The identification of song-driven *zenk* expression in GABAergic neurons in NCM;
- 3) The characterization of roles for GABA during auditory processing in NCM in awake animals. This work has also provided evidence that strongly suggests the existence of a novel mode of sensory processing in NCM that primarily involves disinhibitory circuits.
- 4) The discovery of a sexual dimorphism in a population of GABAergic neurons in NCM.

In the first set of experiments, I demonstrated that GABAergic cells and processes constitute a significant proportion of the total neuronal pool at certain stations of the ascending auditory pathway and throughout song control nuclei. In NCM, in particular, about half of the neuronal cell population is composed of GABAergic neurons, suggesting that inhibitory transmission plays a critical role in the physiology of this auditory area. These GABAergic cells could be divided qualitatively into two sub-populations based on their soma diameters: 1) small GABAergic neurons (approximately 4 to 10 $\mu$ m in diameter) with low zGAD65 expression, that likely represent the typical local inhibitory interneurons found throughout the vertebrate brain; 2) large GABAergic neurons (up to 25 $\mu$ m in diameter), that expressed high levels of zGAD65. Data obtained by other research



groups have demonstrated that projections from the song control nucleus area X to the thalamic nucleus DLM are inhibitory and mediated through large GABAergic neurons (Luo and Perkel, 1999a, b). These two populations of GABAergic neurons were easily detected in my own area X preparations (Chapter 2). It is clear therefore that in area X, the anatomical identity of GABAergic cells (large versus small) reveals a functional property of that circuit. These differences in morphology are also suggested by the current histological evidence obtained in the present work and may likewise be useful to infer functional differences in the caudomedial auditory lobe (CMM, NCM and field L). It is clear from the anatomical data that the majority of GABAergic cells in NCM and CMM are of the smaller type and, presumably, represent local circuit inhibitory neurons. A few of the larger cells, however, could be found in either area. Conversely, the vast majority of GABAergic neurons in field L2 is of the large type and exhibit high levels of zGAD65 expression.

Such findings support the argument that GABAergic projection neurons are likely to influence and/or organize neuronal activity within these telencephalic auditory areas. Furthermore, these data indicate that the majority of inhibitory cells in NCM and CMM are local interneurons, while they suggest that the greatest proportion of GABAergic neurons in field L2 are putative projection neurons. Double fluorescent *in-situ* hybridization (d-FISH) experiments using the activity-dependent gene *zenk* and the GABAergic cell marker zGAD65 revealed that a large population of song-activated cells in NCM and CMM are in fact GABAergic, which provides direct evidence for the participation of inhibitory cells in birdsong auditory processing at telencephalic auditory areas.

The patch-clamp experiments revealed important properties of NCM's GABAergic network. It was found that at resting conditions, inhibitory transmission acts to suppress NCM's excitatory network, which appears to be spontaneously active in the absence of GABA. Pharmacological blockade of GABA-A receptors led to the appearance of large and rhythmic excitatory events. This role for GABAergic transmission in NCM is mediated by local inhibitory neurons given that recordings conducted in conditions where all inputs from CMM and field L to NCM were severed did not affect the observed phenomenon.

Finally, extracellular recordings conducted in the NCM of awake, restrained zebra finches revealed an unconventional role for GABAergic inhibition during auditory processing. It was found that removal of inhibition by blockade of GABA-A receptors induces a synchronization of neuronal firing and suppression of the tonic component of song-evoked responses in NCM. These data suggested that blockade of GABA-A receptors released a secondary inhibition network in NCM which acted to suppress responses to particular song syllables. In addition, these findings suggested that under normal conditions, GABAergic transmission participates in optimizing the fidelity of information transfer/processing in NCM.

### **An Operational Model for NCM**

Integration of the data summarized above allows for the generation of an operational model of NCM circuitry at rest and during auditory processing (Fig. 1). This model proposes that at rest, active GABAergic synapses suppress NCM's excitatory network. During auditory processing, however, inhibition of this

GABAergic circuit (disinhibition) allows for the activation of NCM's excitatory network. Before proceeding to discuss the model, I would like to state that this is a simplified view of how GABAergic circuitry may participate in the generation and processing of auditory information.

#### a) Active GABAergic Synapses at Rest Suppress Excitatory Network

One robust finding of this thesis is that GABAergic synapses are active for resting conditions and, in this state, suppress the excitatory network of NCM (Chapters 3 and 4). In these experiments, the vast majority of neurons that were recorded in NCM slices received spontaneous inhibitory input mediated exclusively through GABA-A receptor activation. Figure 1A represents these spontaneously active synapses indicated in bright red. At resting conditions, these inhibitory cells provide tonic suppression of their putative post-synaptic targets, the excitatory cells in NCM (in Fig. 1A, grey-shading is used to represent on-going suppression of excitatory cells under spontaneously active conditions). These inhibitory cells were interpreted to be local interneurons within NCM. This assumption is based on the finding that recording from a slice preparation in which adjacent areas were dissected out (and their projections into NCM severed) did not affect the frequency or amplitude of the spontaneous inhibitory post-synaptic currents (sIPSCs) over time. Furthermore, in the slice preparation, any intact projections from field L2 to NCM would presumably have little to no spontaneous activity based on findings from extracellular electrophysiological recordings conducted in this region (Terleph et al., 2005).

### b) A Double Inhibitory Circuit

It has been shown that upon auditory stimulation, song-evoked responses are detected in field L2 and NCM (Chew et al., 1995; Chew et al., 1996; Capsius and Leppelsack, 1999; Gehr et al., 1999; Terleph et al., 2005). The extracellular electrophysiological results presented in this thesis are useful to suggest that a “double inhibitory” or “disinhibitory” circuit may mediate key aspects of song-evoked responses in NCM. This hypothesis is substantiated by 1) data that demonstrated that blockade of GABA-A receptors released a putative secondary inhibitory network that acted to suppress NCM’s tonic component of song-evoked responses and 2) the finding that blockade of sIPSCs with BMI application allows for excitatory cells to become active within NCM.

Based on these findings I therefore propose that field L2/NCM operate as indicated in Figure 1B during conditions of auditory stimulation. Auditory stimulation leads to activation of the ascending auditory pathway, including field L2 cells. As mentioned previously, nearly half of the population of field L2 neurons is GABAergic and of the large type, therefore raising the possibility that both inhibitory projection neurons as well as excitatory cells may be directly activated by birdsong auditory stimulation.

The idea that both inhibitory and excitatory cells project from field L2 to NCM is substantiated by the data presented in “Appendix I”, where injections of retrograde rhodamine beads into NCM backfilled cells in field L2. Several backfilled neurons could be co-localized with the marker, zGAD65 indicating that their

neurochemical identity was GABAergic (Appendix I). This co-localization provides a strong reason to postulate that these cells are indeed GABAergic projection neurons that arise from field L and target NCM, and possibly CMM. These experiments also revealed backfilled cells that did not co-localize with zGAD65; these neurons were interpreted to likely be a population of excitatory projection neurons suggesting that parallel projection systems of excitatory and inhibitory transmitters are likely to occur in field L (Appendix I). Figure 1B illustrates the proposed organization of field L projections directed at NCM at rest and during sensory stimulation; inhibitory projection neurons are represented by the bright red cell (activated GABAergic cell) and the black cells indicate activated excitatory neurons.

### c) Disinhibition During Sensory Processing

In order to engage NCM's excitatory output/processing network, the tonic suppression provided by spontaneously active local inhibitory synapses must be counteracted. This could be accomplished by releasing an inhibitory neurotransmitter onto the very interneurons that tonically suppress the excitatory network under resting states. Generally such organizational schemes are referred to as disinhibitory circuits.

One possible mechanism for disinhibition of the excitatory component of NCM is the song-induced activation of field L inhibitory projection neurons. Upon the activation of these putative GABAergic projection neurons, release of GABA onto local inhibitory neurons within NCM could suppress their activity thereby allowing the excitatory network to become active (Fig. 1B).

Another possibility is that the disinhibitory circuitry is intrinsic to NCM: excitatory projections from field L may first target a sub-population of GABAergic neurons within NCM and those, in turn, suppress a second sub-population of inhibitory cells that provide sIPSCs to excitatory NCM neurons (Fig. 1C and D).

A third and final scenario I have explored is that excitatory projection neurons with their cell bodies located in field L may directly target the excitatory neuronal pool in NCM bypassing GABAergic modulation. I argue, however, that this last possibility is unlikely given that normal GABAergic transmission appears to play a significant role in the maintenance of high fidelity transmission in NCM (Chapter 4).

#### d) Physical Requirements of the Double Inhibitory Model

As stated previously, my intention in proposing any model is to provide a framework that subsequent investigations can be based on. It should be noted, however, that this model assumes that inhibitory projections from field L selectively target a sub-population of GABAergic neurons in NCM. There are two experiments that are required to clarify this issue; both of them aim at providing physical evidence for the presence of GABAergic-to-GABAergic cell projections:

1) Local NCM inhibitory interneurons are required to express GABA-A receptors on their surface in order to be modulated by a putative inhibitory input during auditory stimulation. This question can be addressed by using d-FISH with specific probes for zGABA-A receptors and zGAD65. In fact, I collected preliminary evidence for the high expression levels of zGABA-A in the zebra finch NCM (Fig. 2).

The generation and use of fluorescent probes against these mRNA species should shed light into this specific question.

2) Field L inhibitory projection neurons are required to selectively target GABAergic cells in NCM. One approach to address this question would be to fill field L projection neurons and histochemically identify GABAergic neurons within NCM. A careful microscopic evaluation of the synapses between filled neurons and GABAergic neurons within NCM could provide the evidence to support the hypothesis that field L GABAergic neurons target a sub-population of inhibitory neurons within NCM.

### **NCM and the Mammalian Primary Auditory Cortex: Analogous Structures?**

Based on anatomical criteria, it has been proposed that NCM is analogous, if not homologous, to the supragranular layers of the primary auditory cortex (A1) in mammals (Vates et al., 1996; Mello et al., 1998). This suggestion has been advanced primarily with the evidence that NCM is an auditory station that receives input from the thalamo-recipient field L. This issue has been discussed to some extent in chapters 2 and 3. However, in the following paragraphs, I would like propose a re-evaluation of this notion.

#### **a) General Anatomical Organization**

The basic anatomical organization of the caudomedial auditory lobe suggests that NCM may be placed in a position that is analogous to supragranular layers of the mammalian A1. This suggestion is based on the fact that NCM is an auditory area

that receives robust projections from the thalamo-recipient zone (field L; Fig. 3). In the mammalian A1, neurons in the supragranular layers receive a dense innervation from cells located in the granular layer, which in turn are the main targets of medial geniculate nucleus (thalamic) projections (Fig. 3). Based on this general organization, NCM has been proposed to be in an anatomical position that is equivalent to the supragranular layers of A1 (Vates et al., 1996; Mello et al., 1998).

#### b) Organization of the GABAergic Network

The data obtained in this work extended our knowledge on the neurochemical and functional organization of NCM and allows us to further evaluate the similarities and dissimilarities between this songbird auditory telencephalon and the mammalian A1. It was found that GABAergic neurons compose approximately half of the overall population of neurons in NCM. In the mammalian A1, GABAergic neurons are responsible for approximately 25% of the neuronal population (Hendry et al., 1987; Jones, 1993). Given that the majority of inhibitory interneurons are found in the supragranular and granular layers of sensory cortices (Gabbott and Somogyi, 1986; Hendry et al., 1987; Hendry and Jones, 1991; Jones, 1993), high numbers of GABAergic cells detected both in field L and NCM might reflect an over-representation of the distribution of inhibitory neurons in these areas. If this hypothesis is correct, GABAergic neurons should account for a small percentage of the overall neuronal population in the songbird analogue of the A1 infragranular layers. Pyramidal neurons located in the mammalian infragranular layers of primary sensory areas such as the visual, somatosensory and auditory cortices provide



descending projections to subcortical nuclei associated with each sensory modality. In the songbird auditory system, arcopallial neurons, such as those located in the cup region of song nucleus RA, originate descending projections to subcortical auditory nuclei and therefore have been proposed to be analogous to descending projections of A1 (Mello et al., 1998). GABAergic neurons in the RA cup region were quantified to reflect approximately 37% of the overall neuronal population of this area (Chapter 2). Thus, GABAergic neurons are a significantly more prevalent cell type in the songbird auditory telencephalon as compared to its mammalian counterpart. These findings are useful to suggest that the neurochemical organization of the songbird auditory telencephalon, at least as it relates to the GABAergic system, is significantly different from that found in the mammalian auditory cortex.

#### c) Roles for GABAergic Transmission During Sensory Processing

My electrophysiological findings are also useful to suggest that NCM encodes/processes auditory information using mechanisms that are significantly different from those used by mammals. For example, the data presented in Chapter 4 provides clear evidence that local BMI application into NCM shifts originally tonic song-evoked responses into highly phasic responses in awake-restrained zebra finches. These findings are exactly opposite of those found in the mammalian A1, where BMI application tends to shift phasic responses into tonic responses. The findings obtained in this thesis are counter-intuitive in the sense that blockade of inhibition tends to suppress song-evoked responses, suggesting that a BMI-insensitive inhibitory component within NCM is released from control of a BMI-sensitive

network, thereby inhibiting part of the song-evoked responses. In the mammalian auditory system this does not seem to be the case. Excitation appears to be the primary source of information processing in A1, while inhibition appears to contain/restrict excitatory drive to appropriate processing channels.

#### d) Mechanisms Underlying Frequency Discrimination

GABAergic mechanisms have been repeatedly implicated in frequency discrimination in the mammalian auditory system. Blockade of GABA-A receptors, for example, lead to marked expansions of frequency tuning curves of auditory neurons and, therefore, decreased frequency discrimination (Schreiner and Mendelson, 1990; Yang et al., 1992; Ehret and Schreiner, 1997; Suga et al., 1997; Chen and Jen, 2000; Wang et al., 2000). Interfering with GABAergic transmission in the songbird NCM failed to alter frequency tuning characteristics, providing further evidence that the processing strategies at this level of the songbird brain are significantly different from those observed in the mammalian auditory cortex. I should qualify, however, that no frequency tuning differences were detected with BMI treatment when responses were computed for the whole duration of the stimulus. Given that BMI application tended to reorganize the temporal response properties of NCM neurons, I re-analyzed the frequency tuning data with two separate windows: one for the “phasic” component and another one for the “tonic” component. These data can be found in Appendix II and show a significant difference for pre- and post-BMI conditions with respect to frequency discrimination.

### e) Biophysical Properties of Auditory Neurons

The basic biophysical parameters of GABAergic synapses in NCM appear to be significantly different from those observed in the mammalian auditory cortex. For example, in my own patch-clamp experiments in NCM, sIPSCs exhibited average amplitude of 47 pA, average decay time constant of 6.9 milliseconds and an average frequency of approximately 4.6 Hz. Conversely, recordings obtained in the rat A1 under similar conditions revealed that sIPSC amplitude is significantly higher, quantified to approximately 95 pA, and the decay time constant significantly shorter (~3.7 milliseconds) (Hefti and Smith, 2003). In addition, the frequency of these events in the rat is much higher than that observed in the zebra finch NCM, being calculated to approximately 25 Hz (Hefti and Smith, 2003).

The findings discussed above suggest that although the basic anatomical organization of the ascending auditory pathway in avian species resembles that of mammalian auditory systems, several aspects of both the neurochemical organization and the physiology of these areas appear to be significantly different across animal classes. These differences include the general distribution of neurochemically distinct cell types, such as GABAergic neurons, basic biophysical properties of the neurons and synapses embedded in these regions and finally the physiological properties of these regions at rest and during sensory processing.

As discussed in Chapter 4, the wide-spectrum differences outlined above likely evolved independently or divergently in songbirds in response to behavioral requirements and/or ecological and evolutionary pressures. These modifications may

be correlated with auditory processing related to vocal learning behavior, however, experimental data is required to support or refute this hypothesis.

### **Is NCM a Single Brain Region?**

Apart from discussions on the degree of anatomical and functional homology between NCM and the mammalian A1, it is important to consider the internal organization of this songbird auditory region in order to understand how environmental stimuli are encoded and processed in this region. This issue has been discussed to some extent in Chapter 5, so I will just briefly state the considerations associated with this topic and clearly state my own personal view on this matter.

NCM is considered to be a single anatomical entity. Its dorsal, ventral and caudal borders are defined by the ventricular zone, while the rostral aspect of NCM is defined by lamina mesopallialis and field L2a. On the mediolateral axis, NCM is the most medial telencephalic structure, protruding outwards towards the midline. The identification of the NCM's lateral border has been difficult. There is at present no clear lateral border for NCM based on cytoarchitectonic criteria. Therefore, most studies in NCM have been conducted in more medial NCM levels, in order to avoid invading another brain region.

I question, however, whether NCM can be comfortably considered a single auditory structure, even for more medial levels. A number of anatomical, neurochemical, gene expression and electrophysiological studies provide, in my view, evidence that NCM is composed of different sub-domains, or that NCM is in fact composed of multiple functionally distinct brain areas.

On the anatomical front, it has been previously shown that the main bulk of field L projections into NCM target its more rostral aspect, with little projections targeting its caudal portion (Vates et al., 1996). Neurochemical evidence also suggests that rostral and caudal aspects of NCM may constitute different anatomical and functional entities. For example, I showed data on Chapter 5 indicating that aromatase expression is high in caudal, but not rostral NCM. Similarly, calbindin-positive cells are more concentrated in this caudal domain in both males and females. Non-published evidence collected in the Mello laboratory indicates that other genes, such as *Narp*, are expressed in a fashion that is similar to that of calbindin and aromatase, with highest expression located in the caudal domain of NCM.

Analysis of ZENK expression in the songbird NCM has also provided evidence suggesting that NCM is composed of distinct functional domains. For example, Gentner and colleagues have shown that the number of ZENK-positive cells in the ventral NCM of female starlings exposed to sexually relevant conspecific songs is higher than those females exposed to songs in which the sexually attractive features of the song were not present (Gentner et al., 2001; Gentner, 2004). Other regions of NCM did not undergo significant alterations in ZENK expression in response to these experimental protocols, suggesting that sub-domains of NCM (and not the whole nucleus) participate in the discrimination of some behaviorally-relevant auditory stimuli. In another set of studies, ZENK was used to reveal a frequency-dependent organization of the canary NCM. Interestingly, this organization revealed with ZENK-expression was just observed in rostral, but not caudal NCM (Ribeiro et al., 1998).

Finally, robust electrophysiological properties detected in the caudal NCM, such as habituation of responses to repetition of the same auditory stimulus, are not detected in the rostral aspect of this region (Chew et al., 1995).

In this author's opinion the findings described above provide substantial evidence to suggest that NCM is composed of functionally distinct domains. Cells in the caudal NCM, which do not appear to receive robust field L2a projections, appear to exhibit high aromatase, calbindin and Narp expression and undergo experience-dependent habituation. Conversely, the rostral aspect of NCM receives heavy inputs from field L2, exhibit low expression levels for the markers described above, and do not appear to habituate following successive stimulus presentation.

At this point I believe it is premature to propose that the caudal and rostral domains of NCM are in fact two independent anatomical and/or functional entities. The most conservative position is therefore that these highly dissimilar regions are segregated sub-domains of NCM. However, I would not be surprised if future experimentation reveals that two functionally distinct brain regions reside in close apposition in what is currently referred to as nucleus NCM.

### ***zenk* Regulation by Song and Its Role in Auditory Processing in NCM**

*zenk* expression has been used as a marker for neuronal activation in the songbird brain. For example, the activity of basal ganglia circuits involved in the generation of different behavioral contexts (e.g., directed versus undirected singing) has been revealed with *zenk* expression (Jarvis and Nottebohm, 1997; Jarvis et al., 1998). In the songbird NCM, detection of *zenk* expression products (mRNA and

protein) have provided a means to detect song-responsive cells (reviewed in (Mello, 2002a, b; Mello et al., 2004). Using double labeling methods for both RNA and protein, evidence was presented here for the co-localization of *zenk* and zGAD65, demonstrating that a large fraction of song-responsive cells in NCM are in fact GABAergic.

Although *zenk* expression has been used as a neuronal activation mapping tool, it is really important to recognize the limitations and particularities of this approach, as well as to continue investigations on the physiological roles for the protein encoded by this gene. Activity, in fact, has been shown to be necessary, but not sufficient for *zenk* induction. For example, it is known that not all brain regions respond to activation with a *zenk* expression response; some of the clearest examples include thalamic stations in the auditory or visual systems (Mello and Clayton, 1995; Arckens et al., 2000; Pinaud et al., 2003). *zenk* induction is also absent in primary telencephalic thalamo-recipient areas for all major sensory systems in the songbird brain even after systemic treatment with metrazole, a potent GABAergic antagonist thought to induce widespread depolarization of central nervous system networks (Mello and Clayton, 1995). Furthermore, basal *zenk* expression depends on NMDA receptor activation, suggesting that there are specific requirements for *zenk* expression rather than just general membrane depolarization (Cole et al., 1989; Worley et al., 1991). Finally, sustained neuronal activity triggered by song stimulation (up to 6 hours) leads to a suppression of *zenk* expression in the zebra finch NCM (Mello et al., 1995; Mello and Ribeiro, 1998), further indicating that *zenk*

expression is uncoupled from electrophysiological activity for certain brain regions, under certain experimental conditions.

What exactly is *zenk* expression showing us then? Others and I have previously proposed that *zenk* expression may reflect anatomical locations undergoing activity-dependent circuit reorganization or cells and sites that exhibit enhanced neuronal plasticity (Mello et al., 1995; Pinaud et al., 2002b; Pinaud et al., 2002a; Pinaud, 2004, 2005; Pinaud and Tremere, 2005). The lack of *zenk* (NGFI-A) expression in certain thalamic relays upon sensory stimulation strengthens this suggestion given that it has been previously demonstrated that some thalamic nuclei exhibit very limited plasticity (for review see Fox et al., 2002; see also Mello and Clayton, 1995; Arckens et al., 2000; Pinaud et al., 2003). Another argument that has been put forward in support of this theory is that components of the biochemical cascade leading to *zenk* expression might be unavailable in cells that compose these “*zenk*-negative” regions, although experimental data to support this view is currently lacking.

Paradigms that induce significant plastic changes in sensory systems, such as exposure of animals to an enriched sensory environment (EE), also lead to differential induction of the immediate early gene *zenk*. For example, placing adult rodents in an EE triggers robust increases in the dendritic arbors of visual cortical neurons (Volkmar and Greenough, 1972); these increases are paralleled by a significant increase in *zenk* induction in this same area (Wallace et al., 1995; Pinaud et al., 2002a; Pinaud, 2004). Similar experience-dependent changes were also observed for other sensory modalities such as the somatosensory system (Pinaud et al., 2002a).



These increases in *zenk* expression levels over the somatosensory and visual cortices of animals exposed to an EE were not detected in control animals that were left undisturbed in their home cages or that were manipulated to account for any non-specific gene expression (such as that mediated by stress).

These findings clearly indicate that activity alone is not sufficient to guarantee *zenk* induction, as the control animals included in the experiment described above were undergoing visual and tactile experience but did not exhibit *zenk* expression. I argue that *zenk* induction is associated with the generation of specific patterns of activity that likely occur in conditions of enhanced neuronal plasticity, such as sensory deprivation followed by stimulation.

This argument can be further substantiated by a careful analysis of the pattern of *zenk* expression across cortical layers of animals that have undergone enhanced sensory experience. It was found that exposure of animals to an EE triggered *zenk* expression across all cortical layers, with the exception of layer I, of the main sensory systems in the adult rodent. Interestingly, highest expression levels were consistently found in cortical layers III and V while the lowest *zenk* expression levels were detected in the thalamorecipient layer IV (Pinaud et al., 2002a). These results may be related to electrophysiological studies that suggest that layers III and V are potentially more plastic, as measured by their greater ease of inducing changes in synaptic strength such as LTP and LTD (Glazewski and Fox, 1996; Petersen and Sakmann, 2001). Conversely, it has been proposed that low plasticity levels in layer IV could be related to the stability in cortical map representation and possibly the maintenance of fidelity of information transfer at this level (Pinaud, 2004).

Should this hypothesis prove to be correct, low expression levels of the candidate-plasticity gene *zenk* in layer IV might provide a direct visualization of reduced activity in components of the machinery involved in triggering experience-dependent reorganization of circuits in mammalian, and possibly songbird, sensory systems. By association, enhanced *zenk* expression in layers III and V may provide a direct indication of a high density of cells that are participating in the neural plastic response as a function of complex sensory environment exposure.

Enhanced *zenk* expression in the conditions of enhanced sensory drive (e.g., during birdsong auditory stimulation) may thus reflect specific patterns of activity associated with circuit reorganization. One possibility for the recruitment of gene expression programs associated with network rewiring in NCM is that mechanisms for detecting sub-optimal architecture and processing capabilities are in place in this telencephalic region and are potentially involved in optimizing network architecture and synaptic weights in order to appropriately process information contained in this new set of environmental information. This hypothesis remains to be tested experimentally, however.

In sum, I believe that *zenk* expression reveals not only activity patterns in NCM, but may be useful to indicate sites where the mechanistic basis of plastic changes in response to novel stimulation might be engaged by reorganizational pressure on existing brain circuitry. In fact, as a transcriptional regulator, *zenk* is very well positioned to orchestrate the coordinated activation of a large set of genes given that its specific binding site is present in the promoter region of hundreds of genes expressed in the central nervous system. For instance, it has been previously

demonstrated in *in-vitro* essays that the *zenk* (zif268) protein is involved in the transcriptional regulation of synapsin I and II and synaptobrevin genes, as well as the gene that encodes for the monoamine oxidase B gene, the alpha-7 subunit of the nicotinic acetylcholine receptor, neurofilament and the adenosine 5'-triphosphate binding cassette, sub-family A, transporter 2 (ABCA2) (Pospelov et al., 1994; Thiel et al., 1994; Petersohn et al., 1995; Petersohn and Thiel, 1996; Carrasco-Serrano et al., 2000; Wong et al., 2002; Davis et al., 2003). Thus, *zenk* is well positioned to affect the expression of genes involved in a wide range of cellular physiological roles.

For a clear definition on the roles of *zenk* to the physiology of auditory areas in the songbird brain, future work should be directed at identifying *zenk* target genes regulated in NCM as a result of song stimulation. These studies should provide a more complete picture of the effect of sensory experience on the genomic activation (and its consequences) to NCM cells.

The results presented in Chapter 3 provide evidence for the song-induced expression of the IEG *zenk* in neurochemically distinct cell types. By using both double-fluorescence in-situ hybridization and double-immunocytochemical labeling I provided evidence for the presence of GABAergic, as well as non-GABAergic, *zenk*-expressing cells. A question that arises from these results is whether the role of ZENK protein is conserved across these neurochemically distinct cell types.

As discussed previously, *zenk* encodes a transcriptional regulator that potentially controls the expression of a wide variety of genes in the CNS. Given that excitatory and inhibitory cells contribute complementary, yet widely different, roles for sensory physiological responses, the possibility exists that the sets of genes

regulated by *zenk* differs across these different cell types. To my knowledge, this question has not been investigated to date. Currently available methodologies such as single-cell laser capture microscopy and polymerase chain reaction (PCR) amplification provide the means to directly and systematically address this type of question.

### **Final Comments**

I hope to have convinced the reader that GABAergic transmission is highly prevalent and plays a central role in the physiology of the songbird auditory system. In my personal view, the results presented in this thesis contribute with some of the foundations upon which future investigations in this area can be conducted. I would like to close this section by briefly stating some open-ended questions that result from the novel findings obtained with my thesis work.

First, the results presented in Chapter 4 provided evidence that under local antagonism of GABA-A receptors, some song syllables failed to elicit measurable electrophysiological responses in NCM units. It would be interesting to investigate the possibility that these syllables that did not trigger auditory responses may share certain acoustic properties that could provide a connection and/or explanation for the lack of activity under conditions of pharmacological intervention. Equally interesting would be to investigate whether syllables that do evoke responses might share acoustic features that are responsible for triggering electrophysiological responses in NCM.

Second, I have shown that BMI treatment leads to a marked reorganization of the response properties in the time domain whereby sustained, tonic responses were shifted into phasic responses. I would be very curious to study whether the temporal reorganization of these responses affected full song discrimination capabilities of NCM units. As described before, NCM neurons exhibit response preference to conspecific, as compared to heterospecific stimuli. It would be interesting to treat NCM with BMI and test whether this conspecific song preference is abolished. In fact, I conducted this experiment in the Vicario laboratory but the results were inconclusive due to the low number of experimental samples ( $n=2$ ). Future research should clarify whether normal GABAergic transmission is required for NCM conspecific song preference.

Third, the data presented in Chapter 4 clearly demonstrates that BMI treatment suppresses, to a large extent, the tonic component of song-evoked responses and the responses to a number of syllables contained in a full song. This data indicated that a possible “secondary” form of inhibition was released from GABA-A control under BMI treatment and acted to suppress the tonic responses. I was unsuccessful in determining what mechanism accounts for this “secondary” inhibitory circuit. An attempt was made to investigate whether GABA-C receptors contributed to this phenomenon. However, the results obtained in that experiment argued against a role for this receptor type in this process. In future experiments it will be important to repeat these experiments and test specific antagonists directed at GABA-C receptors in order to conclusively exclude the participation of these receptors in the suppression of tonic responses. In addition, testing the role of GABA-B receptors in

this process may shed light into the mechanisms that contribute to this putative “secondary” form of inhibition.

Fourth, the data presented in Chapter 3 provides clear evidence for the expression of *zenk* in GABAergic, as well as non-GABAergic neurons. It will be important to characterize whether ZENK protein acts to regulate different sets of genes in these neurochemically distinct cell types.

Fifth, in Chapter 5 I provide evidence for a robust sexual dimorphism in a sub-population of GABAergic neurons in the adult zebra finch NCM. These calbindin-positive neurons are two times more numerous in males, as compared to females, and are preferentially expressed in a caudal sub-domain of NCM, where the estrogen-synthesizing enzyme aromatase is highly expressed. The spatial correlation of these two markers suggests that sex steroid hormones may play an important role in sensory processing. Two immediate questions arise from these findings. The first is whether sex steroid hormones, in particular estrogen, regulate response properties of the songbird NCM. Electrophysiological approaches coupled to local hormone injections should allow for a direct means of addressing this inquiry. The second question is whether differential hormone levels in NCM are responsible for the dimorphism described here. Interventions such as castration, hormonal replacement and masculinizing females should provide further insight into the mechanisms underlying the sexual dimorphism of the calbindin-positive population in NCM.

It is clear from this work that GABAergic mechanisms are critical to the normal physiology of NCM at rest and during sensory processing. These findings should not be overlooked and/or ignored when interpreting and discussing future

findings obtained in this auditory station. Likewise, it is my opinion that the generation of computer models or theoretical approaches aimed at understanding the roles of NCM to sensory processing, perception, or even the formation of auditory memories, is misdirected from the onset without taking into account the heavy contribution of GABAergic inputs to the physiology of this region. The high prevalence of GABAergic cells throughout the ascending auditory pathway and within the song control system indicates that a lack of consideration of inhibitory mechanisms during experimental design or interpretation of experimental findings will place us farther from truly understanding the role of these brain regions in auditory processing, sensorimotor integration and even song learning.

These years at OHSU, and especially in the Mello laboratory, have appreciably shaped both my personal and professional development. Although it is time to close this chapter of my fledgling career, I will retain fond memories of my time here.

### **Figure 6.1) An Anatomical-Functional NCM Model**

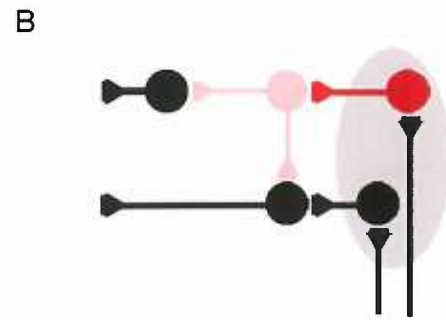
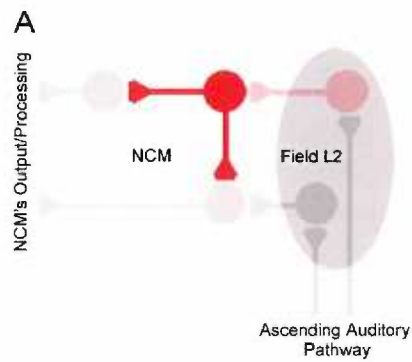
This model suggests that (A) at resting conditions, spontaneously active GABAergic synapses suppress NCM's excitatory network. (B) Upon auditory stimulation, suppression of the spontaneously active GABAergic synapses is made through a secondary inhibitory network that is not active at resting conditions and is activated by auditory stimuli. The inhibition of spontaneously active GABAergic synapses may arise from locations remote to NCM, such as Field L (A and B), as well as from GABAergic neurons intrinsic to NCM (C and D).



## SILENCE (RESTING CONDITIONS)

## AUDITORY STIMULATION

### - Suppression Extrinsic to NCM



### - Suppression Intrinsic to NCM

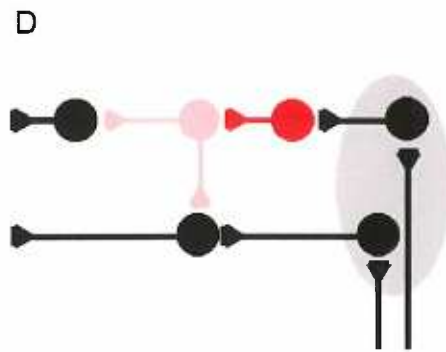
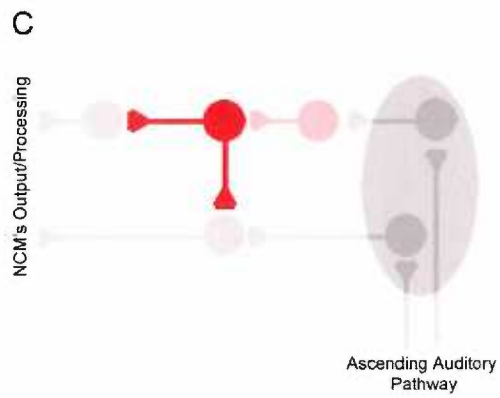
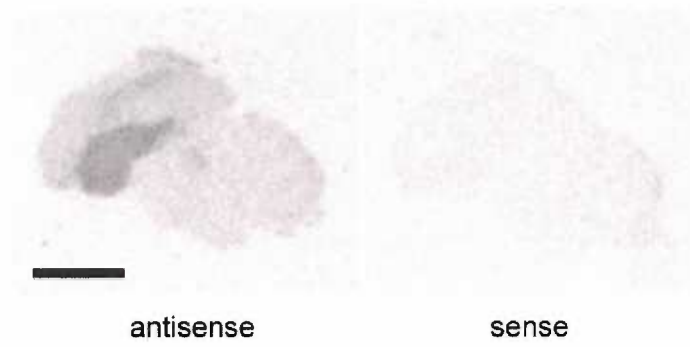


**Figure 6.2) zGABA-A is Highly Expressed in the Zebra Finch NCM**

The top panel is composed with autoradiographic images of parasagittal sections through caudomedial auditory lobe that have been hybridized against a radioactive zGABA-A antisense (left) and sense (right) riboprobes. zGABA-A is highly expressed throughout the brain, including NCM and Field L. Highest expression of zGABA-A is observed in the striatum. Scale bar = 4mm.

The bottom panel depicts fluorescent in-situ hybridization photomicrographs of zGABA-A expression in NCM at two different magnifications: 20x (A and B) and 40x (C and D). Scale bars = 250um.

### Radioactive in-situ hybridization



### Fluorescent in-situ hybridization

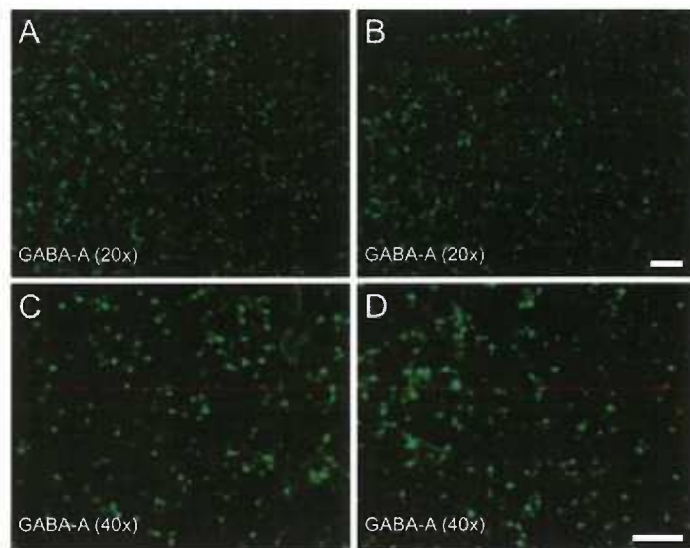


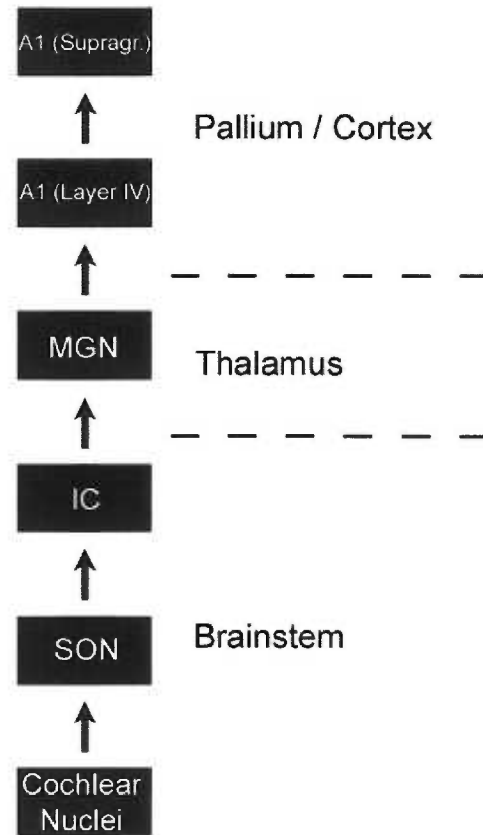
**Figure 6.3) Basic Organization of the Avian and Mammalian Ascending Auditory Pathway**

The box diagrams illustrate the main stations of the ascending auditory pathway in birds (left column) and mammals (right column). Both schematics illustrate the presence of a set of brainstem nuclei, a single thalamic station, a telencephalic/cortical thalamo-recipient layer, and intra-telencephalic/cortical connections. Abbreviations: SON, superior olivary nucleus; MLd, dorsal part of the lateral mesencephalic nucleus; Ov, nucleus Ovoidalis; NCM, caudomedial nidopallium; CMM, caudomedial mesopallium; IC, inferior colliculus; MGN, medial geniculate nucleus; A1, primary auditory cortex.

## Avian



## Mammal



## **APPENDIX I**

### **PRELIMINARY EVIDENCE FOR THE NEUROCHEMICAL IDENTITY OF PROJECTION NEURONS IN THE SONGBIRD FIELD L AND NCM**

In Chapters 2 and 3 I provided evidence for the existence of two qualitatively different populations of GABAergic neurons in the caudomedial auditory lobe. In both CMM and NCM, the majority of GABAergic neurons were small (4-10 $\mu$ m in diameter), while few large inhibitory neurons (>15 $\mu$ m) could be found distributed evenly throughout these regions. Conversely, Field L2 appeared to be composed primarily of GABAergic neurons of the larger type. We suggested that this morphological dichotomy could reflect a functional difference in this population of neurons, where the large GABAergic cells could reflect projection neurons while the small cells likely compose the pool of local circuit GABAergic interneurons.

In order to investigate this possibility experimentally, I stereotactically injected a retrograde tracer (rhodamine beads) into NCM of anesthetized birds. Animals were allowed to recover for 5 days and were sacrificed by decapitation, following the protocol detailed in Chapter 3. The injection procedure backfilled projection neurons in both Field L2 and CMM. Subsequently, tissue from injected animals was double-labeled with our zGAD65 probe (green Alexa tag) through in-situ hybridization (details on Chapter 3). This double labeling allowed for the detection of GABAergic (as evidenced by zGAD65 expression) projection neurons (as evidenced by rhodamine backfill).

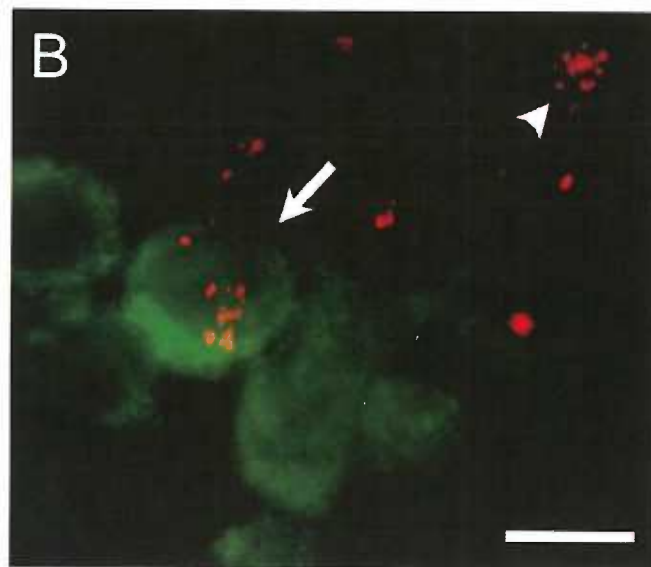
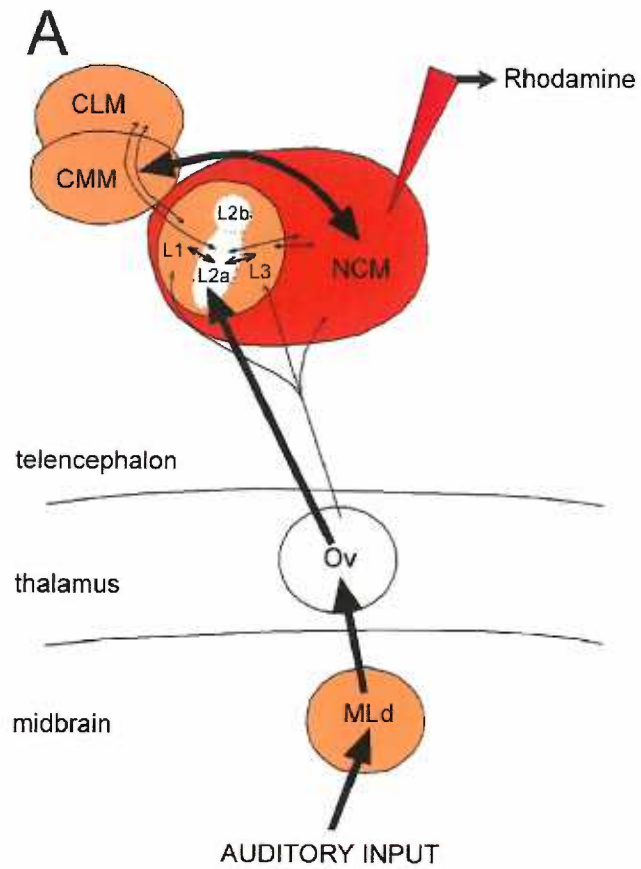
In Fig. 1 I present a photomicrograph obtained from Field L2 depicting large zGAD65-positive cells (green neurons). Selected backfilled neurons are indicated by the white arrowhead and arrow. These preliminary injections provide evidence for the presence of large GABAergic projection neurons in Field L2, as they exhibit co-localization of rhodamine beads and zGAD65 (arrow). It is noteworthy that although

a percentage of large zGAD65-expressing cells were co-localized with rhodamine beads (arrow), other neurons that were backfilled but did not express zGAD65 were also found (arrowhead). In addition, zGAD65-positive neurons that did not exhibit backfilling were observed in these preparations. These preliminary data suggest that 1) some large GABAergic neurons in Field L2 are projection neurons and 2) Field L2 projections arise from both excitatory and inhibitory neurons, unlike what is commonly assumed in the songbird neurobiology field. These findings suggest that interpretation of electrophysiological and modeling data aimed at understanding the physiology of auditory areas during sensory processing and/or memory formation should take into consideration the more complex connectivity networks observed in the caudomedial auditory lobe. Such considerations should provide a more accurate representation and understanding of the physiology of auditory areas in the songbird brain. Future work should be aimed at more carefully defining the connectivity of the caudomedial auditory lobe.



**Figure A1.1) Some GABAergic cells in Field L and NCM are projection neurons**

(A) Schematic depicting the general organization of the ascending auditory pathway in the zebra finch. Rhodamine injections were placed in NCM (red area). Backfilled neurons were detected in Field L. (B) Co-localization of rhodamine beads and zGAD65 expression reveals GABAergic projection neurons. The arrowhead indicates a projection neuron that does not express zGAD65 and is presumably an excitatory cell. Scale bar = 10 $\mu$ m.



## **APPENDIX II**

### **FURTHER ANALYSIS ON THE EFFECTS OF BICUCULLINE ON FREQUENCY TUNING CURVES IN THE NCM OF AWAKE-RESTRAINED ZEBRA FINCHES**

The results presented in Chapter 4 provide clear evidence that local bicuculline methiodide (BMI) treatment led to a marked reorganization of the temporal properties of song-evoked responses of NCM neurons. It was found that BMI application triggered:

- 1) Synchronization of neuronal responses, especially to the onset of the stimulus presentation.
- 2) Suppression of the tonic (sustained) component of song-evoked responses.

The cartoon represented in Fig. 1 illustrates a comparison between the temporal pattern of response to a single song syllable with (red) and without (blue) BMI. These data suggest that GABAergic mechanisms normally shape the temporal pattern of response by shifting activity from phasic period into the tonic period. One of the questions investigated in Chapter 4 was whether the reorganization of response properties induced by BMI treatment affected perceptual discrimination of auditory stimuli in NCM neurons. A common approach to investigate sound discrimination in the auditory system is to characterize neuronal frequency tuning in areas of interest. In fact, in the mammalian auditory system, frequency tuning curves undergo significant widening upon blockade of inhibitory transmission (Yang et al., 1992; Ehret and Schreiner, 1997; Suga et al., 1997; Chen and Jen, 2000). In our experiments, however, local BMI application did not affect frequency tuning curves, suggesting that frequency discrimination is preserved in conditions of GABA-A receptor blockade in NCM.

As stated above, BMI application enhances the amplitude of responses to stimulus onset, while it reduces the tonic responses throughout the stimulus presentation. It is therefore possible that by analyzing frequency tuning for the full duration of the stimulus (250 msec), a possible difference in pre- versus post-BMI treatment may have been diluted by combining phasic versus tonic response windows. In order to explore this possibility I further analyzed the frequency tuning data in two discrete bins, rather than as a full response set: 1) *phasic bin*: a 50 msec window at 10 msec into stimulus onset; 2) *tonic bin*: a 70 msec window placed immediately following the phasic window. Control period for rms correction was a 500 msec window included immediately prior to stimulus onset.

Fig. 2 includes three representative channels from birds where frequency tuning curves were obtained. Stimuli were pure tones of increasing frequencies (each data point is 250 Hz apart). By separating phasic from tonic components of the response, it was observed that frequency tuning curves follow a trend similar to that observed in the cartoon presented in Fig. 1: Responses to pure tones tended to get reorganized after BMI application, with significantly higher response amplitude for the phasic component and lower response for the tonic component of the responses, as compared to pre-BMI conditions (Fig. 2). Interestingly, the tuning of NCM units after GABA-A receptor antagonism tended to widen during the phasic component of the response. These data provide evidence for decrease frequency discrimination capabilities for NCM units under BMI influence especially for periods within the first 50 msec of the response.

**Figure A2.1) Illustration of BMI-Induced Reorganization of Song-Evoked Response Temporal Properties**

Cartoon comparing the temporal pattern of response to a single song syllable with BMI (red) and without (blue), based on the data obtained in Chapter 4. This data suggests that GABAergic mechanisms normally shape the temporal pattern of the response by shifting activity from the tonic period into the phasic period.

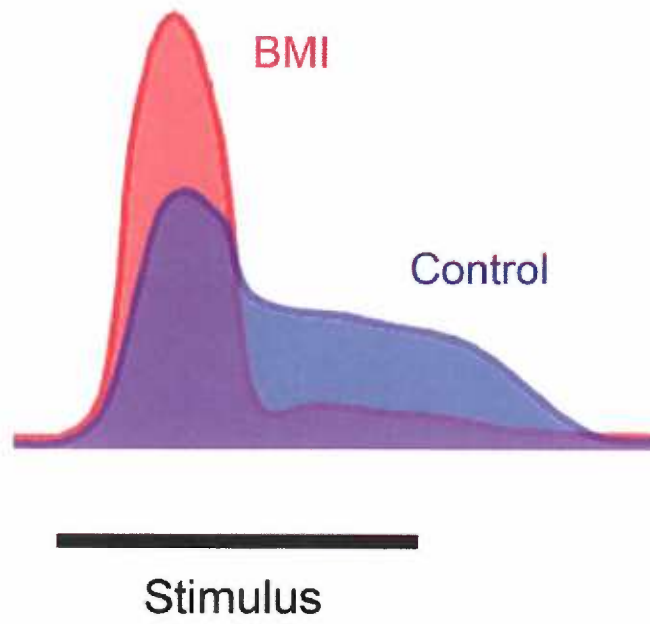
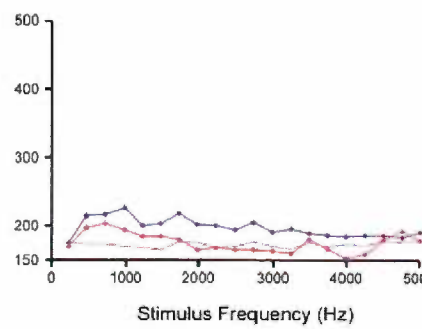
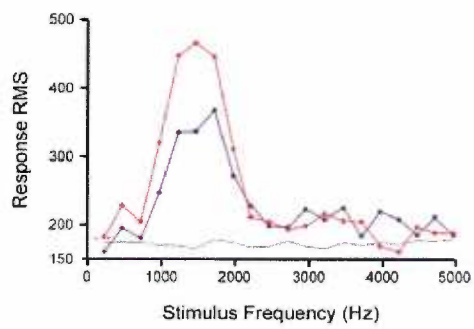
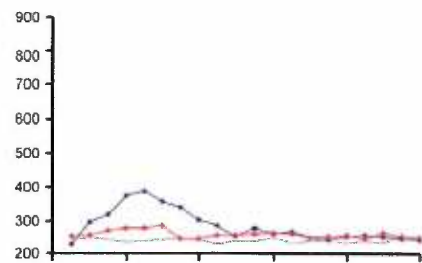
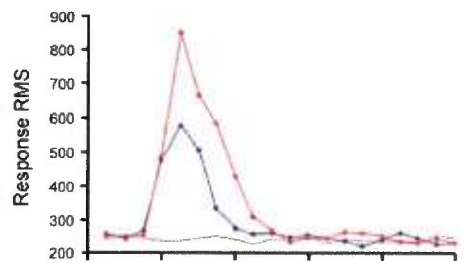
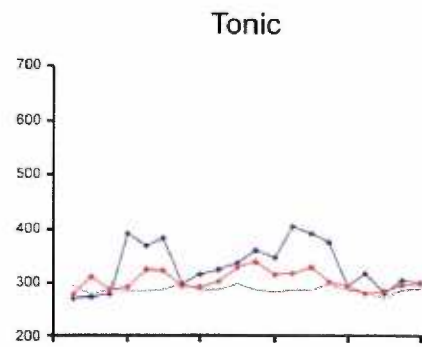
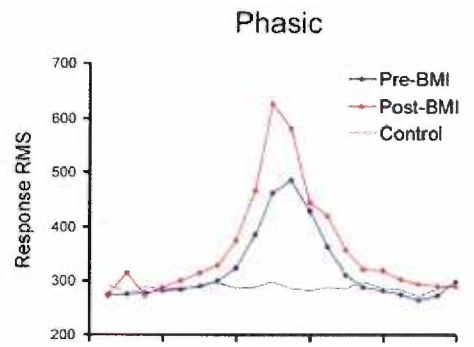


**Figure A2.2) Effects of BMI on Frequency Tuning Curves for Tonic and Phasic  
Bins**

Separation of phasic and tonic components in these three representative channels reveal that under GABA-A antagonism, tone-evoked responses are higher for the phasic (left column), but lower for the tonic component (right column) of the responses. Frequency tuning curves tend to be wider, especially for the phasic component (left column), under BMI treatment.





## REFERENCES

- Adkins-Regan E, Mansukhani V, Seiwert C, Thompson R (1994) Sexual differentiation of brain and behavior in the zebra finch: critical periods for effects of early estrogen treatment. *J Neurobiol* 25:865-877.
- Ahman AK, Wagberg F, Mattsson MO (1996) Two glutamate decarboxylase forms corresponding to the mammalian GAD65 and GAD67 are expressed during development of the chick telencephalon. *Eur J Neurosci* 8:2111-2117.
- Akhtar ND, Land PW (1991) Activity-dependent regulation of glutamic acid decarboxylase in the rat barrel cortex: effects of neonatal versus adult sensory deprivation. *J Comp Neurol* 307:200-213.
- Alloway KD, Burton H (1986) Bicuculline-induced alterations in neuronal responses to controlled tactile stimuli in the second somatosensory cortex of the cat: a microiontophoretic study. *Somatosens Res* 3:197-211.
- Alloway KD, Burton H (1991) Differential effects of GABA and bicuculline on rapidly- and slowly-adapting neurons in primary somatosensory cortex of primates. *Exp Brain Res* 85:598-610.
- Alloway KD, Rosenthal P, Burton H (1989) Quantitative measurements of receptive field changes during antagonism of GABAergic transmission in primary somatosensory cortex of cats. *Exp Brain Res* 78:514-532.
- Ambalavanar R, McCabe BJ, Potter KN, Horn G (1999) Learning-related fos-like immunoreactivity in the chick brain: time-course and co-localization with GABA and parvalbumin. *Neuroscience* 93:1515-1524.

Arckens L, Van Der Gucht E, Eysel UT, Orban GA, Vandesande F (2000)

Investigation of cortical reorganization in area 17 and nine extrastriate visual areas through the detection of changes in immediate early gene expression as induced by retinal lesions. *J Comp Neurol* 425:531-544.

Arnold AP (2004) Sex chromosomes and brain gender. *Nat Rev Neurosci* 5:701-708.

Bading H, Ginty DD, Greenberg ME (1993) Regulation of gene expression in hippocampal neurons by distinct calcium signaling pathways. *Science* 260:181-186.

Ball GF, Auger CJ, Bernard DJ, Charlier TD, Sartor JJ, Ritters LV, Balthazart J (2004) Seasonal plasticity in the song control system: multiple brain sites of steroid hormone action and the importance of variation in song behavior. *Ann N Y Acad Sci* 1016:586-610.

Balthazart J, Foidart A, Wilson EM, Ball GF (1992) Immunocytochemical localization of androgen receptors in the male songbird and quail brain. *J Comp Neurol* 317:407-420.

Barnard EA (1995) The molecular biology of GABAA receptors and their structural determinants. *Adv Biochem Psychopharmacol* 48:1-16.

Bartlett EL, Stark JM, Guillery RW, Smith PH (2000) Comparison of the fine structure of cortical and collicular terminals in the rat medial geniculate body. *Neuroscience* 100:811-828.

Batini C, Compoin C, Buisseret-Delmas C, Daniel H, Guegan M (1992) Cerebellar nuclei and the nucleocortical projections in the rat: retrograde tracing coupled to GABA and glutamate immunohistochemistry. *J Comp Neurol* 315:74-84.

- Batuev AS, Alexandrov AA, Scheynikov NA (1982) Picrotoxin action on the receptive fields of the cat sensorimotor cortex neurons. *J Neurosci Res* 7:49-55.
- Benevento LA, Creutzfeldt OD, Kuhnt U (1972) Significance of intracortical inhibition in the visual cortex. *Nat New Biol* 238:124-126.
- Bernard DJ, Bentley GE, Balthazart J, Turek FW, Ball GF (1999) Androgen receptor, estrogen receptor alpha, and estrogen receptor beta show distinct patterns of expression in forebrain song control nuclei of European starlings. *Endocrinology* 140:4633-4643.
- Blakemore C, Tobin EA (1972) Lateral inhibition between orientation detectors in the cat's visual cortex. *Exp Brain Res* 15:439-440.
- Bland BH, Oddie SD (2001) Theta band oscillation and synchrony in the hippocampal formation and associated structures: the case for its role in sensorimotor integration. *Behav Brain Res* 127:119-136.
- Bolam JP, Hanley JJ, Booth PA, Bevan MD (2000) Synaptic organisation of the basal ganglia. *J Anat* 196 ( Pt 4):527-542.
- Bolhuis JJ, Zijlstra GG, den Boer-Visser AM, Van Der Zee EA (2000) Localized neuronal activation in the zebra finch brain is related to the strength of song learning. *Proc Natl Acad Sci U S A* 97:2282-2285.
- Bolhuis JJ, Hetebrij E, Den Boer-Visser AM, De Groot JH, Zijlstra GG (2001) Localized immediate early gene expression related to the strength of song learning in socially reared zebra finches. *Eur J Neurosci* 13:2165-2170.

- Bolz J, Gilbert CD (1986) Generation of end-inhibition in the visual cortex via interlaminar connections. *Nature* 320:362-365.
- Bonke BA, Bonke D, Scheich H (1979) Connectivity of the auditory forebrain nuclei in the guinea fowl (*Numida meleagris*). *Cell Tissue Res* 200:101-121.
- Boord RL (1968) Ascending projections of the primary cochlear nuclei and nucleus laminaris in the pigeon. *J Comp Neurol* 133:523-541.
- Bottjer SW, Miesner EA, Arnold AP (1984) Forebrain lesions disrupt development but not maintenance of song in passerine birds. *Science* 224:901-903.
- Bottjer SW, Brady JD, Walsh JP (1998) Intrinsic and synaptic properties of neurons in the vocal-control nucleus IMAN from in vitro slice preparations of juvenile and adult zebra finches. *J Neurobiol* 37:642-658.
- Bottjer SW, Halsema KA, Brown SA, Miesner EA (1989) Axonal connections of a forebrain nucleus involved with vocal learning in zebra finches. *J Comp Neurol* 279:312-326.
- Brager DH, Sickel MJ, McCarthy MM (2000) Developmental sex differences in calbindin-D(28K) and calretinin immunoreactivity in the neonatal rat hypothalamus. *J Neurobiol* 42:315-322.
- Brainard MS, Doupe AJ (2000) Auditory feedback in learning and maintenance of vocal behaviour. *Nat Rev Neurosci* 1:31-40.
- Brainard MS, Knudsen EI, Esterly SD (1992) Neural derivation of sound source location: resolution of spatial ambiguities in binaural cues. *J Acoust Soc Am* 91:1015-1027.

- Braun K, Scheich H, Heizmann CW, Hunziker W (1991) Parvalbumin and calbindin-D28K immunoreactivity as developmental markers of auditory and vocal motor nuclei of the zebra finch. *Neuroscience* 40:853-869.
- Brauth SE, McHale CM, Brasher CA, Dooling RJ (1987) Auditory pathways in the budgerigar. I. Thalamo-telencephalic projections. *Brain Behav Evol* 30:174-199.
- Brenowitz EA (1991) Altered perception of species-specific song by female birds after lesions of a forebrain nucleus. *Science* 251:303-305.
- Brenowitz EA (1997) Comparative approaches to the avian song system. *J Neurobiol* 33:517-531.
- Brenowitz EA, Arnold AP (1985) Lack of sexual dimorphism in steroid accumulation in vocal control brain regions of duetting song birds. *Brain Res* 344:172-175.
- Brenowitz EA, Arnold AP, Levin RN (1985) Neural correlates of female song in tropical duetting birds. *Brain Res* 343:104-112.
- Bruckner S, Hyson RL (1998) Effect of GABA on the processing of interaural time differences in nucleus laminaris neurons in the chick. *Eur J Neurosci* 10:3438-3450.
- Bubser M, de Brabander JM, Timmerman W, Feenstra MG, Erdtsieck-Ernste EB, Rinkens A, van Uum JF, Westerink BH (1998) Disinhibition of the mediodorsal thalamus induces fos-like immunoreactivity in both pyramidal and GABA-containing neurons in the medial prefrontal cortex of rats, but does not affect prefrontal extracellular GABA levels. *Synapse* 30:156-165.

- Burek MJ, Nordeen KW, Nordeen EJ (1995) Estrogen promotes neuron addition to an avian song-control nucleus by regulating post-mitotic events. *Brain Res Dev Brain Res* 85:220-224.
- Capsius B, Leppelsack H (1999) Response patterns and their relationship to frequency analysis in auditory forebrain centers of a songbird. *Hear Res* 136:91-99.
- Cardin JA, Schmidt MF (2003) Song system auditory responses are stable and highly tuned during sedation, rapidly modulated and unselective during wakefulness, and suppressed by arousal. *J Neurophysiol* 90:2884-2899.
- Cardin JA, Schmidt MF (2004) Auditory responses in multiple sensorimotor song system nuclei are co-modulated by behavioral state. *J Neurophysiol* 91:2148-2163.
- Carr CE, Konishi M (1990) A circuit for detection of interaural time differences in the brain stem of the barn owl. *J Neurosci* 10:3227-3246.
- Carrasco-Serrano C, Viniegra S, Ballesta JJ, Criado M (2000) Phorbol ester activation of the neuronal nicotinic acetylcholine receptor alpha7 subunit gene: involvement of transcription factor Egr-1. *J Neurochem* 74:932-939.
- Catchpole CK, Slater PJB (1995) Bird song: biological themes and variations. Cambridge: Cambridge University Press.
- Chagnac-Amitai Y, Connors BW (1989a) Synchronized excitation and inhibition driven by intrinsically bursting neurons in neocortex. *J Neurophysiol* 62:1149-1162.

- Chagnac-Amitai Y, Connors BW (1989b) Horizontal spread of synchronized activity in neocortex and its control by GABA-mediated inhibition. *J Neurophysiol* 61:747-758.
- Chaudhuri A (1997) Neural activity mapping with inducible transcription factors. *Neuroreport* 8:v-ix.
- Chen QC, Jen PH (2000) Bicuculline application affects discharge patterns, rate-intensity functions, and frequency tuning characteristics of bat auditory cortical neurons. *Hear Res* 150:161-174.
- Cheng HY, Clayton DF (2004) Activation and habituation of extracellular signal-regulated kinase phosphorylation in zebra finch auditory forebrain during song presentation. *J Neurosci* 24:7503-7513.
- Chew SJ, Vicario DS, Nottebohm F (1996) A large-capacity memory system that recognizes the calls and songs of individual birds. *Proc Natl Acad Sci U S A* 93:1950-1955.
- Chew SJ, Mello C, Nottebohm F, Jarvis E, Vicario DS (1995) Decrements in auditory responses to a repeated conspecific song are long-lasting and require two periods of protein synthesis in the songbird forebrain. *Proc Natl Acad Sci U S A* 92:3406-3410.
- Chomczynski P, Sacchi N (1987) Single-step method of RNA isolation by acid guanidinium thiocyanate-phenol-chloroform extraction. *Anal Biochem* 162:156-159.



- Chowdhury SA, Rasmusson DD (2003) Corticocortical inhibition of peripheral inputs within primary somatosensory cortex: the role of GABA(A) and GABA(B) receptors. *J Neurophysiol* 90:851-856.
- Christy B, Nathans D (1989) DNA binding site of the growth factor-inducible protein Zif268. *Proc Natl Acad Sci U S A* 86:8737-8741.
- Churchill L, Kalivas PW (1994) A topographically organized gamma-aminobutyric acid projection from the ventral pallidum to the nucleus accumbens in the rat. *J Comp Neurol* 345:579-595.
- Clayton DF, Huecas ME, Sinclair-Thompson EY, Nastiuk KL, Nottebohm F (1988) Probes for rare mRNAs reveal distributed cell subsets in canary brain. *Neuron* 1:249-261.
- Cobos I, Puelles L, Martinez S (2001) The avian telencephalic subpallium originates inhibitory neurons that invade tangentially the pallium (dorsal ventricular ridge and cortical areas). *Dev Biol* 239:30-45.
- Coggeshall RE, Lekan HA (1996) Methods for determining numbers of cells and synapses: a case for more uniform standards of review. *J Comp Neurol* 364:6-15.
- Cole AJ, Saffen DW, Baraban JM, Worley PF (1989) Rapid increase of an immediate early gene messenger RNA in hippocampal neurons by synaptic NMDA receptor activation. *Nature* 340:474-476.
- Conlee JW, Parks TN (1986) Origin of ascending auditory projections to the nucleus mesencephalicus lateralis pars dorsalis in the chicken. *Brain Res* 367:96-113.

- Cooke B, Hegstrom CD, Villeneuve LS, Breedlove SM (1998) Sexual differentiation of the vertebrate brain: principles and mechanisms. *Front Neuroendocrinol* 19:323-362.
- Cotman CW, Monaghan DT, Ganong AH (1988) Excitatory amino acid neurotransmission: NMDA receptors and Hebb-type synaptic plasticity. *Annu Rev Neurosci* 11:61-80.
- Creutzfeldt OD, Kuhnt U, Benevento LA (1974) An intracellular analysis of visual cortical neurones to moving stimuli: response in a co-operative neuronal network. *Exp Brain Res* 21:251-274.
- Cynx J, Nottebohm F (1992a) Testosterone facilitates some conspecific song discriminations in castrated zebra finches (*Taeniopygia guttata*). *Proc Natl Acad Sci U S A* 89:1376-1378.
- Cynx J, Nottebohm F (1992b) Role of gender, season, and familiarity in discrimination of conspecific song by zebra finches (*Taeniopygia guttata*). *Proc Natl Acad Sci U S A* 89:1368-1371.
- Dave AS, Yu AC, Margoliash D (1998) Behavioral state modulation of auditory activity in a vocal motor system. *Science* 282:2250-2254.
- Davis W, Jr., Chen ZJ, Ile KE, Tew KD (2003) Reciprocal regulation of expression of the human adenosine 5'-triphosphate binding cassette, sub-family A, transporter 2 (ABCA2) promoter by the early growth response-1 (EGR-1) and Sp-family transcription factors. *Nucleic Acids Res* 31:1097-1107.
- Daw NW, Stein PS, Fox K (1993) The role of NMDA receptors in information processing. *Annu Rev Neurosci* 16:207-222.

- De Weerd P, Pinaud R, Bertini G (2005) Plasticity in V1 induced by perceptual learning. In: Plasticity in the visual system: from genes to circuits (Pinaud R, Tremere LA, De Weerd P, eds), p (in press). Boston: Springer Scientific Press.
- DeFelipe J (1997) Types of neurons, synaptic connections and chemical characteristics of cells immunoreactive for calbindin-D28K, parvalbumin and calretinin in the neocortex. *J Chem Neuroanat* 14:1-19.
- Del Negro C, Edeline JM (2001) Differences in auditory and physiological properties of HVc neurons between reproductively active male and female canaries (*Serinus canaria*). *Eur J Neurosci* 14:1377-1389.
- Del Negro C, Edeline JM (2002) Sex and season influence the proportion of thin spike cells in the canary HVc. *Neuroreport* 13:2005-2009.
- Del Negro C, Kreutzer M, Gahr M (2000) Sexually stimulating signals of canary (*Serinus canaria*) songs: evidence for a female-specific auditory representation in the HVc nucleus during the breeding season. *Behav Neurosci* 114:526-542.
- Denisenko-Nehrbass NI, Jarvis E, Scharff C, Nottebohm F, Mello CV (2000) Site-specific retinoic acid production in the brain of adult songbirds. *Neuron* 27:359-370.
- DeVoogd T, Nottebohm F (1981) Gonadal hormones induce dendritic growth in the adult avian brain. *Science* 214:202-204.
- Doetsch GS, Norelle A, Mark EK, Standage GP, Lu SM, Lin RC (1993) Immunoreactivity for GAD and three peptides in somatosensory cortex and thalamus of the raccoon. *Brain Res Bull* 31:553-563.

- Doupe AJ (1993) A neural circuit specialized for vocal learning. *Curr Opin Neurobiol* 3:104-111.
- Doupe AJ (1997) Song- and order-selective neurons in the songbird anterior forebrain and their emergence during vocal development. *J Neurosci* 17:1147-1167.
- Doupe AJ, Konishi M (1991) Song-selective auditory circuits in the vocal control system of the zebra finch. *Proc Natl Acad Sci U S A* 88:11339-11343.
- Dykes RW, Landry P, Metherate R, Hicks TP (1984) Functional role of GABA in cat primary somatosensory cortex: shaping receptive fields of cortical neurons. *J Neurophysiol* 52:1066-1093.
- Dziema H, Oatis B, Butcher GQ, Yates R, Hoyt KR, Obrietan K (2003) The ERK/MAP kinase pathway couples light to immediate-early gene expression in the suprachiasmatic nucleus. *Eur J Neurosci* 17:1617-1627.
- Ebner FF, Armstrong-James MA (1990) Intracortical processes regulating the integration of sensory information. *Prog Brain Res* 86:129-141.
- Ehret G, Schreiner CE (1997) Frequency resolution and spectral integration (critical band analysis) in single units of the cat primary auditory cortex. *J Comp Physiol [A]* 181:635-650.
- Ehret G, Egorova M, Hage SR, Muller BA (2003) Spatial map of frequency tuning-curve shapes in the mouse inferior colliculus. *Neuroreport* 14:1365-1369.
- Eysel UT, Shevelev IA, Lazareva NA, Sharaev GA (1998) Orientation tuning and receptive field structure in cat striate neurons during local blockade of intracortical inhibition. *Neuroscience* 84:25-36.

- Fairen A, DeFelipe J, Regidor J (1984) Non pyramidal neurons: general account. In: Cellular components of the cerebral cortex (Peters A, Jones EG, eds), pp 201-253. New York: Plenum Press.
- Ferragamo MJ, Haresign T, Simmons JA (1998) Frequency tuning, latencies, and responses to frequency-modulated sweeps in the inferior colliculus of the echolocating bat, *Eptesicus fuscus*. *J Comp Physiol [A]* 182:65-79.
- Fiorillo CD, Williams JT (1998) Glutamate mediates an inhibitory postsynaptic potential in dopamine neurons. *Nature* 394:78-82.
- Fox K, Wallace H, Glazewski S (2002) Is there a thalamic component to experience-dependent cortical plasticity? *Philos Trans R Soc Lond B Biol Sci* 357:1709-1715.
- Freund TF, Meskenaite V (1992) gamma-Aminobutyric acid-containing basal forebrain neurons innervate inhibitory interneurons in the neocortex. *Proc Natl Acad Sci U S A* 89:738-742.
- Fujita I, Konishi M (1991) The role of GABAergic inhibition in processing of interaural time difference in the owl's auditory system. *J Neurosci* 11:722-739.
- Fukui I, Ohmori H (2004) Tonotopic gradients of membrane and synaptic properties for neurons of the chicken nucleus magnocellularis. *J Neurosci* 24:7514-7523.
- Funabiki K, Koyano K, Ohmori H (1998) The role of GABAergic inputs for coincidence detection in the neurones of nucleus laminaris of the chick. *J Physiol* 508 ( Pt 3):851-869.
- Fusani L, Hutchison JB, Gahr M (2001) Testosterone regulates the activity and expression of aromatase in the canary neostriatum. *J Neurobiol* 49:1-8.

- Gabbott PL, Somogyi P (1986) Quantitative distribution of GABA-immunoreactive neurons in the visual cortex (area 17) of the cat. *Exp Brain Res* 61:323-331.
- Gabbott PL, Somogyi J, Stewart MG, Hamori J (1986) GABA-immunoreactive neurons in the rat cerebellum: a light and electron microscope study. *J Comp Neurol* 251:474-490.
- Gahwiler BH, Brown DA (1985) GABAB-receptor-activated K<sup>+</sup> current in voltage-clamped CA3 pyramidal cells in hippocampal cultures. *Proc Natl Acad Sci U S A* 82:1558-1562.
- Gazzaley AH, Weiland NG, McEwen BS, Morrison JH (1996) Differential regulation of NMDAR1 mRNA and protein by estradiol in the rat hippocampus. *J Neurosci* 16:6830-6838.
- Gehr DD, Capsius B, Grabner P, Gahr M, Leppelsack HJ (1999) Functional organisation of the field-L-complex of adult male zebra finches. *Neuroreport* 10:375-380.
- Gentner TQ (2004) Neural systems for individual song recognition in adult birds. *Ann N Y Acad Sci* 1016:282-302.
- Gentner TQ, Margoliash D (2003) Neuronal populations and single cells representing learned auditory objects. *Nature* 424:669-674.
- Gentner TQ, Hulse SH, Duffy D, Ball GF (2001) Response biases in auditory forebrain regions of female songbirds following exposure to sexually relevant variation in male song. *J Neurobiol* 46:48-58.
- Gerfen CR (1988) Synaptic organization of the striatum. *J Electron Microsc Tech* 10:265-281.

- Gierdalski M, Jablonska B, Siucinska E, Lech M, Skibinska A, Kossut M (2001) Rapid regulation of GAD67 mRNA and protein level in cortical neurons after sensory learning. *Cereb Cortex* 11:806-815.
- Glazewski S, Fox K (1996) Time course of experience-dependent synaptic potentiation and depression in barrel cortex of adolescent rats. *J Neurophysiol* 75:1714-1729.
- Gonzalez-Albo MC, Elston GN, DeFelipe J (2001) The human temporal cortex: characterization of neurons expressing nitric oxide synthase, neuropeptides and calcium-binding proteins, and their glutamate receptor subunit profiles. *Cereb Cortex* 11:1170-1181.
- Gould E, Woolley CS, Frankfurt M, McEwen BS (1990) Gonadal steroids regulate dendritic spine density in hippocampal pyramidal cells in adulthood. *J Neurosci* 10:1286-1291.
- Grisham W, Arnold AP (1994) Distribution of GABA-like immunoreactivity in the song system of the zebra finch. *Brain Res* 651:115-122.
- Gritti I, Mainville L, Jones BE (1993) Codistribution of GABA- with acetylcholine-synthesizing neurons in the basal forebrain of the rat. *J Comp Neurol* 329:438-457.
- Gritti I, Manns ID, Mainville L, Jones BE (2003) Parvalbumin, calbindin, or calretinin in cortically projecting and GABAergic, cholinergic, or glutamatergic basal forebrain neurons of the rat. *J Comp Neurol* 458:11-31.
- Halle F, Gahr M, Pieneman AW, Kreutzer M (2002) Recovery of song preferences after excitotoxic HVC lesion in female canaries. *J Neurobiol* 52:1-13.

- Hata Y, Tsumoto T, Sato H, Hagihara K, Tamura H (1988) Inhibition contributes to orientation selectivity in visual cortex of cat. *Nature* 335:815-817.
- Hefti BJ, Smith PH (2003) Distribution and kinetic properties of GABAergic inputs to layer V pyramidal cells in rat auditory cortex. *J Assoc Res Otolaryngol* 4:106-121.
- Heizmann CW (1992) Calcium-binding proteins: basic concepts and clinical implications. *Gen Physiol Biophys* 11:411-425.
- Hendry SH, Jones EG (1991) GABA neuronal subpopulations in cat primary auditory cortex: co-localization with calcium binding proteins. *Brain Res* 543:45-55.
- Hendry SH, Schwark HD, Jones EG, Yan J (1987) Numbers and proportions of GABA-immunoreactive neurons in different areas of monkey cerebral cortex. *J Neurosci* 7:1503-1519.
- Hendry SH, Fuchs J, deBlas AL, Jones EG (1990) Distribution and plasticity of immunocytochemically localized GABAA receptors in adult monkey visual cortex. *J Neurosci* 10:2438-2450.
- Herbison AE (1997) Estrogen regulation of GABA transmission in rat preoptic area. *Brain Res Bull* 44:321-326.
- Herbison AE, Fenelon VS (1995) Estrogen regulation of GABAA receptor subunit mRNA expression in preoptic area and bed nucleus of the stria terminalis of female rat brain. *J Neurosci* 15:2328-2337.
- Herdegen T, Leah JD (1998) Inducible and constitutive transcription factors in the mammalian nervous system: control of gene expression by Jun, Fos and Krox, and CREB/ATF proteins. *Brain Res Brain Res Rev* 28:370-490.



- Herrada G, Dulac C (1997) A novel family of putative pheromone receptors in mammals with a topographically organized and sexually dimorphic distribution. *Cell* 90:763-773.
- Hicks TP, Dykes RW (1983) Receptive field size for certain neurons in primary somatosensory cortex is determined by GABA-mediated intracortical inhibition. *Brain Res* 274:160-164.
- Hicks TP, Albus K, Kaneko T, Baumfalk U (1993) Examination of the effects of cholecystokinin 26-33 and neuropeptide Y on responses of visual cortical neurons of the cat. *Neuroscience* 52:263-279.
- Hogan D, Terwilleger ER, Berman NE (1992) Development of subpopulations of GABAergic neurons in cat visual cortical areas. *Neuroreport* 3:1069-1072.
- Hollmann M, Heinemann S (1994) Cloned glutamate receptors. *Annu Rev Neurosci* 17:31-108.
- Hollrigel GS, Soltesz I (1997) Slow kinetics of miniature IPSCs during early postnatal development in granule cells of the dentate gyrus. *J Neurosci* 17:5119-5128.
- Holzenberger M, Jarvis ED, Chong C, Grossman M, Nottebohm F, Scharff C (1997) Selective expression of insulin-like growth factor II in the songbird brain. *J Neurosci* 17:6974-6987.
- Horn G (2004) Pathways of the past: the imprint of memory. *Nat Rev Neurosci* 5:108-120.
- Hubel DH, Wiesel TN (1962) Receptive fields, binocular interaction and functional architecture in the cat's visual cortex. *J Physiol* 160:106-154.

- Hubel DH, Wiesel TN (1968) Receptive fields and functional architecture of monkey striate cortex. *J Physiol* 195:215-243.
- Hunziker W, Schrickel S (1988) Rat brain calbindin D28: six domain structure and extensive amino acid homology with chicken calbindin D28. *Mol Endocrinol* 2:465-473.
- Isaacson JS, Solis JM, Nicoll RA (1993) Local and diffuse synaptic actions of GABA in the hippocampus. *Neuron* 10:165-175.
- Jarvis ED, Nottebohm F (1997) Motor-driven gene expression. *Proc Natl Acad Sci U S A* 94:4097-4102.
- Jarvis ED, Mello CV (2000) Molecular mapping of brain areas involved in parrot vocal communication. *J Comp Neurol* 419:1-31.
- Jarvis ED, Schwabl H, Ribeiro S, Mello CV (1997) Brain gene regulation by territorial singing behavior in freely ranging songbirds. *Neuroreport* 8:2073-2077.
- Jarvis ED, Scharff C, Grossman MR, Ramos JA, Nottebohm F (1998) For whom the bird sings: context-dependent gene expression. *Neuron* 21:775-788.
- Jarvis ED, Ribeiro S, da Silva ML, Ventura D, Vielliard J, Mello CV (2000) Behaviourally driven gene expression reveals song nuclei in hummingbird brain. *Nature* 406:628-632.
- Jin H, Clayton DF (1997) Localized changes in immediate-early gene regulation during sensory and motor learning in zebra finches. *Neuron* 19:1049-1059.

- Johnson F, Bottjer SW (1993) Hormone-induced changes in identified cell populations of the higher vocal center in male canaries. *J Neurobiol* 24:400-418.
- Jones EG (1993) GABAergic neurons and their role in cortical plasticity in primates. *Cereb Cortex* 3:361-372.
- Jones KA, Borowsky B, Tamm JA, Craig DA, Durkin MM, Dai M, Yao WJ, Johnson M, Gunwaldsen C, Huang LY, Tang C, Shen Q, Salon JA, Morse K, Laz T, Smith KE, Nagarathnam D, Noble SA, Branchek TA, Gerald C (1998) GABA(B) receptors function as a heteromeric assembly of the subunits GABA(B)R1 and GABA(B)R2. *Nature* 396:674-679.
- Kaczmarek L, Robertson HA (2002) Immediate early genes and inducible transcription factors in mapping of the central nervous system function and dysfunction. Amsterdam: Elsevier Science B.V.
- Karten HJ (1967) The organization of the ascending auditory pathway in the pigeon (*Columba livia*). I. Diencephalic projections of the inferior colliculus (nucleus mesencephali lateralis, pars dorsalis). *Brain Res* 6:409-427.
- Karten HJ (1968) The ascending auditory pathway in the pigeon (*Columba livia*). II. Telencephalic projections of the nucleus ovoidalis thalami. *Brain Res* 11:134-153.
- Karten HJ (1991) Homology and evolutionary origins of the 'neocortex'. *Brain Behav Evol* 38:264-272.
- Karten HJ, Shimizu T (1989) The origins of neocortex: connections and lamination as distinct events in evolution. *J Cogn Neurosci* 1:291-301.

- Kaupmann K, Malitschek B, Schuler V, Heid J, Froestl W, Beck P, Mosbacher J, Bischoff S, Kulik A, Shigemoto R, Karschin A, Bettler B (1998) GABA(B)-receptor subtypes assemble into functional heteromeric complexes. *Nature* 396:683-687.
- Kautz D, Wagner H (1998) GABAergic inhibition influences auditory motion-direction sensitivity in barn owls. *J Neurophysiol* 80:172-185.
- Kawaguchi Y, Katsumaru H, Kosaka T, Heizmann CW, Hama K (1987) Fast spiking cells in rat hippocampus (CA1 region) contain the calcium-binding protein parvalbumin. *Brain Res* 416:369-374.
- Kelley DB, Nottebohm F (1979) Projections of a telencephalic auditory nucleus-field L-in the canary. *J Comp Neurol* 183:455-469.
- Knapska E, Kaczmarek L (2004) A gene for neuronal plasticity in the mammalian brain: Zif268/Egr-1/NGFI-A/Krox-24/TIS8/ZENK? *Prog Neurobiol* 74:183-211.
- Knudsen EI, Konishi M (1978) Space and frequency are represented separately in auditory midbrain of the owl. *J Neurophysiol* 41:870-884.
- Knudsen EI, Zheng W, DeBello WM (2000) Traces of learning in the auditory localization pathway. *Proc Natl Acad Sci U S A* 97:11815-11820.
- Konishi M (1965a) Effects of deafening on song development in American robins and black-headed grosbeaks. *Z Tierpsychol* 22:584-599.
- Konishi M (1965b) The role of auditory feedback in the control of vocalization in the white-crowned sparrow. *Z Tierpsychol* 22:770-783.

- Koppl C, Manley GA, Konishi M (2000) Auditory processing in birds. *Curr Opin Neurobiol* 10:474-481.
- Krnjevic K (1984) Some functional consequences of GABA uptake by brain cells. *Neurosci Lett* 47:283-287.
- Kroodsma DE, Miller EH (1982) *Acoustic communication in birds*. New York: Academic Press.
- Kroodsma DE, Miller EH (1996) *Ecology and evolution of acoustic communication in birds*. Ithaca, NY: Cornell University Press.
- Kroodsma DE, Houlihan PW, Fallon PA, Wells JA (1997) Song development by grey catbirds. *Anim Behav* 54:457-464.
- Kubke MF, Carr CE (2000) Development of the auditory brainstem of birds: comparison between barn owls and chickens. *Hear Res* 147:1-20.
- Kubke MF, Massoglia DP, Carr CE (2004) Bigger brains or bigger nuclei? Regulating the size of auditory structures in birds. *Brain Behav Evol* 63:169-180.
- Kuner R, Kohr G, Grunewald S, Eisenhardt G, Bach A, Kornau HC (1999) Role of heteromer formation in GABAB receptor function. *Science* 283:74-77.
- Kyriazi H, Carvell GE, Brumberg JC, Simons DJ (1998) Laminar differences in bicuculline methiodide's effects on cortical neurons in the rat whisker/barrel system. *Somatosens Mot Res* 15:146-156.
- Lachica EA, Rubsamen R, Rubel EW (1994) GABAergic terminals in nucleus magnocellularis and laminaris originate from the superior olivary nucleus. *J Comp Neurol* 348:403-418.

- Leitner S, Nicholson J, Leisler B, DeVogd TJ, Catchpole CK (2002) Song and the song control pathway in the brain can develop independently of exposure to song in the sedge warbler. *Proc R Soc Lond B Biol Sci* 269:2519-2524.
- Leonardo A, Konishi M (1999) Decrystallization of adult birdsong by perturbation of auditory feedback. *Nature* 399:466-470.
- Levin MD, Kubke MF, Schneider M, Wenthold R, Carr CE (1997) Localization of AMPA-selective glutamate receptors in the auditory brainstem of the barn owl. *J Comp Neurol* 378:239-253.
- Lewald J (2004) Gender-specific hemispheric asymmetry in auditory space perception. *Brain Res Cogn Brain Res* 19:92-99.
- Luddens H, Korpi ER, Seeburg PH (1995) GABAA/benzodiazepine receptor heterogeneity: neurophysiological implications. *Neuropharmacology* 34:245-254.
- Luo M, Perkel DJ (1999a) Long-range GABAergic projection in a circuit essential for vocal learning. *J Comp Neurol* 403:68-84.
- Luo M, Perkel DJ (1999b) A GABAergic, strongly inhibitory projection to a thalamic nucleus in the zebra finch song system. *J Neurosci* 19:6700-6711.
- Luscher C, Jan LY, Stoffel M, Malenka RC, Nicoll RA (1997) G protein-coupled inwardly rectifying K<sup>+</sup> channels (GIRKs) mediate postsynaptic but not presynaptic transmitter actions in hippocampal neurons. *Neuron* 19:687-695.
- Macdonald RL, Olsen RW (1994) GABAA receptor channels. *Annu Rev Neurosci* 17:569-602.

- Maggi A, Perez J (1984) Progesterone and estrogens in rat brain: modulation of GABA (gamma-aminobutyric acid) receptor activity. *Eur J Pharmacol* 103:165-168.
- Manunta Y, Edeline JM (1997) Effects of noradrenaline on frequency tuning of rat auditory cortex neurons. *Eur J Neurosci* 9:833-847.
- Margoliash D (1983) Acoustic parameters underlying the responses of song-specific neurons in the white-crowned sparrow. *J Neurosci* 3:1039-1057.
- Margoliash D (1997) Functional organization of forebrain pathways for song production and perception. *J Neurobiol* 33:671-693.
- Markram H, Toledo-Rodriguez M, Wang Y, Gupta A, Silberberg G, Wu C (2004) Interneurons of the neocortical inhibitory system. *Nat Rev Neurosci* 5:793-807.
- Marler P, Waser MS (1977) Role of auditory feedback in canary song development. *J Comp Physiol Psychol* 91:8-16.
- Marler P, Doupe AJ (2000) Singing in the brain. *Proc Natl Acad Sci U S A* 97:2965-2967.
- Marler P, Mundinger P, Waser MS, Lutjen A (1972) Effects of acoustical stimulation and deprivation on song development in red-winged blackbirds (*Agelaius phoeniceus*). *Anim Behav* 20:586-606.
- McCabe BJ, Horn G (1994) Learning-related changes in Fos-like immunoreactivity in the chick forebrain after imprinting. *Proc Natl Acad Sci U S A* 91:11417-11421.

- McCasland JS, Konishi M (1981) Interaction between auditory and motor activities in an avian song control nucleus. *Proc Natl Acad Sci U S A* 78:7815-7819.
- McGuire BA, Gilbert CD, Rivlin PK, Wiesel TN (1991) Targets of horizontal connections in macaque primary visual cortex. *J Comp Neurol* 305:370-392.
- Mello C, Nottebohm F, Clayton D (1995) Repeated exposure to one song leads to a rapid and persistent decline in an immediate early gene's response to that song in zebra finch telencephalon. *J Neurosci* 15:6919-6925.
- Mello CV (2002a) Mapping vocal communication pathways in birds with inducible gene expression. *J Comp Physiol A Neuroethol Sens Neural Behav Physiol* 188:943-959.
- Mello CV (2002b) Immediate early gene (IEG) expression mapping of vocal communication areas in the avian brain. In: Immediate early genes and inducible transcription factors in mapping of the central nervous system function and dysfunction (Kaczmarek L, Robertson HA, eds), pp 59-101. Amsterdam: Elsevier Science B.V.
- Mello CV, Clayton DF (1994) Song-induced ZENK gene expression in auditory pathways of songbird brain and its relation to the song control system. *J Neurosci* 14:6652-6666.
- Mello CV, Clayton DF (1995) Differential induction of the ZENK gene in the avian forebrain and song control circuit after metrazole-induced depolarization. *J Neurobiol* 26:145-161.
- Mello CV, Ribeiro S (1998) ZENK protein regulation by song in the brain of songbirds. *J Comp Neurol* 393:426-438.



- Mello CV, Vicario DS, Clayton DF (1992) Song presentation induces gene expression in the songbird forebrain. *Proc Natl Acad Sci U S A* 89:6818-6822.
- Mello CV, Velho TA, Pinaud R (2004) Song-induced gene expression: a window on song auditory processing and perception. *Ann N Y Acad Sci* 1016:263-281.
- Mello CV, Jarvis ED, Denisenko N, Rivas M (1997) Isolation of song-regulated genes in the brain of songbirds. *Methods Mol Biol* 85:205-217.
- Mello CV, Vates GE, Okuhata S, Nottebohm F (1998) Descending auditory pathways in the adult male zebra finch (*Taeniopygia guttata*). *J Comp Neurol* 395:137-160.
- Meredith RM, Floyer-Lea AM, Paulsen O (2003) Maturation of long-term potentiation induction rules in rodent hippocampus: role of GABAergic inhibition. *J Neurosci* 23:11142-11146.
- Metzdorf R, Gahr M, Fusani L (1999) Distribution of aromatase, estrogen receptor, and androgen receptor mRNA in the forebrain of songbirds and nonsongbirds. *J Comp Neurol* 407:115-129.
- Misgeld U, Bijak M, Jarolimek W (1995) A physiological role for GABAB receptors and the effects of baclofen in the mammalian central nervous system. *Prog Neurobiol* 46:423-462.
- Mizukami S, Nishizuka M, Arai Y (1983) Sexual difference in nuclear volume and its ontogeny in the rat amygdala. *Exp Neurol* 79:569-575.
- Mody I, De Koninck Y, Otis TS, Soltesz I (1994) Bridging the cleft at GABA synapses in the brain. *Trends Neurosci* 17:517-525.

- Monsivais P, Rubel EW (2001) Accommodation enhances depolarizing inhibition in central neurons. *J Neurosci* 21:7823-7830.
- Monsivais P, Yang L, Rubel EW (2000) GABAergic inhibition in nucleus magnocellularis: implications for phase locking in the avian auditory brainstem. *J Neurosci* 20:2954-2963.
- Mooney R (1999) Sensitive periods and circuits for learned birdsong. *Curr Opin Neurobiol* 9:121-127.
- Morales B, Choi SY, Kirkwood A (2002) Dark rearing alters the development of GABAergic transmission in visual cortex. *J Neurosci* 22:8084-8090.
- Morrisett RA, Mott DD, Lewis DV, Swartzwelder HS, Wilson WA (1991) GABAB-receptor-mediated inhibition of the N-methyl-D-aspartate component of synaptic transmission in the rat hippocampus. *J Neurosci* 11:203-209.
- Muller CM, Leppelsack HJ (1985) Feature extraction and tonotopic organization in the avian auditory forebrain. *Exp Brain Res* 59:587-599.
- Muller CM, Scheich H (1988) Contribution of GABAergic inhibition to the response characteristics of auditory units in the avian forebrain. *J Neurophysiol* 59:1673-1689.
- Munoz A, DeFelipe J, Jones EG (2001) Patterns of GABA(B)R1a,b receptor gene expression in monkey and human visual cortex. *Cereb Cortex* 11:104-113.
- Murphy TH, Worley PF, Nakabeppu Y, Christy B, Gastel J, Baraban JM (1991) Synaptic regulation of immediate early gene expression in primary cultures of cortical neurons. *J Neurochem* 57:1862-1872.

- Narins PM, Capranica RR (1976) Sexual differences in the auditory system of the tree frog *Eleutherodactylus coqui*. *Science* 192:378-380.
- Nordeen KW, Nordeen EJ (1992) Auditory feedback is necessary for the maintenance of stereotyped song in adult zebra finches. *Behav Neural Biol* 57:58-66.
- Nordeen KW, Nordeen EJ (1993) Long-term maintenance of song in adult zebra finches is not affected by lesions of a forebrain region involved in song learning. *Behav Neural Biol* 59:79-82.
- Nordeen KW, Nordeen EJ (1997) Anatomical and synaptic substrates for avian song learning. *J Neurobiol* 33:532-548.
- Nordeen KW, Nordeen EJ (2004) Synaptic and molecular mechanisms regulating plasticity during early learning. *Ann N Y Acad Sci* 1016:416-437.
- Nottebohm F (1980) Testosterone triggers growth of brain vocal control nuclei in adult female canaries. *Brain Res* 189:429-436.
- Nottebohm F (1999) The anatomy and timing of vocal learning in birds. In: *The design of animal communication* (Konishi M, ed), pp 63-110. Cambridge: MIT Press.
- Nottebohm F, Arnold AP (1976) Sexual dimorphism in vocal control areas of the songbird brain. *Science* 194:211-213.
- Nottebohm F, Arnold AP (1979) Songbirds' brains: sexual dimorphism. *Science* 206:769.
- Nottebohm F, Stokes TM, Leonard CM (1976) Central control of song in the canary, *Serinus canarius*. *J Comp Neurol* 165:457-486.

- Nottebohm F, Kelley DB, Paton JA (1982) Connections of vocal control nuclei in the canary telencephalon. *J Comp Neurol* 207:344-357.
- Overholt EM, Rubel EW, Hyson RL (1992) A circuit for coding interaural time differences in the chick brainstem. *J Neurosci* 12:1698-1708.
- Parent A, Cote PY, Lavoie B (1995) Chemical anatomy of primate basal ganglia. *Prog Neurobiol* 46:131-197.
- Parks TN, Rubel EW (1975) Organization and development of brain stem auditory nuclei of the chicken: organization of projections from n. magnocellularis to n. laminaris. *J Comp Neurol* 164:435-448.
- Parks TN, Rubel EW (1978) Organization and development of the brain stem auditory nuclei of the chicken: primary afferent projections. *J Comp Neurol* 180:439-448.
- Pasteels B, Miki N, Hatakenaka S, Pochet R (1987) Immunohistochemical cross-reactivity and electrophoretic comigration between calbindin D-27 kDa and visinin. *Brain Res* 412:107-113.
- Peruzzi D, Bartlett E, Smith PH, Oliver DL (1997) A monosynaptic GABAergic input from the inferior colliculus to the medial geniculate body in rat. *J Neurosci* 17:3766-3777.
- Peters A, Jones EG (1984) Cellular components of the cerebral cortex. New York: Plenum Press.
- Petersen CC, Sakmann B (2001) Functionally independent columns of rat somatosensory barrel cortex revealed with voltage-sensitive dye imaging. *J Neurosci* 21:8435-8446.

- Petersohn D, Thiel G (1996) Role of zinc-finger proteins Sp1 and zif268/egr-1 in transcriptional regulation of the human synaptobrevin II gene. *Eur J Biochem* 239:827-834.
- Petersohn D, Schoch S, Brinkmann DR, Thiel G (1995) The human synapsin II gene promoter. Possible role for the transcription factor zif268/egr-1, polyoma enhancer activator 3, and AP2. *J Biol Chem* 270:24361-24369.
- Pinaud R (2004) Experience-dependent immediate early gene expression in the adult central nervous system: evidence from enriched-environment studies. *Int J Neurosci* 114:321-333.
- Pinaud R (2005) Critical calcium-regulated biochemical and gene expression programs involved in experience-dependent plasticity. In: *Plasticity in the visual system: from genes to circuits* (Pinaud R, Tremere LA, De Weerd P, eds), pp 153-180. New York: Springer Scientific Press.
- Pinaud R, Tremere LA (2005) Experience-dependent retinal circuit rewiring: involvement of immediate early genes. In: *Plasticity in the visual system: from genes to circuits* (Pinaud R, Tremere LA, De Weerd P, eds), pp 79-95. New York: Springer Scientific Press.
- Pinaud R, Velho TA, Mello CV (2005) GABA immunoreactivity in auditory and song control brain areas of zebra finches. *J Comp Neurol* accepted pending revisions.
- Pinaud R, Tremere LA, Penner MR, Hess FF, Robertson HA, Currie RW (2002a) Complexity of sensory environment drives the expression of candidate-plasticity gene, nerve growth factor induced-A. *Neuroscience* 112:573-582.

- Pinaud R, Tremere LA, Penner MR, Hess FF, Barnes S, Robertson HA, Currie RW (2002b) Plasticity-driven gene expression in the rat retina. *Brain Res Mol Brain Res* 98:93-101.
- Pinaud R, Velho TA, Jeong JK, Tremere LA, Leao RM, von Gersdorff H, Mello CV (2004) GABAergic neurons participate in the brain's response to birdsong auditory stimulation. *Eur J Neurosci* 20:1318-1330.
- Pinaud R, Vargas CD, Ribeiro S, Monteiro MV, Tremere LA, Vianney P, Delgado P, Mello CV, Rocha-Miranda CE, Volchan E (2003) Light-induced Egr-1 expression in the striate cortex of the opossum. *Brain Res Bull* 61:139-146.
- Poirier P, Samson FK, Imig TJ (2003) Spectral shape sensitivity contributes to the azimuth tuning of neurons in the cat's inferior colliculus. *J Neurophysiol* 89:2760-2777.
- Pollak GD, Burger RM, Klug A (2003) Dissecting the circuitry of the auditory system. *Trends Neurosci* 26:33-39.
- Pospelov VA, Pospelova TV, Julien JP (1994) AP-1 and Krox-24 transcription factors activate the neurofilament light gene promoter in P19 embryonal carcinoma cells. *Cell Growth Differ* 5:187-196.
- Prieto JJ, Peterson BA, Winer JA (1994a) Laminar distribution and neuronal targets of GABAergic axon terminals in cat primary auditory cortex (AI). *J Comp Neurol* 344:383-402.
- Prieto JJ, Peterson BA, Winer JA (1994b) Morphology and spatial distribution of GABAergic neurons in cat primary auditory cortex (AI). *J Comp Neurol* 344:349-382.

- Princivalle A, Regondi MC, Frassoni C, Bowery NG, Spreafico R (2000) Distribution of GABA(B) receptor protein in somatosensory cortex and thalamus of adult rats and during postnatal development. *Brain Res Bull* 52:397-405.
- Qian H, Pan Y, Zhu Y, Khalili P (2005) Picrotoxin accelerates relaxation of GABAC receptors. *Mol Pharmacol* 67:470-479.
- Ramanathan S, Hanley JJ, Deniau JM, Bolam JP (2002) Synaptic convergence of motor and somatosensory cortical afferents onto GABAergic interneurons in the rat striatum. *J Neurosci* 22:8158-8169.
- Ramoá AS, Paradiso MA, Freeman RD (1988) Blockade of intracortical inhibition in kitten striate cortex: effects on receptive field properties and associated loss of ocular dominance plasticity. *Exp Brain Res* 73:285-296.
- Reiner A, Perkel DJ, Bruce LL, Butler AB, Csillag A, Kuenzel W, Medina L, Paxinos G, Shimizu T, Striedter G, Wild M, Ball GF, Durand S, Gunturkun O, Lee DW, Mello CV, Powers A, White SA, Hough G, Kubikova L, Smulders TV, Wada K, Dugas-Ford J, Husband S, Yamamoto K, Yu J, Siang C, Jarvis ED, Gunturkun O (2004) Revised nomenclature for avian telencephalon and some related brainstem nuclei. *J Comp Neurol* 473:377-414.
- Reynolds GP, Zhang ZJ, Beasley CL (2001) Neurochemical correlates of cortical GABAergic deficits in schizophrenia: selective losses of calcium binding protein immunoreactivity. *Brain Res Bull* 55:579-584.
- Reynolds GP, Abdul-Monim Z, Neill JC, Zhang ZJ (2004) Calcium binding protein markers of GABA deficits in schizophrenia--postmortem studies and animal models. *Neurotox Res* 6:57-61.

- Ribeiro S, Mello CV (2000) Gene expression and synaptic plasticity in the auditory forebrain of songbirds. *Learn Mem* 7:235-243.
- Ribeiro S, Cecchi GA, Magnasco MO, Mello CV (1998) Toward a song code: evidence for a syllabic representation in the canary brain. *Neuron* 21:359-371.
- Rogers JH (1992) Immunohistochemical markers in rat cortex: co-localization of calretinin and calbindin-D28k with neuropeptides and GABA. *Brain Res* 587:147-157.
- Roof RL (1993) The dentate gyrus is sexually dimorphic in prepubescent rats: testosterone plays a significant role. *Brain Res* 610:148-151.
- Rubel EW, Parks TN (1975) Organization and development of brain stem auditory nuclei of the chicken: tonotopic organization of n. magnocellularis and n. laminaris. *J Comp Neurol* 164:411-433.
- Ruppert C, Sandrasagra A, Anton B, Evans C, Schweitzer ES, Tobin AJ (1993) Rat-1 fibroblasts engineered with GAD65 and GAD67 cDNAs in retroviral vectors produce and release GABA. *J Neurochem* 61:768-771.
- Saldanha CJ, Clayton NS, Schlinger BA (1999) Androgen metabolism in the juvenile oscine forebrain: a cross-species analysis at neural sites implicated in memory function. *J Neurobiol* 40:397-406.
- Saldanha CJ, Tuerk MJ, Kim YH, Fernandes AO, Arnold AP, Schlinger BA (2000) Distribution and regulation of telencephalic aromatase expression in the zebra finch revealed with a specific antibody. *J Comp Neurol* 423:619-630.
- Salin PA, Prince DA (1996) Spontaneous GABAA receptor-mediated inhibitory currents in adult rat somatosensory cortex. *J Neurophysiol* 75:1573-1588.



- Sambrook J, Fritsch EF, Maniatis T (1989) Molecular cloning: a laboratory manual, 2nd Edition. Cold Spring Harbor, NY: Cold Spring Harbor Laboratory.
- Saper CB (1996) Any way you cut it: a new journal policy for the use of unbiased counting methods. *J Comp Neurol* 364:5.
- Saper CB, Sawchenko PE (2003) Magic peptides, magic antibodies: guidelines for appropriate controls for immunohistochemistry. *J Comp Neurol* 465:161-163.
- Sarter M, Bruno JP (2002) The neglected constituent of the basal forebrain corticopetal projection system: GABAergic projections. *Eur J Neurosci* 15:1867-1873.
- Sastry BR, Morishita W, Yip S, Shew T (1997) GABA-ergic transmission in deep cerebellar nuclei. *Prog Neurobiol* 53:259-271.
- Sato H, Sando I, Takahashi H (1991) Sexual dimorphism and development of the human cochlea. Computer 3-D measurement. *Acta Otolaryngol* 111:1037-1040.
- Scanziani M, Gahwiler BH, Thompson SM (1993) Presynaptic inhibition of excitatory synaptic transmission mediated by alpha adrenergic receptors in area CA3 of the rat hippocampus in vitro. *J Neurosci* 13:5393-5401.
- Scharff C, Nottebohm F (1991) A comparative study of the behavioral deficits following lesions of various parts of the zebra finch song system: implications for vocal learning. *J Neurosci* 11:2896-2913.
- Scharff C, Nottebohm F, Cynx J (1998) Conspecific and heterospecific song discrimination in male zebra finches with lesions in the anterior forebrain pathway. *J Neurobiol* 36:81-90.

- Scheich H, Bonke BA, Bonke D, Langner G (1979) Functional organization of some auditory nuclei in the guinea fowl demonstrated by the 2-deoxyglucose technique. *Cell Tissue Res* 204:17-27.
- Schlinger BA (1997) Sex steroids and their actions on the birdsong system. *J Neurobiol* 33:619-631.
- Schmidt MF, Konishi M (1998) Gating of auditory responses in the vocal control system of awake songbirds. *Nat Neurosci* 1:513-518.
- Schreiner CE, Mendelson JR (1990) Functional topography of cat primary auditory cortex: distribution of integrated excitation. *J Neurophysiol* 64:1442-1459.
- Schumacher M, Coirini H, McEwen BS (1989) Regulation of high-affinity GABA<sub>A</sub> receptors in specific brain regions by ovarian hormones. *Neuroendocrinology* 50:315-320.
- Segovia S, Guillaumon A (1982) Effects of sex steroids on the development of the vomeronasal organ in the rat. *Brain Res* 281:209-212.
- Segovia S, Guillaumon A (1993) Sexual dimorphism in the vomeronasal pathway and sex differences in reproductive behaviors. *Brain Res Brain Res Rev* 18:51-74.
- Sen K, Theunissen FE, Doupe AJ (2001) Feature analysis of natural sounds in the songbird auditory forebrain. *J Neurophysiol* 86:1445-1458.
- Shen P, Schlinger BA, Campagnoni AT, Arnold AP (1995) An atlas of aromatase mRNA expression in the zebra finch brain. *J Comp Neurol* 360:172-184.
- Sickel MJ, McCarthy MM (2000) Calbindin-D28k immunoreactivity is a marker for a subdivision of the sexually dimorphic nucleus of the preoptic area of the rat:

- developmental profile and gonadal steroid modulation. *J Neuroendocrinol* 12:397-402.
- Sillito AM (1975a) The effectiveness of bicuculline as an antagonist of GABA and visually evoked inhibition in the cat's striate cortex. *J Physiol* 250:287-304.
- Sillito AM (1975b) The contribution of inhibitory mechanisms to the receptive field properties of neurones in the striate cortex of the cat. *J Physiol* 250:305-329.
- Sillito AM (1977) Inhibitory processes underlying the directional specificity of simple, complex and hypercomplex cells in the cat's visual cortex. *J Physiol* 271:699-720.
- Sillito AM (1979) Inhibitory mechanisms influencing complex cell orientation selectivity and their modification at high resting discharge levels. *J Physiol* 289:33-53.
- Sillito AM, Versiani V (1977) The contribution of excitatory and inhibitory inputs to the length preference of hypercomplex cells in layers II and III of the cat's striate cortex. *J Physiol* 273:775-790.
- Sillito AM, Kemp JA, Milson JA, Berardi N (1980) A re-evaluation of the mechanisms underlying simple cell orientation selectivity. *Brain Res* 194:517-520.
- Simerly RB (1998) Organization and regulation of sexually dimorphic neuroendocrine pathways. *Behav Brain Res* 92:195-203.
- Simerly RB (2002) Wired for reproduction: organization and development of sexually dimorphic circuits in the mammalian forebrain. *Annu Rev Neurosci* 25:507-536.

- Simpson HB, Vicario DS (1990) Brain pathways for learned and unlearned vocalizations differ in zebra finches. *J Neurosci* 10:1541-1556.
- Sisneros JA, Forlano PM, Deitcher DL, Bass AH (2004) Steroid-dependent auditory plasticity leads to adaptive coupling of sender and receiver. *Science* 305:404-407.
- Sivaramakrishnan S, Sterbing-D'Angelo SJ, Filipovic B, D'Angelo WR, Oliver DL, Kuwada S (2004) GABA( A) synapses shape neuronal responses to sound intensity in the inferior colliculus. *J Neurosci* 24:5031-5043.
- Smith AJ, Owens S, Forsythe ID (2000) Characterisation of inhibitory and excitatory postsynaptic currents of the rat medial superior olive. *J Physiol* 529 Pt 3:681-698.
- Smith Y, Bolam JP (1990) The output neurones and the dopaminergic neurones of the substantia nigra receive a GABA-containing input from the globus pallidus in the rat. *J Comp Neurol* 296:47-64.
- Smith Y, Parent A, Seguela P, Descarries L (1987) Distribution of GABA-immunoreactive neurons in the basal ganglia of the squirrel monkey (*Saimiri sciureus*). *J Comp Neurol* 259:50-64.
- Soghomonian JJ, Martin DL (1998) Two isoforms of glutamate decarboxylase: why? *Trends Pharmacol Sci* 19:500-505.
- Sohrabji F, Nordeen EJ, Nordeen KW (1990) Selective impairment of song learning following lesions of a forebrain nucleus in the juvenile zebra finch. *Behav Neural Biol* 53:51-63.

- Somogyi P, Cowey A, Halasz N, Freund TF (1981) Vertical organization of neurones accumulating 3H-GABA in visual cortex of rhesus monkey. *Nature* 294:761-763.
- Spiro JE, Dalva MB, Mooney R (1999) Long-range inhibition within the zebra finch song nucleus RA can coordinate the firing of multiple projection neurons. *J Neurophysiol* 81:3007-3020.
- Stefanova N, Ovtcharoff W (2000) Sexual dimorphism of the bed nucleus of the stria terminalis and the amygdala. *Adv Anat Embryol Cell Biol* 158:III-X, 1-78.
- Stokes TM, Leonard CM, Nottebohm F (1974) The telencephalon, diencephalon, and mesencephalon of the canary, *Serinus canaria*, in stereotaxic coordinates. *J Comp Neurol* 156:337-374.
- Suga N, Zhang Y, Yan J (1997) Sharpening of frequency tuning by inhibition in the thalamic auditory nucleus of the mustached bat. *J Neurophysiol* 77:2098-2114.
- Sullivan WE, Konishi M (1984) Segregation of stimulus phase and intensity coding in the cochlear nucleus of the barn owl. *J Neurosci* 4:1787-1799.
- Takahashi T, Moiseff A, Konishi M (1984) Time and intensity cues are processed independently in the auditory system of the owl. *J Neurosci* 4:1781-1786.
- Takahashi TT, Konishi M (1988) Projections of nucleus angularis and nucleus laminaris to the lateral lemniscal nuclear complex of the barn owl. *J Comp Neurol* 274:212-238.
- Tchernichovski O, Mitra PP, Lints T, Nottebohm F (2001) Dynamics of the vocal imitation process: how a zebra finch learns its song. *Science* 291:2564-2569.

- Terleph TA, Mello CV, Vicario DS (2005) Auditory topography and temporal response dynamics of canary caudal telencephalon. (submitted).
- Terpstra NJ, Bolhuis JJ, den Boer-Visser AM (2004) An analysis of the neural representation of birdsong memory. *J Neurosci* 24:4971-4977.
- Thiel G, Schoch S, Petersohn D (1994) Regulation of synapsin I gene expression by the zinc finger transcription factor zif268/egr-1. *J Biol Chem* 269:15294-15301.
- Thompson SM, Capogna M, Scanziani M (1993) Presynaptic inhibition in the hippocampus. *Trends Neurosci* 16:222-227.
- Thorpe WH (1958) The learning of song patterns by birds, with especial references to the song of the chaffinch, *Fringilla coelebs*. *Ibis* 100:535-570.
- Tremere L, Hicks TP, Rasmusson DD (2001a) Expansion of receptive fields in raccoon somatosensory cortex in vivo by GABA(A) receptor antagonism: implications for cortical reorganization. *Exp Brain Res* 136:447-455.
- Tremere L, Hicks TP, Rasmusson DD (2001b) Role of inhibition in cortical reorganization of the adult raccoon revealed by microiontophoretic blockade of GABA(A) receptors. *J Neurophysiol* 86:94-103.
- Tremere LA, Pinaud R, De Weerd P (2003) Contributions of inhibitory mechanisms to perceptual completion and cortical reorganization. In: Filling-in: from perceptual completion to cortical reorganization (Pessoa L, De Weerd P, eds), pp 295-322. New York: Oxford University Press.
- Vates GE, Nottebohm F (1995) Feedback circuitry within a song-learning pathway. *Proc Natl Acad Sci U S A* 92:5139-5143.

- Vates GE, Broome BM, Mello CV, Nottebohm F (1996) Auditory pathways of caudal telencephalon and their relation to the song system of adult male zebra finches. *J Comp Neurol* 366:613-642.
- Veenman CL, Reiner A (1994) The distribution of GABA-containing perikarya, fibers, and terminals in the forebrain and midbrain of pigeons, with particular reference to the basal ganglia and its projection targets. *J Comp Neurol* 339:209-250.
- Vicario DS, Yohay KH (1993) Song-selective auditory input to a forebrain vocal control nucleus in the zebra finch. *J Neurobiol* 24:488-505.
- Vicario DS, Raksin JN (2000) Possible roles for GABAergic inhibition in the vocal control system of the zebra finch. *Neuroreport* 11:3631-3635.
- Vicario DS, Raksin JN, Naqvi NH, Thande N, Simpson HB (2002) The relationship between perception and production in songbird vocal imitation: what learned calls can teach us. *J Comp Physiol A Neuroethol Sens Neural Behav Physiol* 188:897-908.
- Volkmar FR, Greenough WT (1972) Rearing complexity affects branching of dendrites in the visual cortex of the rat. *Science* 176:1145-1147.
- Wallace CS, Withers GS, Weiler IJ, George JM, Clayton DF, Greenough WT (1995) Correspondence between sites of NGFI-A induction and sites of morphological plasticity following exposure to environmental complexity. *Brain Res Mol Brain Res* 32:211-220.

- Walrond JP, Govind CK, Huestis SE (1993) Two structural adaptations for regulating transmitter release at lobster neuromuscular synapses. *J Neurosci* 13:4831-4845.
- Wang J, Caspary D, Salvi RJ (2000) GABA-A antagonist causes dramatic expansion of tuning in primary auditory cortex. *Neuroreport* 11:1137-1140.
- Warchol ME, Dallos P (1990) Neural coding in the chick cochlear nucleus. *J Comp Physiol [A]* 166:721-734.
- Wenstrup JJ (1999) Frequency organization and responses to complex sounds in the medial geniculate body of the mustached bat. *J Neurophysiol* 82:2528-2544.
- Werhahn KJ, Mortensen J, Kaelin-Lang A, Boroojerdi B, Cohen LG (2002) Cortical excitability changes induced by deafferentation of the contralateral hemisphere. *Brain* 125:1402-1413.
- White JH, Wise A, Main MJ, Green A, Fraser NJ, Disney GH, Barnes AA, Emson P, Foord SM, Marshall FH (1998) Heterodimerization is required for the formation of a functional GABA(B) receptor. *Nature* 396:679-682.
- Wild JM (2004) Functional neuroanatomy of the sensorimotor control of singing. *Ann N Y Acad Sci* 1016:438-462.
- Wild JM, Karten HJ, Frost BJ (1993) Connections of the auditory forebrain in the pigeon (*Columba livia*). *J Comp Neurol* 337:32-62.
- Wild JM, Williams MN, Suthers RA (2001) Parvalbumin-positive projection neurons characterise the vocal premotor pathway in male, but not female, zebra finches. *Brain Res* 917:235-252.



- Wild JM, Williams MN, Howie GJ, Mooney R (2005) Calcium-binding proteins define interneurons in HVC of the zebra finch (*Taeniopygia guttata*). *J Comp Neurol* 483:76-90.
- Williams H (1985) Sexual dimorphism of auditory activity in the zebra finch song system. *Behav Neural Biol* 44:470-484.
- Williams H, Nottebohm F (1985) Auditory responses in avian vocal motor neurons: a motor theory for song perception in birds. *Science* 229:279-282.
- Wimer RE, Wimer C (1985) Three sex dimorphisms in the granule cell layer of the hippocampus in house mice. *Brain Res* 328:105-109.
- Winer JA, Larue DT (1996) Evolution of GABAergic circuitry in the mammalian medial geniculate body. *Proc Natl Acad Sci U S A* 93:3083-3087.
- Winer JA, Larue DT, Pollak GD (1995) GABA and glycine in the central auditory system of the mustache bat: structural substrates for inhibitory neuronal organization. *J Comp Neurol* 355:317-353.
- Winer JA, Saint Marie RL, Larue DT, Oliver DL (1996) GABAergic feedforward projections from the inferior colliculus to the medial geniculate body. *Proc Natl Acad Sci U S A* 93:8005-8010.
- Winfield DA, Brooke RN, Sloper JJ, Powell TP (1981) A combined Golgi-electron microscopic study of the synapses made by the proximal axon and recurrent collaterals of a pyramidal cell in the somatic sensory cortex of the monkey. *Neuroscience* 6:1217-1230.

- Wisden W, Errington ML, Williams S, Dunnett SB, Waters C, Hitchcock D, Evan G, Bliss TV, Hunt SP (1990) Differential expression of immediate early genes in the hippocampus and spinal cord. *Neuron* 4:603-614.
- Wong WK, Ou XM, Chen K, Shih JC (2002) Activation of human monoamine oxidase B gene expression by a protein kinase C MAPK signal transduction pathway involves c-Jun and Egr-1. *J Biol Chem* 277:22222-22230.
- Woolley CS, McEwen BS (1992) Estradiol mediates fluctuation in hippocampal synapse density during the estrous cycle in the adult rat. *J Neurosci* 12:2549-2554.
- Woolley SM, Rubel EW (1997) Bengalese finches *Lonchura Striata domestica* depend upon auditory feedback for the maintenance of adult song. *J Neurosci* 17:6380-6390.
- Worley PF, Christy BA, Nakabeppu Y, Bhat RV, Cole AJ, Baraban JM (1991) Constitutive expression of zif268 in neocortex is regulated by synaptic activity. *Proc Natl Acad Sci U S A* 88:5106-5110.
- Yang L, Pollak GD, Resler C (1992) GABAergic circuits sharpen tuning curves and modify response properties in the mustache bat inferior colliculus. *J Neurophysiol* 68:1760-1774.
- Yang L, Monsivais P, Rubel EW (1999) The superior olivary nucleus and its influence on nucleus laminaris: a source of inhibitory feedback for coincidence detection in the avian auditory brainstem. *J Neurosci* 19:2313-2325.

- Young SR, Rubel EW (1983) Frequency-specific projections of individual neurons in chick brainstem auditory nuclei. *J Neurosci* 3:1373-1378.
- Zeigler HP, Marler P (2004) *Behavioral Neurobiology of Birdsong*. New York: New York Academy of Sciences.
- Zhang D, Pan ZH, Awobuluyi M, Lipton SA (2001) Structure and function of GABA(C) receptors: a comparison of native versus recombinant receptors. *Trends Pharmacol Sci* 22:121-132.
- Zheng W, Knudsen EI (1999) Functional selection of adaptive auditory space map by GABAA-mediated inhibition. *Science* 284:962-965.
- Zheng W, Knudsen EI (2001) Gabaergic inhibition antagonizes adaptive adjustment of the owl's auditory space map during the initial phase of plasticity. *J Neurosci* 21:4356-4365.
- Zhu Y, Li H, Zhou L, Wu JY, Rao Y (1999) Cellular and molecular guidance of GABAergic neuronal migration from an extracortical origin to the neocortex. *Neuron* 23:473-485.
- Ziemann U, Muellbacher W, Hallett M, Cohen LG (2001) Modulation of practice-dependent plasticity in human motor cortex. *Brain* 124:1171-1181.